

**Chapter - 4**  
**Results**  
**and**  
**Discussion**

## 4.1 Introduction

This chapter deals with the results obtained using the techniques like X-ray diffraction (XRD), Energy Dispersive X-Ray Analysis (EDAX), Field Emission Scanning Electron Microscope (FE-SEM), Photoluminescence (PL) and Thermoelectric electric measurements, which were used to characterize the samples and to obtain its properties.

## 4.2 X-RAY Diffraction Analysis of the synthesized samples

The samples synthesized in the laboratory by the Solid-State and Precipitation method are characterized here using X-RAY Diffraction technique for the structural analysis. The samples were subjected to EDAX analysis to confirm the presence of elements. The results are presented below.

### 4.2.1 X-RAY Diffraction Pattern of undoped and Mn/ Eu/ Tb doped

#### Cerium Sulphide Synthesized by Solid State Method

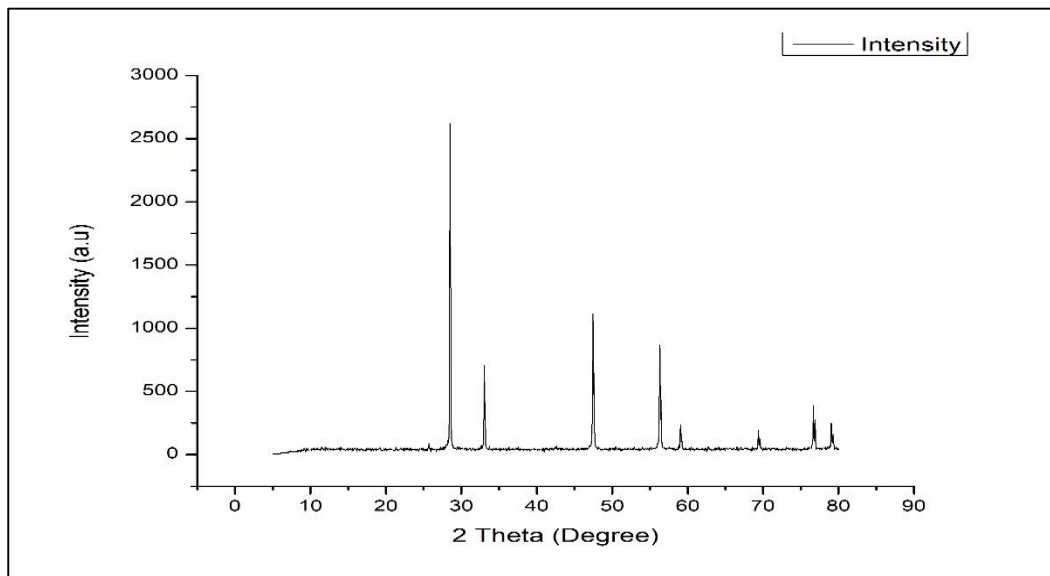
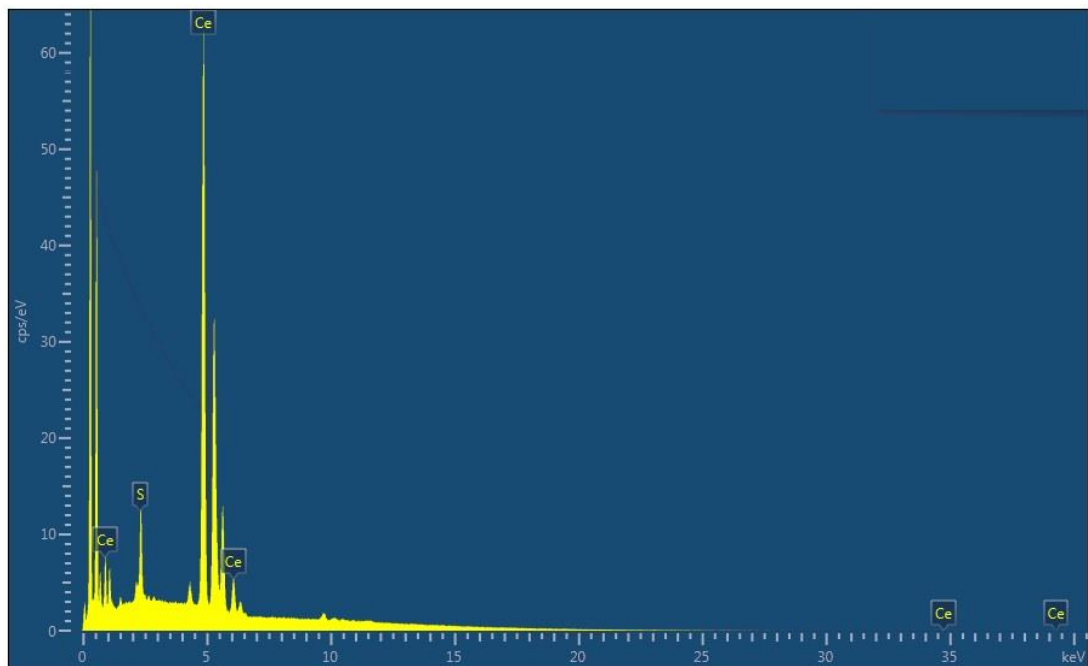


Figure 4-1: XRD peaks of undoped Ce<sub>2</sub>S<sub>3</sub> [CeU-SS]

**Table 4-1: XRD Peaks Matching with JCPDS Data for Ce<sub>2</sub>S<sub>3</sub> [CeU-SS]**

<b>Ce<sub>2</sub>S<sub>3</sub></b>				
<b>2 Theta (degree)</b>	<b>Intensity</b>	<b>d-spacing (Calculated)</b>	<b>d-Spacing (JCPDS-43- 0799)</b>	<b>hkl</b>
28.5137	2620	3.1250	3.120	111
33.0589	709	2.7085	2.71	200
47.4684	1117	1.9155	1.914	220
56.3300	864	1.6332	1.620	311
59.0752	234	1.5626	1.559	222
69.4215	194	1.3531	1.369	400
76.7128	344	1.2416	1.251	331
79.0880	251	1.2108	1.217	420



**Figure 4-2: EDAX Peaks of Undoped Ce<sub>2</sub>S<sub>3</sub> [CeU-SS]**

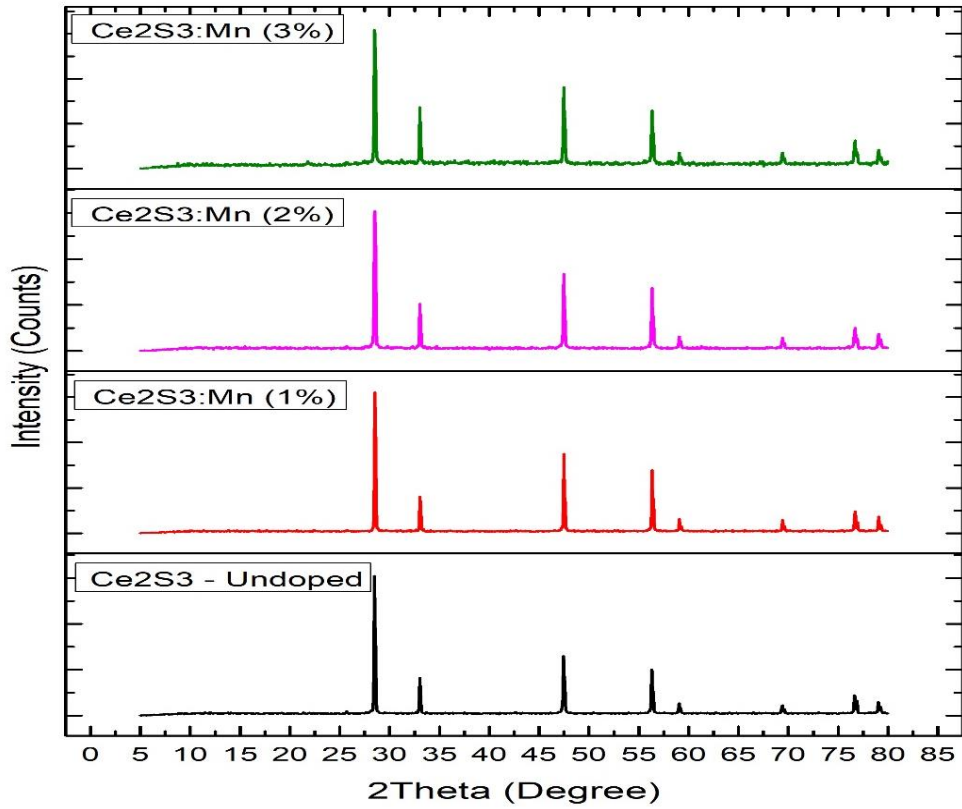


Figure 4-3: XRD Peaks of undoped and Mn doped Ce<sub>2</sub>S<sub>3</sub> [CeU-SS, CeM1-SS, CeM2-SS, CeM3-SS]

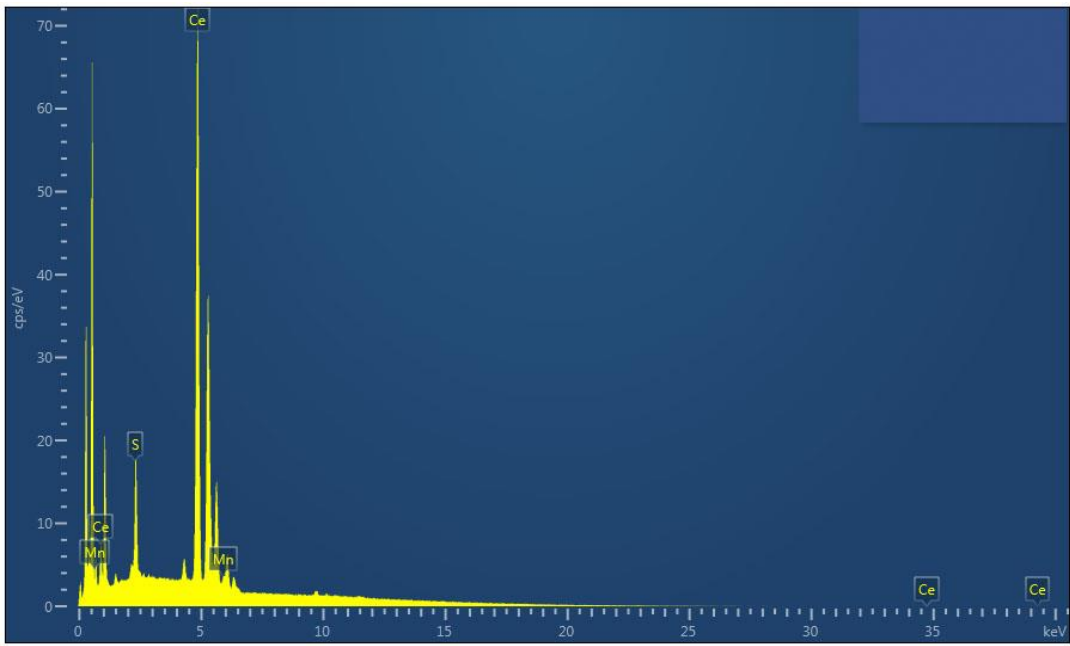


Figure 4-4: EDAX Peaks of Mn doped Ce<sub>2</sub>S<sub>3</sub> [CeM-SS]

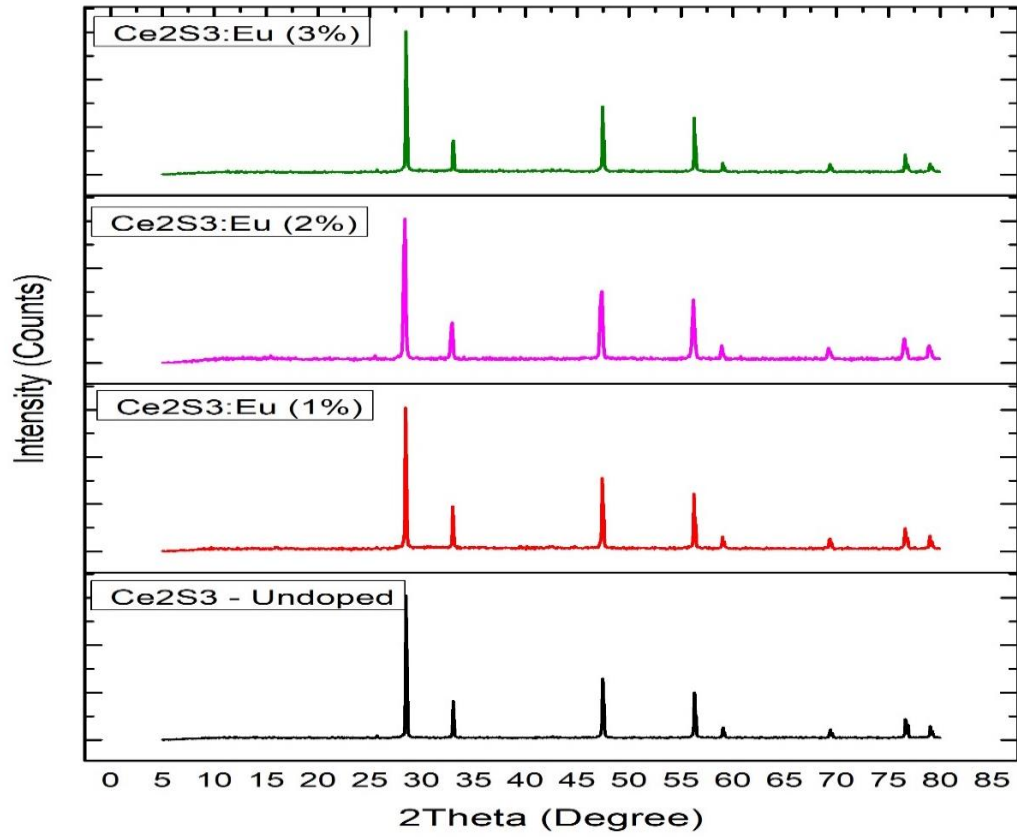


Figure 4-5: XRD Peaks of undoped and Eu doped Ce<sub>2</sub>S<sub>3</sub> [CeU-SS, CeE1-SS, CeE2-SS, CeE3-SS]

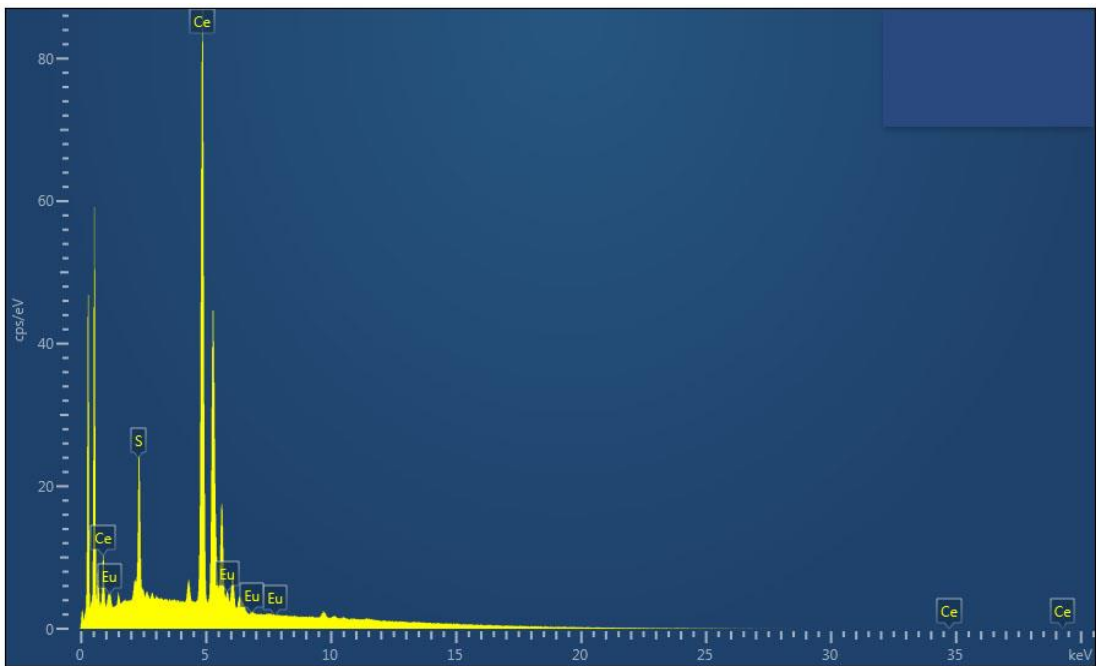


Figure 4.6: EDAX Peaks of Eu doped Ce<sub>2</sub>S<sub>3</sub> [CeE-SS]

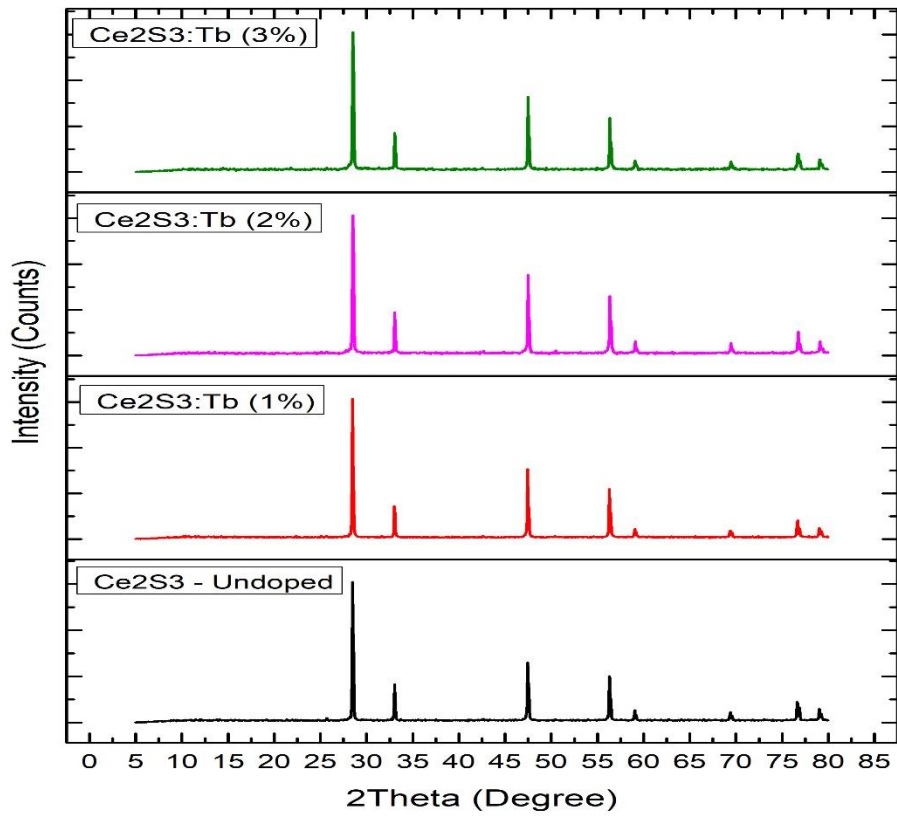


Figure 4-7: XRD Peaks of undoped and Tb doped Ce<sub>2</sub>S<sub>3</sub> [CeU-SS, CeT1-SS, CeT2-SS, CeT3-SS]

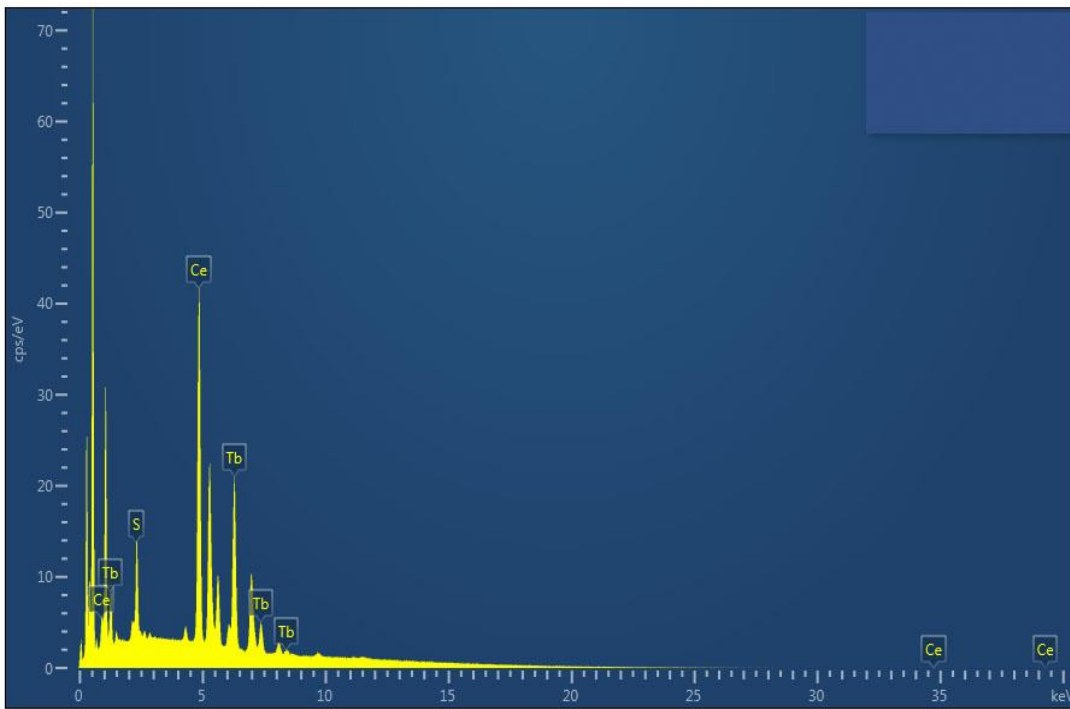


Figure 4.8: EDAX Peaks of Tb doped Ce<sub>2</sub>S<sub>3</sub> [CeT-SS]

The Figures 4-1, 4-3, 4-5 and 4-7 show the X-Ray diffraction patterns of undoped  $\text{Ce}_2\text{S}_3$  and  $\text{Ce}_2\text{S}_3$  doped with Manganese, Europium and Terbium. It is seen that the XRD patterns of undoped and doped  $\text{Ce}_2\text{S}_3$  are identical, which is in conformity with the results reported elsewhere. The formation of  $\text{Ce}_2\text{S}_3$  is confirmed from the results of the XRD patterns and the peaks therein [1]. The sharp peak at  $2\Theta = 28.5137$  having the highest intensity is the characteristic peak of (111) plane. As seen from Table 4-1, the d- values of the peaks match with the standard values of JCPDS card no. 43-0799, which is for  $\alpha$  -  $\text{Ce}_2\text{S}_3$ .

The pattern indicates high degree of crystallinity and confirms the formation of alpha ( $\alpha$ ) phase with orthorhombic structure [2-4]. Rare earth sulphides are usually found in the orthorhombic  $\alpha$  – phase below temperatures of 1100 °C, the intermediate tetragonal  $\beta$  - phase at temperatures between 1100-1300 °C and cubic  $\gamma$  – phase at temperatures above 1350 °C [5].

Taking the Lanthanum compounds as reference, as they have been also synthesized in this study, Cerium has electrons in the 4f shell which is an inner shell closer to the nucleus and hence these electrons experience greater nuclear force. Hence, the  $\alpha$  – phase is the preferred structure for lighter lanthanides which generally have an orthorhombic structure with space group of Pnma (62) [6].

The EDAX results shown in Figures 4-2, 4-4, 4-6 and 4-8 confirm the presence of all the elements. EDAX study was carried out for one of the doped samples.

#### 4.2.2 X-RAY Diffraction Pattern of undoped and Mn/ Eu/ Tb doped Gadolinium Sulphide Synthesized by Solid State Method

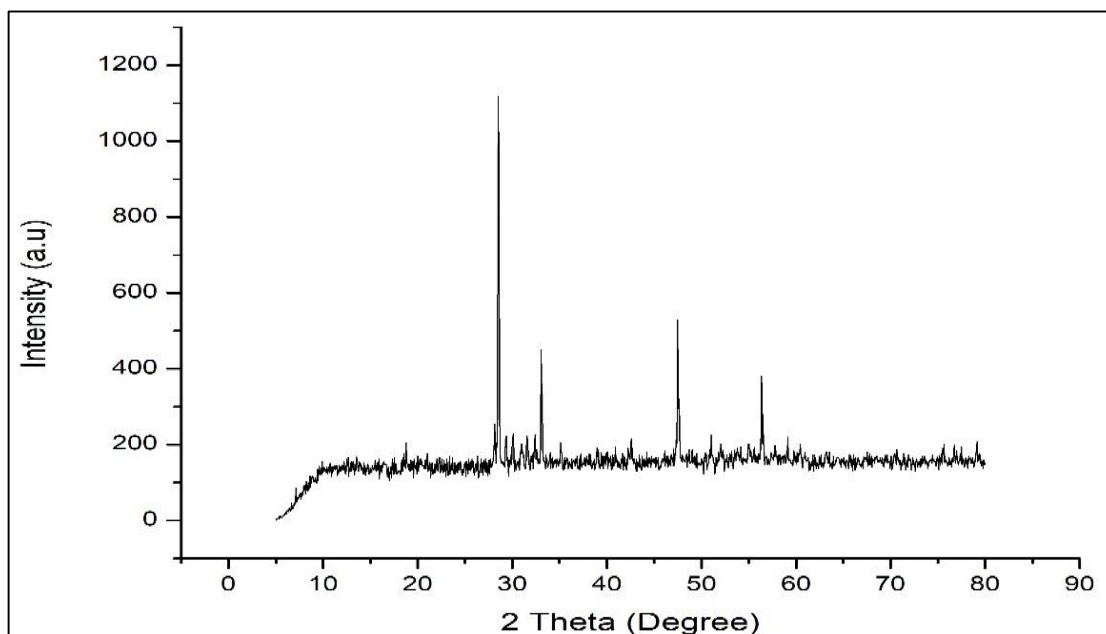


Figure 4-9: XRD Peaks of undoped  $Gd_2S_3$  [GdU-SS]

Table 4-2: XRD Peaks Matching with JCPDS Data for  $Gd_2S_3$  [GdU-SS]

$Gd_2S_3$				
2 Theta (degree)	Intensity	d-spacing Calculated	d- Spacing JCPDS-76-0265	hkl
18.8232	162	4.7111	4.7337	102
28.5942	1119	3.1196	3.1118	210
31.6319	223	2.8266	2.82	203
33.1001	450	2.7045	2.7075	212
35.0239	161	2.5602	2.5662	104
47.5289	530	1.9117	1.9492	020
55.0217	200	1.6677	1.6657	504
56.3886	380	1.6305	1.6273	610
60.4894	201	1.5294	1.5264	415

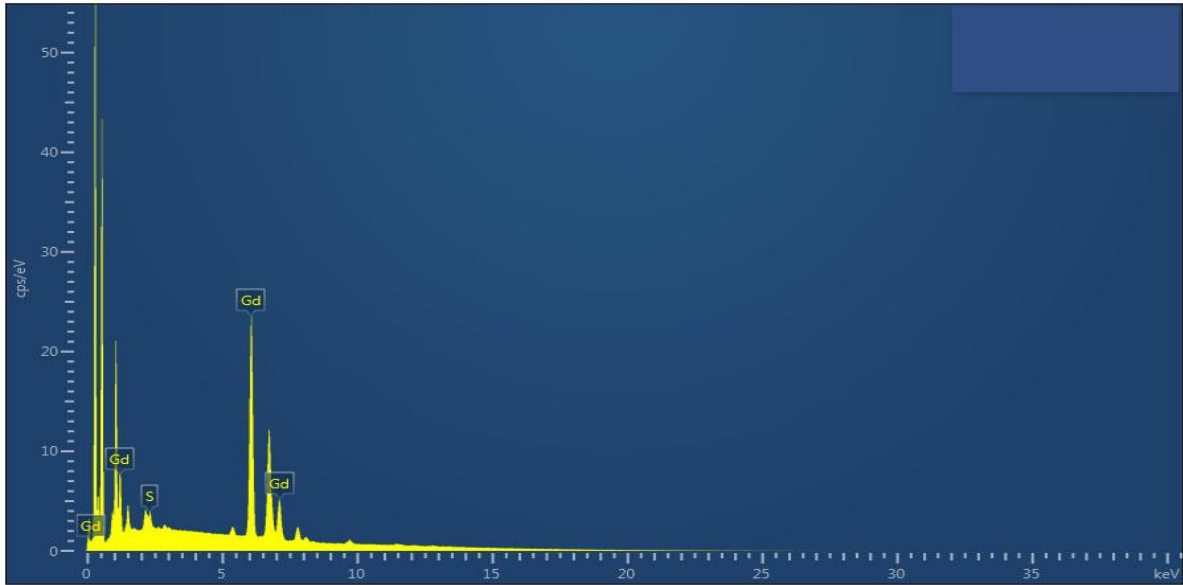


Figure 4-10: EDAX Peaks of undoped  $Gd_2S_3$  [GdU-SS]

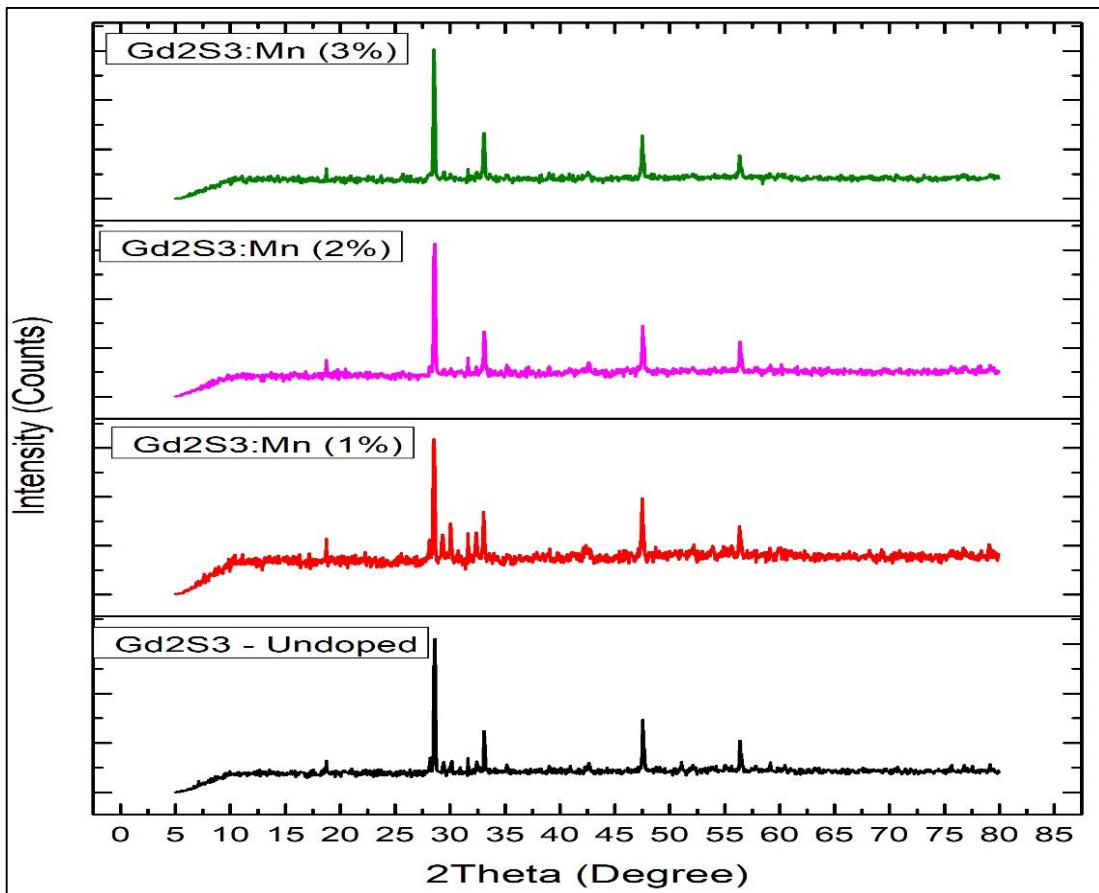


Figure 4-11: XRD Peaks of undoped and Mn doped  $Gd_2S_3$  [GdU-SS, GdM1-SS, GdM2-SS, GdM3-SS]

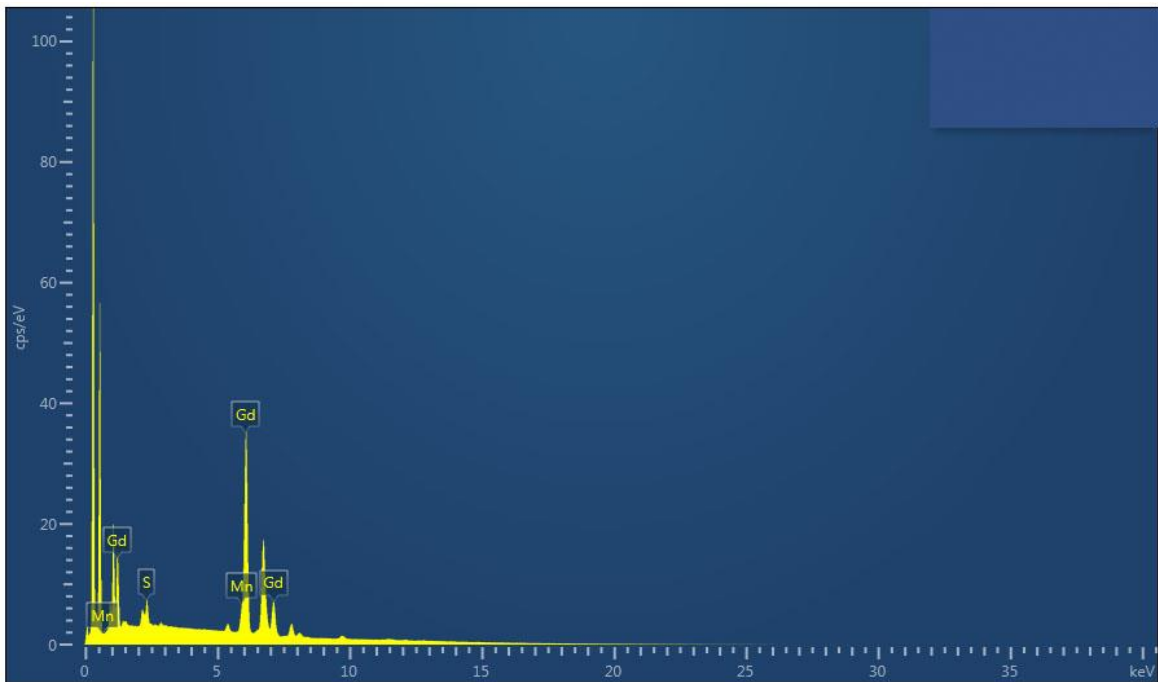


Figure 4-12: EDAX Peaks of Mn doped  $Gd_2S_3$  [GdM-SS]

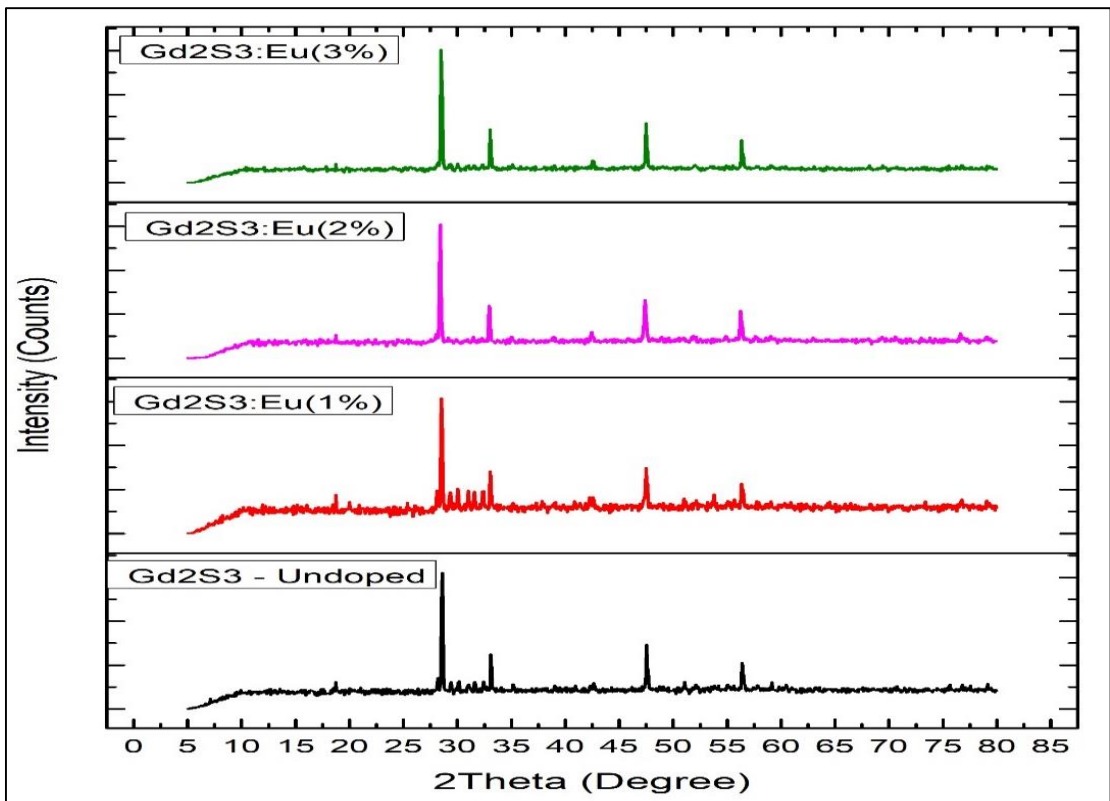


Figure 4-13: XRD Peaks of undoped and Eu doped  $Gd_2S_3$  [GdU-SS, GdE1-SS, GdE2-SS, GdE3-SS]

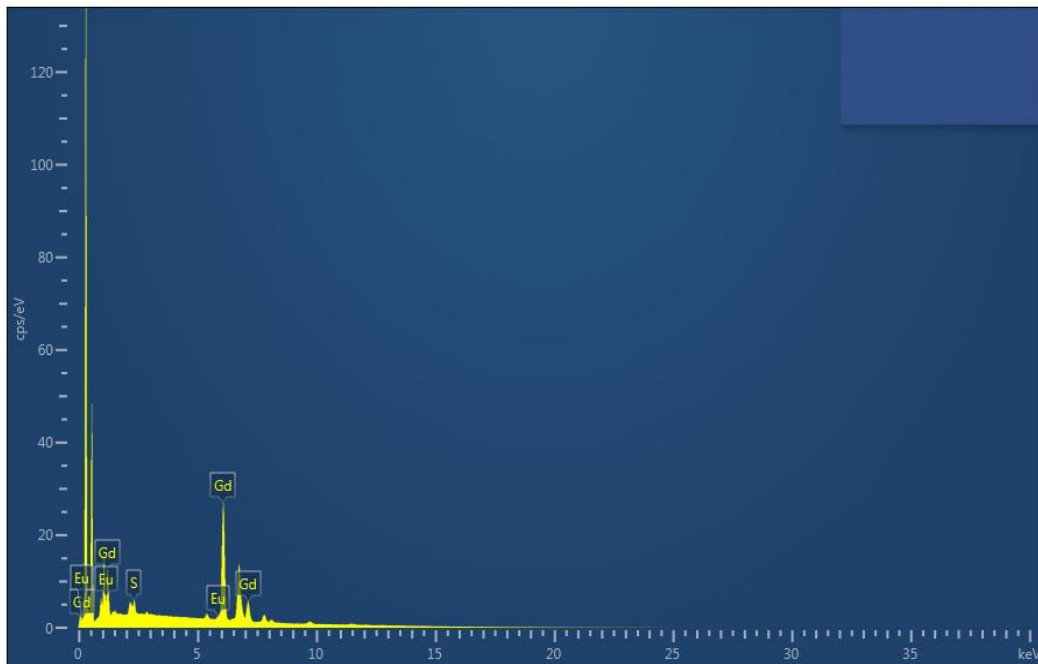


Figure 4-14: EDAX Peaks of Eu doped  $Gd_2S_3$  [GdE-SS]

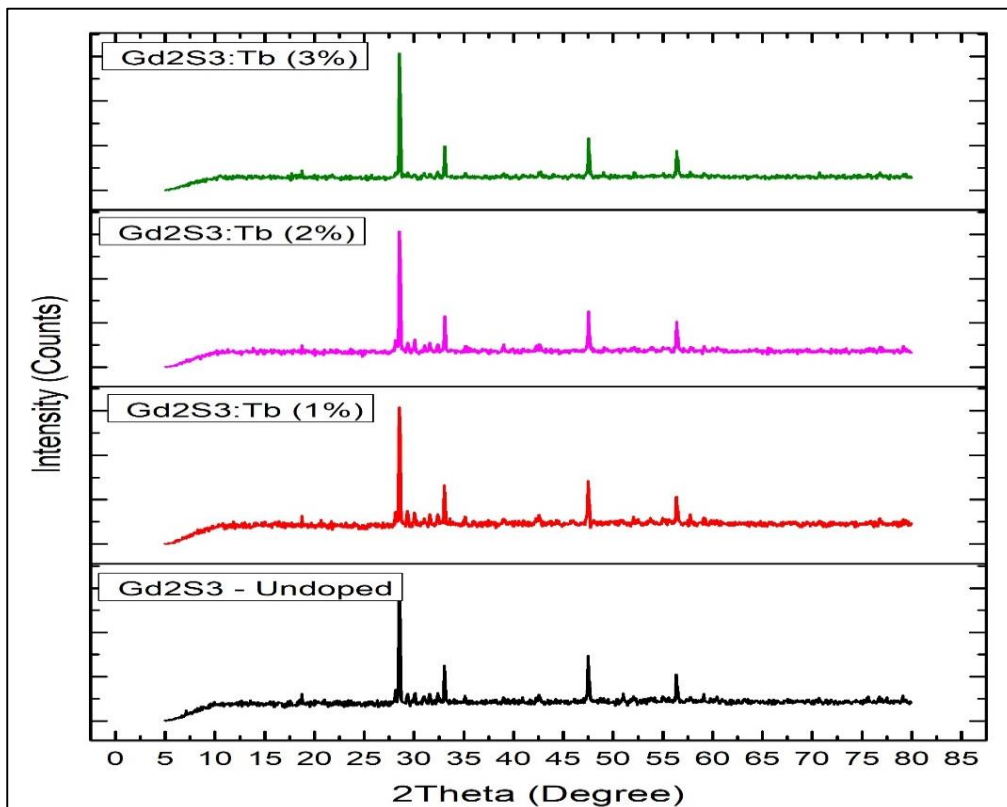


Figure 4-15: XRD Peaks of undoped and Tb doped  $Gd_2S_3$  [GdU-SS, GdT1-SS, GdT2-SS, GdT3-SS]

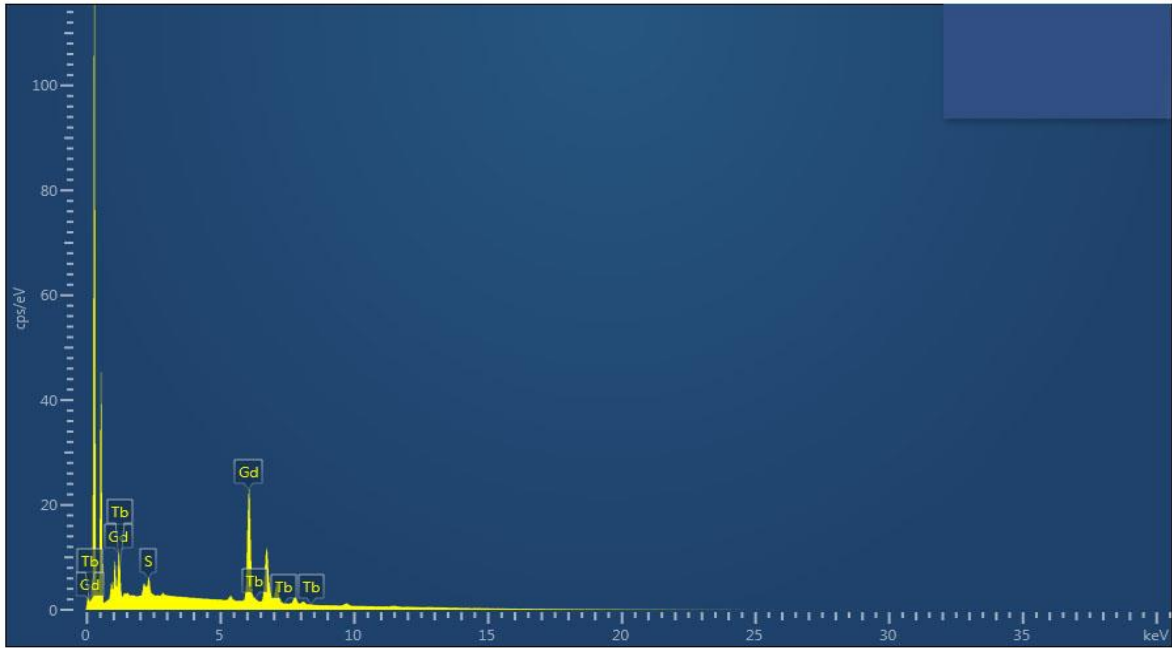


Figure 4-16: EDAX Peaks of Tb doped  $Gd_2S_3$  [GdT-SS]

The Figures 4-9, 4-11, 4-13 and 4-15 show the X-Ray diffraction patterns of undoped  $Gd_2S_3$  and  $Gd_2S_3$  doped with Manganese, Europium and Terbium. It is seen that the XRD patterns of undoped and doped  $Gd_2S_3$  are identical, which is in conformity with the results reported elsewhere [7]. The formation of  $Gd_2S_3$  is confirmed from the results of the XRD patterns and the peaks therein. The sharp peak at  $2\theta = 28.5942$  having the highest intensity is the characteristic peak corresponding to (210) plane. As seen from Table 4-2, the d- values of the peaks match with the standard values of JCPDS card no. 76-0265, which is for  $\alpha$  -  $Gd_2S_3$ .

The pattern indicates high degree of crystallinity and conforms the formation of alpha ( $\alpha$ ) phase with orthorhombic structure [8]. This orthorhombic system has space group of Pnma (62) [6]. Gadolinium has a half filled electronic configuration which makes it much more stable than other lanthanides. The  $\alpha$  – phase of  $Gd_2S_3$  is stable at temperatures below 1200 °C and transforms to  $\beta$  and  $\gamma$  phases at higher temperatures [9]. This suitably explains the formation of  $\alpha$  – phase of  $Gd_2S_3$  in our study. The EDAX results shown in Figures 4-10, 4-12, 4-14 and 4-16 confirm the presence of all the elements. EDAX study was carried out for one of the doped sample.

### 4.2.3 X-RAY Diffraction Pattern of undoped and Mn/ Eu/ Tb doped Lanthanum Sulphide Synthesized by Solid State Method

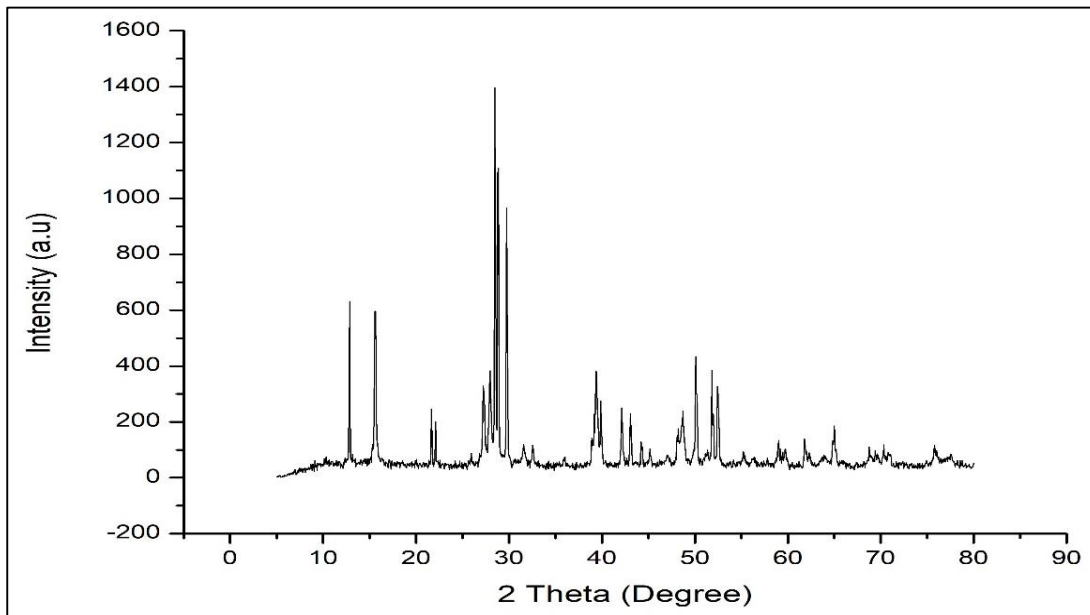


Figure 4-17: XRD Peaks of undoped  $\text{La}_2\text{S}_3$  [LaU-SS]

**Table 4-3: XRD Peaks Matching with JCPDS Data for La<sub>2</sub>S<sub>3</sub> [LaU-SS]**

La <sub>2</sub> S <sub>3</sub>					
2Theta (degree)	Intensity	d-spacing Calculated	d-Standard JCPDS- $\alpha$ -71- 2349 JCPDS- $\beta$ -43- 0340	Phase	hkl
12.7985	249	6.9121	6.9049	$\alpha$	101
15.6337	596	5.6643	5.5244	$\alpha$	102
21.6583	247	4.1004	4.1706	$\beta$	321
27.8348	232	3.203	3.2374	$\beta$	116
28.493	1398	3.1304	3.1076	$\alpha$	203
29.7587	965	3.0001	3.0348	$\alpha$	113
39.3779	382	2.2866	2.2876	$\beta$	604
42.1117	251	2.1442	2.147	$\beta$	615
43.0736	229	2.0985	2.0846	$\beta$	642
44.3393	110	2.0415	2.0455	$\beta$	428
48.6933	239	1.8687	1.862	$\alpha$	402
50.1108	435	1.8191	1.812	$\alpha$	124
51.8322	386	1.7626	1.7684	$\alpha$	208
59.0212	134	1.5639	1.5615	$\alpha$	323
61.8057	141	1.5	1.494	$\beta$	6111
64.9953	186	1.4338	1.4353	$\alpha$	227
68.7417	111	1.3645	1.3598	$\alpha$	033
75.7789	117	1.2543	1.2557	$\alpha$	234

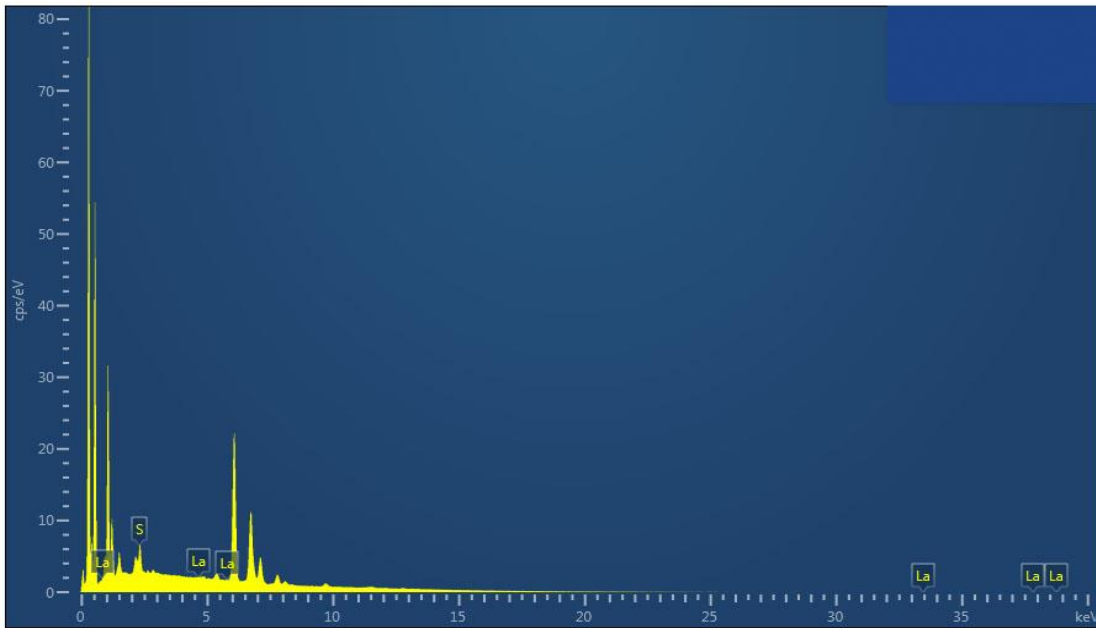


Figure 4-18: EDAX Peaks of undoped  $\text{La}_2\text{S}_3$  [LaU-SS]

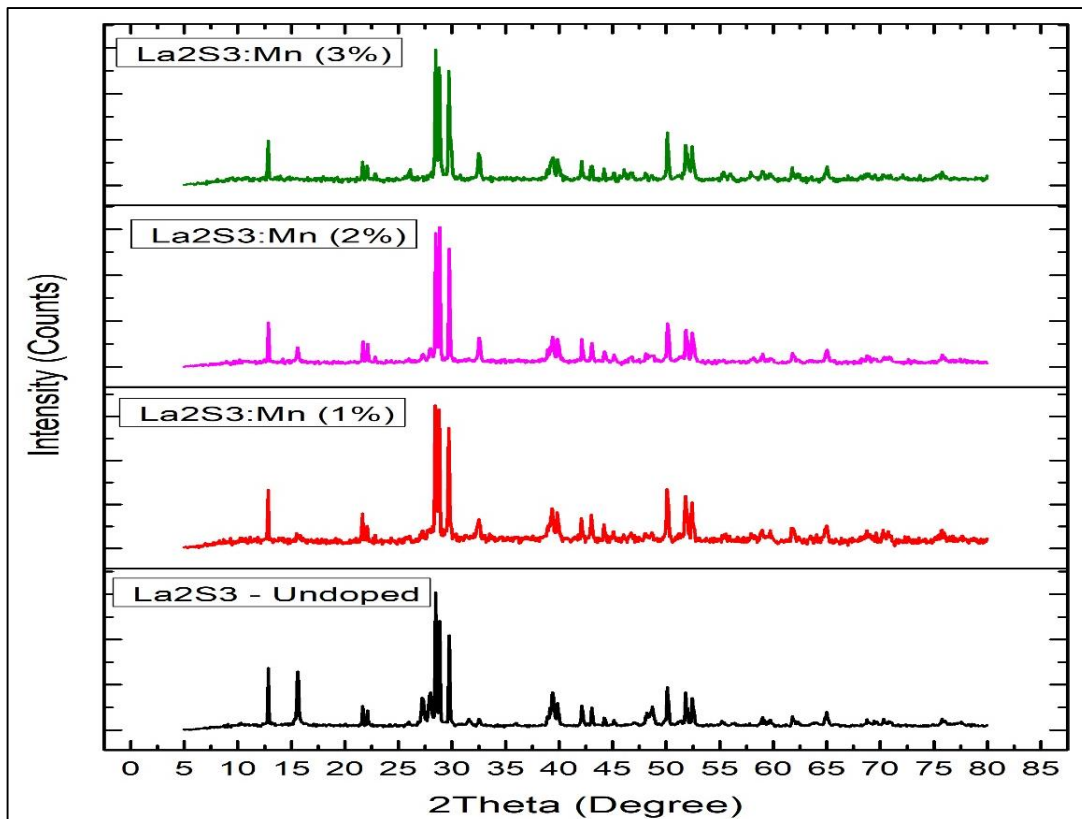


Figure 4-19: XRD Peaks of undoped and Mn doped  $\text{La}_2\text{S}_3$  [LaU-SS, LaM1-SS, LaM2-SS, LaM3-SS]

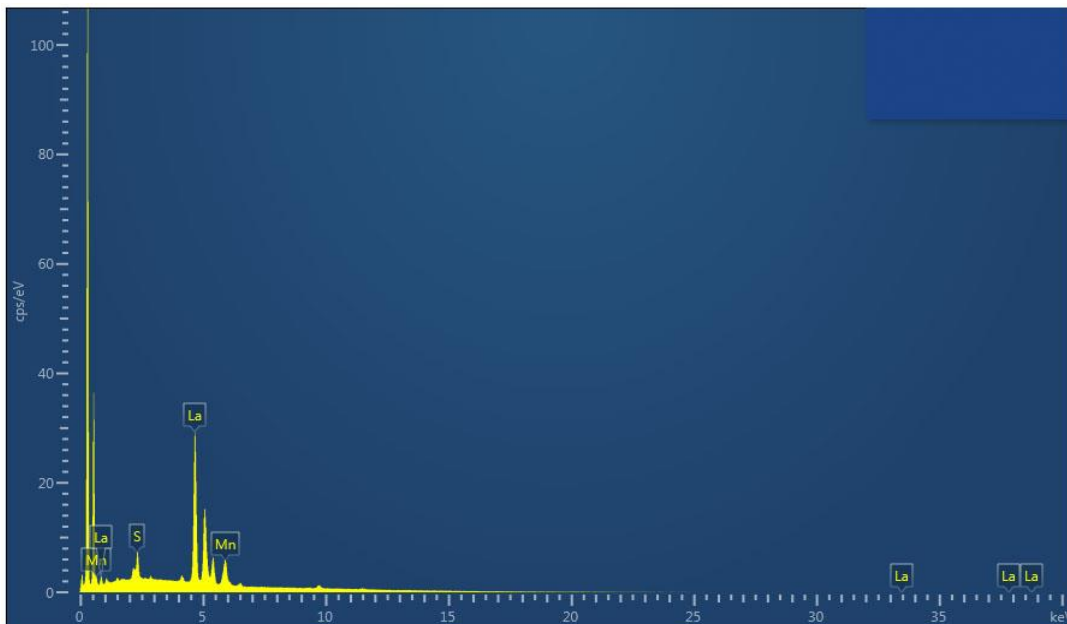


Figure 4-20: EDAX Peaks of Mn doped  $\text{La}_2\text{S}_3$  [LaM-SS]

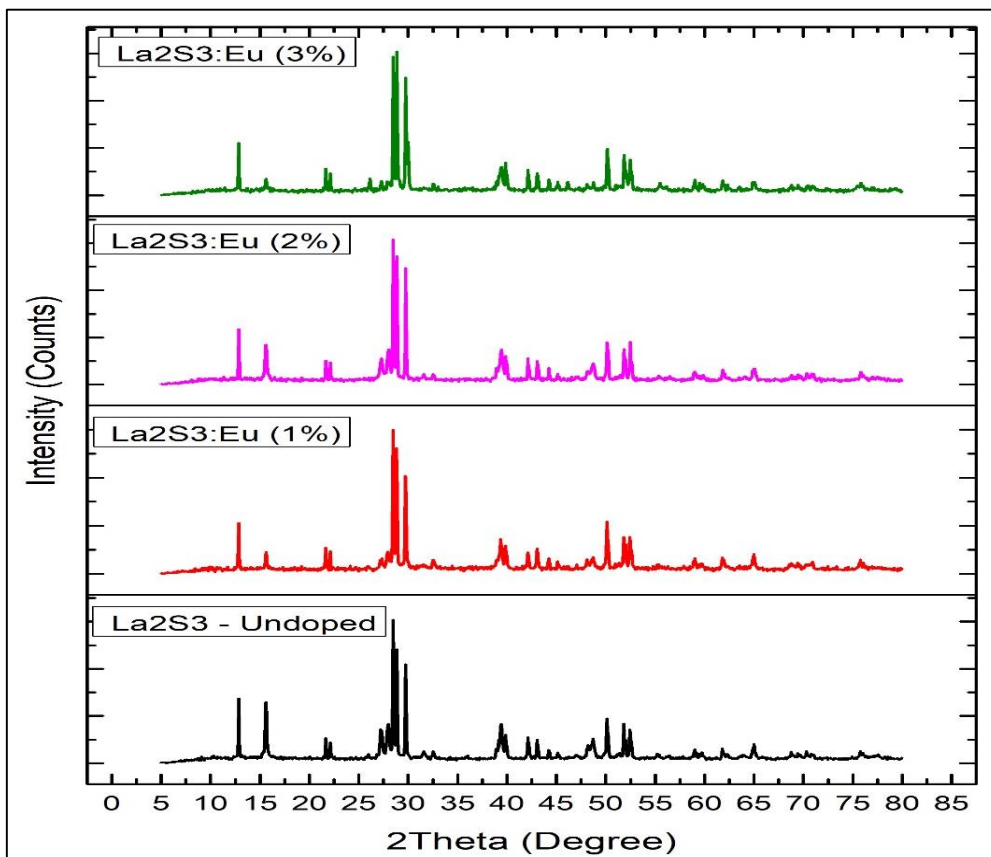


Figure 4-21: XRD Peaks of undoped and Eu doped  $\text{La}_2\text{S}_3$  [LaU-SS, LaE1-SS, LaE2-SS, LaE3-SS]

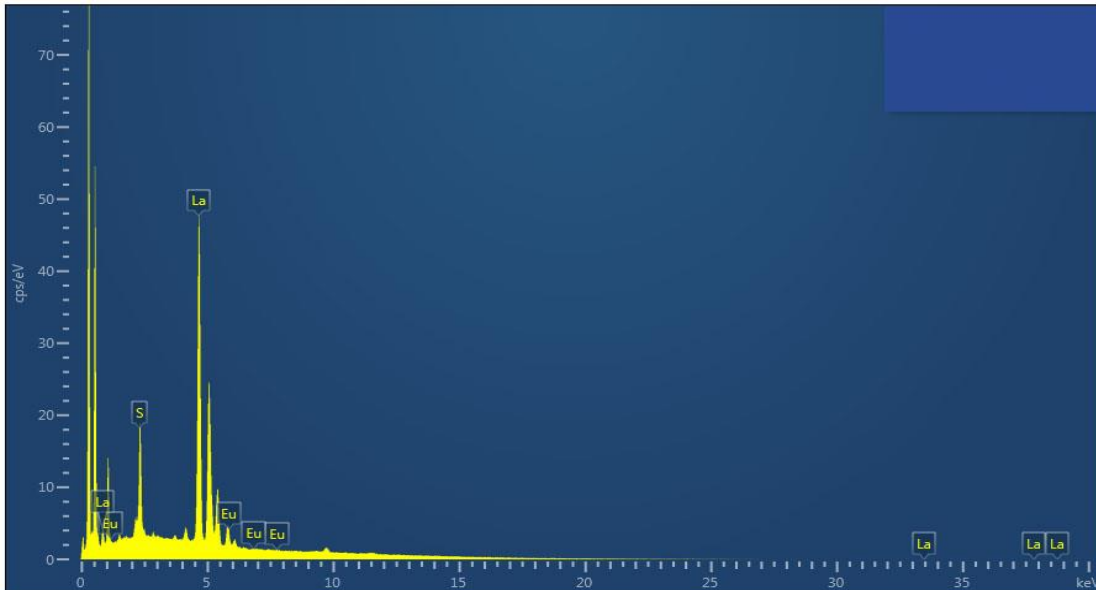


Figure 4-22: EDAX Peaks of Eu doped  $\text{La}_2\text{S}_3$  [LaE-SS]

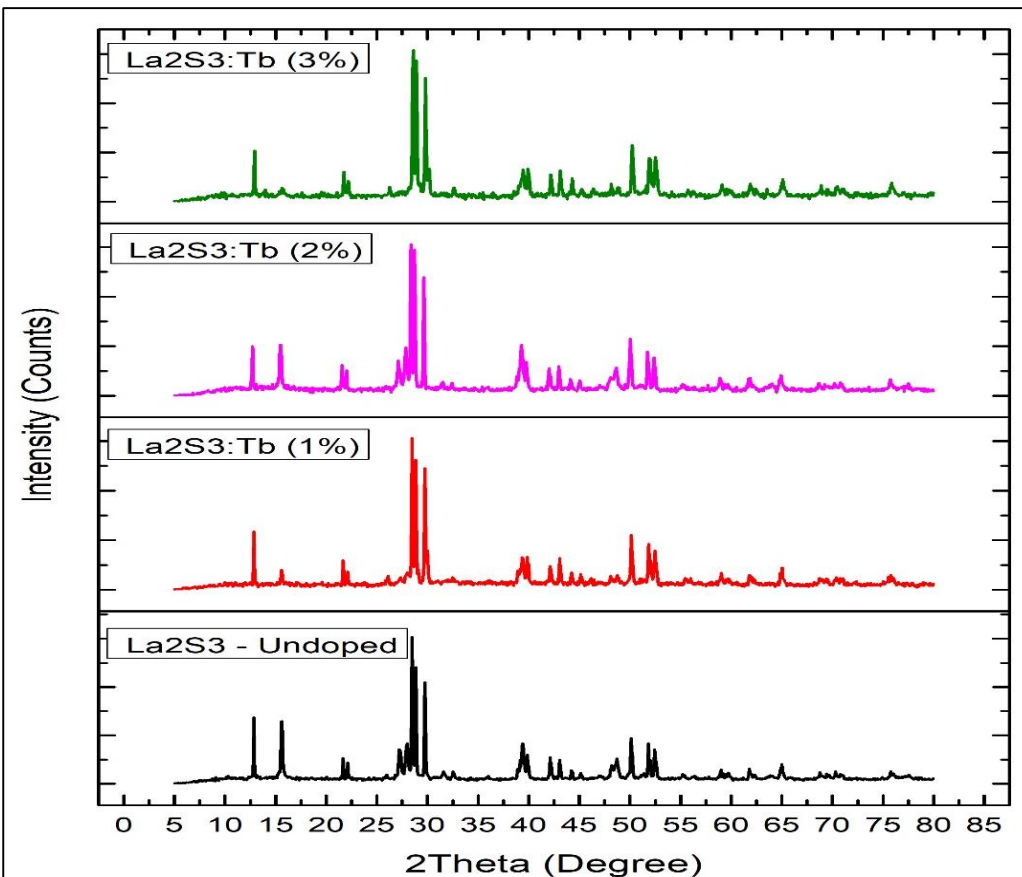


Figure 4-23: XRD Peaks of undoped and Tb doped  $\text{La}_2\text{S}_3$  [LaU-SS, LaT1-SS, LaT2-SS, LaT3-SS]

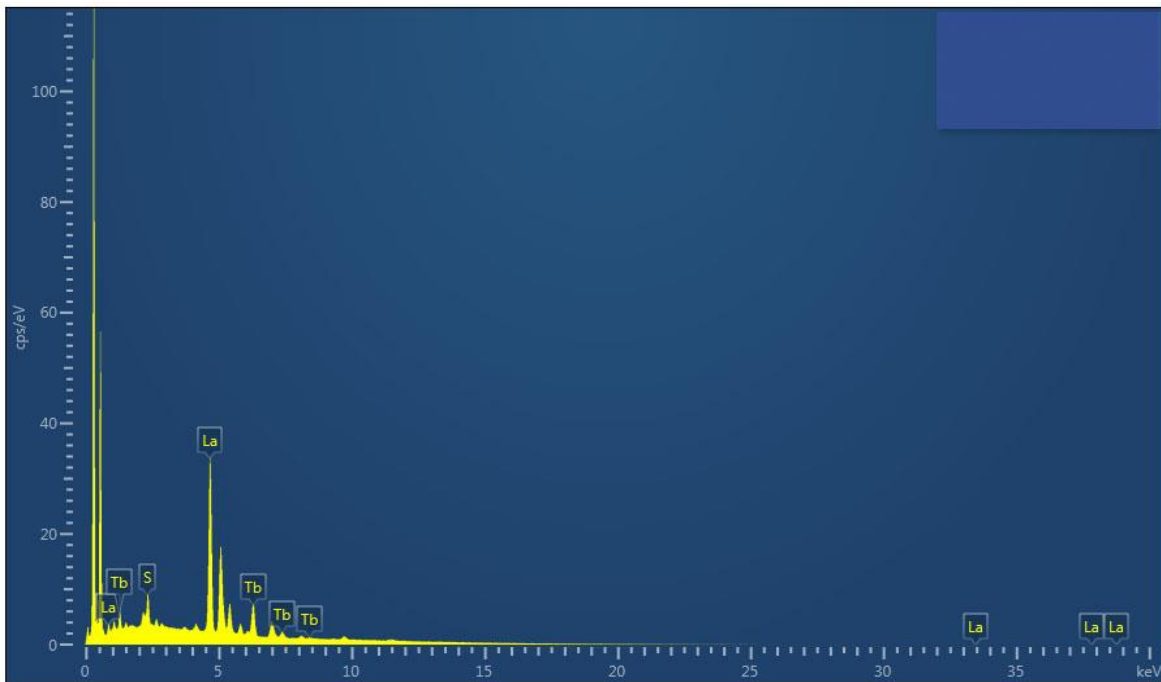


Figure 4-24: EDAX Peaks of Tb doped  $\text{La}_2\text{S}_3$  [LaT-SS]

The Figures 4-17, 4-19, 4-21 and 4-23 depict the X-Ray diffraction patterns of undoped  $\text{La}_2\text{S}_3$  and  $\text{La}_2\text{S}_3$  doped with Manganese, Europium and Terbium. It is seen that the XRD patterns of undoped and doped  $\text{La}_2\text{S}_3$  are identical. However, unlike other samples, two phases have been observed – alpha ( $\alpha$ ) and beta ( $\beta$ ). As seen from Table 4-3, the d-values of synthesized  $\text{La}_2\text{S}_3$  are found to match the patterns of the standard reference JCPDS card no. 71-2349 ( $\alpha$  - phase) and JCPDS-43-0340 ( $\beta$  - phase).

The pattern indicates high degree of crystallinity and has a mixed phase of orthogonal and tetragonal structure [10,11]. The  $\alpha$  – phase has a space group of Pnma (62) while the  $\beta$  – phase has a space group of 141/acd (142) [6]. The highest intensity peak of  $\alpha$  – phase corresponds to  $2\theta = 28.493$  and represents the (203) plane. The second highest peak corresponding to  $2\theta = 29.7587$  in this phase represents the (113) plane.

The highest intensity peak of  $\beta$  – phase corresponds to  $2\theta = 39.3779$  and represents the (604) plane.

Lanthanum is the simplest of the lanthanides which does not have any 4f shell electron. The  $\alpha$  – phase of  $\text{La}_2\text{S}_3$  transforms to the  $\beta$  – phase at temperature around  $1200^\circ\text{C}$  and to the  $\gamma$  – Phase at temperatures above  $1350^\circ\text{C}$ . In our study we have obtained a mixed phase of  $\alpha$

and  $\beta$ . This can be attributed to the fact that during the solid state reaction, some of the atoms of the precursors may have achieved the temperature of 1200 °C and beyond and hence the higher temperature  $\beta$  – phase is also obtained. The EDAX results shown in Figures 4-18, 4-20, 4-22 and 4-24 confirm the presence of all the elements. EDAX study was carried out for one of the doped samples.

#### 4.2.4 X-RAY Diffraction Pattern of undoped and Mn/ Eu/ Tb doped Yttrium Sulphide Synthesized by Solid State Method

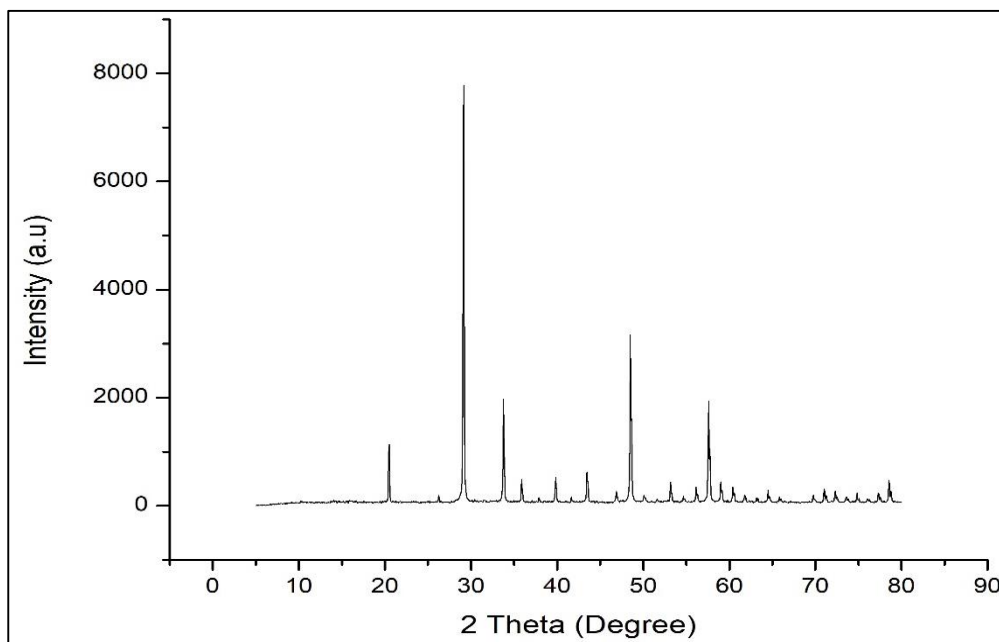


Figure 4-25: XRD Peaks of undoped  $Y_2S_3$  [YU-SS]

**Table 4-4: XRD Peaks Matching with JCPDS Data for Y<sub>2</sub>S<sub>3</sub> [YU-SS]**

<b>Y<sub>2</sub>S<sub>3</sub></b>				
<b>2 Theta (degree)</b>	<b>Intensity</b>	<b>d-spacing Calculated</b>	<b>d-Standard JCPDS-79-2250</b>	<b>hkl</b>
20.4939	1133	4.3307	4.3315	400
29.1511	7784	3.0612	3.0634	402
33.7582	1974	2.6532	2.6539	312
35.8846	482	2.5007	2.5032	113
39.8841	328	2.2587	2.2556	313
43.4787	628	2.0799	2.0829	114
48.4908	3165	1.8760	1.8785	<u>3</u> 21
53.1485	366	1.7220	1.7285	405
57.6037	1933	1.5990	1.5979	<u>8</u> 05
59.0212	447	1.5639	1.5625	<u>7</u> 21
60.3882	342	1.5317	1.5317	804
69.3998	73	1.3532	1.3517	-

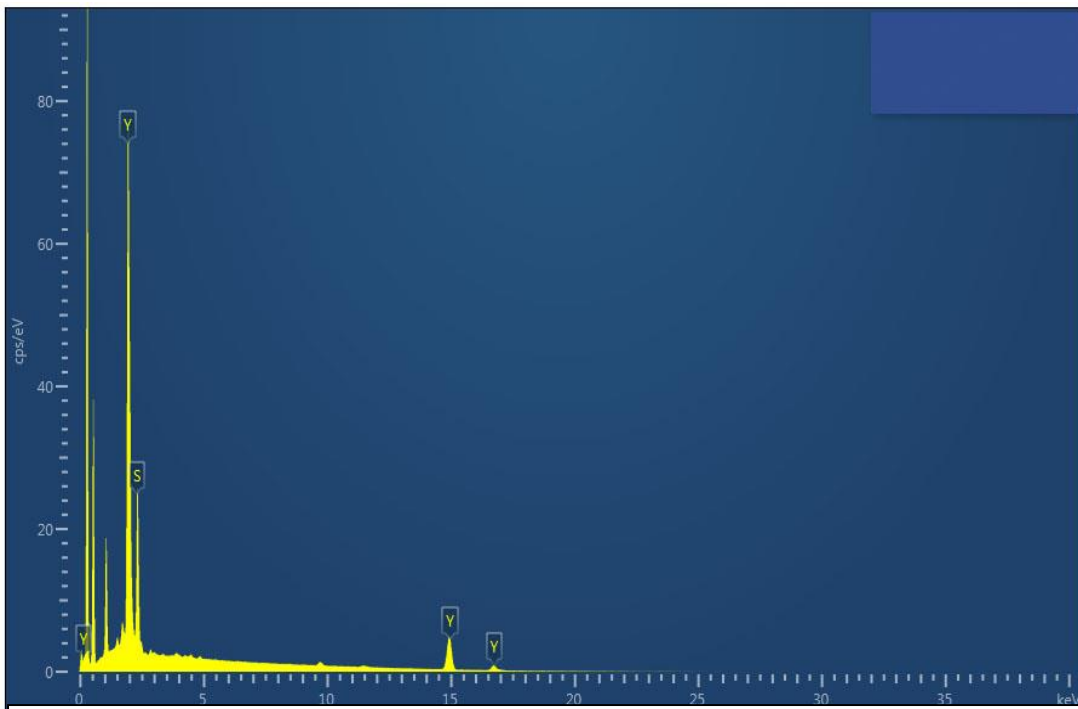


Figure 4-26: EDAX Peaks of undoped Y<sub>2</sub>S<sub>3</sub>[YU-SS]

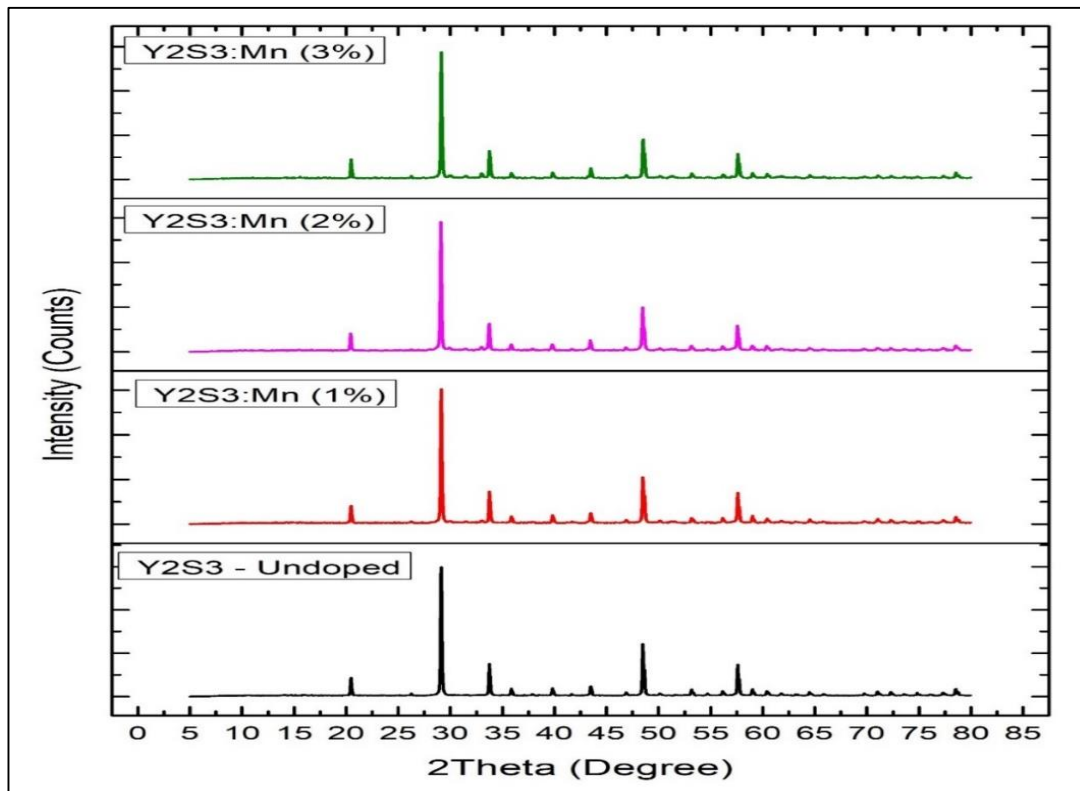


Figure 4-27: XRD Peaks of undoped and Mn doped Y<sub>2</sub>S<sub>3</sub> [YU-SS, YM1-SS, YM2-SS, YM3-SS]

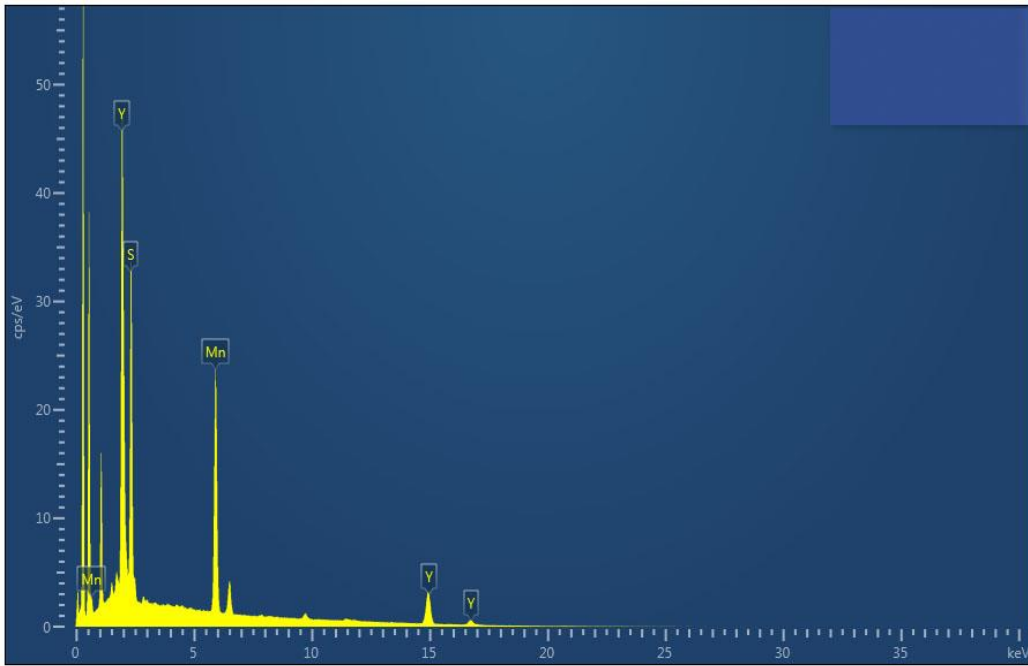


Figure 4-28: EDAX Peaks of Mn doped  $Y_2S_3$  [YM-SS]

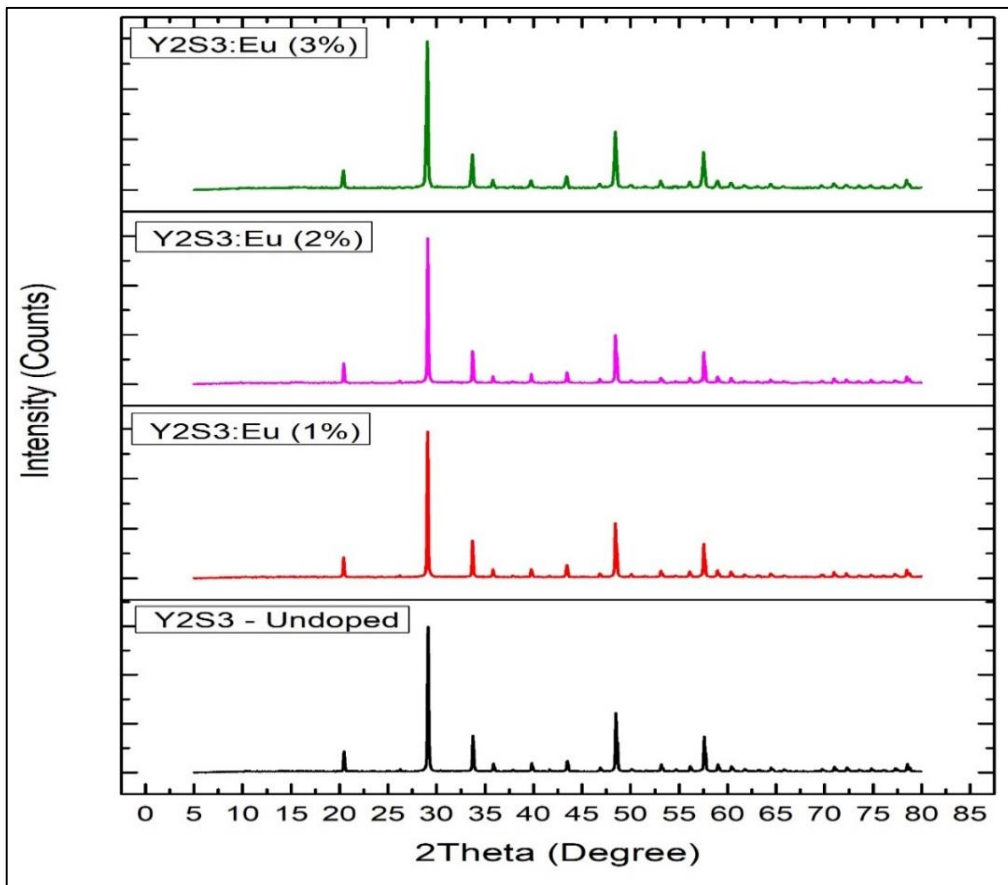


Figure 4-29: XRD Peaks of undoped and Eu doped  $Y_2S_3$  [YU-SS, YE1-SS, YE2-SS, YE3-SS]

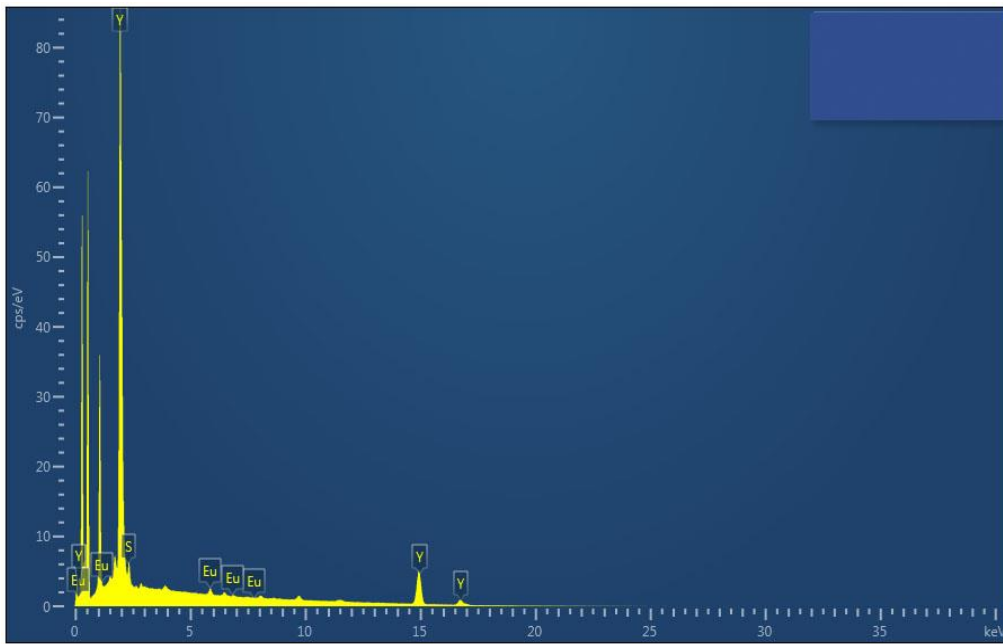


Figure 4-30: EDAX Peaks of Eu doped  $Y_2S_3$  [YE-SS]

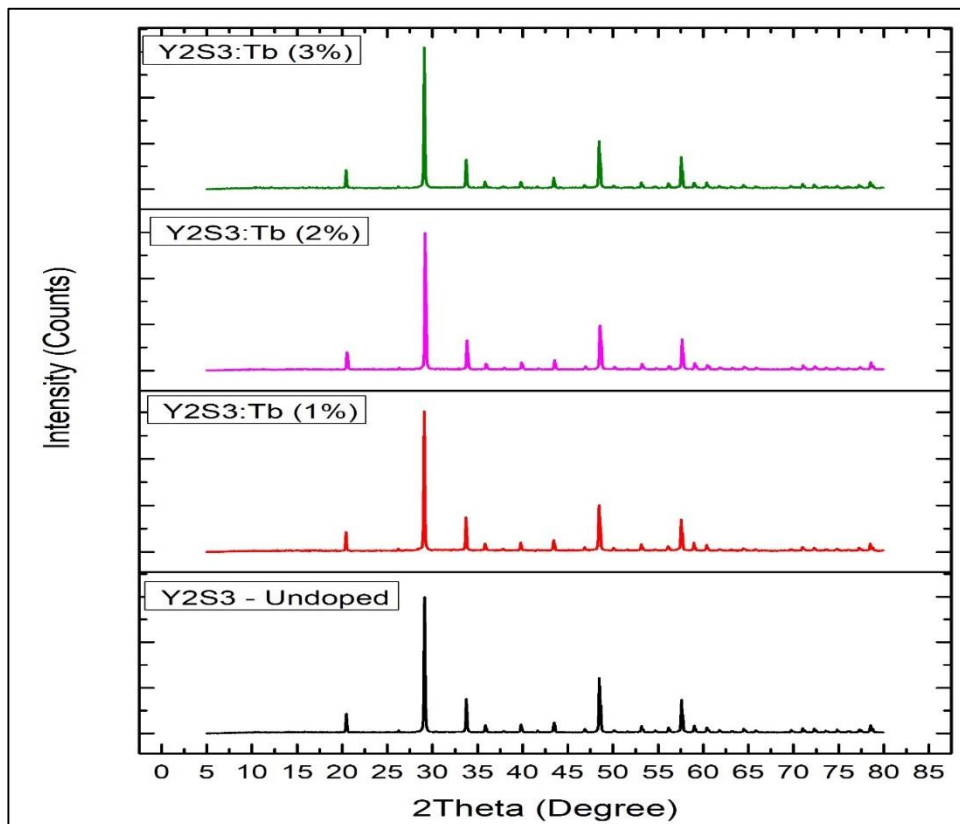


Figure 4-31: XRD Peaks of undoped and Tb doped  $Y_2S_3$  [YU-SS, YT1-SS, YT2-SS, YT3-SS]

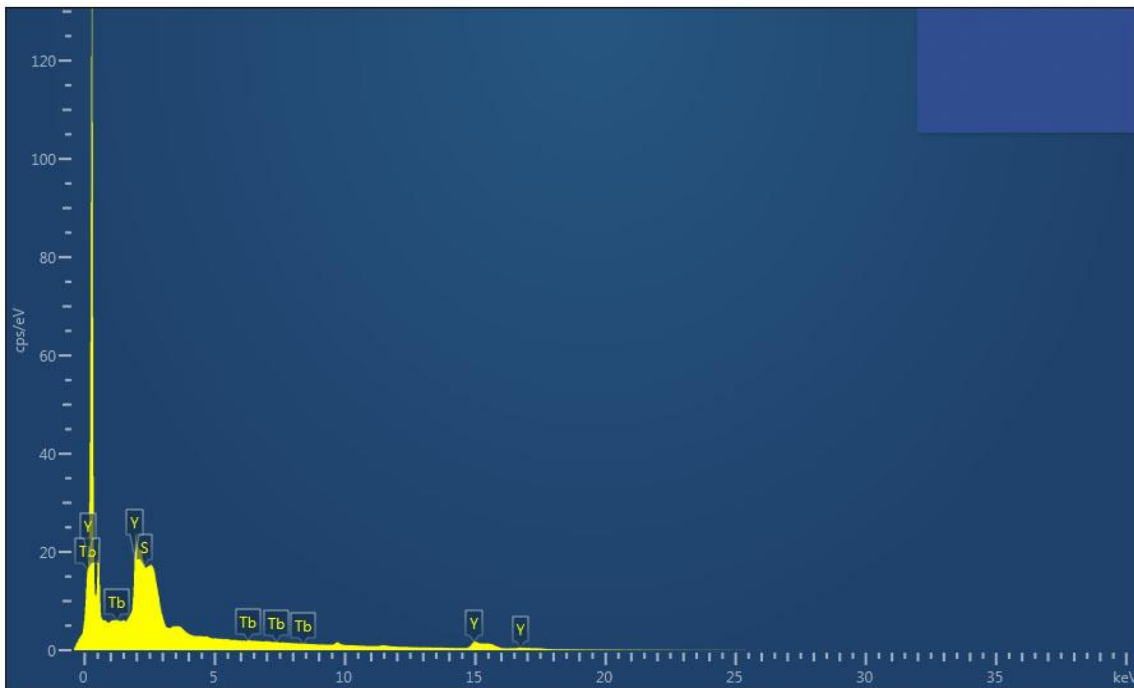


Figure 4-32: EDAX Peaks of Tb doped  $Y_2S_3$  [YT-SS]

The X-Ray diffraction patterns of undoped  $Y_2S_3$  and  $Y_2S_3$  doped with Manganese, Europium and Terbium are shown in the Figures 4-25, 4-27, 4-29 and 4-31. It can be seen that the XRD patterns of undoped and doped  $Y_2S_3$  are identical. The literature also reports the same. The formation of  $Y_2S_3$  is confirmed from Table 4-4 which shows the matching of d-values of synthesized sample and the d-values of the standard JCPDS card no. 79-2250 [12]. The major peak value obtained at  $2\theta = 29.1511$  corresponds to (402) plane. The pattern indicates high degree of crystallinity and confirms the formation of monoclinic delta ( $\delta$ ) phase. The  $\delta$  – phase is a very low symmetry monoclinic system with space group P21/m (11) [6]. Yttrium Sulphide is only found in the  $\delta$  – phase only which justifies the result that we have obtained in this study. The EDAX results shown in Figures 4-26, 4-28, 4-30 and 4-32 confirms the presence of all the elements. EDAX study was carried out for one of the doped samples.

#### 4.2.5 X-RAY Diffraction Pattern of Cerium Sulphide Synthesized by Precipitation Method

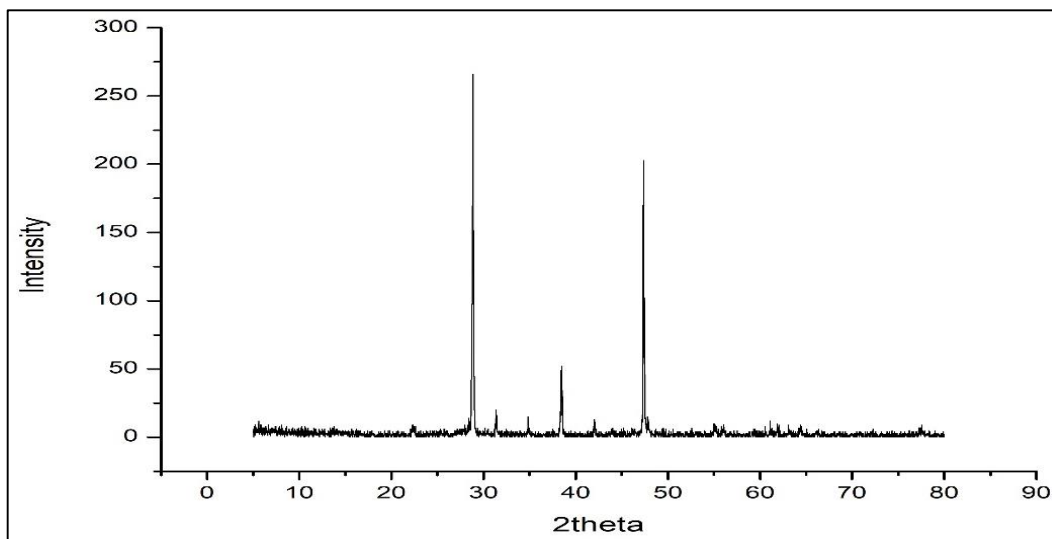


Figure 4-33: XRD Peaks of  $Ce_2S_3$  synthesized by Precipitation Method [CeU-P]

Table 4-5: XRD Peaks Matching with JCPDS Data for  $Ce_2S_3$  [CeU-P]

$Ce_2S_3$				
2 Theta (degree)	Intensity	d-spacing Calculated	d-Spacing JCPDS-43-0799	hkl
28.86	266	3.09	3.12	(100)
31.32	14	2.85	2.83	(110)
34.82	15	2.57	2.53	(141)
38.42	49	2.34	2.38	(320)
47.34	203	1.92	1.91	(122)

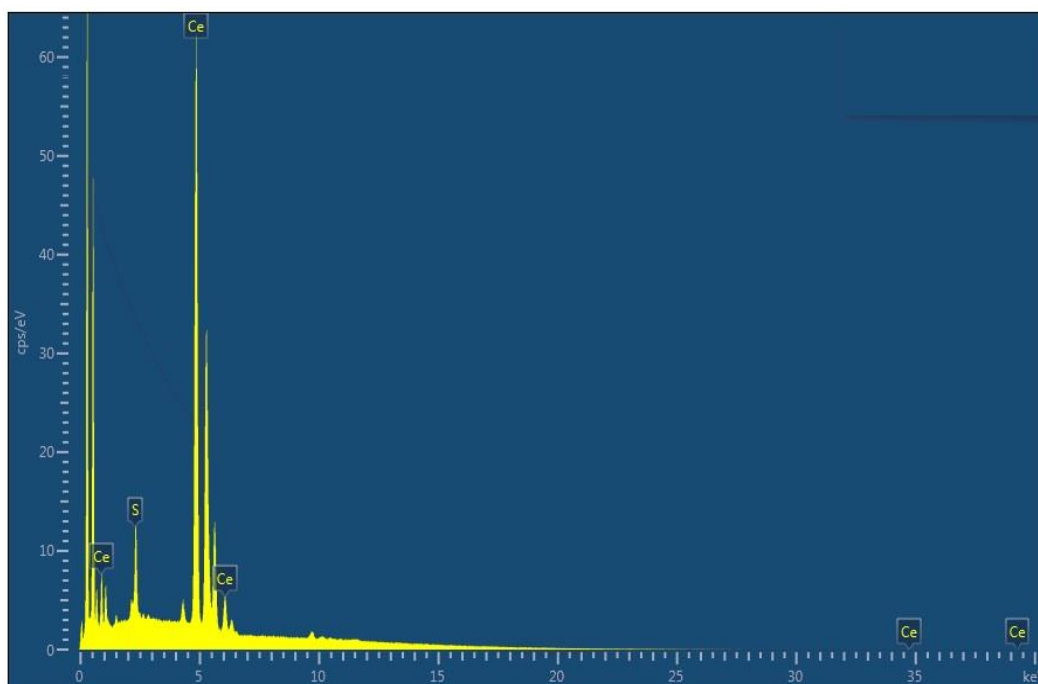


Figure 4-34: EDAX Peaks of Ce<sub>2</sub>S<sub>3</sub> [CeU-P]

Figure 4-33 shows the X-Ray diffraction pattern of Ce<sub>2</sub>S<sub>3</sub> synthesized by Precipitation method. The XRD results of the undoped and the doped samples were exactly similar. The formation of Ce<sub>2</sub>S<sub>3</sub> is confirmed from the results of the XRD patterns and peaks [1]. The sharp peak at  $2\theta = 28.86$  having the highest intensity is the characteristic peak of (111) plane. As seen from Table 4-5, the d- values of the peaks match with the standard values of JCPDS card no. 43-0799 for  $\alpha$  - Ce<sub>2</sub>S<sub>3</sub>. The pattern indicates good degree of crystallinity and signifies predominantly alpha ( $\alpha$ ) phase formation with orthorhombic nature [2-4]. The  $\alpha$  – phase is the preferred structure for lighter lanthanides and has an orthorhombic structure with space group Pnma (62) [6].

As compared to the XRD pattern of Ce<sub>2</sub>S<sub>3</sub> synthesized by solid state method, the intensity of the peaks of Ce<sub>2</sub>S<sub>3</sub> synthesized by precipitation method is quite low. Both the methods give the same  $\alpha$  – phase of Ce<sub>2</sub>S<sub>3</sub>. Two of the highest intensity peaks in both the patterns remain the same. However, there is a variation in the hkl values of peaks with lower intensities. This can be attributed to the decrease in crystallite size of the material due to different synthesis methods, as this decrease may lead to increase in lattice strain and consequently the lattice parameters. The EDAX results shown in Figure 4-34 confirm the presence of all the elements.

#### 4.2.6 X-RAY Diffraction Pattern of Gadolinium Sulphide Synthesized by Precipitation Method

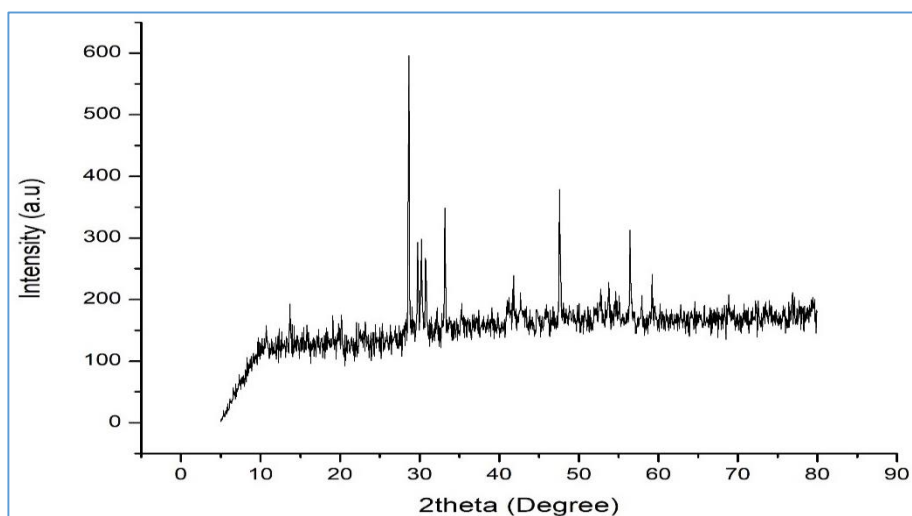


Figure 4-35: XRD Peaks of  $Gd_2S_3$  Prepared by Precipitation Method [GdU-P]

Table 4-6: XRD Peaks Matching with JCPDS Data for  $Gd_2S_3$  [GdU-P]

$Gd_2S_3$				
2 Theta (degree)	Intensity	d-spacing Calculated	d- Spacing JCPDS-76-0265	hkl
28.54	412	3.125	3.1552	(210)
29.75	293	3.000	3.0093	(112)
33.15	349	2.700	2.7075	(212)
41.60	173	2.169	2.1648	(411)
47.57	379	1.909	1.9492	(020)
56.43	313	1.62	1.6273	(322)
59.22	241	1.55	1.5549	( 612 )

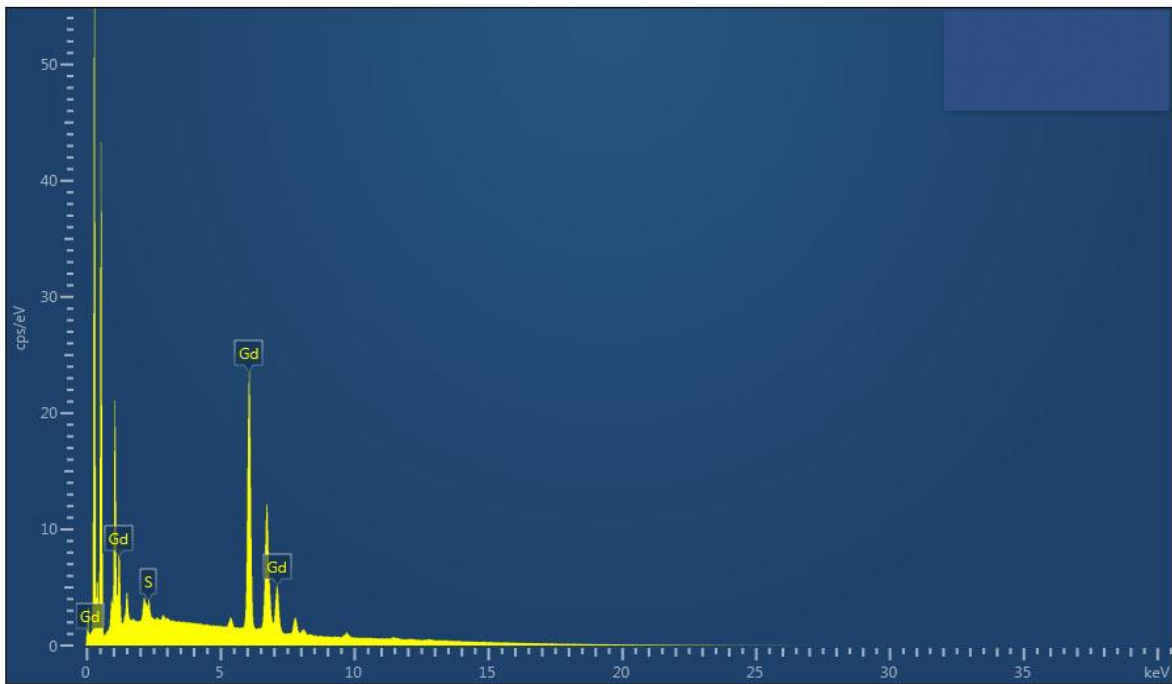


Figure 4-36: EDAX Peaks of Gd<sub>2</sub>S<sub>3</sub> [GdU-P]

The Figure 4-35 shows the X-Ray diffraction pattern of Gd<sub>2</sub>S<sub>3</sub> synthesized by Precipitation Method. The XRD results of the undoped and the doped samples in case of Solid State method were exactly similar. The formation of Gd<sub>2</sub>S<sub>3</sub> is confirmed from the results of the XRD patterns and peaks. The sharp peak at  $2\theta = 28.54$  having the highest intensity is the characteristic peak corresponding to (210) plane. As seen from Table 4-6, the d- values of the peaks match with the standard values of JCPDS card no. 76-0265 for  $\alpha$  - Gd<sub>2</sub>S<sub>3</sub>. The pattern indicates good degree of crystallinity and signifies predominantly the orthorhombic alpha ( $\alpha$ ) phase [8]. This orthorhombic system has space group Pnma (62) [6]. In this case also, in comparison to solid state method XRD pattern, the Precipitation method XRD has low intensity. However, the highest intensity and second highest intensity peaks have the same  $2\theta$  value. There is no change in the phase of Gd<sub>2</sub>S<sub>3</sub>. The intensity and hkl values are different for other peaks which can be attributed to the reasons already stated above. The EDAX result shown in Figure 4-36 confirms the presence of all the elements.

#### 4.2.7 X-RAY Diffraction Pattern of Lanthanum Sulphide Synthesized by Precipitation Method

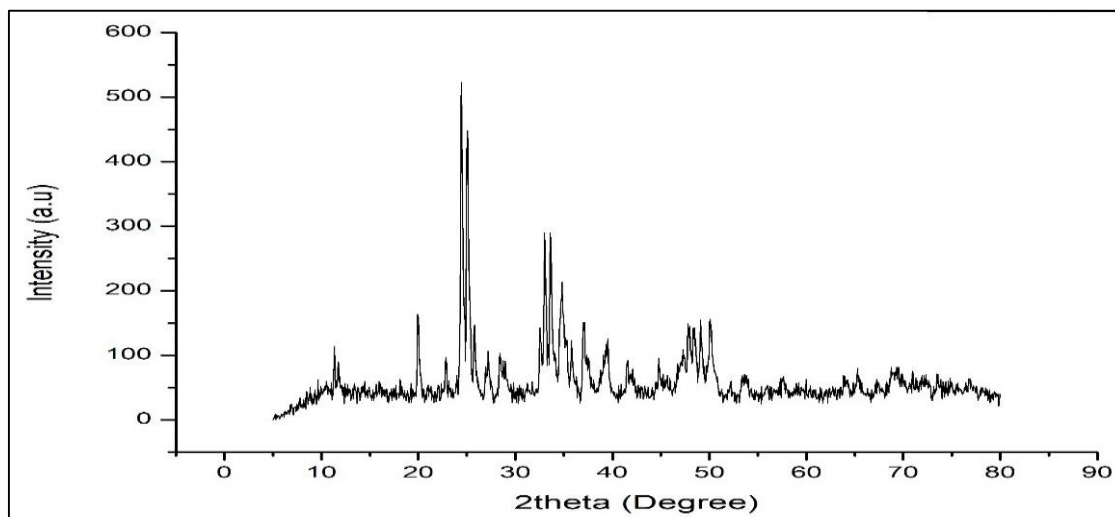


Figure 4-37: XRD Peaks of  $\text{La}_2\text{S}_3$  Prepared by Precipitation Method [LaU-P]

Table 4-7: XRD Peaks Matching with JCPDS Data for  $\text{La}_2\text{S}_3$  [LaU-P]

$\text{La}_2\text{S}_3$					
2Theta (degree)	Intensity	d-spacing Calculated	d-Standard JCPDS- $\alpha$ - 71-2349 JCPDS- $\beta$ - 43-0340	Phase	hkl
11.381	85	7.76	7.67	$\beta$	(200)
19.93	164	4.45	4.38	$\beta$	(312)
24.29	166	3.66	3.66	$\beta$	(411)
32.99	290	2.71	2.71	$\beta$	(400)
34.77	188	2.57	2.59	$\beta$	(544)
36.99	151	2.42	2.47	$\beta$	(336)
39.07	101	2.30	2.30	$\alpha$	(303)
47.93	140	1.89	1.89	$\beta$	(811)

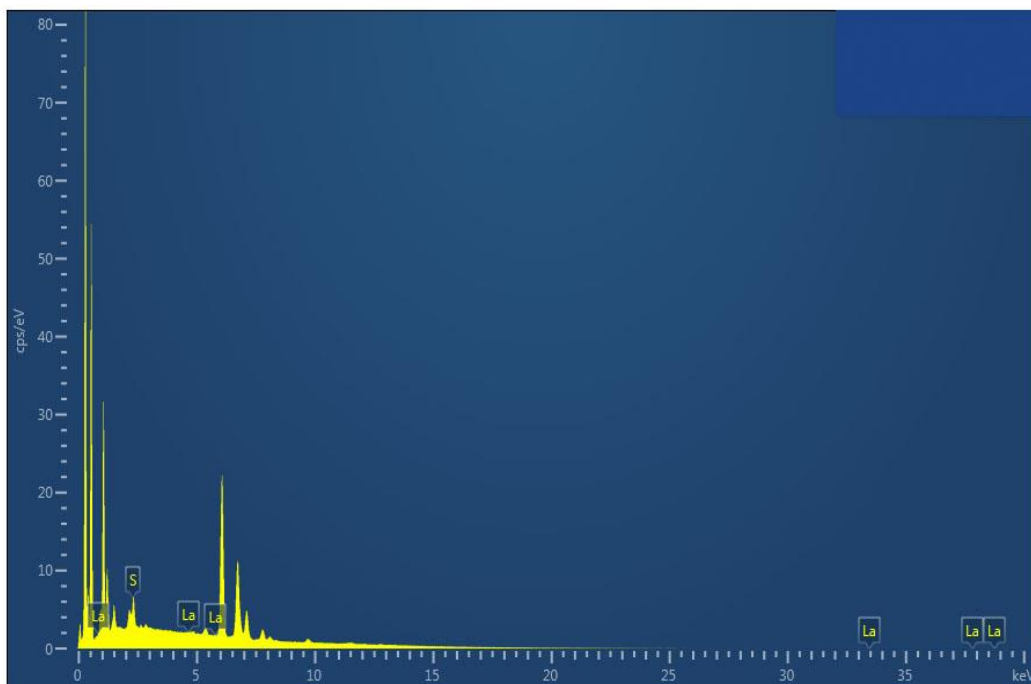


Figure 4-38: EDAX Peaks of La<sub>2</sub>S<sub>3</sub> [LaU-P]

Figure 4-37 shows the X-Ray diffraction pattern of La<sub>2</sub>S<sub>3</sub> prepared by Precipitation Method. The XRD results of the undoped and the doped samples were exactly similar. As seen from Table 4-3, the d-values of synthesized La<sub>2</sub>S<sub>3</sub> samples are predominantly found to match the pattern of JCPDS-43-0340 ( $\beta$  - phase) while one of peaks matches with the standard reference JCPDS card no. 71-2349 ( $\alpha$  - phase). The pattern indicates high degree of crystallinity and the structure is predominantly tetragonal ( $\beta$  - phase) in nature. There is a trace of orthorhombic ( $\alpha$  - phase) [10,11]. The  $\alpha$  - phase has a space group Pnma (62) while the  $\beta$  - phase has a space group 141/acd (142) [6]. The most intense peak corresponds to  $2\Theta = 32.99$  in  $\beta$  - phase. It represents the (400) plane. The second highest peak corresponding to  $2\Theta = 34.77$  also matches with  $\beta$  - phase and represents the (544) plane. It can be observed from table 4-7 that, as compared to the Solid State method, in Precipitation method, the proportion of  $\beta$  - phase is highly increased. This can be seen from the fact that the two high intensity peaks in samples prepared by Solid State method, which were in  $\alpha$  - phase have not been found in the samples prepared by Precipitation method giving  $\beta$  - phase. The EDAX result shown in Figure 4-38 confirms the presence of all the elements.

#### 4.2.8 X-RAY Diffraction Pattern of Yttrium Sulphide Synthesized by Precipitation Method

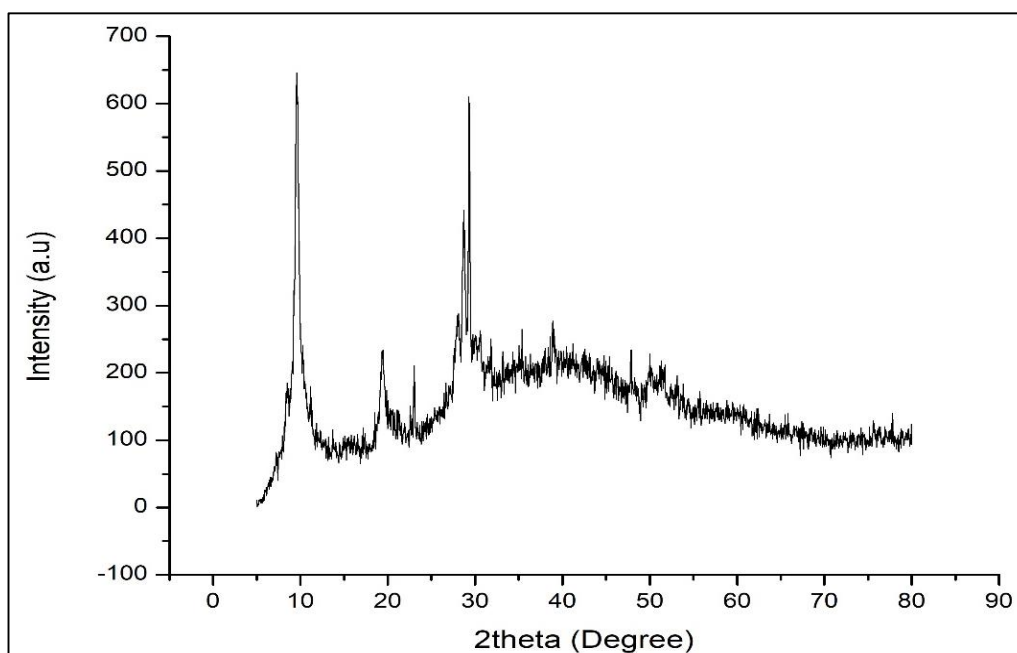


Figure 4-39: XRD Peaks of  $Y_2S_3$  Prepared by Precipitation Method [YU-P]

Table 4-8: XRD Peaks Matching with JCPDS Data for  $Y_2S_3$  [YU-P]

$Y_2S_3$				
2 Theta (degree)	Intensity	d-spacing Calculated	d-Standard JCPDS-79-2250	hkl
9.46	506	9.35	9.33	(-101)
19.23	202	4.61	4.65	(-202)
23.03	211	3.86	3.78	(401)
29.30	610	3.05	3.04	(-212)
35.02	241	2.56	2.54	(-104)
38.57	254	2.33	2.33	(-404)
47.83	234	1.90	1.91	(504)

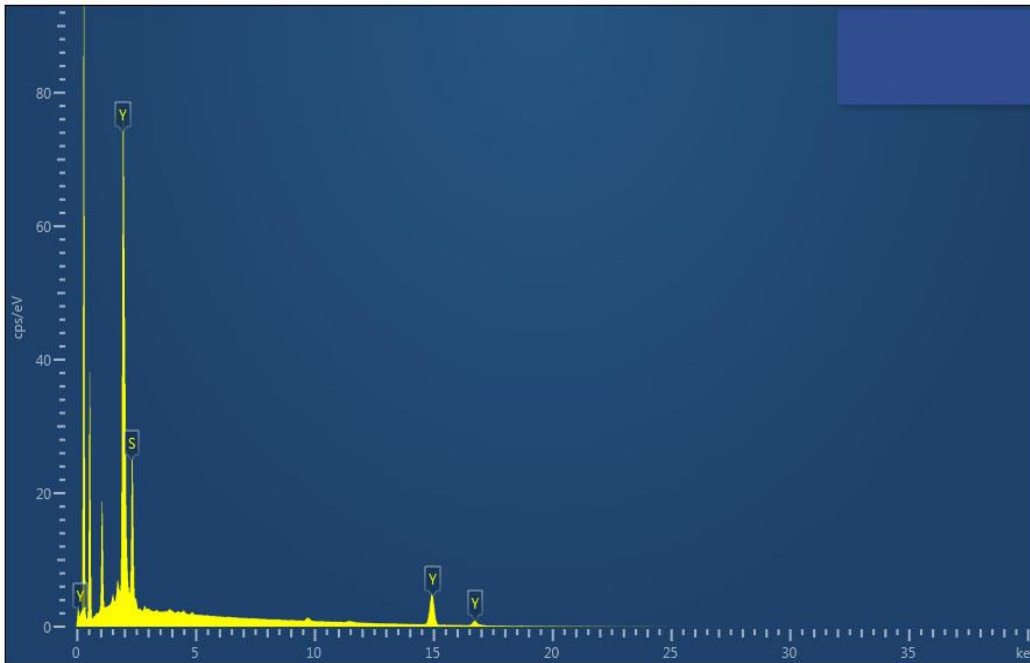


Figure 4-40: EDAX Peaks of Y<sub>2</sub>S<sub>3</sub> [YU-P]

The X-Ray diffraction patterns of Y<sub>2</sub>S<sub>3</sub> is shown in Figure 4-39. The formation of Y<sub>2</sub>S<sub>3</sub> is confirmed from table 4-8 which shows the matching of d-values of synthesized sample and the d-values of the standard JCPDS card no. 79-2250 [12]. The highest intensity peak was obtained at  $2\theta = 29.30$  which corresponds to (-212) plane. The pattern indicates crystallinity and signifies predominantly the monoclinic delta ( $\delta$ ) phase formation. The  $\delta$  – phase is a very low symmetry monoclinic system with space group P21/m (11) [6]. Yttrium Sulphide is found in the  $\delta$  – phase only. This justifies the result that we have obtained in this study. When compared to the XRD plot of Solid State method, the XRD of Precipitation method has a very low intensity. The EDAX results shown in Figure 4-40 confirms the presence of all the elements.

### 4.3 Crystallite Size of Synthesized samples

The average crystallite size was calculated by using the Debye – Scherrer formula. The values are given in Table 4-9, 4-10 and 4-11.

**Table 4-9: Crystallite Size for undoped samples synthesized by Solid State Method**

Sample Name	Crystallite Size (nm)
Ce <sub>2</sub> S <sub>3</sub> [CeU-SS]	96.68
Gd <sub>2</sub> S <sub>3</sub> [GdU-SS]	106.32
La <sub>2</sub> S <sub>3</sub> [LaU-SS]	23.12
Y <sub>2</sub> S <sub>3</sub> [YU-SS]	103.07

**Table 4-10: Crystallite Size for undoped samples synthesized by Precipitation Method**

Sample Name	Crystallite Size (nm)
Ce <sub>2</sub> S <sub>3</sub> [CeU-P]	52.92
Gd <sub>2</sub> S <sub>3</sub> [GdU-P]	70.97
La <sub>2</sub> S <sub>3</sub> [LaU-P]	12.79
Y <sub>2</sub> S <sub>3</sub> [YU-P]	17.82

**Table 4-11: Crystallite Size for Solid State samples doped with Mn/Eu/Tb**

Sample Name	Crystallite Size (nm)		
	(1%) Doping	(2%) Doping	(3%) Doping
Ce <sub>2</sub> S <sub>3</sub> :Mn [CeM-SS] 5% [CU-SS]	107.91	95.98	96.54
Ce <sub>2</sub> S <sub>3</sub> :Eu [CeE-SS]	97.93	98.79	99.30
Ce <sub>2</sub> S <sub>3</sub> :Tb [CeT-SS]	102.22	99.10	97.99
Gd <sub>2</sub> S <sub>3</sub> :Mn [GdM-SS]	102.38	99.48	96.25

Sample Name	Crystallite Size (nm)		
	(1%) Doping	(2%) Doping	(3%) Doping
Gd <sub>2</sub> S <sub>3</sub> :Eu [GdE-SS]	102.88	102.02	100.93
Gd <sub>2</sub> S <sub>3</sub> :Tb [GdT-SS]	104.77	103.09	100.48
La <sub>2</sub> S <sub>3</sub> :Mn [LaM-SS]	25.82	25.23	24.60
La <sub>2</sub> S <sub>3</sub> :Eu [LaE-SS]	24.66	24.46	22.67
La <sub>2</sub> S <sub>3</sub> :Tb [LaT-SS]	24.45	21.88	20.73
Y <sub>2</sub> S <sub>3</sub> :Mn [YM-SS]	93.71	90.26	91.70
Y <sub>2</sub> S <sub>3</sub> :Eu [YE-SS] Y <sub>2</sub> S <sub>3</sub> :Mn [YM-SS]	94.18	95.69	63.37
Y <sub>2</sub> S <sub>3</sub> :Tb [YT-SS]	94.06	93.65	93.95

The crystallite size of the samples synthesized by the Solid State method show that the samples are in bulk form. The crystallite size of the samples synthesized by Precipitation method are much smaller as compared to the Solid State samples clearly indicating movement towards nanoscale. The crystallite size obtained from doped Solid State samples does not follow a fixed rule but varies. In some cases, the Vegard's law is obeyed while in other cases, it is violated. For most cases, the crystallite size decreases with increase in doping percentage.

#### 4.4 Morphological Analysis

Samples synthesized and prepared by Solid State and Precipitation methods were analyzed by Field Emission Scanning Electron Microscope (FE-SEM) technique for the morphological analysis. Following are the results obtained for samples prepared by these two methods:

#### 4.4.1 Cerium Sulphide ( $\text{Ce}_2\text{S}_3$ ) by Solid State Method

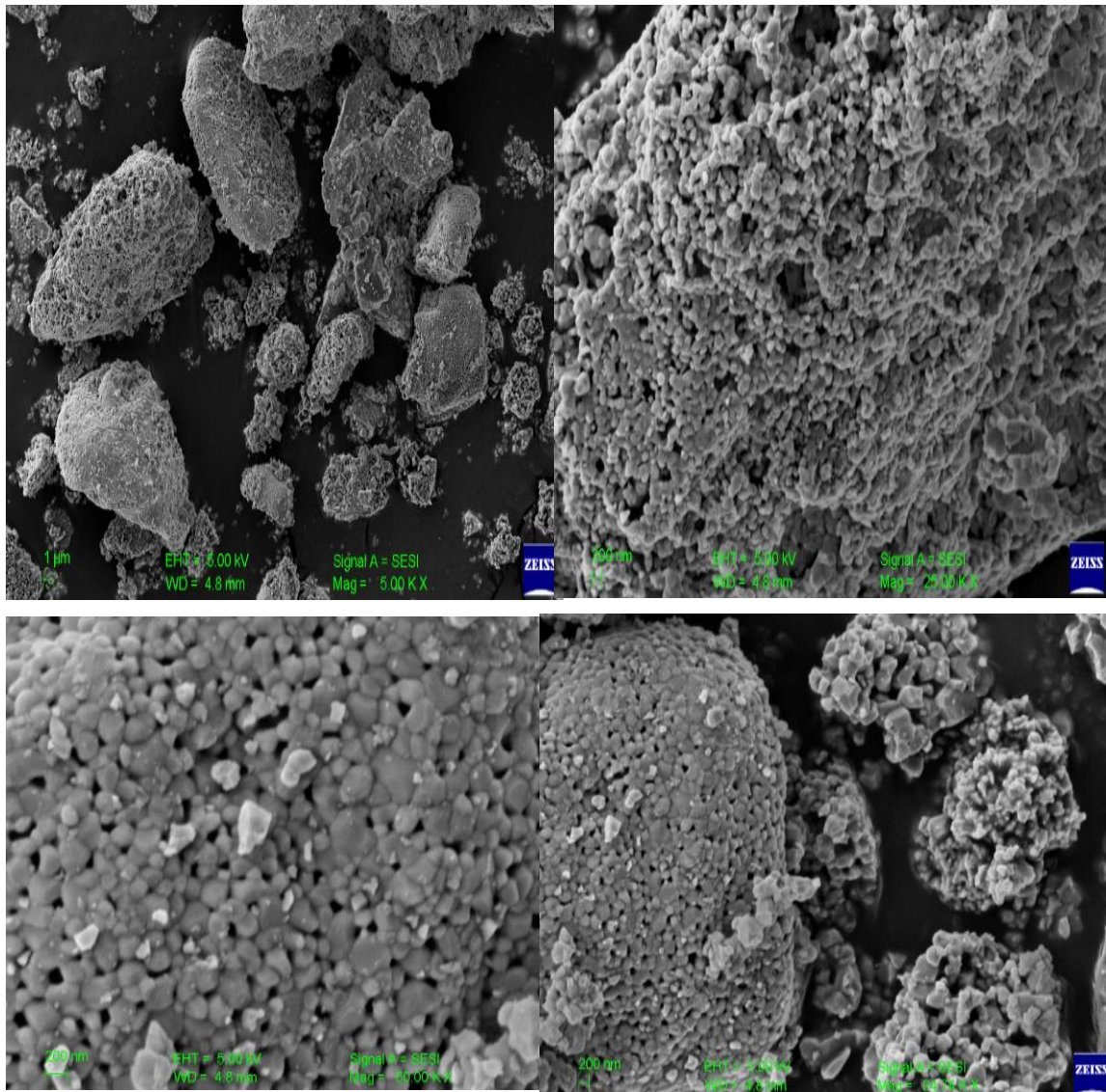


Figure 4-41: FESEM of Cerium Sulphide ( $\text{Ce}_2\text{S}_3$ ) [CeU-SS]

The Fig. 4-41 shows the Field Emission Scanning Electron Microscope (FESEM) of the Cerium Sulphide ( $\text{Ce}_2\text{S}_3$ ) prepared by Solid State Method. The morphology of material as seen from the image was like chunks of particles with porosity bonded together to form different shapes and sizes. All the particles are arranged in scattered regions.

#### 4.4.2 Gadolinium Sulphide ( $Gd_2S_3$ ) by Solid State Method

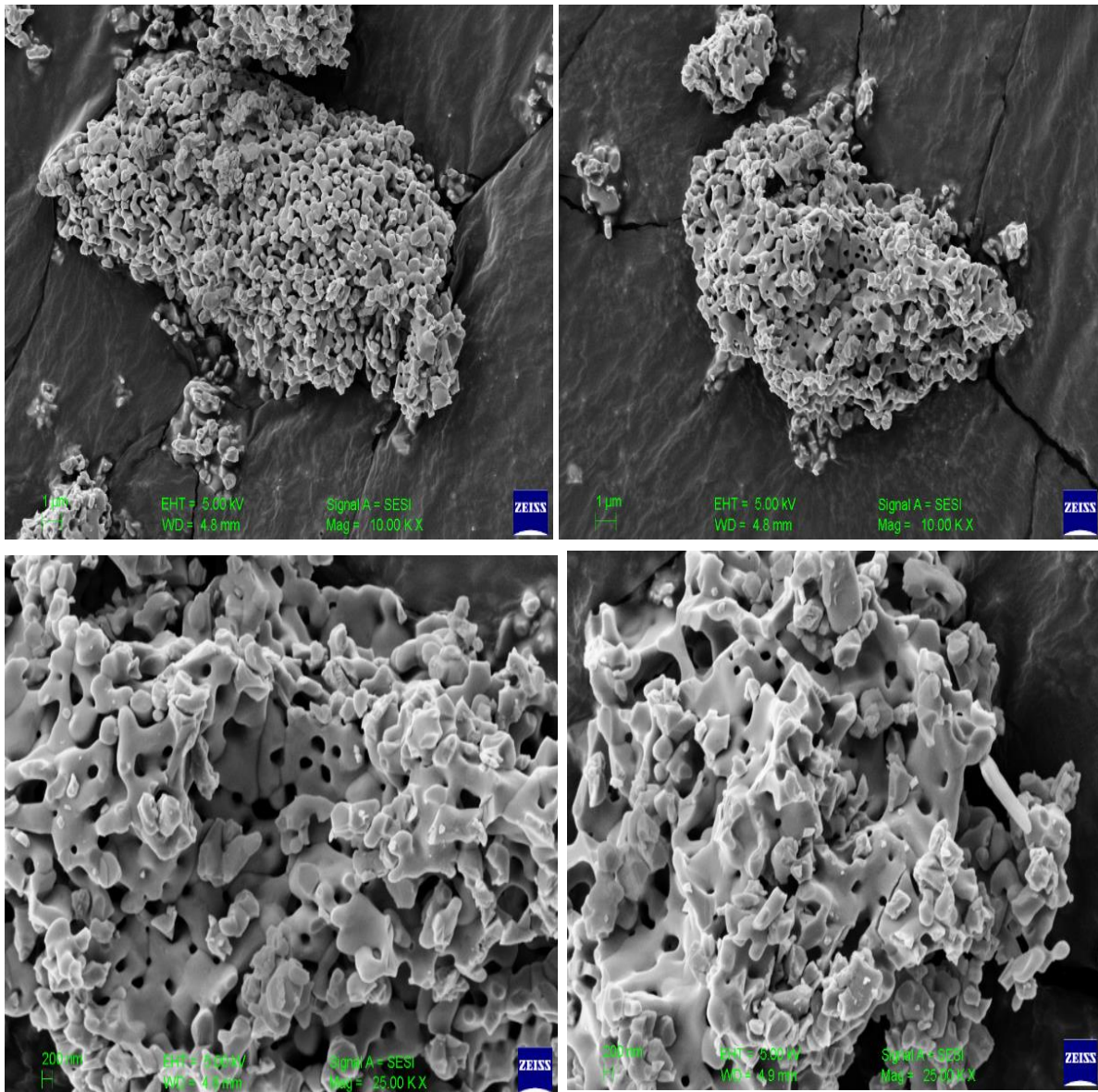


Figure 4-42: FESEM of Gadolinium Sulphide ( $Gd_2S_3$ ) [GdU-SS]

As shown in the Fig. 4-42, consider the Field Emission Scanning Electron Microscope (FESEM) of Gadolinium Sulphide ( $Gd_2S_3$ ) synthesized by Solid-State Method. The image shows that the formation of material was in the cluster form. The particles are like blooming and rolling over each other and have an elongated rounded edge structure. The material has numerous pores on its surface.

#### 4.4.3 Lanthanum Sulphide ( $\text{La}_2\text{S}_3$ ) by Solid State Method

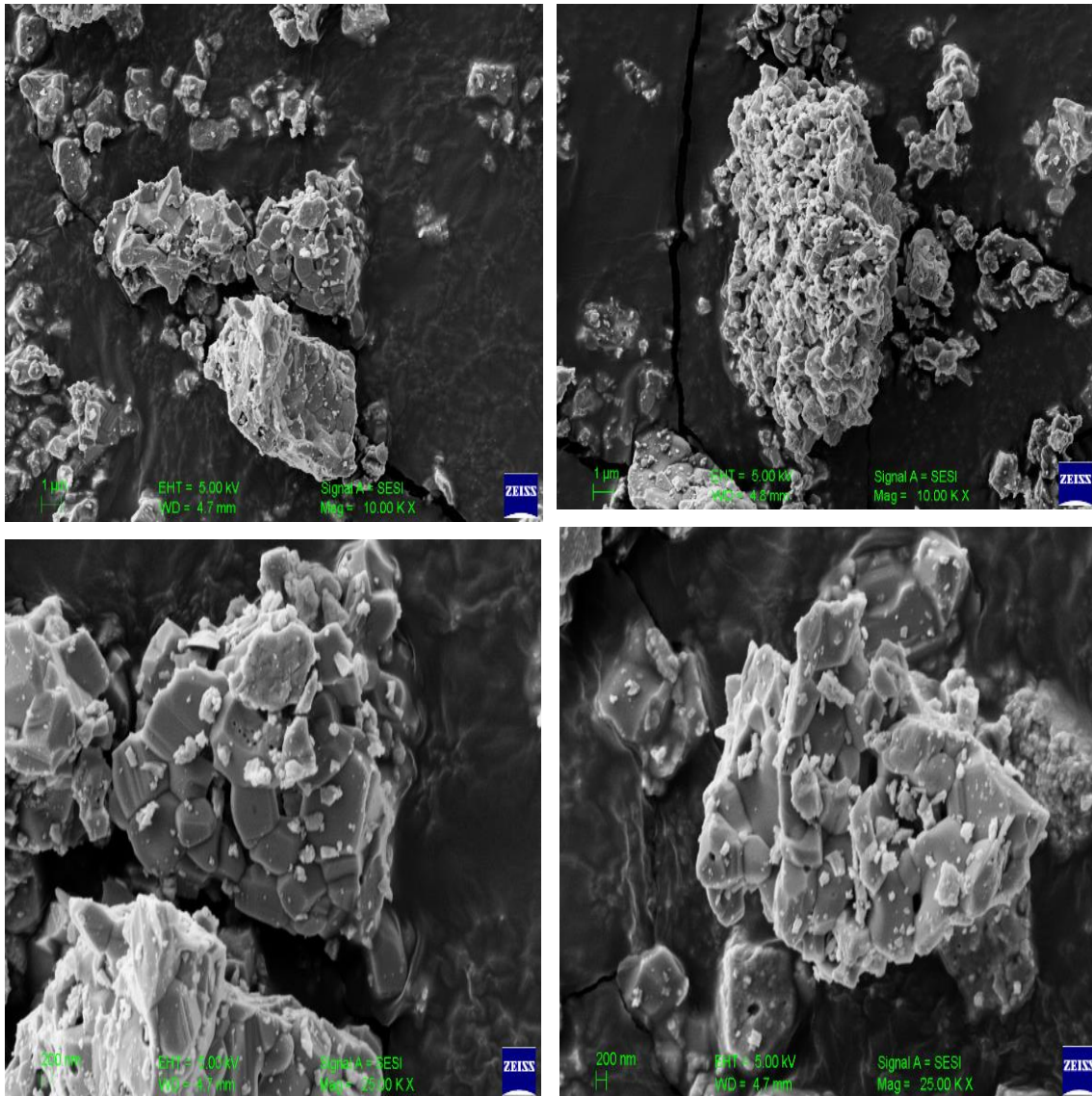


Figure 4-43: FESEM of Lanthanum Sulphide ( $\text{La}_2\text{S}_3$ ) [LaU-SS]

Figure 4-43 shows the Field Emission Scanning Electron Microscope (FESEM) for the Lanthanum Sulphide ( $\text{La}_2\text{S}_3$ ) samples prepared by the Solid-State Method. The different visual chunks of particles are seen in the images: one is scattered or dispersive and on other side, it is bonded with each other. The particles are arranged like a rock formation and seem to have cuboidal structures bonded with each other.

#### 4.4.4 Yttrium Sulphide ( $Y_2S_3$ ) by Solid State Method

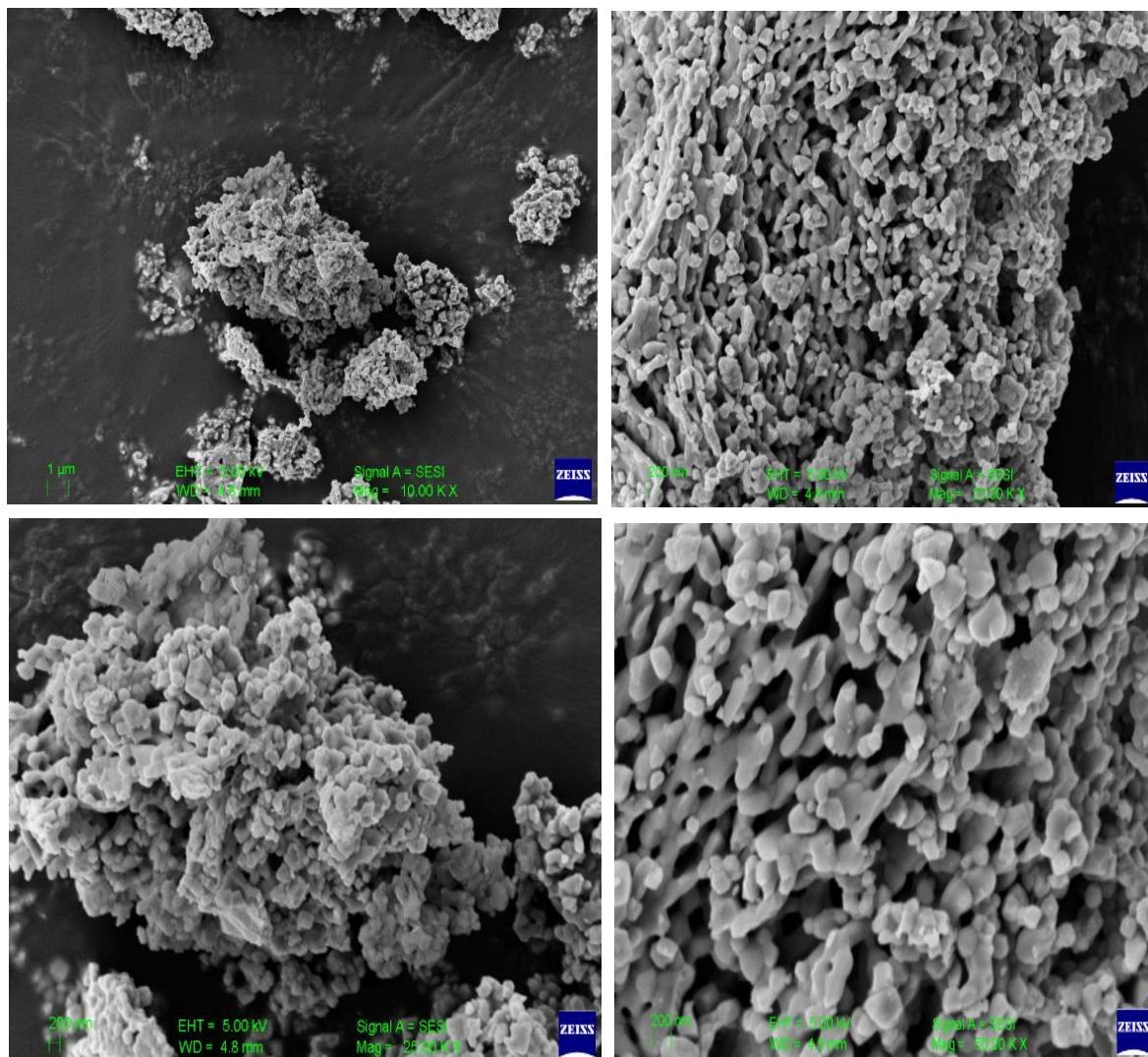


Figure 4-44: FESEM of Yttrium Sulphide ( $Y_2S_3$ ) [YU-SS]

The Fig.4-44 shows the Field Emission Scanning Electron Microscope (FESEM) for the Yttrium Sulphide ( $Y_2S_3$ ) samples prepared by the Solid-State Method. The image shows formation similar to lumps of the particles that are closely spaced to each other. The particles are arranged in different manner in the form of elongated rounded structures.

#### 4.4.5 Cerium Sulphide ( $Ce_2S_3$ ) by Precipitation Method

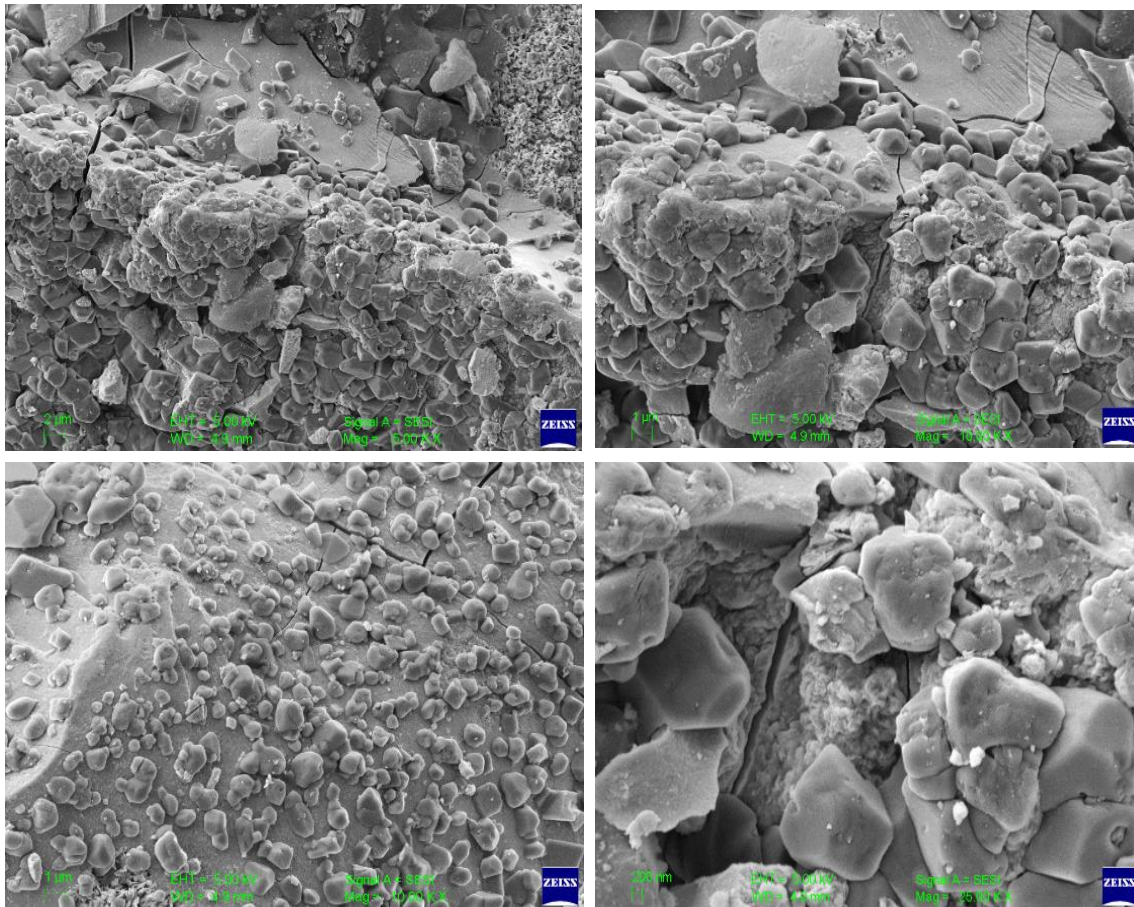


Figure 4-45: FESEM of Cerium Sulphide ( $Ce_2S_3$ ) [CeU-P]

The fig.4-45 shows the Field Emission Scanning Electron Microscope (FESEM) for the Cerium Sulphide ( $Ce_2S_3$ ) samples prepared by the Precipitation method. The formation can be seen in the form of kinks of the particles which are closely spaced to each other. The particles are smooth and have vivid shapes but are mostly cuboidal. As compared to the SEM images of samples synthesized by Solid State Method, these images are more smooth and distinct.

#### 4.4.6 Gadolinium Sulphide ( $Gd_2S_3$ ) by Precipitation Method

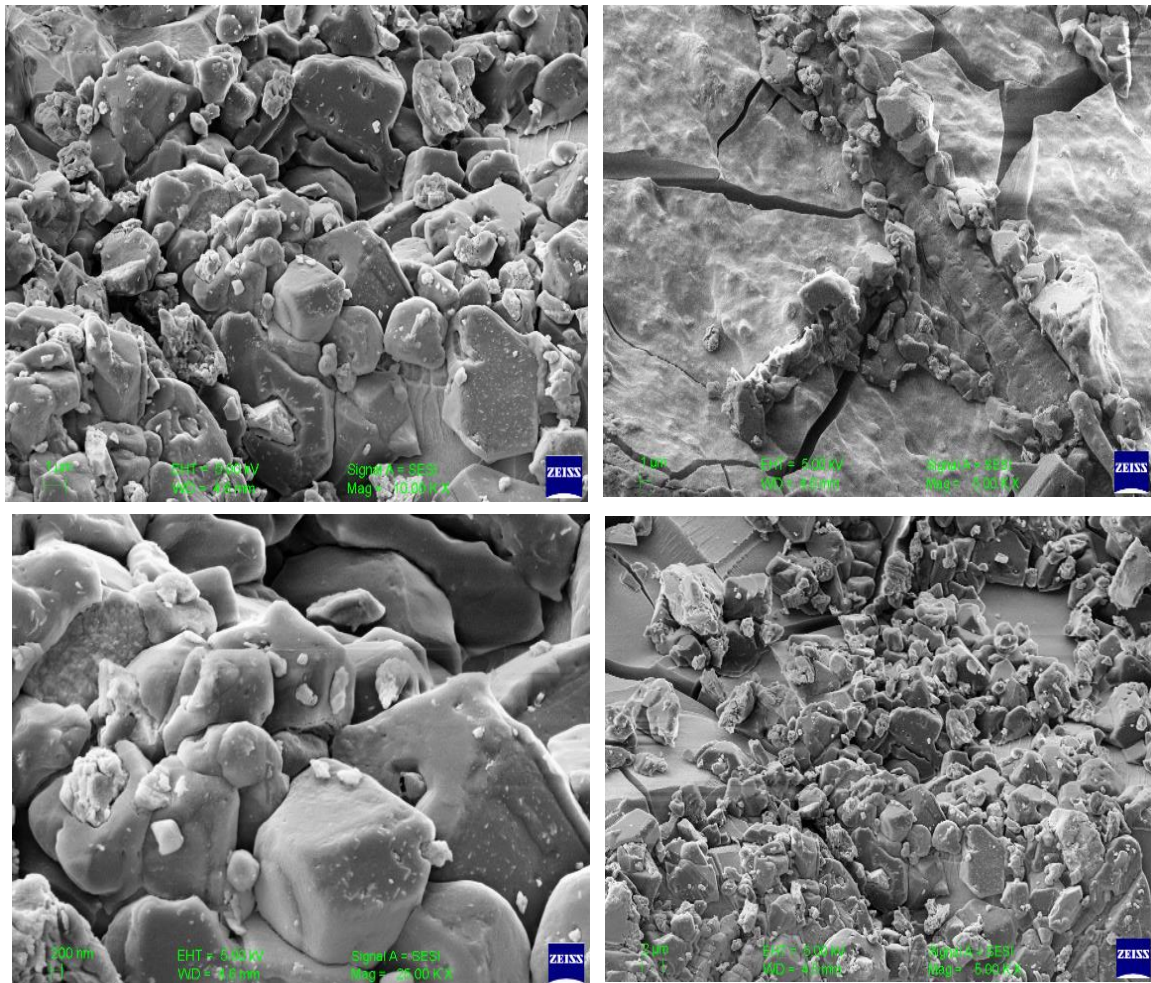


Figure 4-46: FESEM of Gadolinium Sulphide ( $Gd_2S_3$ ) [GdU-P]

Fig.4-46 shows the Field Emission Scanning Electron Microscope (FESEM) images of Gadolinium Sulphide ( $Gd_2S_3$ ) synthesized by Precipitation method. The image shows that the formation of material was in the cuboidal bunch form. The particles are smooth and are very close to each other. As compared to the SEM images of Solid State Method, these images are more distinct, more rounded and show almost no pores on the surface.

#### 4.4.7 Lanthanum Sulphide ( $\text{La}_2\text{S}_3$ ) by Precipitation Method

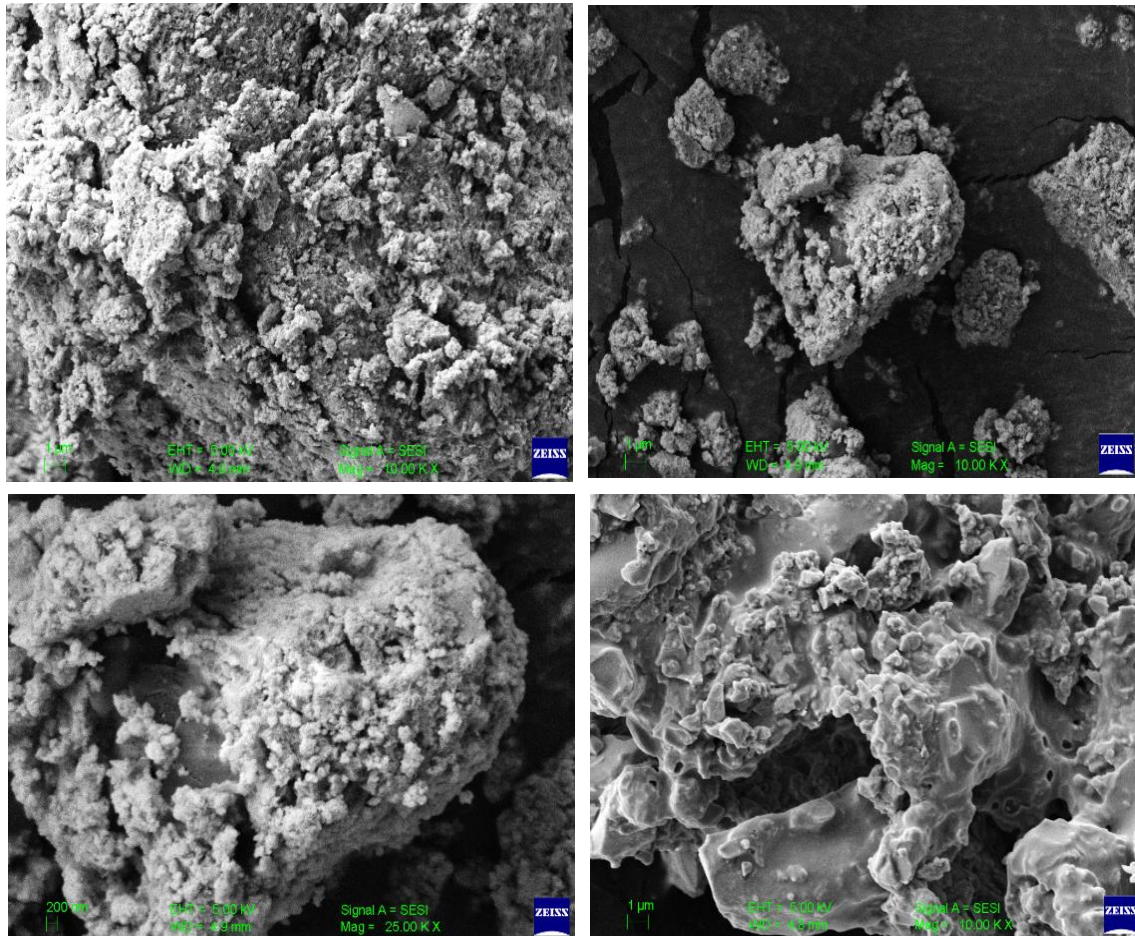


Figure 4-47: FESEM of Lanthanum Sulphide ( $\text{La}_2\text{S}_3$ ) [LaU-P]

The Fig.4-47 elaborates the Field Emission Scanning Electron Microscope (FESEM) of the Lanthanum Sulphide ( $\text{La}_2\text{S}_3$ ) prepared by Precipitation method. The morphology of material as seen from the image was like a conglomeration of particles bonded together to form different shapes and sizes. All the particles are arranged in scattered regions showing rock formation and this scattering is much more as compared with their Solid State counterpart.

#### 4.4.8 Yttrium Sulphide ( $Y_2S_3$ ) by Precipitation Method

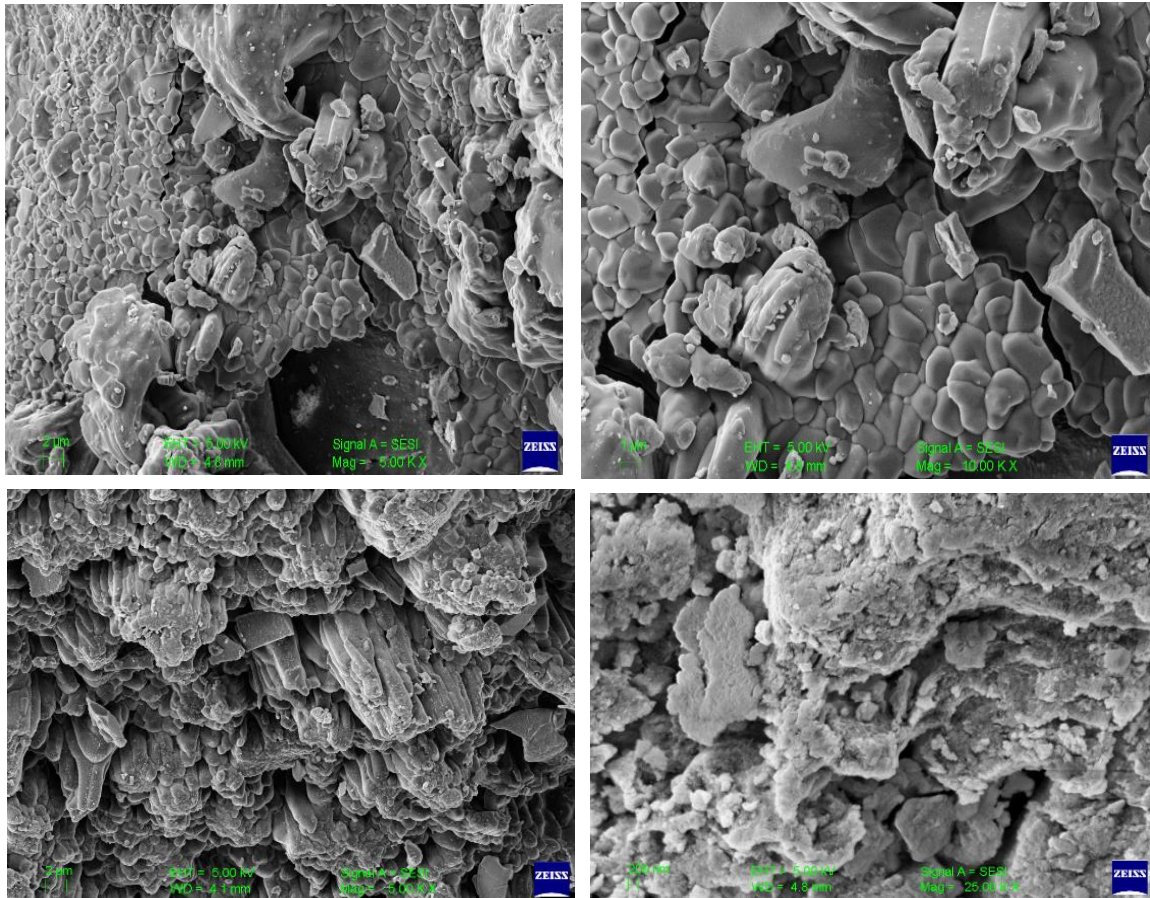


Figure 4-48: FESEM of Yttrium Sulphide ( $Y_2S_3$ ) [YU-P]

The Fig.4-48 shows the Field Emission Scanning Electron Microscope (FESEM) for the Yttrium Sulphide ( $Y_2S_3$ ) samples prepared by the Precipitation method. The formation of particles is compact with respect to each other. The particles are arranged in different manner, somewhere they are in the form of rounded agglomerates while somewhere they are in the form of elongated structures. As compared to its Solid State material, the precipitation sample is more distinctly separated and shows some order.

## 4.5 Photoluminescence Analysis (PL)

The excitation and emission spectra of the set of samples synthesized by Solid State method and Precipitation method are presented here.

The Manganese doped samples of rare earth sulphides of Cerium, Gadolinium, Lanthanum and Yttrium were very dark in colour. Some samples of Eu and Tb doped Cerium sulphide also had very dark red- maroonish colour. They did not give emission. Some of the samples synthesized by precipitation method did not give satisfactory results.

Only those samples which gave good PL results have been mentioned here.

The Europium (Eu) doped  $\text{Ce}_2\text{S}_3$  samples being dark in colour did not give luminescence and hence their excitation and emission spectra could not be obtained.

## Samples synthesized by Solid State Method

### 4.5.1 PL of Terbium (Tb) doped Cerium Sulphide ( $\text{Ce}_2\text{S}_3$ ) synthesized by Solid State Method

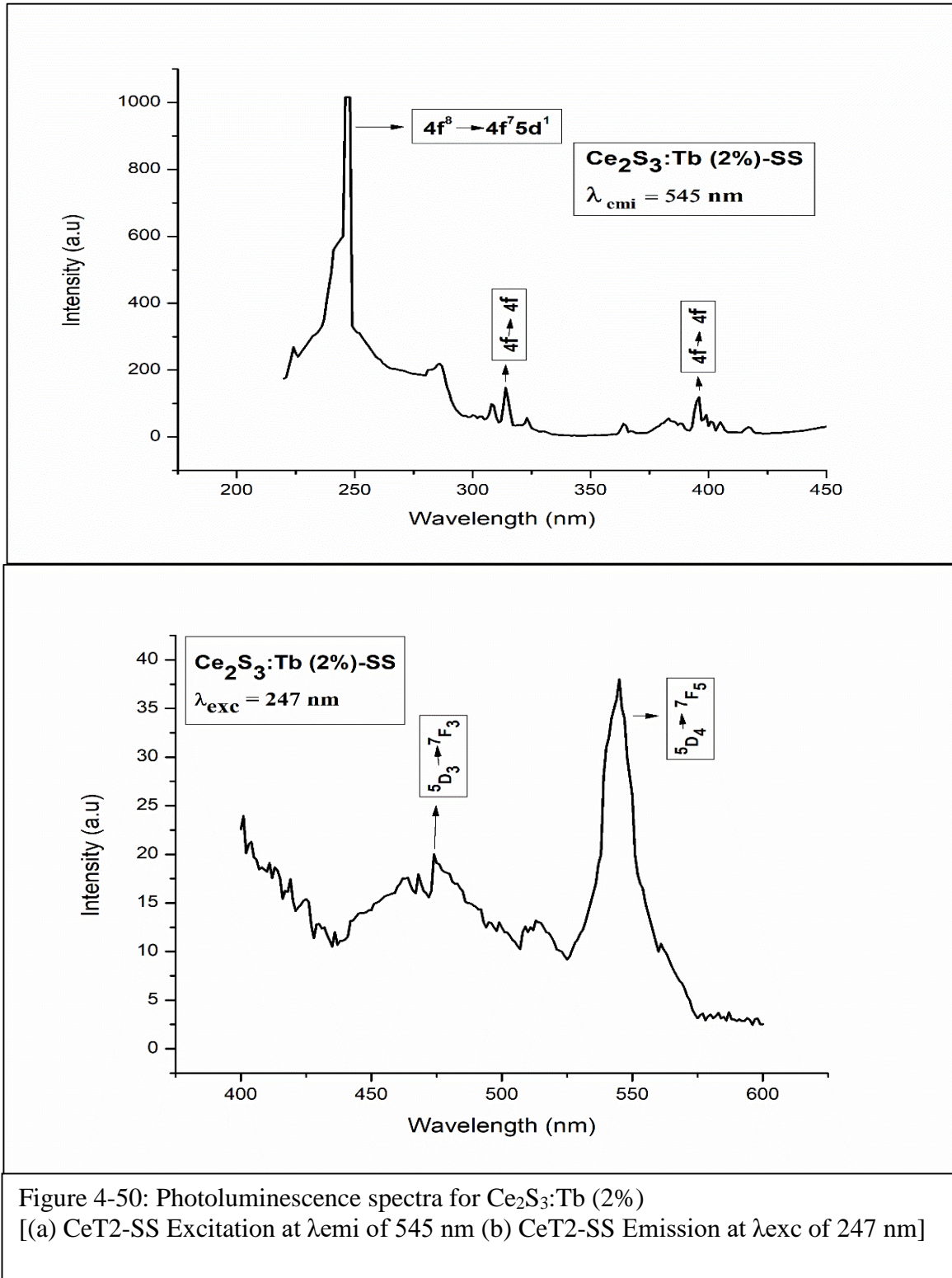


Figure 4-50: Photoluminescence spectra for  $\text{Ce}_2\text{S}_3:\text{Tb}$  (2%)  
[(a)  $\text{CeT}_2\text{-SS}$  Excitation at  $\lambda_{\text{emi}}$  of 545 nm (b)  $\text{CeT}_2\text{-SS}$  Emission at  $\lambda_{\text{exc}}$  of 247 nm]

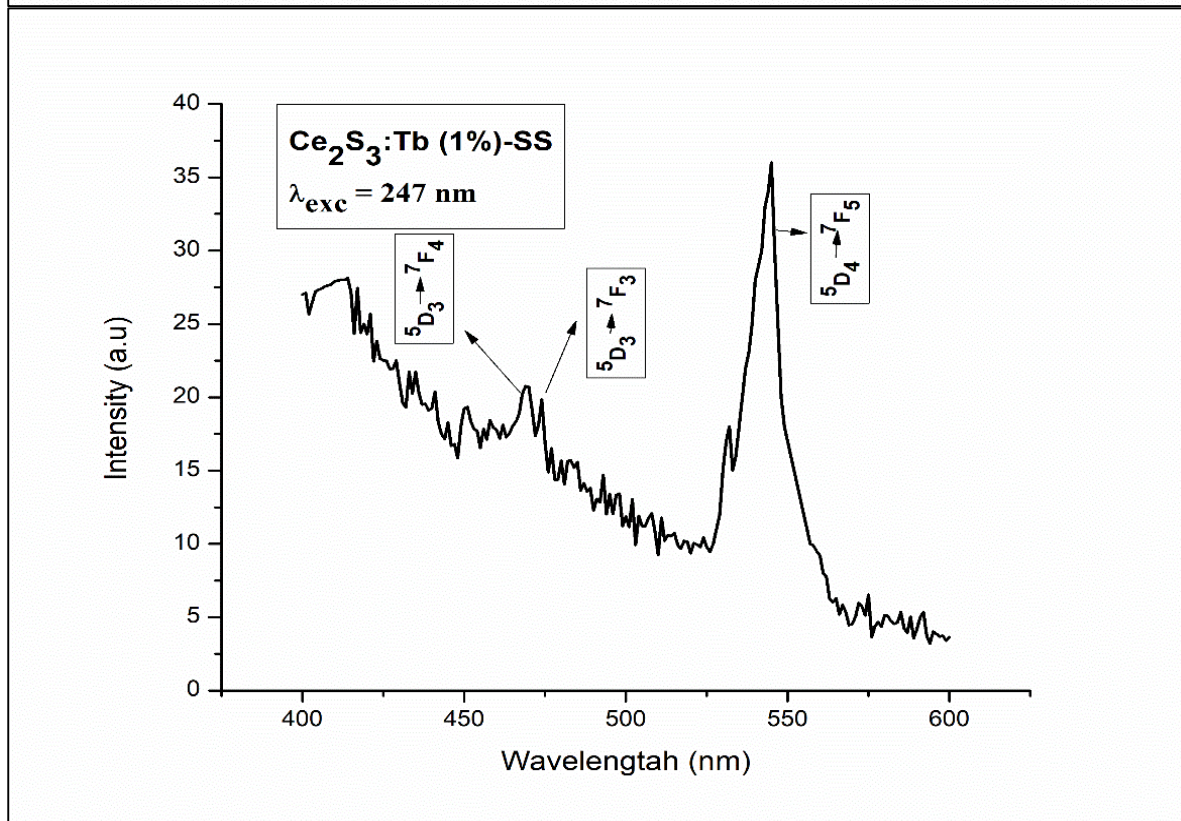
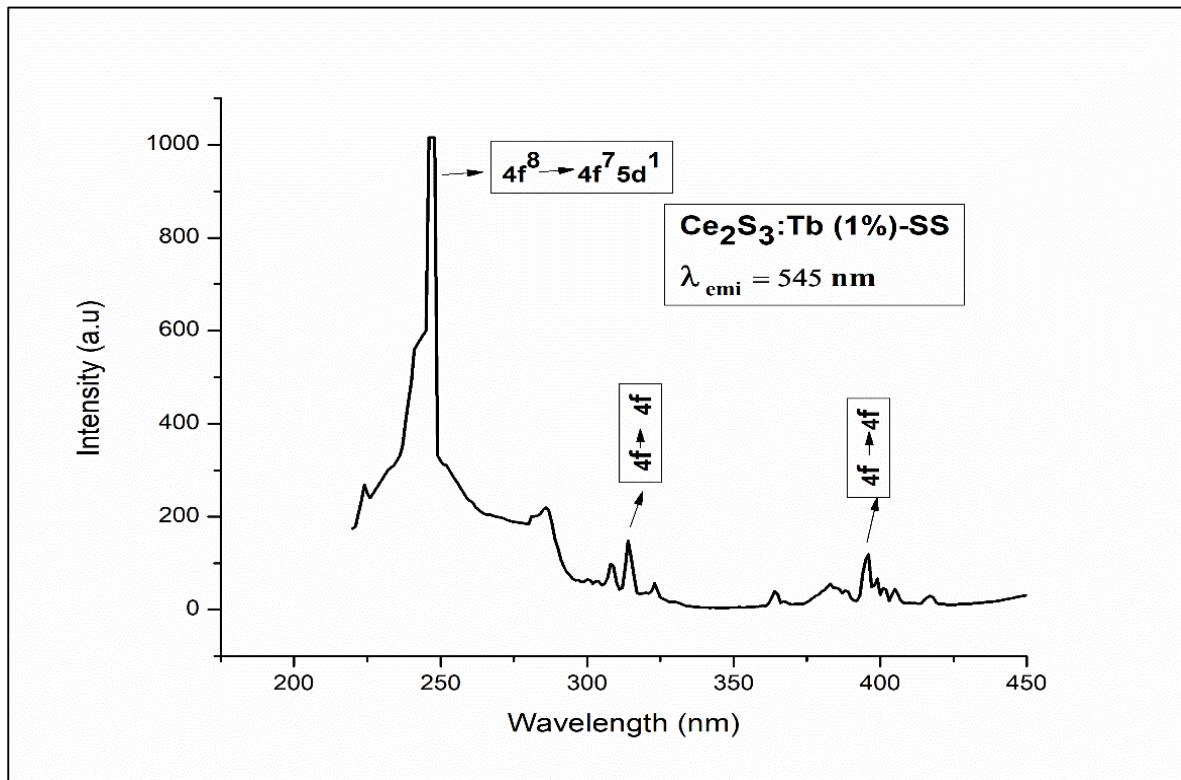


Figure 4-49: Photoluminescence spectra for Ce<sub>2</sub>S<sub>3</sub>:Tb (1%)  
 [(a) CeT1-SS Excitation at  $\lambda_{\text{emi}}$  545 nm (b) CeT1-SS Emission at  $\lambda_{\text{exc}}$  of 247 nm]

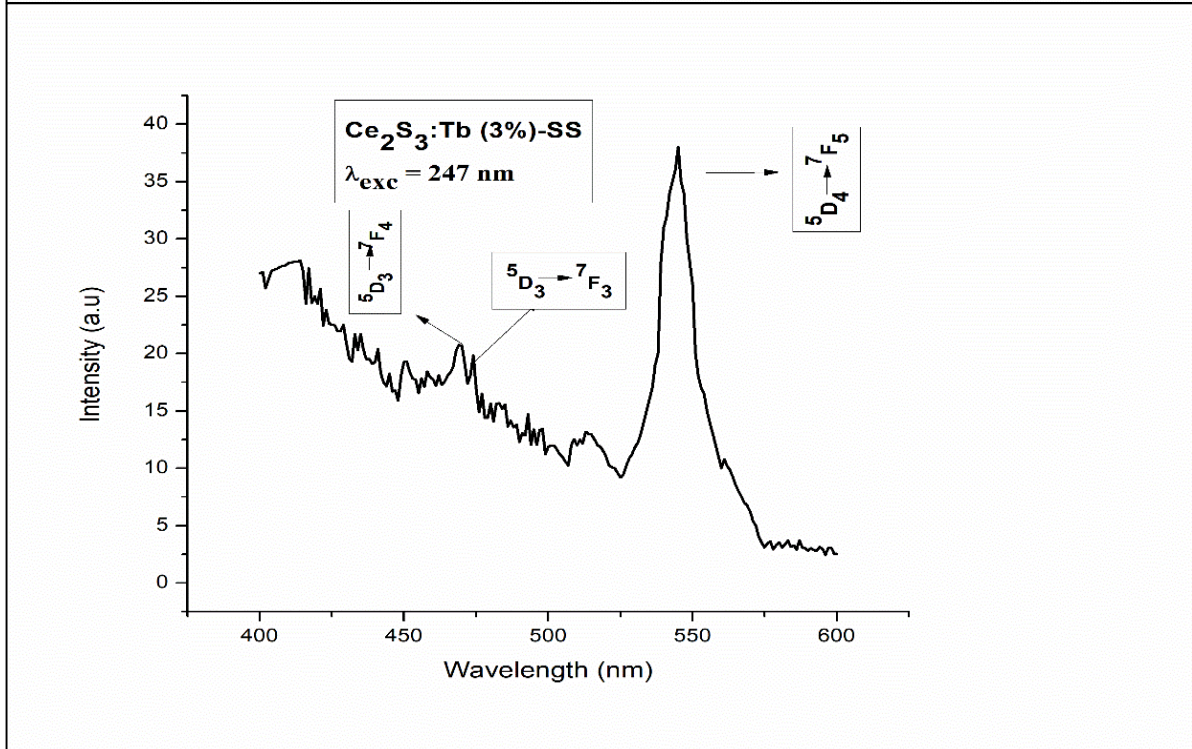
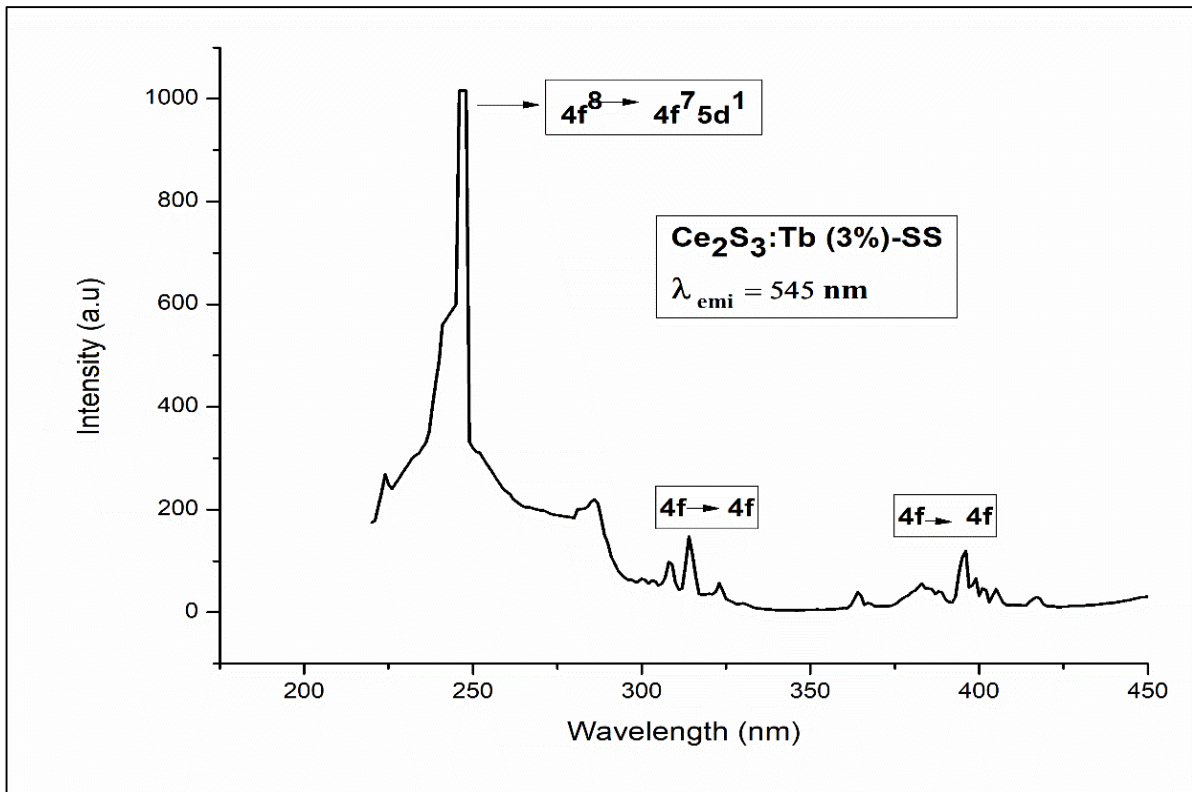


Figure 4-51: Photoluminescence spectra for Ce<sub>2</sub>S<sub>3</sub>:Tb (3%)  
 [(a) CeT3-SS Excitation at  $\lambda_{\text{emi}}$  of 545 nm (b) CeT3-SS Emission at  $\lambda_{\text{exc}}$  of 247 nm]

The Photoluminescence characteristics of Cerium Sulphide were evaluated on the basis of emission and excitation results at room temperature. The graphs in Fig. 4-49, 4-50 and 4-51 show excitation and emission spectra of  $\text{Ce}_2\text{S}_3$  for 1%, 2% and 3% of Tb doping. The excitation spectrum shows an intense peak at 247 nm which is due to the  $4f^8 \rightarrow 4f^7 5d^1$  transition of  $\text{Tb}^{3+}$  ion, while the series of absorption lines from 300 to 400 nm are attributed to the 4f–4f transitions of  $\text{Tb}^{3+}$  ions.

The emission spectrum consists of two sets of lines, the blue emission lines and strong green emission lines. The ground and the first excited levels of  $\text{Tb}^{3+}$  are split by spin–orbit coupling and the transitions from the  $^5\text{D}_4$  and  $^5\text{D}_3$  multiplets to the different  $^7\text{F}_j$  multiplets result in the generation of green and blue emissions [13]. The emission peaks at 468 nm and 474 nm give blue emissions corresponding to the  $^5\text{D}_3 \rightarrow ^7\text{F}_4$  and  $^5\text{D}_3 \rightarrow ^7\text{F}_3$  transitions while the sharp and intense peak at 545 nm gives green emission associated with the  $^5\text{D}_4 \rightarrow ^7\text{F}_5$  transition of  $\text{Tb}^{3+}$  ions. From the graphs, it can be seen that the blue emission peaks are more intense in 2% Tb doping while it decreases considerably in 3% Tb doping.

#### 4.5.2 PL of Europium (Eu) Doped Gadolinium Sulphide ( $Gd_2S_3$ ) synthesized by Solid State Method

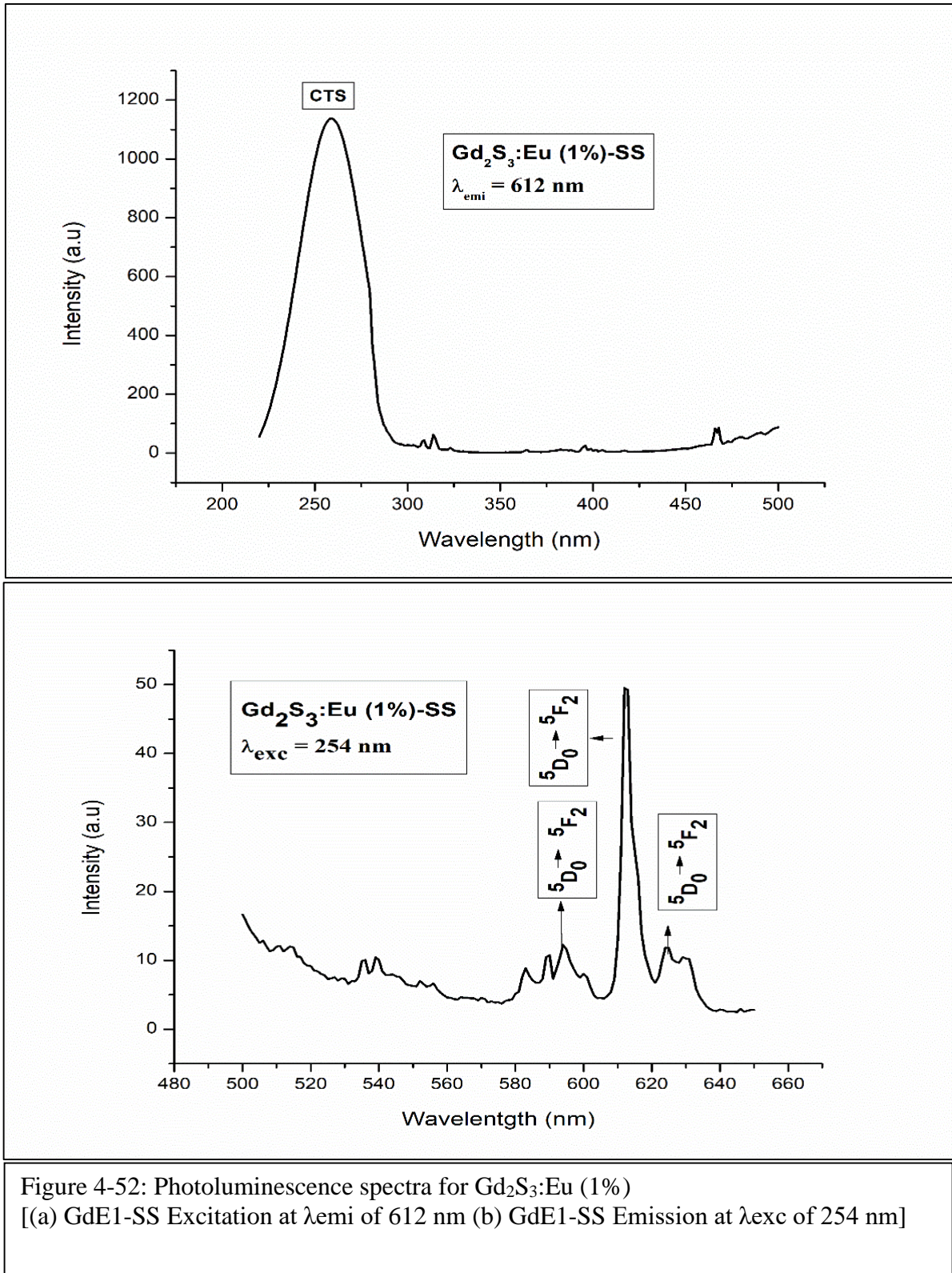
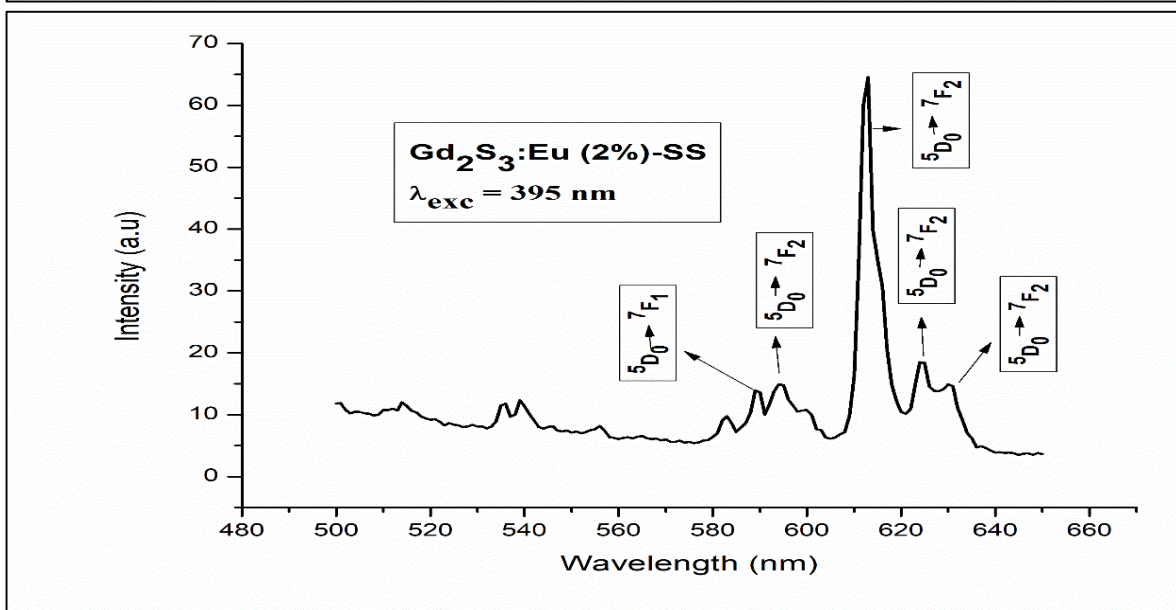
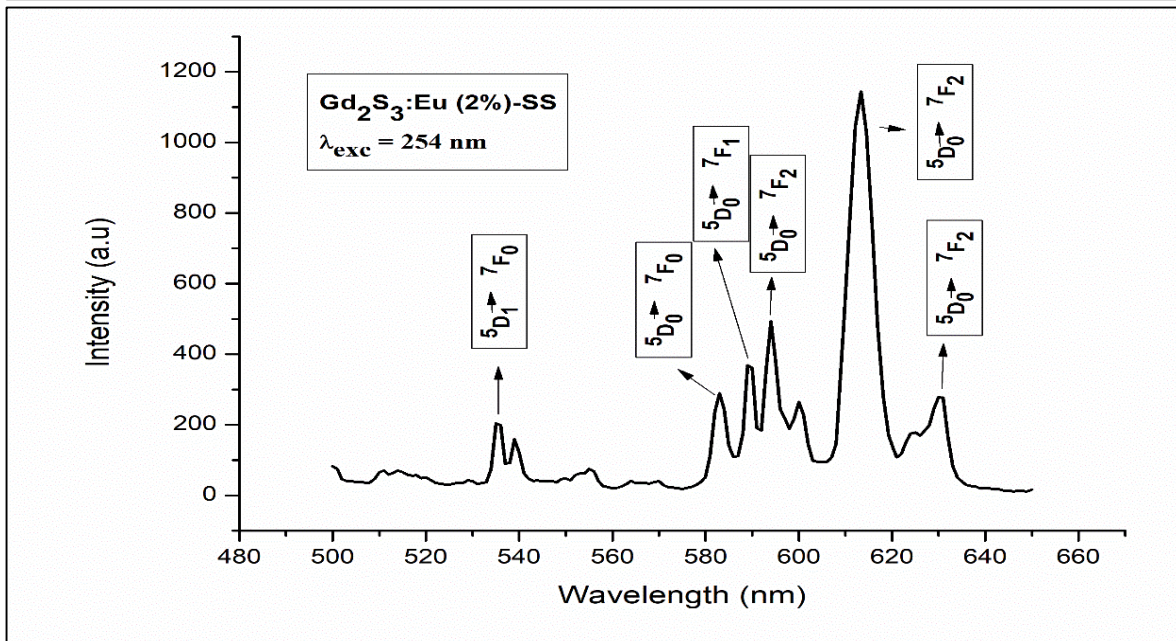
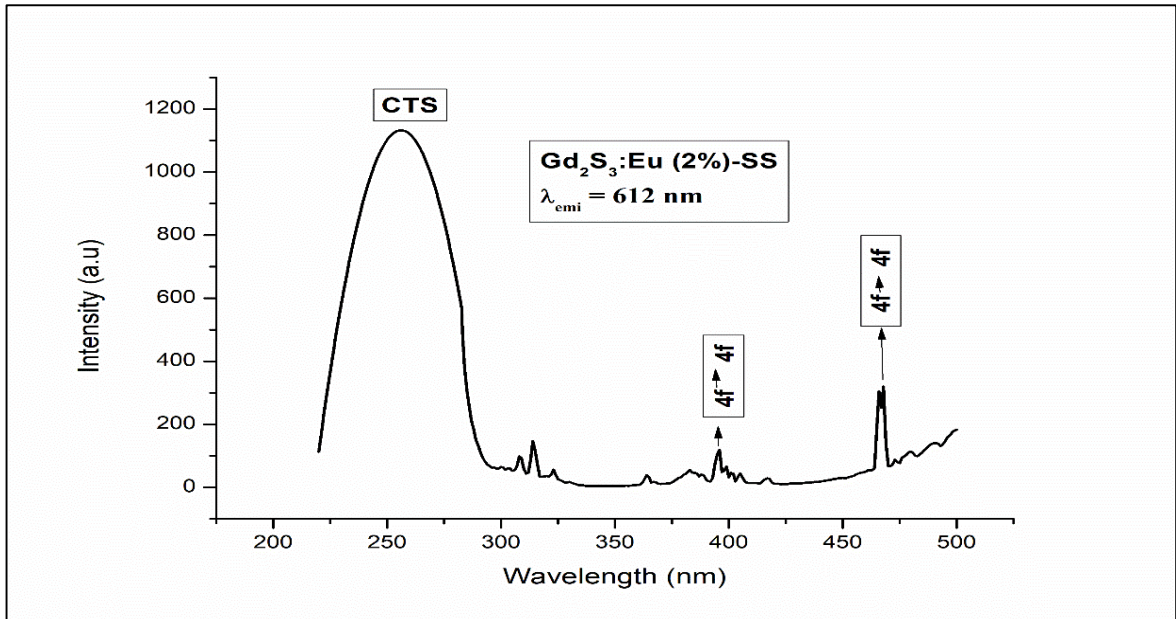


Figure 4-52: Photoluminescence spectra for  $Gd_2S_3:Eu$  (1%) [(a) GdE1-SS Excitation at  $\lambda_{emi}$  of 612 nm (b) GdE1-SS Emission at  $\lambda_{exc}$  of 254 nm]



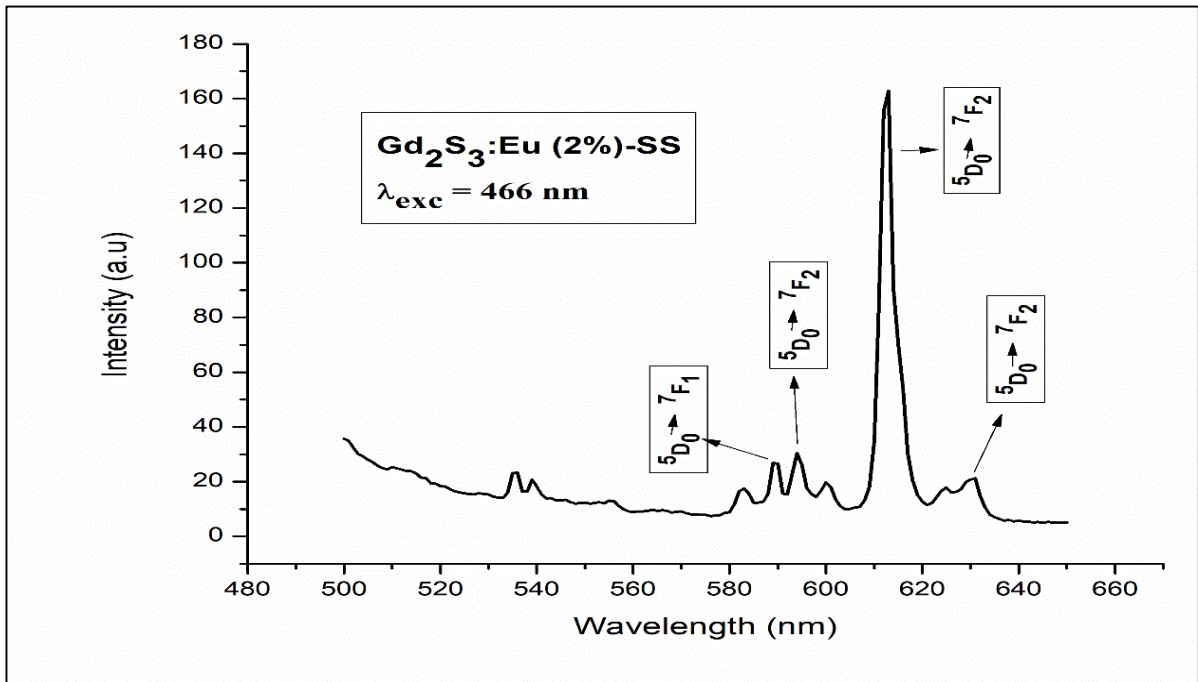


Figure 4-53: Photoluminescence spectra for  $Gd_2S_3:Eu (2\%)$   
 [(a)  $GdE_2$ -SS Excitation at  $\lambda_{emi}$  of 612 nm (b)  $GdE_2$ -SS Emission at  $\lambda_{exc}$  of 254 nm  
 (c)  $GdE_2$ -SS Emission at  $\lambda_{exc}$  of 395 nm (d)  $GdE_2$ -SS Emission at  $\lambda_{exc}$  of 395 nm]

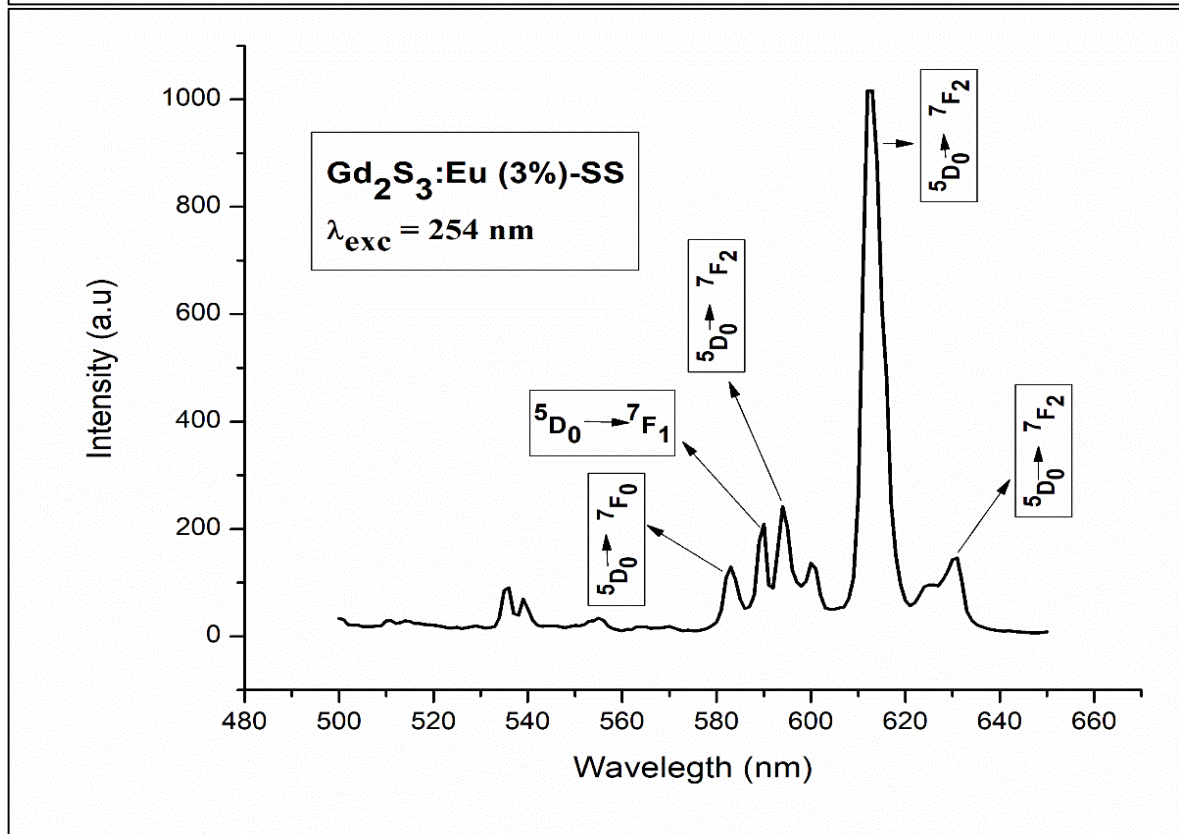
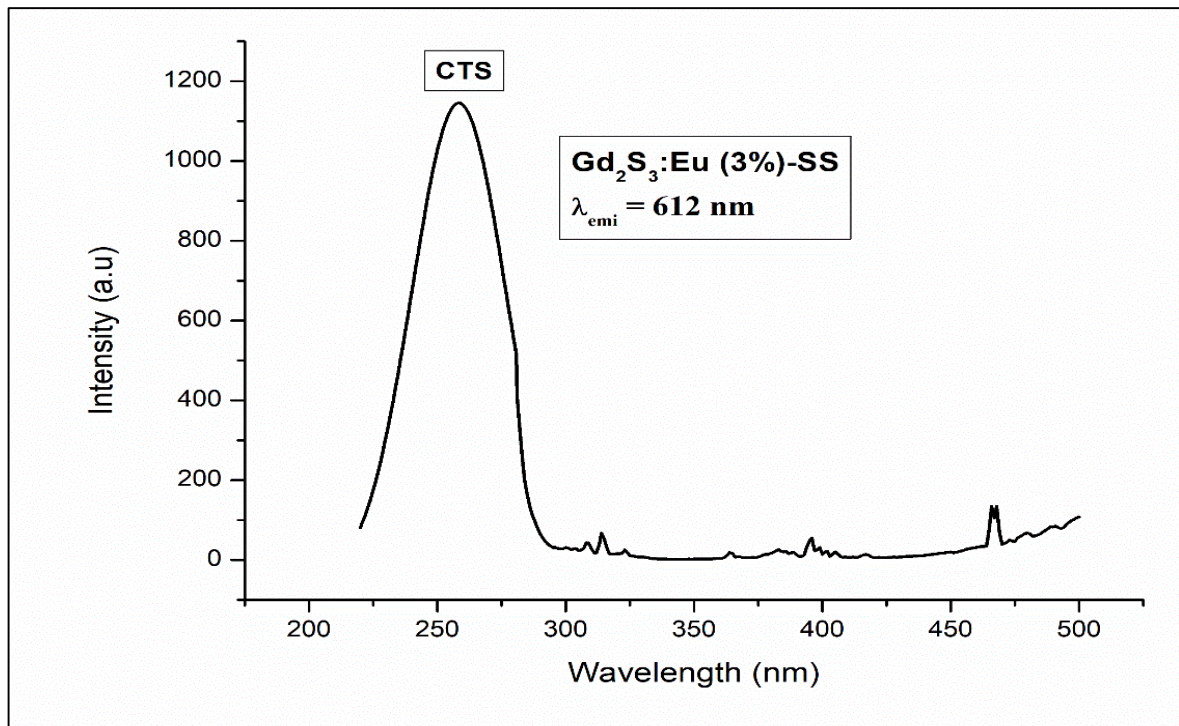


Figure 4-54: Photoluminescence spectra for  $Gd_2S_3:Eu (3\%)$   
 [(a) GdE3-SS Excitation at  $\lambda_{emi}$  of 612 nm (b) GdE3-SS Emission at  $\lambda_{exc}$  of 254 nm]

The graphs in Fig. 4-52, 4-53 and 4-54 show excitation and emission spectra of 1%, 2% and 3% Eu doped Gd<sub>2</sub>S<sub>3</sub>. The excitation spectra of Gd<sub>2</sub>S<sub>3</sub> for 1% to 3% Eu doping show an intense peak at 254 nm which is due to the charge transfer (CTS) transition of Eu<sup>3+</sup> ions. In 2% Eu doping, there are additional small peaks at 395 nm and 466 nm due to the 4f–4f transitions of Eu<sup>3+</sup> ions.

The emission spectrum of 1% Eu doping shows an intense peak at 612 nm corresponding to the transition  $^5D_0 \rightarrow ^7F_2$  and two weak peaks at 593 nm and 625 nm due to Stark splitting of the same transition.

The emission spectra of 2% Eu doping for excitation of 254 nm shows highest peak at 613 nm corresponding to  $^5D_0 \rightarrow ^7F_2$  transition and additional peaks at 535 nm, 583 nm, 588 nm, 593 nm and 630 nm which can be associated to the transitions  $^5D_1 \rightarrow ^7F_0$  (535 nm),  $^5D_0 \rightarrow ^7F_0$  (583 nm),  $^5D_0 \rightarrow ^7F_1$  (588 nm) and  $^5D_0 \rightarrow ^7F_2$  (593 and 630 nm) of Eu<sup>3+</sup> ions. The same sample excited at 395 nm, gives intense peak at 613 nm ( $^5D_0 \rightarrow ^7F_2$ ) with additional peaks at 588 nm ( $^5D_0 \rightarrow ^7F_1$ ), 593 nm, 625 nm and 630 nm, the last three being associated with the  $^5D_0 \rightarrow ^7F_2$  transition. For excitation of 466 nm, it shows the same features with an intense peak at 613 nm and other weak peaks due to transitions  $^5D_0 \rightarrow ^7F_1$  (588 nm) and  $^5D_0 \rightarrow ^7F_2$  (593 nm, 613 nm and 630 nm) in the red region.

The PL spectra of 3% Eu doping shows peaks at 582 nm ( $^5D_0 \rightarrow ^7F_0$ ) and 590 nm, 593 nm, 630 nm with highest intensity peak at 613 nm, all associated to the transition  $^5D_0 \rightarrow ^7F_2$  of Eu<sup>3+</sup> ions.

It can be seen from the figures that intensity increases with Eu doping from 1% to 2% and then decreases for 3% of Eu doping. For 1% Eu<sup>3+</sup> ions, the number of photoluminescence centres are less and hence the luminescent intensity is relatively low. With the increase of Eu<sup>3+</sup> ions concentration to 2%, the photoluminescent intensity increases. When the concentration of Eu<sup>3+</sup> increases to 3%, it becomes a relatively heavily doped phosphor with increase in the number of activator ions. Hence, the interaction of Eu<sup>3+</sup>  $\rightarrow$  Eu<sup>3+</sup> increases, which leads to increase in phonon transitions resulting in concentration quenching. Thus, the emission intensity decreases.

### 4.5.3 PL of Terbium (Tb) Doped Gadolinium Sulphide ( $Gd_2S_3$ ) synthesized by Solid State Method

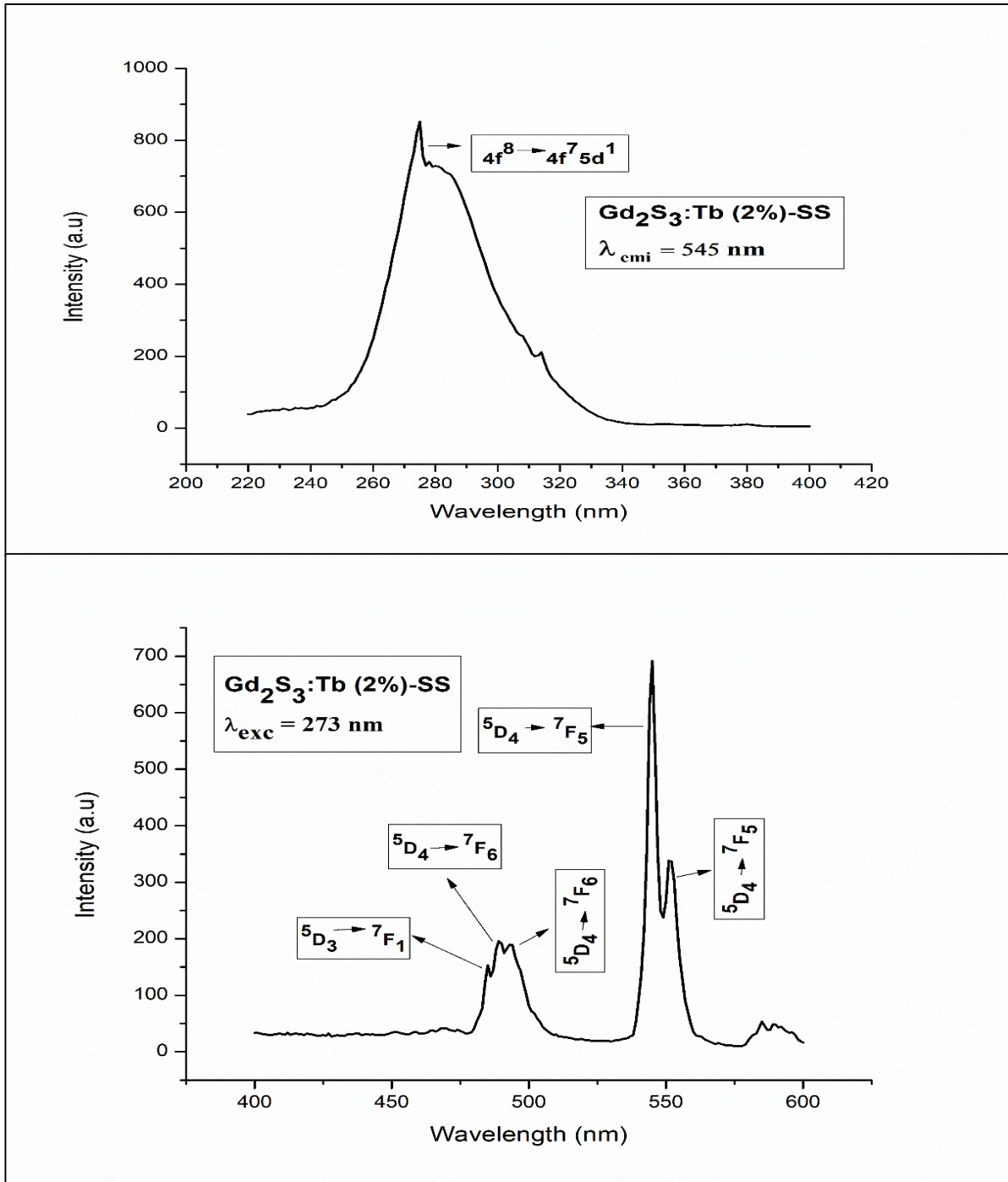


Figure 4-56: Photoluminescence spectra for  $Gd_2S_3:Tb$  (2%)  
 [(a)  $Gd_2S_3:Tb$ -SS Excitation at  $\lambda_{emi}$  of 545 nm (b)  $Gd_2S_3:Tb$ -SS Emission at  $\lambda_{exc}$  of 273 nm]

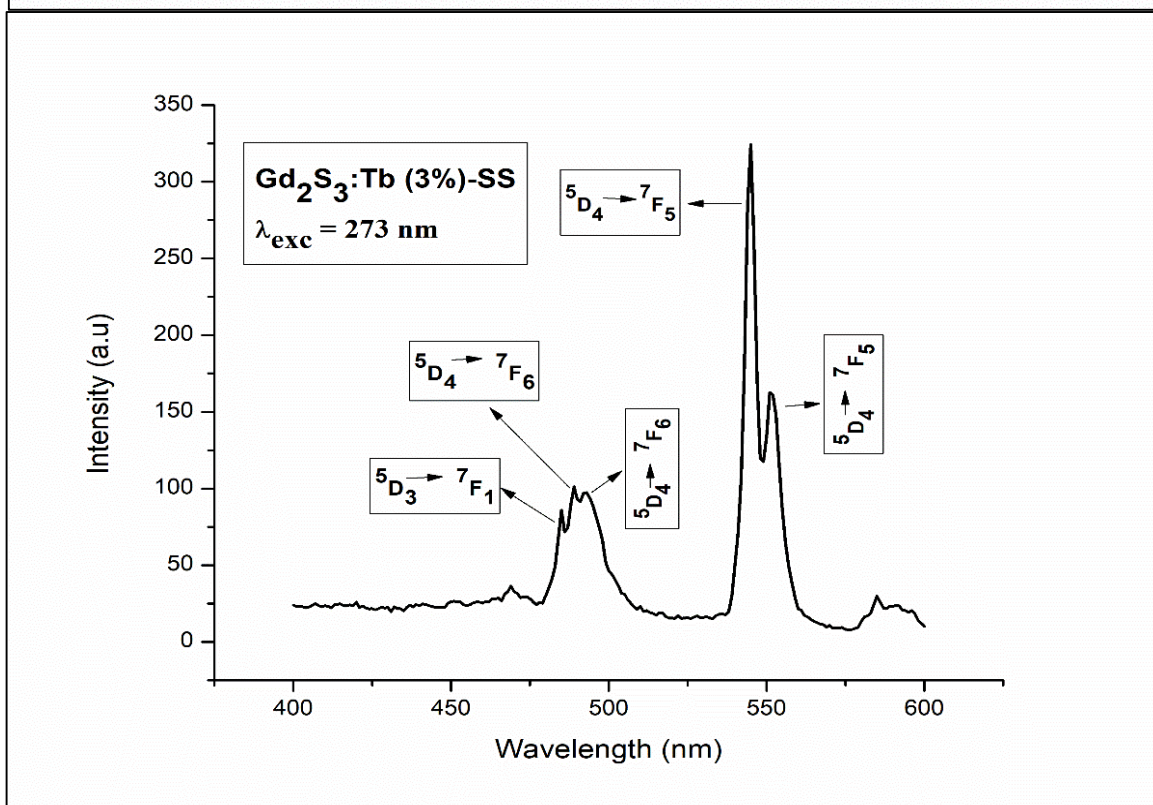
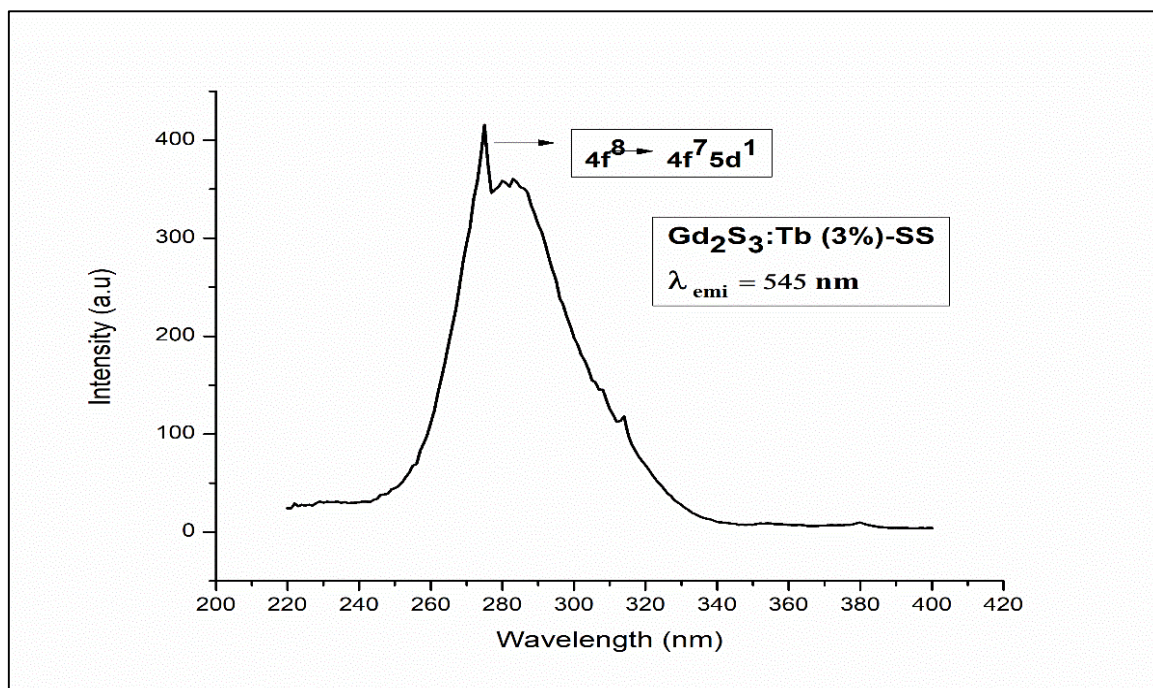


Figure 4-57: Photoluminescence spectra for Gd<sub>2</sub>S<sub>3</sub>:Tb (3%)  
 [(a) GdT3-SS Excitation at  $\lambda_{emi}$  of 545 nm (b) GdT3-SS Emission at  $\lambda_{exc}$  of 273 nm]

The graphs in Fig. 4-55 to 4-57 show excitation and emission spectra of  $\text{Gd}_2\text{S}_3$  with 1%, 2% and 3% of Tb doping. The excitation spectra for all the three doping percentages show an intense peak at 273 nm which is due to the  $4f^8 \rightarrow 4f^7 5d^1$

transition of  $\text{Tb}^{3+}$  ion.

The emission spectrum consists of lines in the blue and green region. The ground and the first excited levels of  $\text{Tb}^{3+}$  are split by spin-orbit coupling and the transitions from the  $^5\text{D}_4$  and  $^5\text{D}_3$  multiplets to the different  $^7\text{F}_J$  multiplets result in the generation of blue and green emissions [12]. For all the doping percentages, the emission peak at 484 nm gives blue emission corresponding to the  $^5\text{D}_3 \rightarrow ^7\text{F}_1$  transition while the sharp intense peaks at 544 nm and 552 nm are associated with the  $^5\text{D}_4 \rightarrow ^7\text{F}_5$  transition along with a small peak at 489 nm, which is associated with  $^5\text{D}_4 \rightarrow ^7\text{F}_6$  transition of  $\text{Tb}^{3+}$  ions. The photoluminescence intensity decreases with increase in doping percentage.

#### 4.5.4 PL of Europium (Eu) Doped Lanthanum Sulphide ( $\text{La}_2\text{S}_3$ ) synthesized by Solid State Method

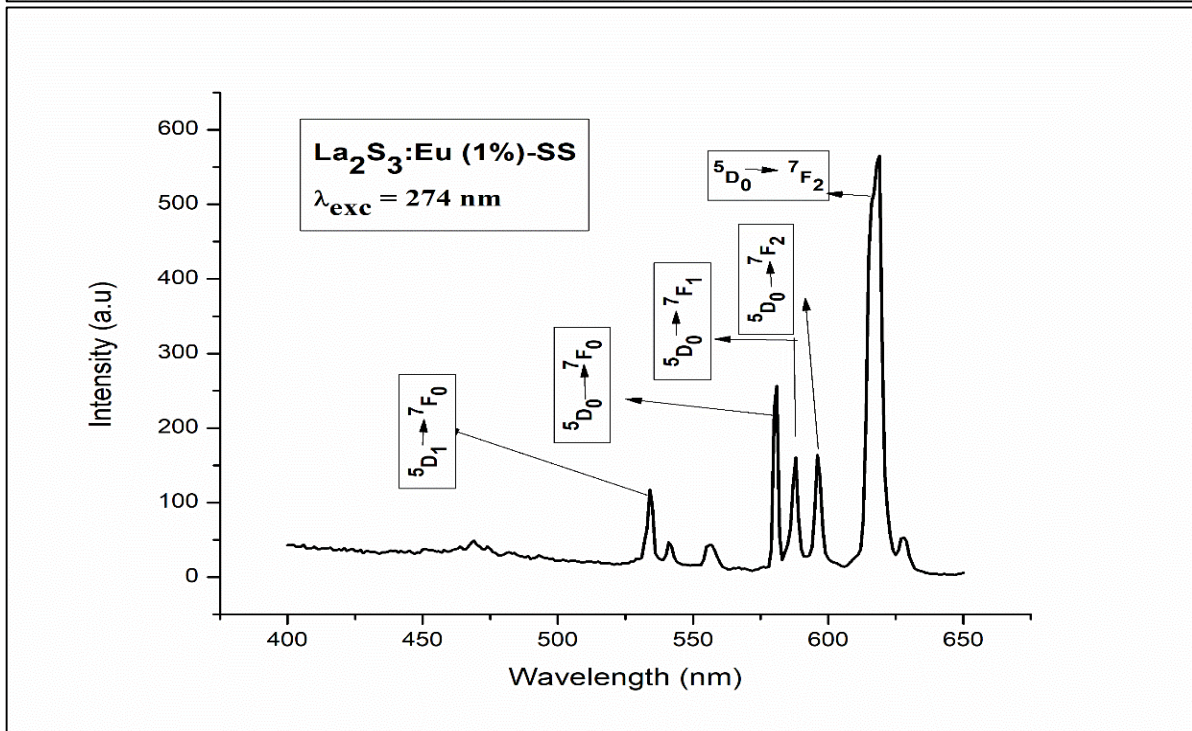
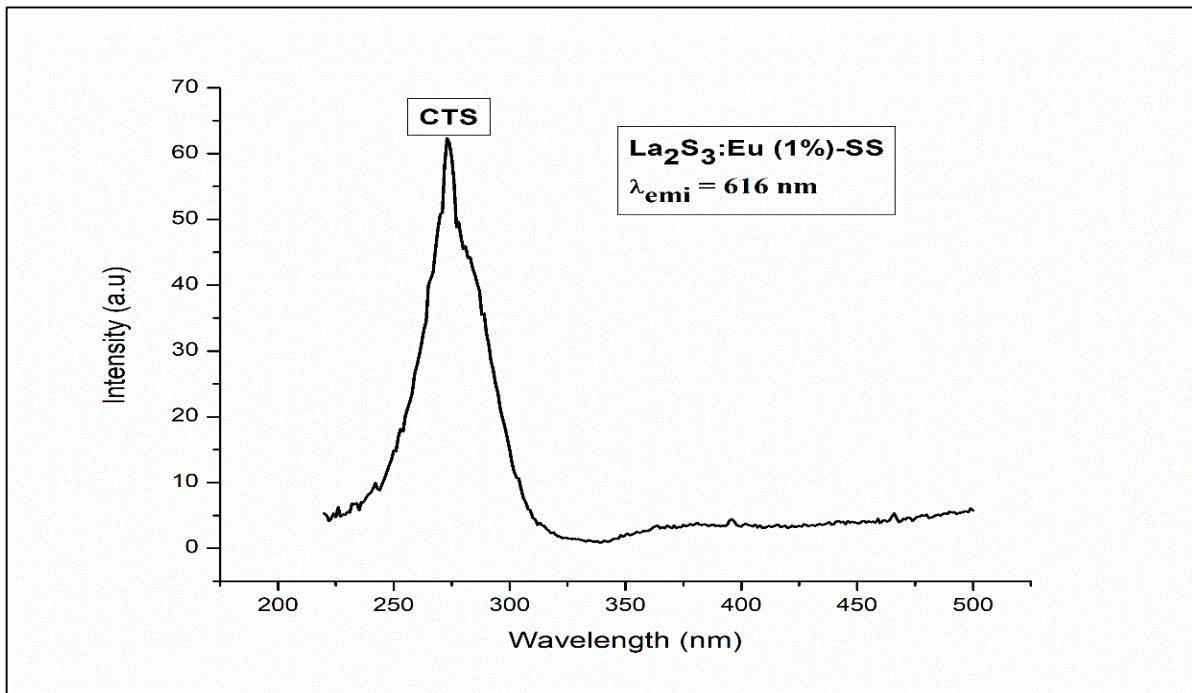
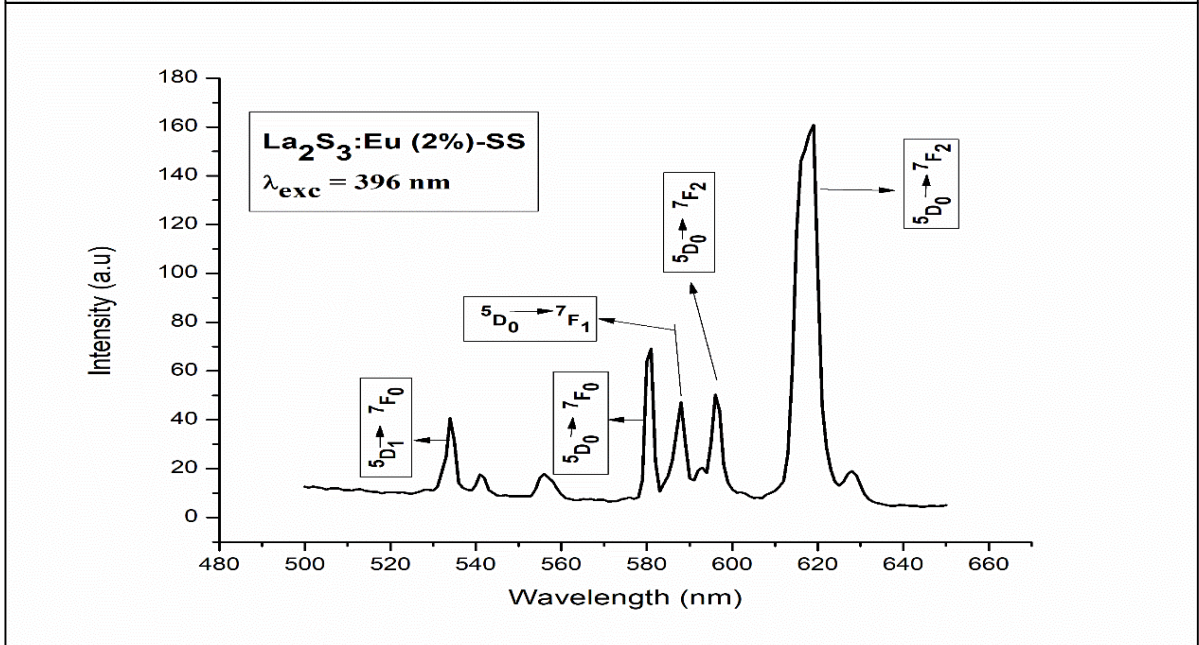
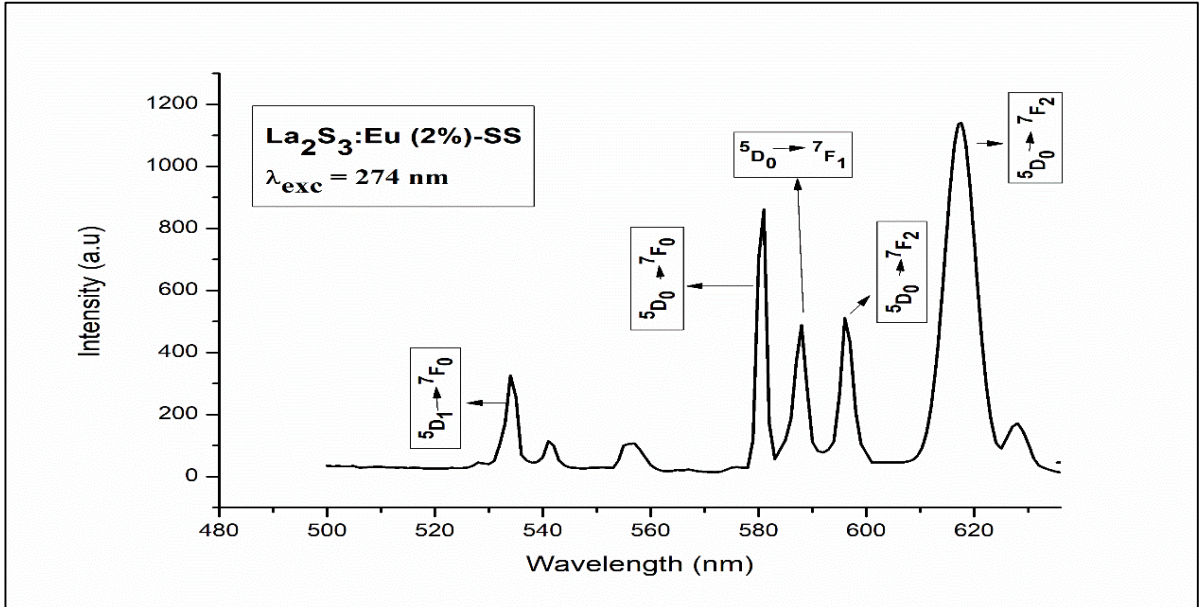
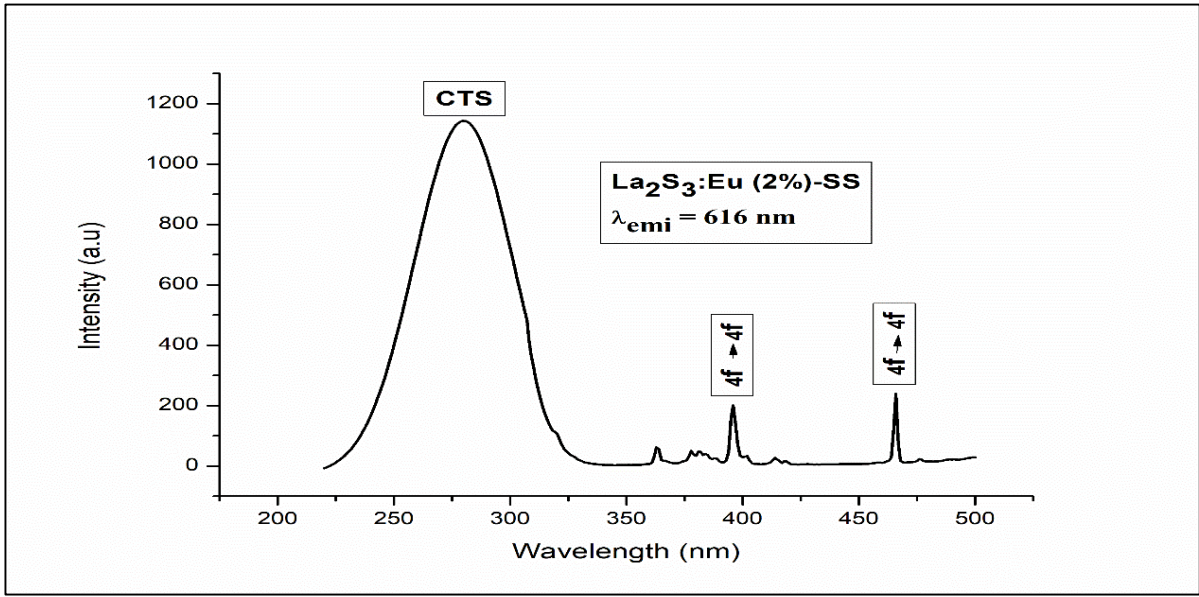


Figure 4-58: Photoluminescence spectra for  $\text{La}_2\text{S}_3:\text{Eu (1\%)}$   
[(a)  $\text{La}_2\text{S}_3:\text{Eu (1\%)-SS}$  Excitation at  $\lambda_{\text{emi}}$  of 616 nm (b)  $\text{La}_2\text{S}_3:\text{Eu (1\%)-SS}$  Emission at  $\lambda_{\text{exc}}$  of 274 nm]



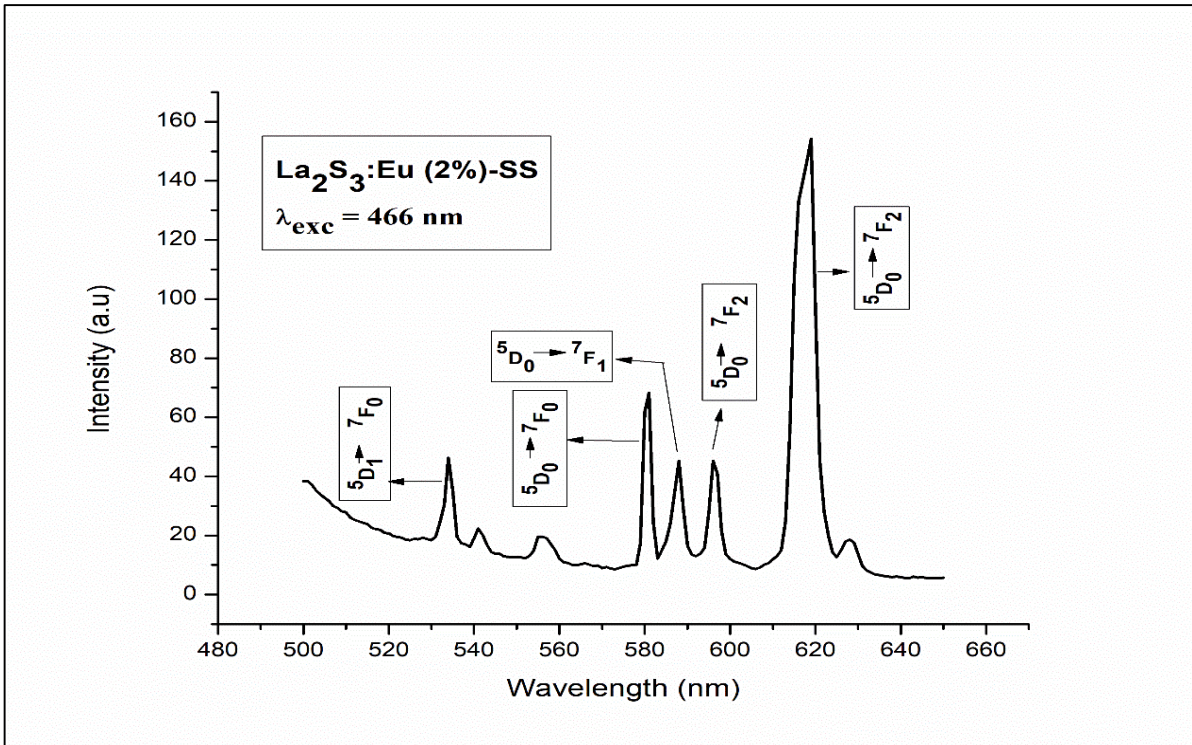


Figure 4-59: Photoluminescence spectra for  $\text{La}_2\text{S}_3:\text{Eu (2\%)}$   
 [(a) LaE2-SS Excitation at  $\lambda_{\text{emi}}$  of 616 nm (b) LaE2-SS Emission at  $\lambda_{\text{exc}}$  of 274 nm  
 (c) LaE2-SS Emission at  $\lambda_{\text{exc}}$  of 396 nm (d) LaE2-SS Emission at  $\lambda_{\text{exc}}$  of 466 nm]

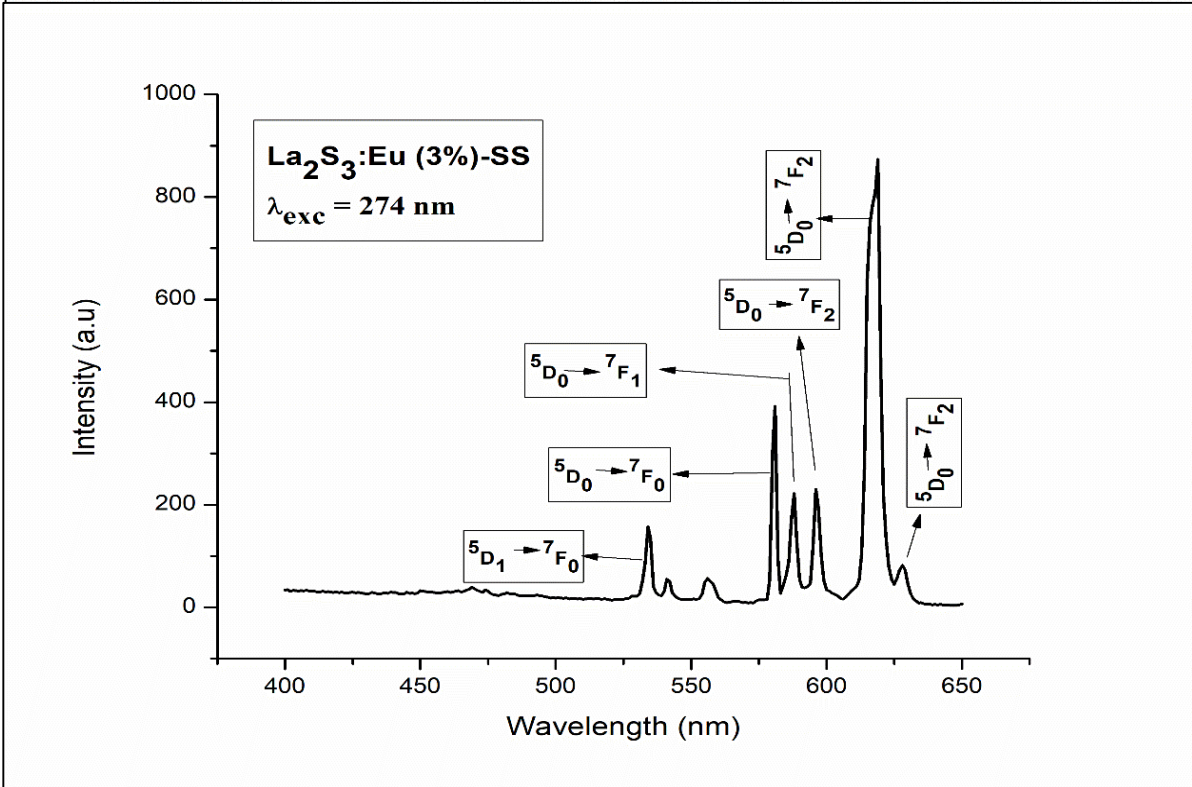
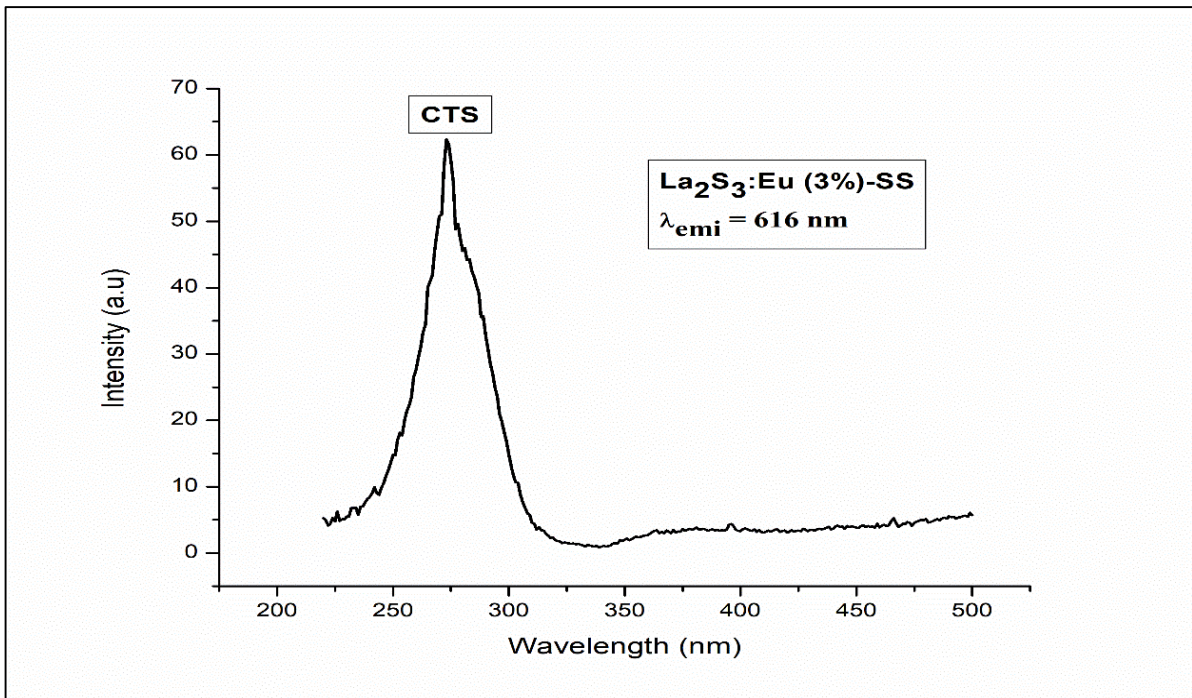
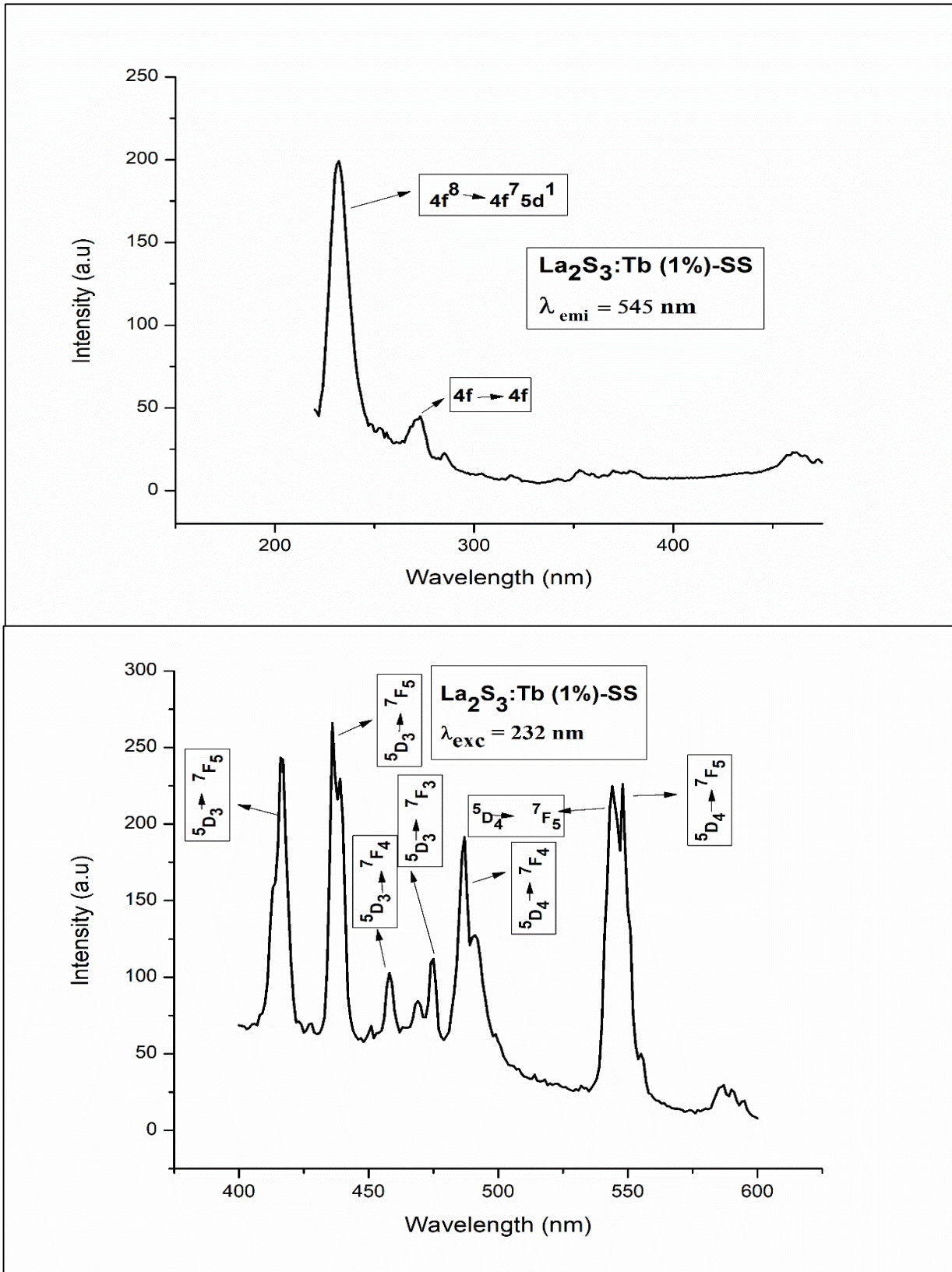


Figure 4-60: Photoluminescence spectra for La<sub>2</sub>S<sub>3</sub>:Eu (3%)  
 [(a) LaE3-SS Excitation at  $\lambda_{\text{emi}}$  of 616 nm (b) LaE3-SS Emission at  $\lambda_{\text{exc}}$  of 274 nm]

The graphs in Fig. 4-58 to 4-60 show excitation and emission spectra of  $\text{La}_2\text{S}_3$  doped with 1%, 2% and 3% of Eu at room temperature. The excitation spectra of  $\text{La}_2\text{S}_3$  for all concentrations of Eu doping show an intense peak at 274 nm which is due to the charge transfer (CTS) transition of  $\text{Eu}^{3+}$  ions while in 2% Eu doping, there are additional small peaks at 396 nm and 466 nm due to the 4f-4f transitions of  $\text{Eu}^{3+}$  ions.

At an excitation of 274 nm, the emission spectrum shows an intense peak at 618 nm corresponding to the  $^5\text{D}_0 \rightarrow ^7\text{F}_2$  transition for all the doping percentages. The other peaks observed in the PL spectra located at 534 nm, 580 nm, 589 nm and 596 nm are assigned to the transitions  $^5\text{D}_1 \rightarrow ^7\text{F}_0$ ,  $^5\text{D}_0 \rightarrow ^7\text{F}_0$ ,  $^5\text{D}_0 \rightarrow ^7\text{F}_1$  and  $^5\text{D}_0 \rightarrow ^7\text{F}_2$  of  $\text{Eu}^{3+}$  ions respectively. In 2% Eu doping, an additional small peak is observed at 627 nm which is also attributed to the  $^5\text{D}_0 \rightarrow ^7\text{F}_2$  transition. In 2% Eu doped sample, excitation at 396 nm and 466 nm also yielded the same peaks at 534 nm, 580 nm, 587 nm, 596 nm and 627 nm corresponding to the transitions  $^5\text{D}_1 \rightarrow ^7\text{F}_0$ ,  $^5\text{D}_0 \rightarrow ^7\text{F}_0$ ,  $^5\text{D}_0 \rightarrow ^7\text{F}_1$  and  $^5\text{D}_0 \rightarrow ^7\text{F}_2$  (596, 627 nm) of  $\text{Eu}^{3+}$  ions. The highest intensity peak is observed at the same value of 618 nm due to the  $^5\text{D}_0 \rightarrow ^7\text{F}_2$  transition of  $\text{Eu}^{3+}$  ions. It can be seen that as doping percentage of Eu is increased from 1% to 2%, the intensity of emission increases and then for 3% of Eu doping, the intensity falls. The range of emission spectra spreading over orange-red region is more for 2% Eu doping which has the highest intensity.

### 4.5.5 PL of Terbium (Tb) Doped Lanthanum Sulphide ( $\text{La}_2\text{S}_3$ ) synthesized by Solid State Method



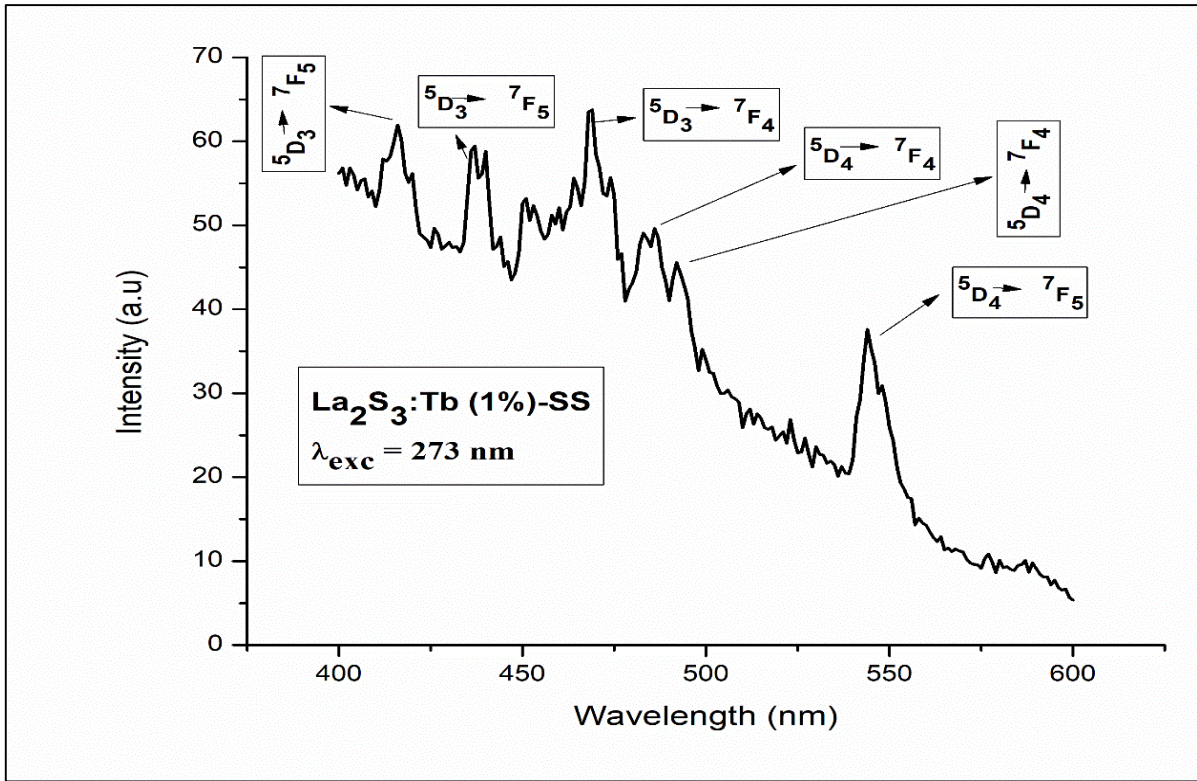
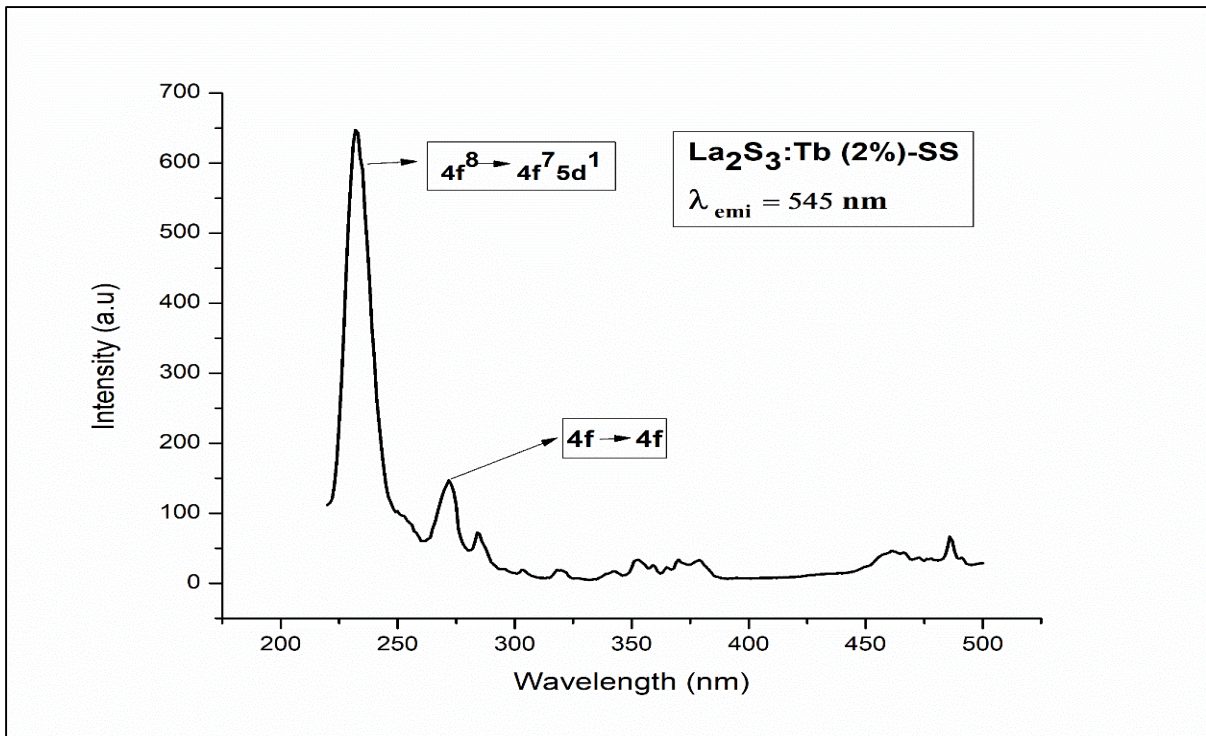


Figure 4-61: Photoluminescence spectra for  $\text{La}_2\text{S}_3:\text{Tb (1\%)}$   
 [(a) LaT1-SS Excitation at  $\lambda_{\text{emi}}$  of 545 nm (b) LaT1-SS Emission at  $\lambda_{\text{exc}}$  of 232 nm  
 (c) LaT1-SS Emission at  $\lambda_{\text{exc}}$  of 273 nm]



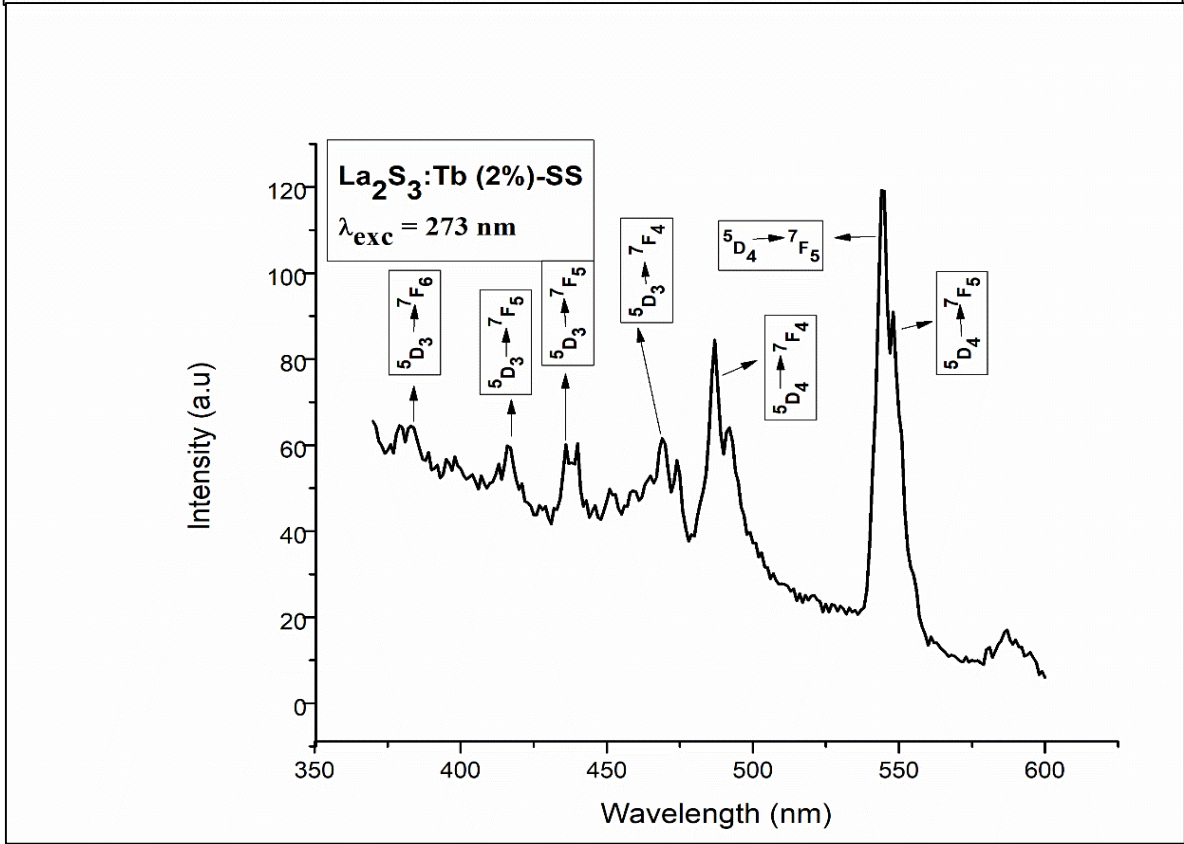
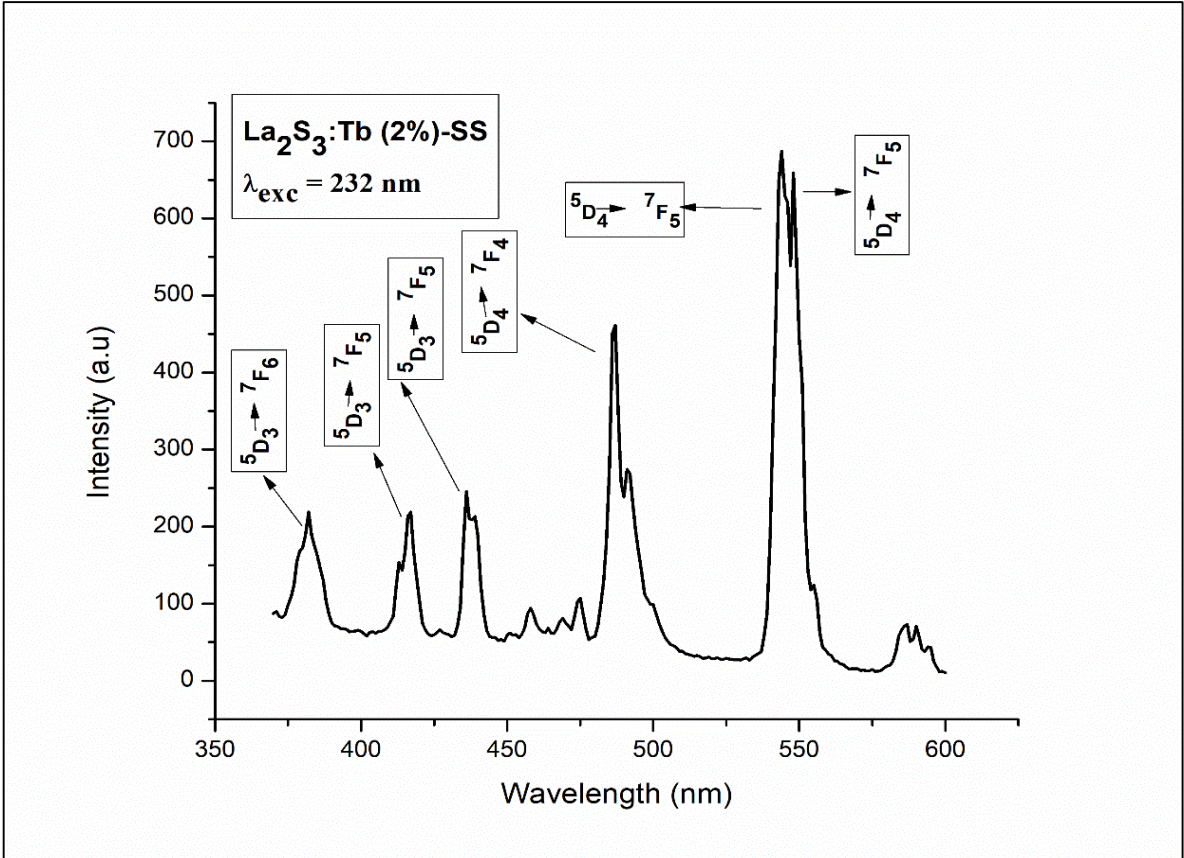
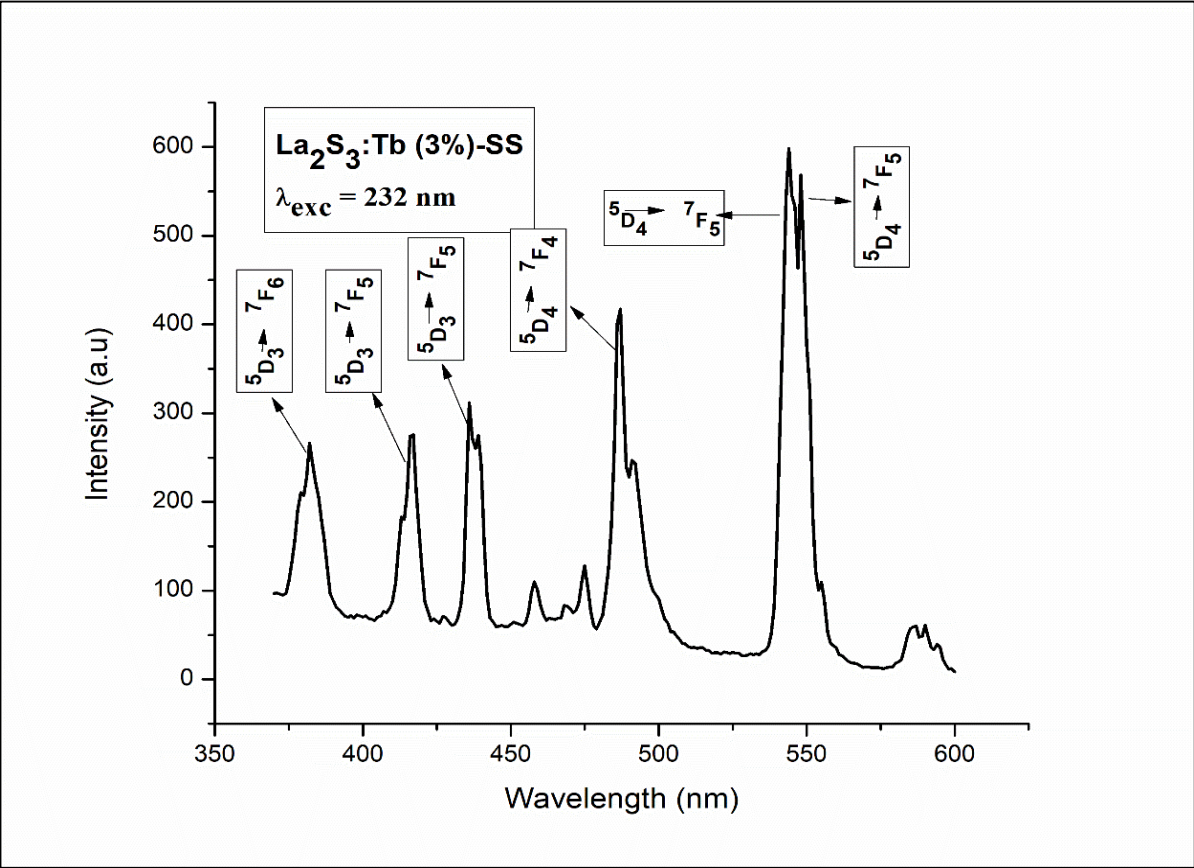
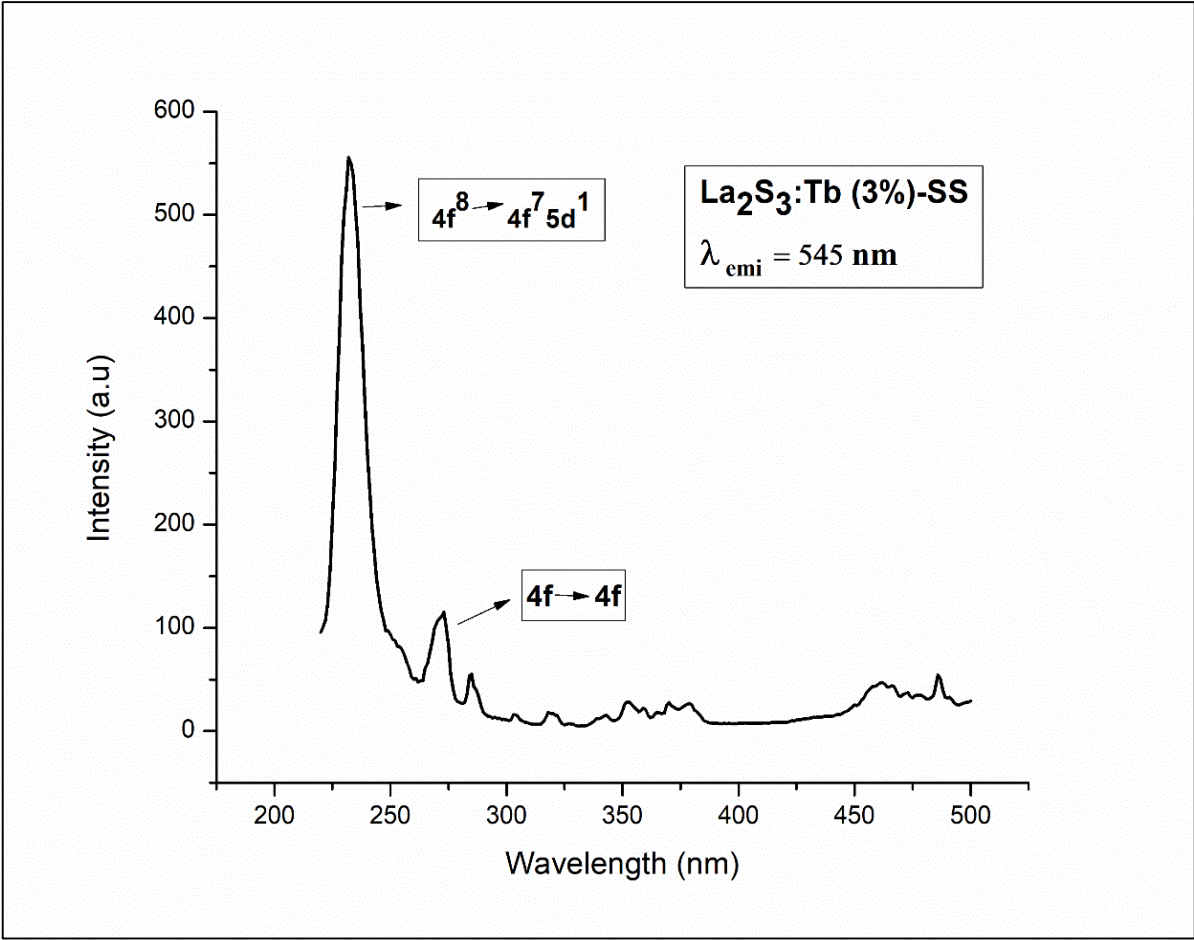


Figure 4-62: Photoluminescence spectra for La<sub>2</sub>S<sub>3</sub>:Tb (2%)  
 [(a) LaT2-SS Excitation at  $\lambda_{emi}$  of 545 nm (b) LaT2-SS Emission at  $\lambda_{exc}$  of 232 nm  
 (c) LaT2-SS Emission at  $\lambda_{exc}$  of 273 nm]



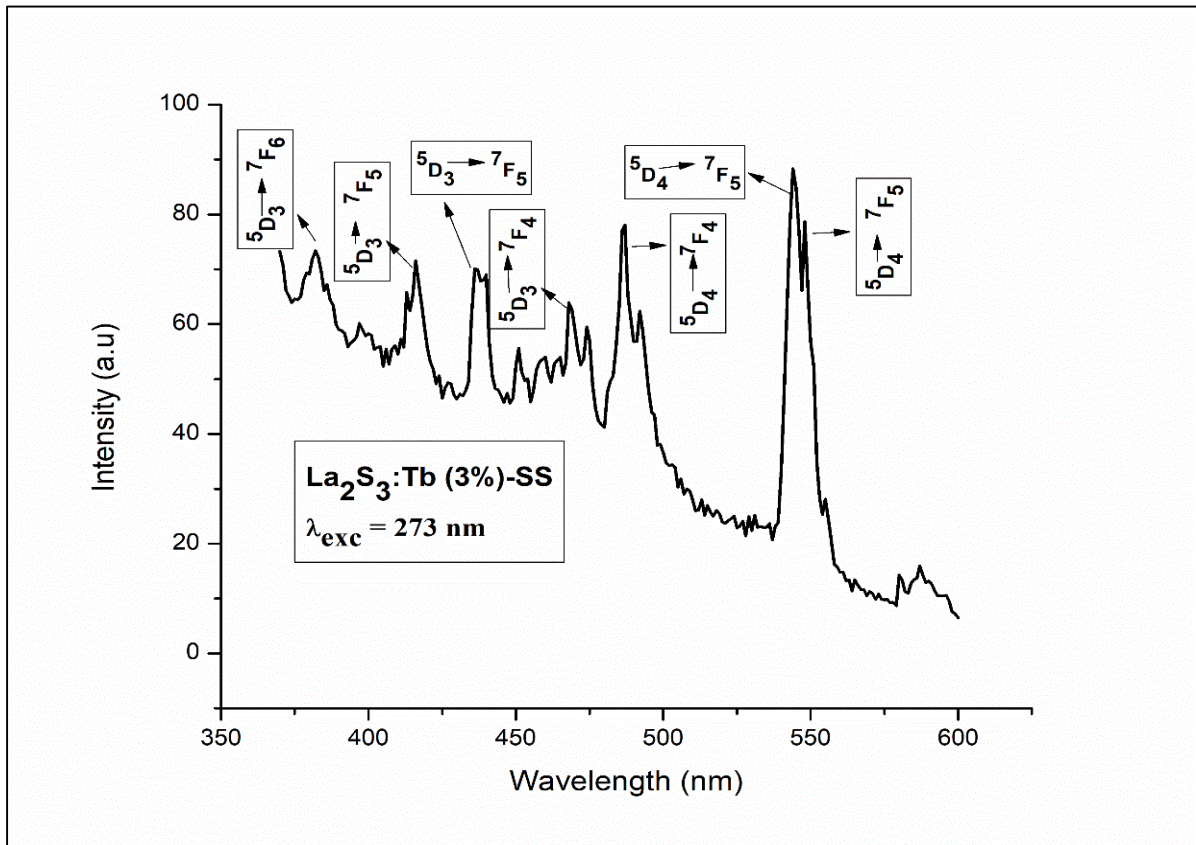


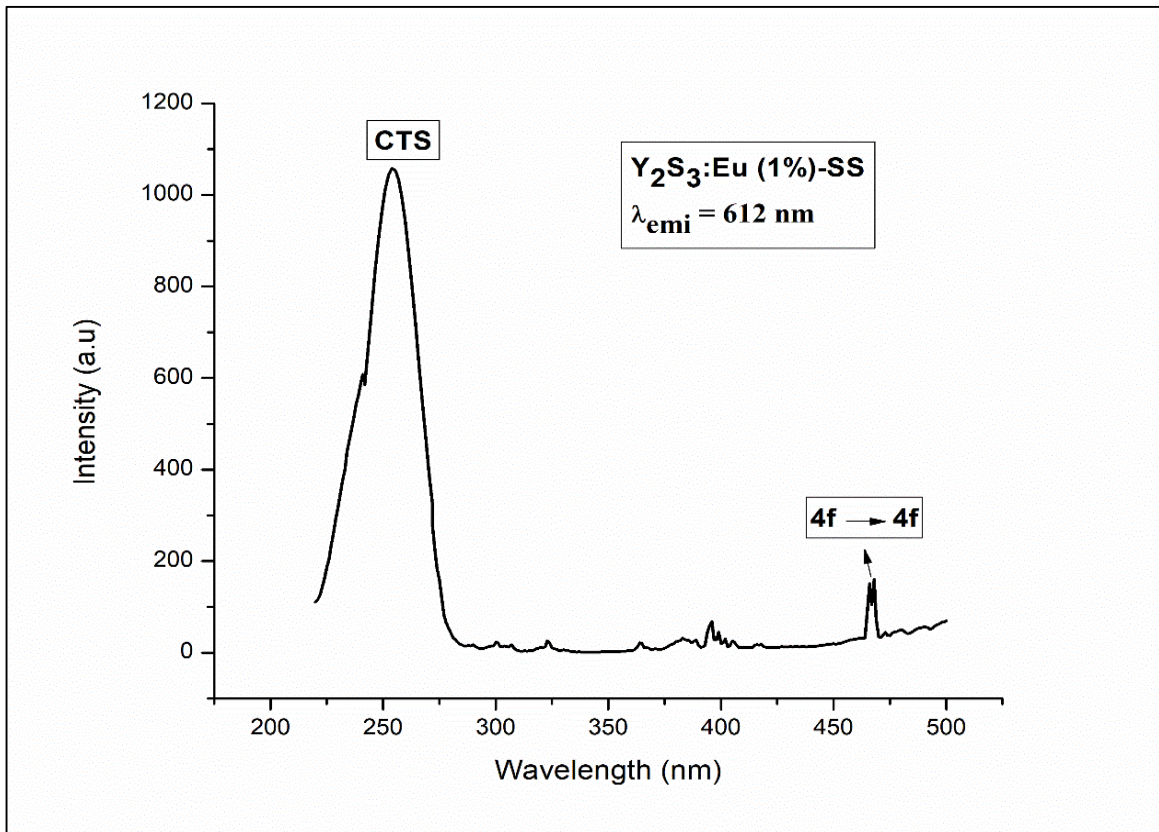
Figure 4-63: Photoluminescence spectra for La<sub>2</sub>S<sub>3</sub>:Tb (3%)  
 [(a) LaT3-SS Excitation at λ<sub>emi</sub> of 545 nm (b) LaT3-SS Emission at λ<sub>exc</sub> of 232 nm  
 (c) LaT3-SS Emission at λ<sub>exc</sub> of 273 nm]

The graphs in Fig. 4-61, 4-62 and 4-63 show excitation and emission spectra of 1%, 2% and 3% Tb doped La<sub>2</sub>S<sub>3</sub>. The excitation spectrum shows an intense peak at 232 nm which is due to the  $4f^8 \rightarrow 4f^7 5d^1$  transition of Tb<sup>3+</sup> ion and an additional small peak at 273 nm can be attributed to the 4f–4f transitions of Tb<sup>3+</sup> ions.

The emission spectrum again consists of two sets of blue and green emission lines. For 1% Tb doping at an excitation of 232 nm, the emission peaks at 415 nm, 436 nm, 457 nm and 475 nm give blue emission corresponding to the 5D<sub>3</sub> → 7F<sub>5</sub>, 5D<sub>3</sub> → 7F<sub>5</sub>, 5D<sub>3</sub> → 7F<sub>4</sub> and 5D<sub>3</sub> → 7F<sub>3</sub> transitions while the sharp and intense peaks at 544 nm and 547 nm give green emission associated with the 5D<sub>4</sub> → 7F<sub>5</sub> transition of Tb<sup>3+</sup> ions. For 2% and 3% Tb doping at an excitation of 232nm, blue emission peaks are observed at 383 nm, 416nm, 435 nm, and 487 nm corresponding to the transitions 5D<sub>3</sub> → 7F<sub>6</sub>, 5D<sub>3</sub> → 7F<sub>5</sub>, 5D<sub>3</sub> → 7F<sub>5</sub> and 5D<sub>3</sub> → 7F<sub>1</sub> while the sharp and intense peaks at 544 nm and 547 nm give green emission associated with the 5D<sub>4</sub> → 7F<sub>5</sub> transition of Tb<sup>3+</sup> ions.

When excited at 273 nm, the Tb doped samples show the same peaks as for  $\lambda_{exc} = 232$ . In addition, one more peak in the blue region corresponding to the transition  $^5D_3 \rightarrow ^7F_4$  is observed at 468 nm. Only one intense peak at 544 nm is seen in the green region and the 547 nm peak gets diminished. The luminescent intensity increases from 1% to 2% of Tb doping and decreases when doping percentage becomes 3%.

#### 4.5.6 PL of Europium (Eu) Doped Yttrium Sulphide ( $Y_2S_3$ ) synthesized by Solid State Method



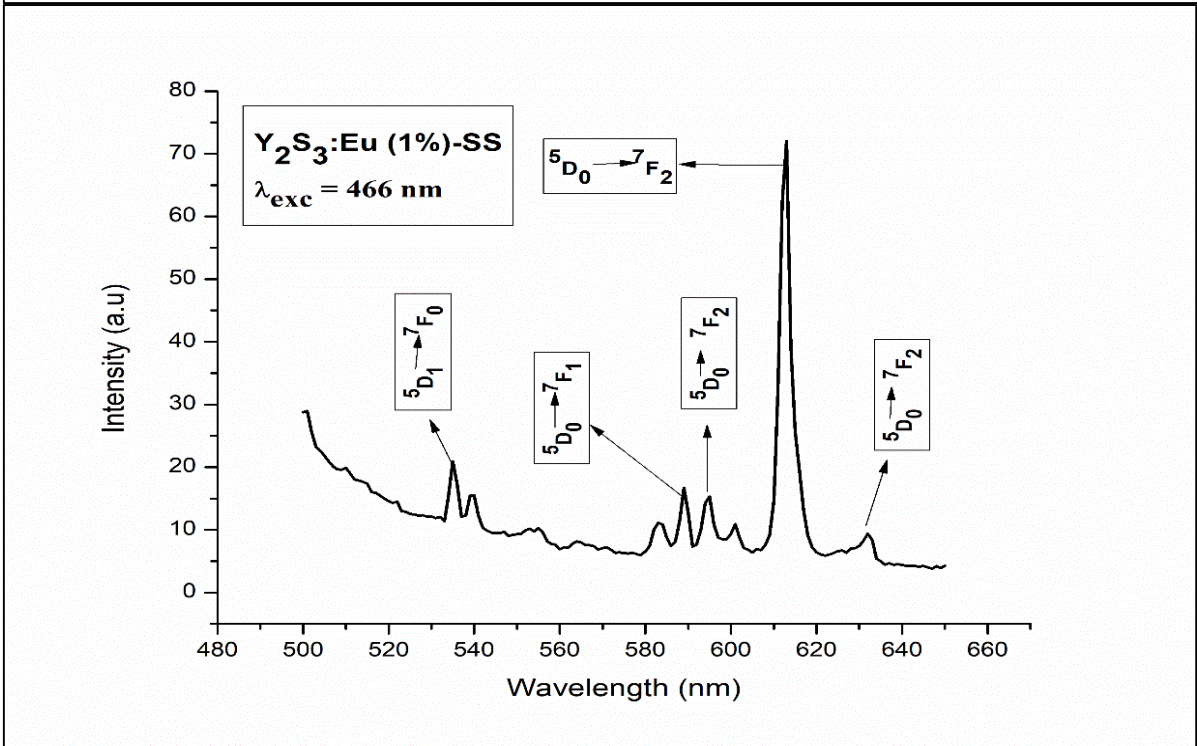
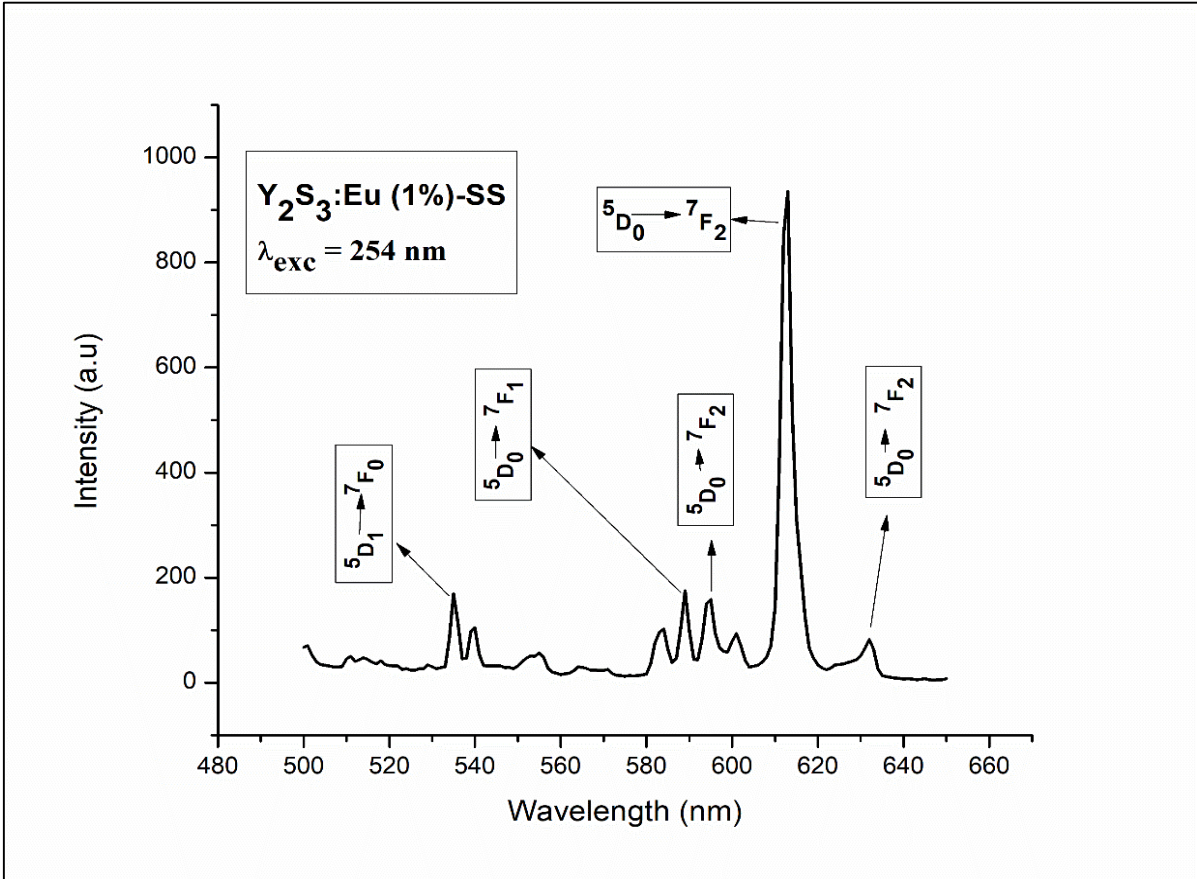
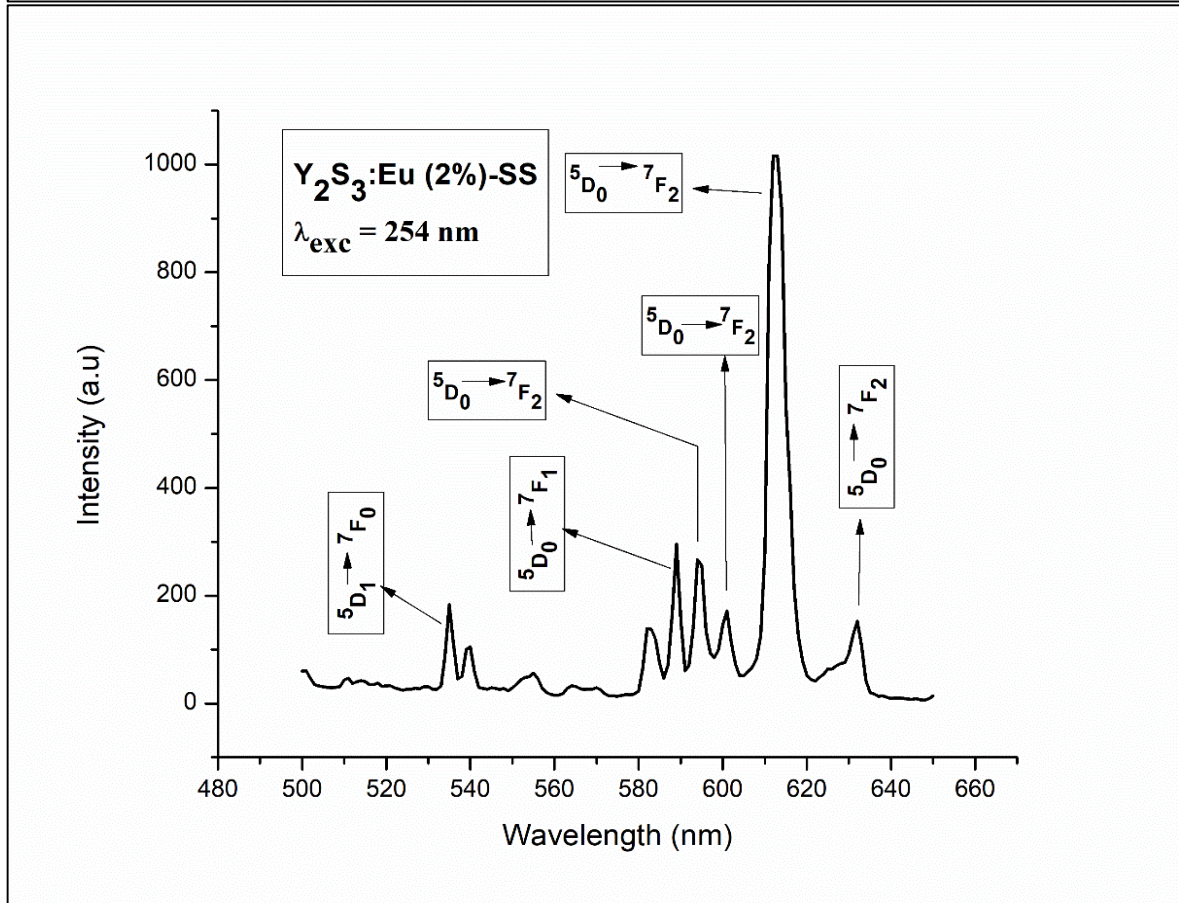
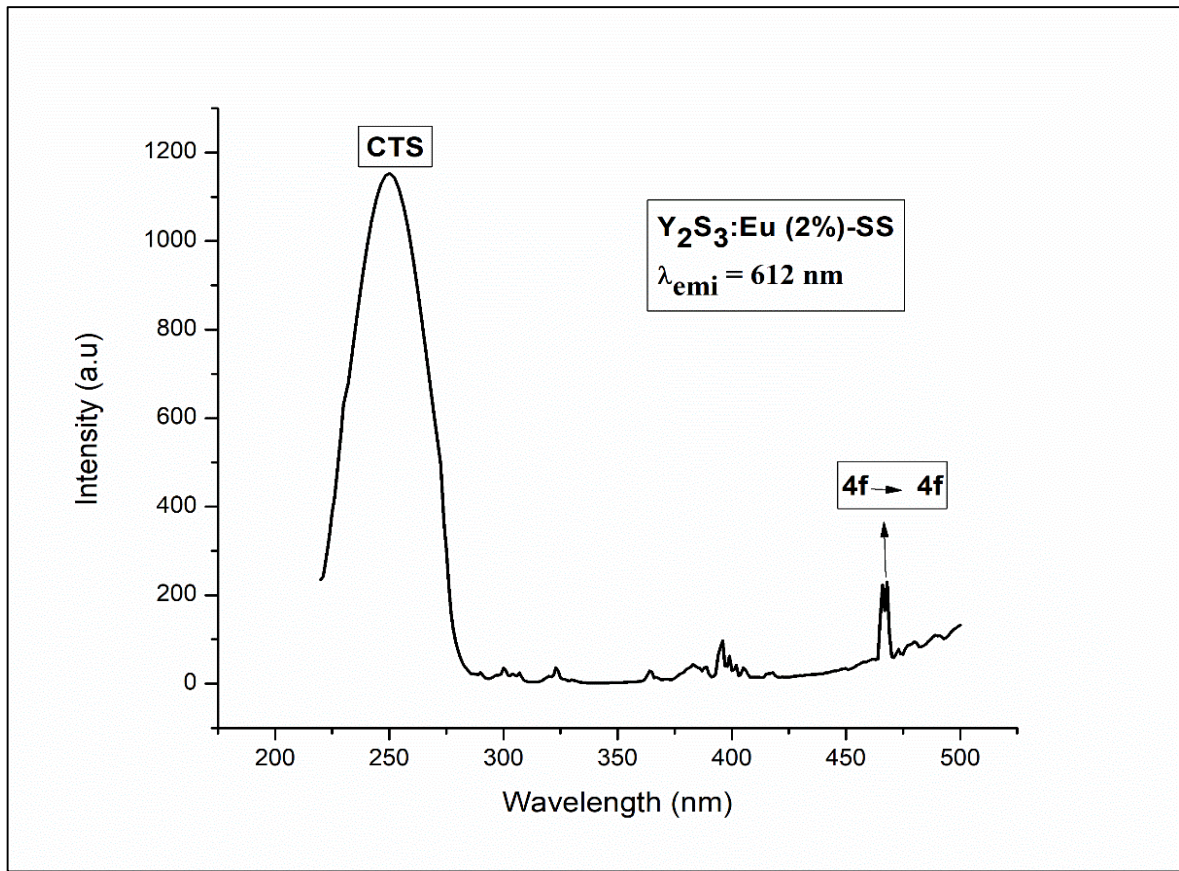


Figure 4-64: Photoluminescence spectra for  $Y_2S_3:Eu$  (1%)  
 [(a) YE1-SS Excitation at  $\lambda_{emi}$  of 612 nm (b) YE1-SS Emission at  $\lambda_{exc}$  of 254 nm  
 (c) YE1-SS Emission at  $\lambda_{exc}$  of 466 nm]



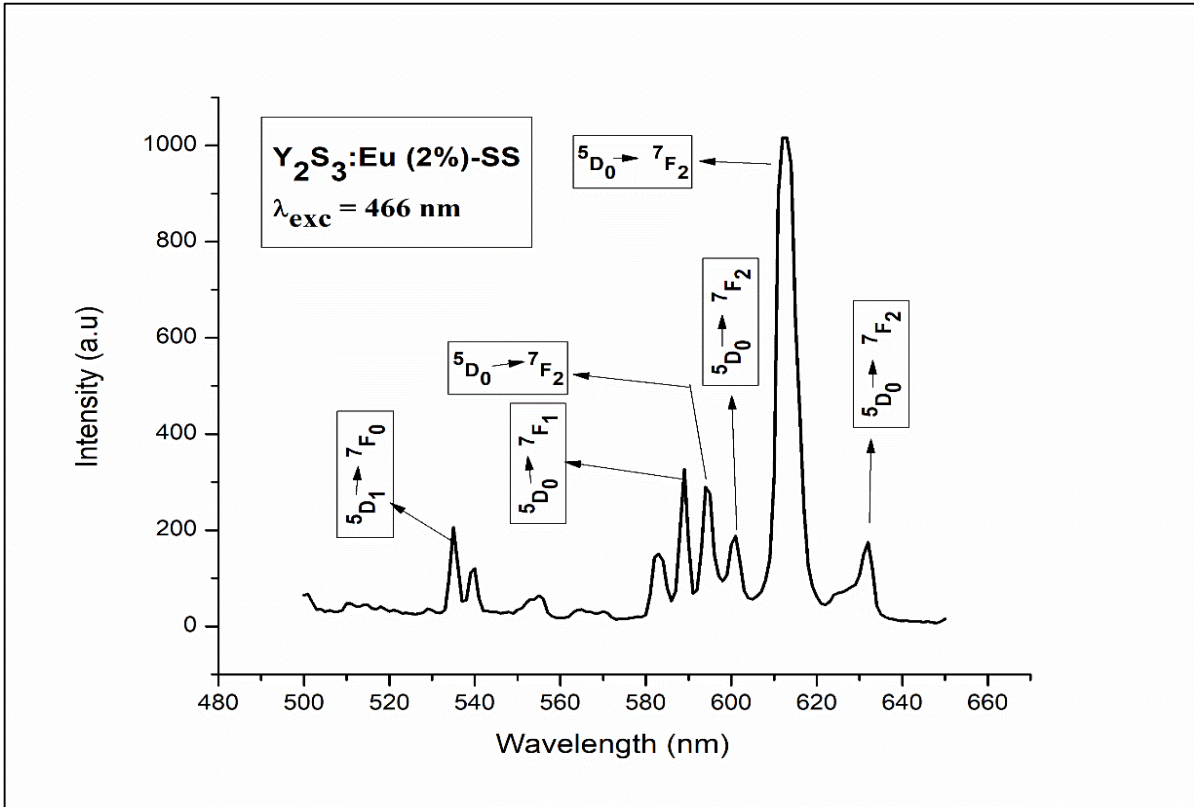
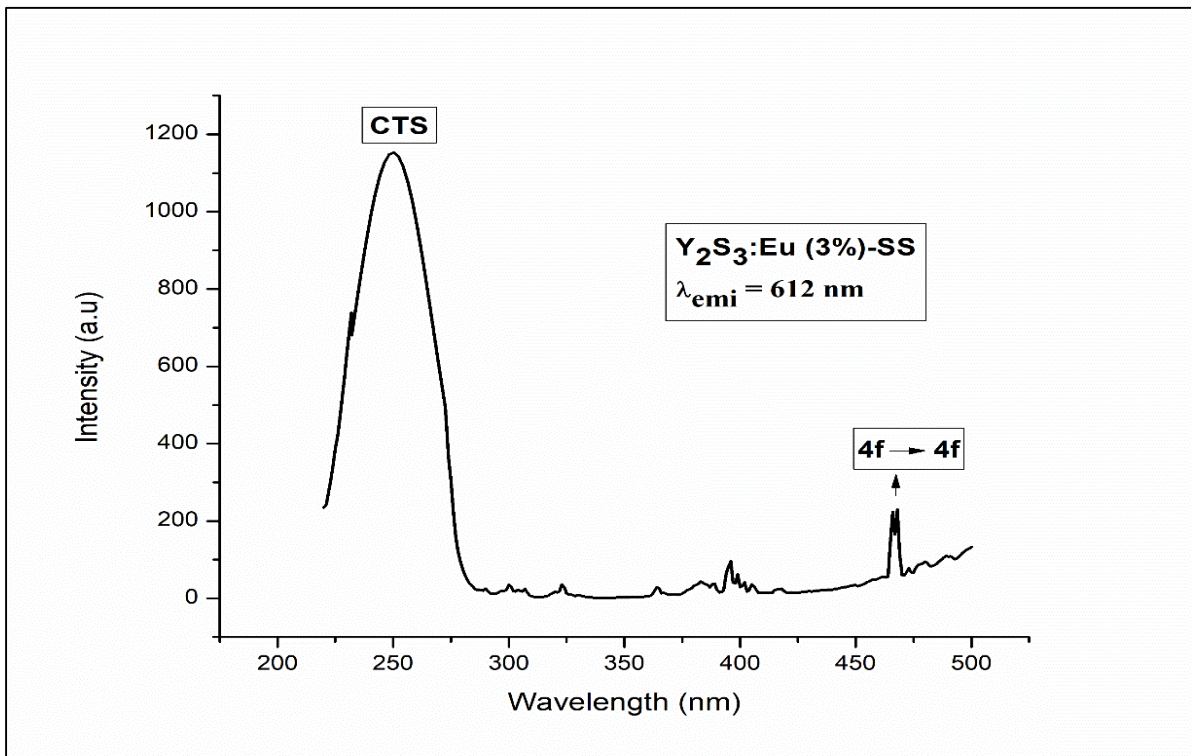


Figure 4-65: Photoluminescence spectra for  $Y_2S_3:Eu$  (2%)  
 [(a) YE2-SS Excitation at  $\lambda_{emi}$  of 612 nm (b) YE2-SS Emission at  $\lambda_{exc}$  of 254 nm  
 (c) YE2-SS Emission at  $\lambda_{exc}$  of 466 nm]



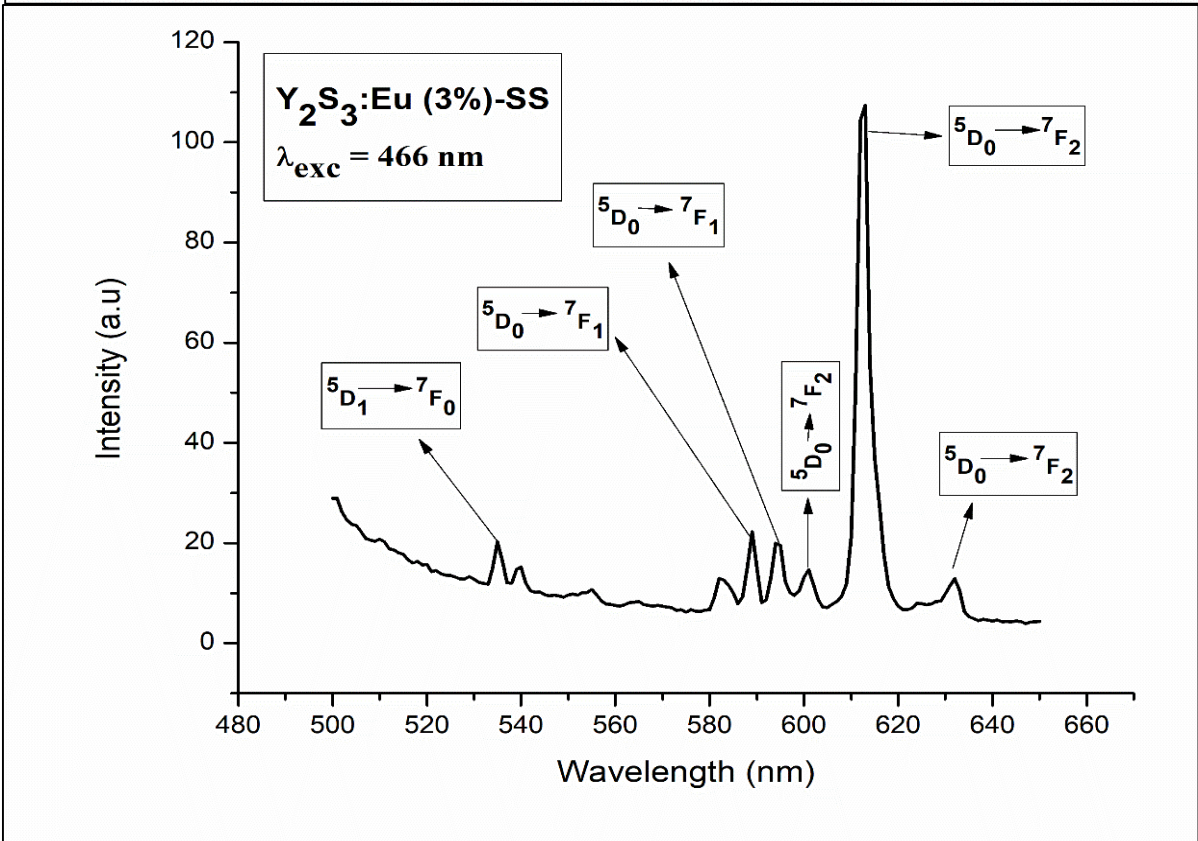
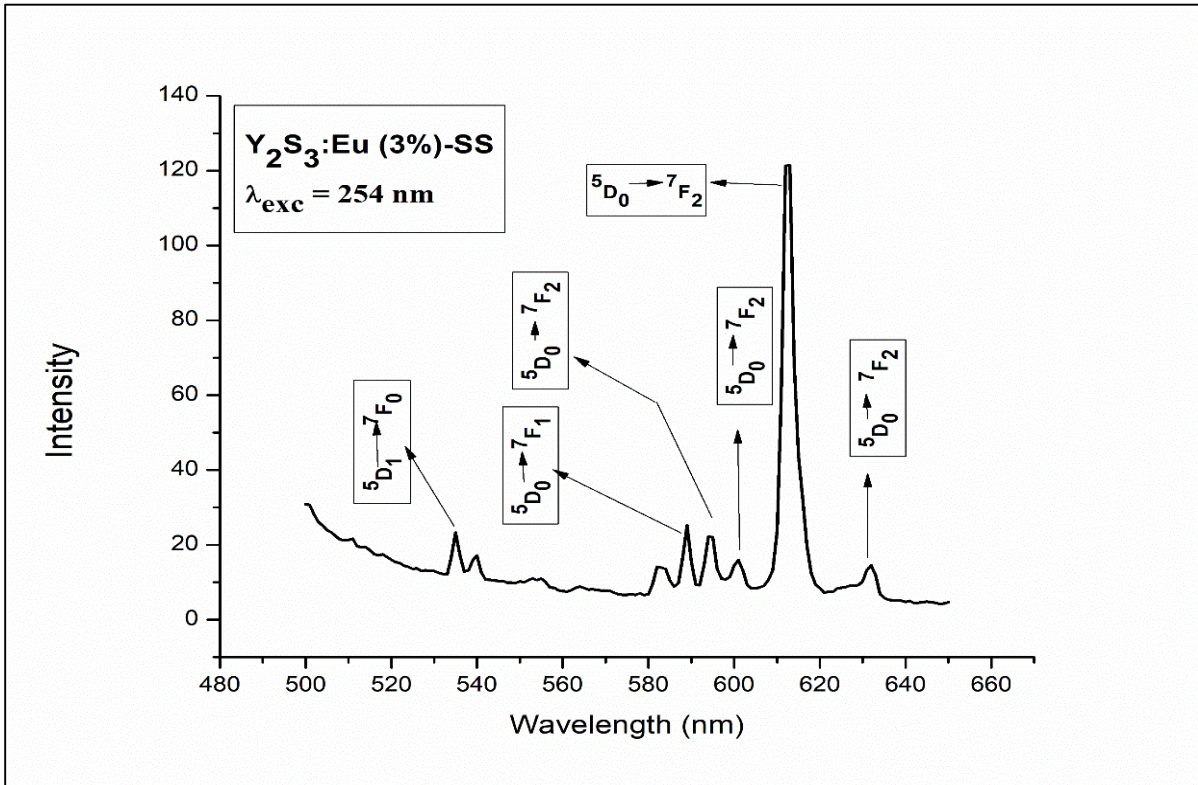


Figure 4-66 Photoluminescence spectra for  $Y_2S_3:Eu$  (3%)  
 [(a) YE3-SS Excitation at  $\lambda_{emi}$  of 612 nm (b) YE3-SS Emission at  $\lambda_{exc}$  of 254 nm  
 (c) YE3-SS Emission at  $\lambda_{exc}$  of 466 nm]

The excitation and emission spectra of 1%, 2% and 3% Eu doped  $Y_2S_3$  are shown in Fig. 4-64 to 4-66. The excitation spectra of  $Y_2S_3$  for all the doping percentages of Eu show an intense peak at 254 nm which is due to the charge transfer (CTS) transition of  $Eu^{3+}$  ions and additional small peak at 466 nm due to the 4f–4f transitions of  $Eu^{3+}$  ions.

For an excitation of 254 nm and 466 nm, the emission spectrum of all the doping percentages from 1% to 3% of Eu shows an intense peak at 613 nm corresponding to the  $^5D_0 \rightarrow ^7F_2$  transition. The other peaks observed in the PL spectra are located at 535 nm, 588 nm, 595 nm and 631 nm which can be attributed to the transitions  $^5D_1 \rightarrow ^7F_0$ ,  $^5D_0 \rightarrow ^7F_1$ ,  $^5D_0 \rightarrow ^7F_2$  and  $^5D_0 \rightarrow ^7F_2$  of  $Eu^{3+}$  ions. In 2% and 3% Eu doping, an additional small peak is observed at 600 nm which can be attributed to the  $^5D_0 \rightarrow ^7F_2$  transition of  $Eu^{3+}$  ions. It can be seen that as doping percentage of Eu is increased from 1% to 2%, the intensity of emissions increases and then for 3% of Eu doping, the intensity decreases.

**4.5.7 PL of Terbium (Tb) Doped Yttrium Sulphide ( $Y_2S_3$ ) synthesized by Solid State Method**

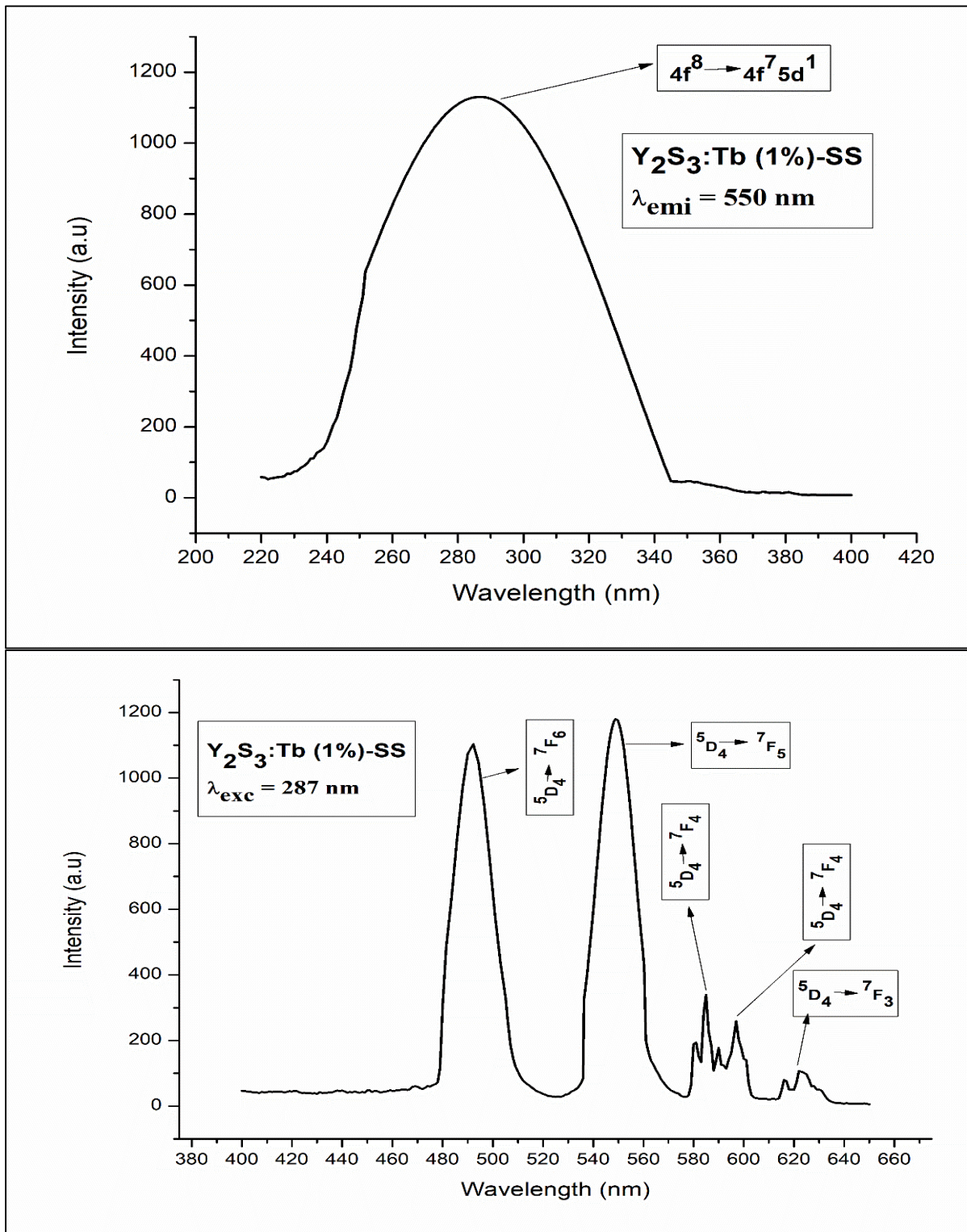


Figure 4-67: Photoluminescence spectra for  $Y_2S_3:Tb$  (1%)  
 [(a) YT1-SS Excitation at  $\lambda_{emi}$  of 550 nm (b) YT1-SS Emission at  $\lambda_{exc}$  of 287 nm]

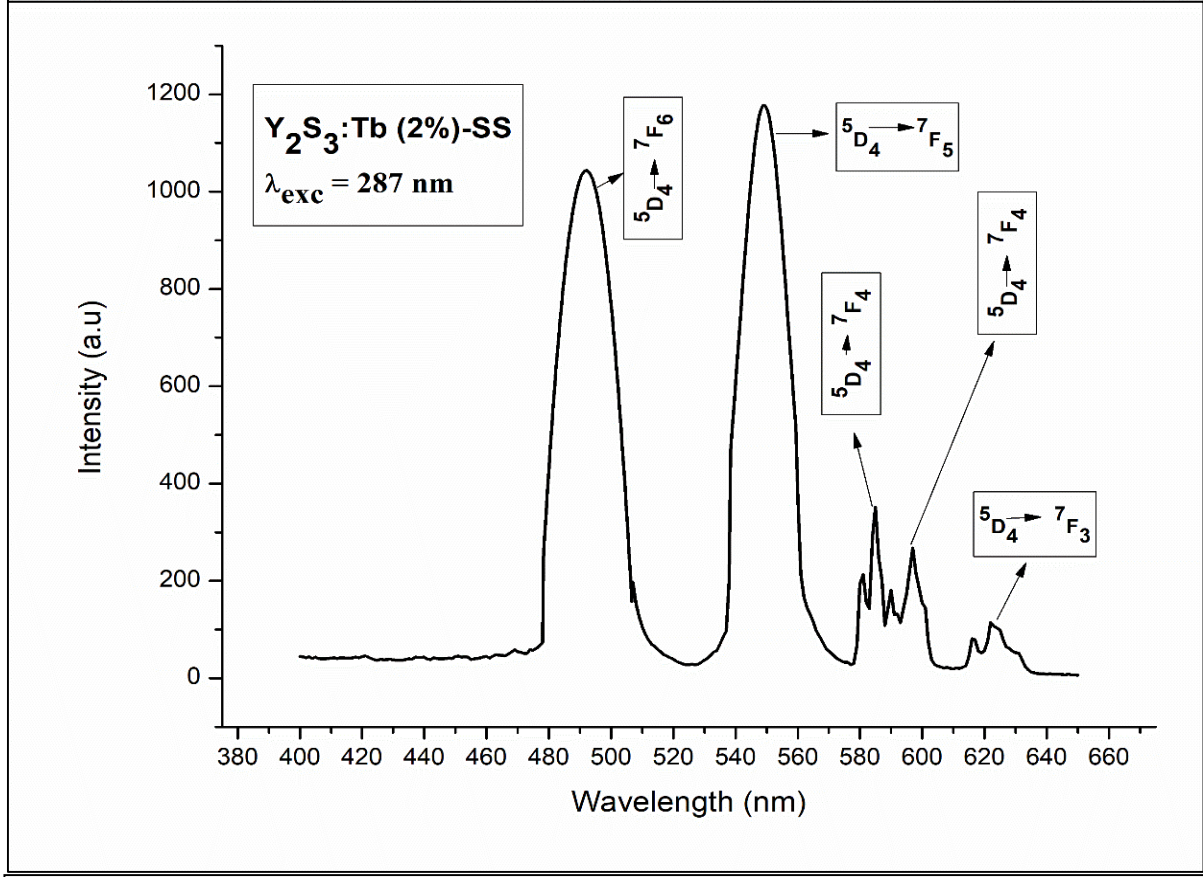
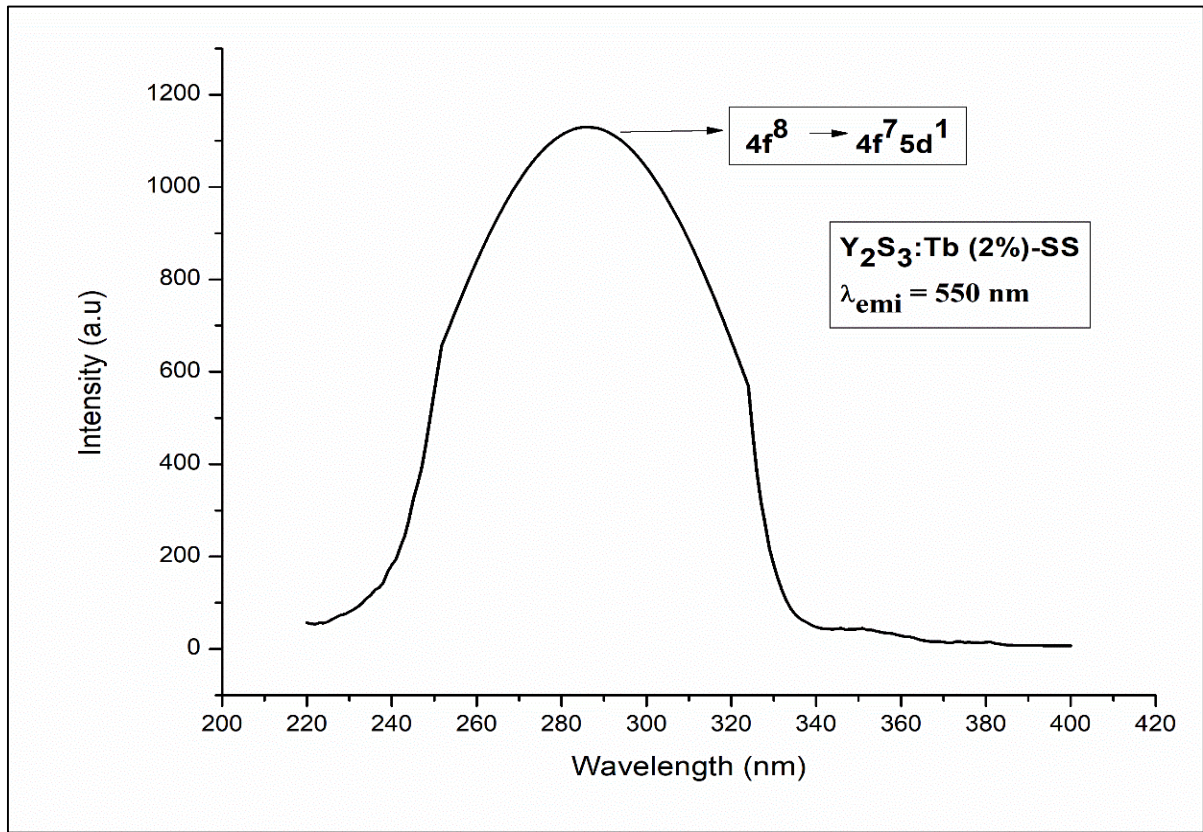


Figure 4-68: Photoluminescence spectra for  $Y_2S_3:Tb$  (2%)  
 [(a) YT2-SS Excitation at  $\lambda_{emi}$  of 550 nm (b) YT2-SS Emission at  $\lambda_{exc}$  of 287 nm]

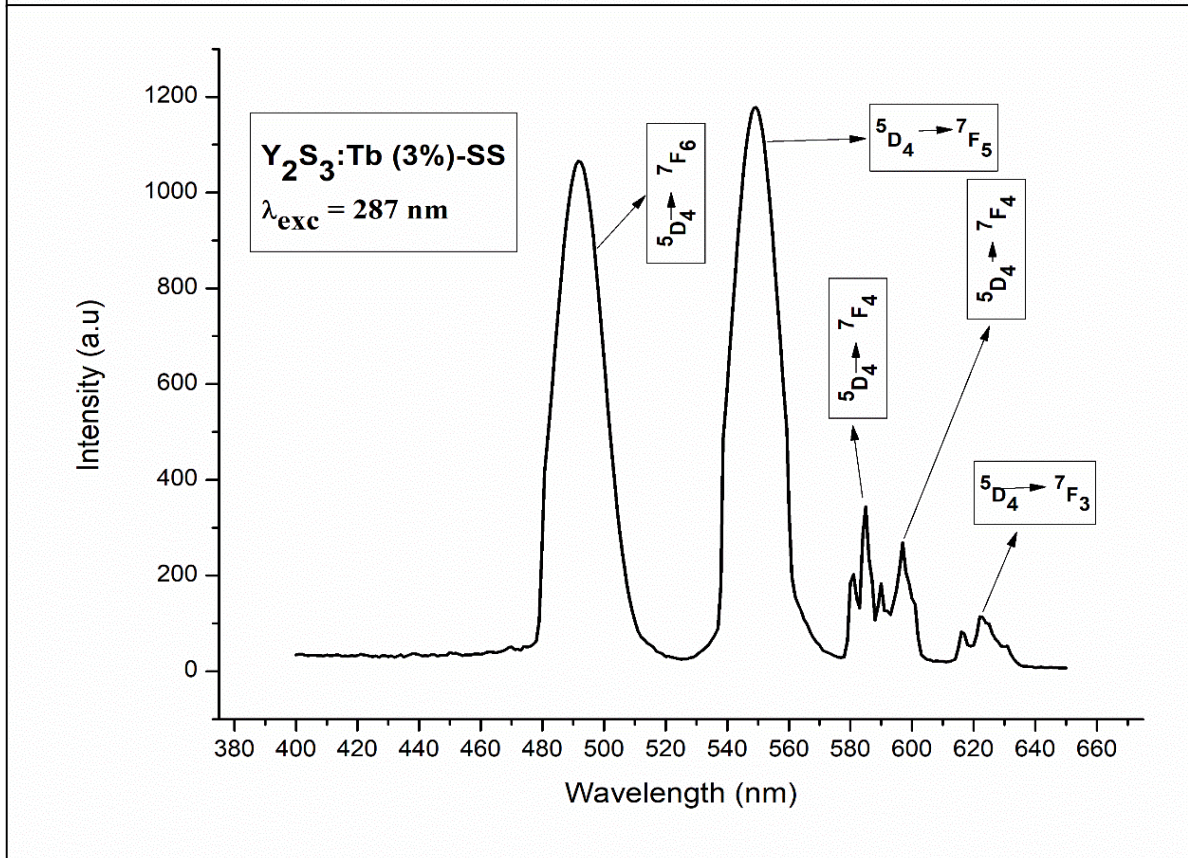
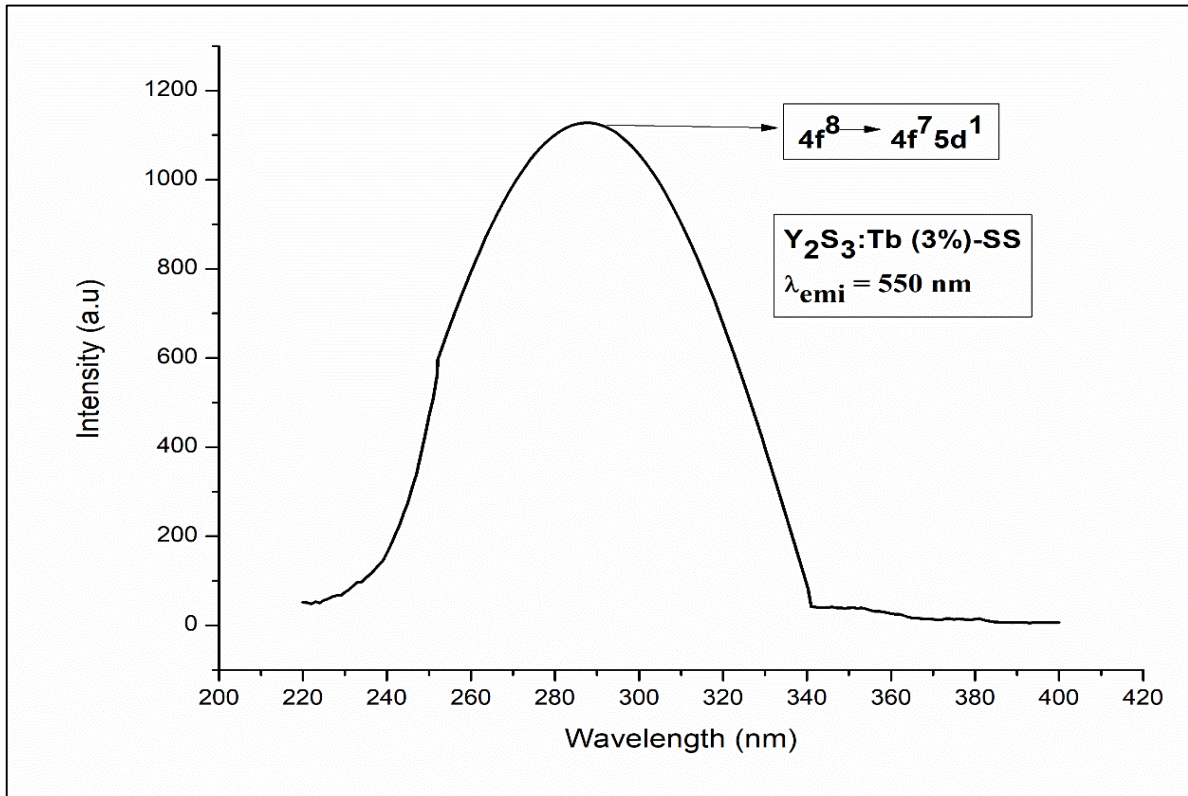


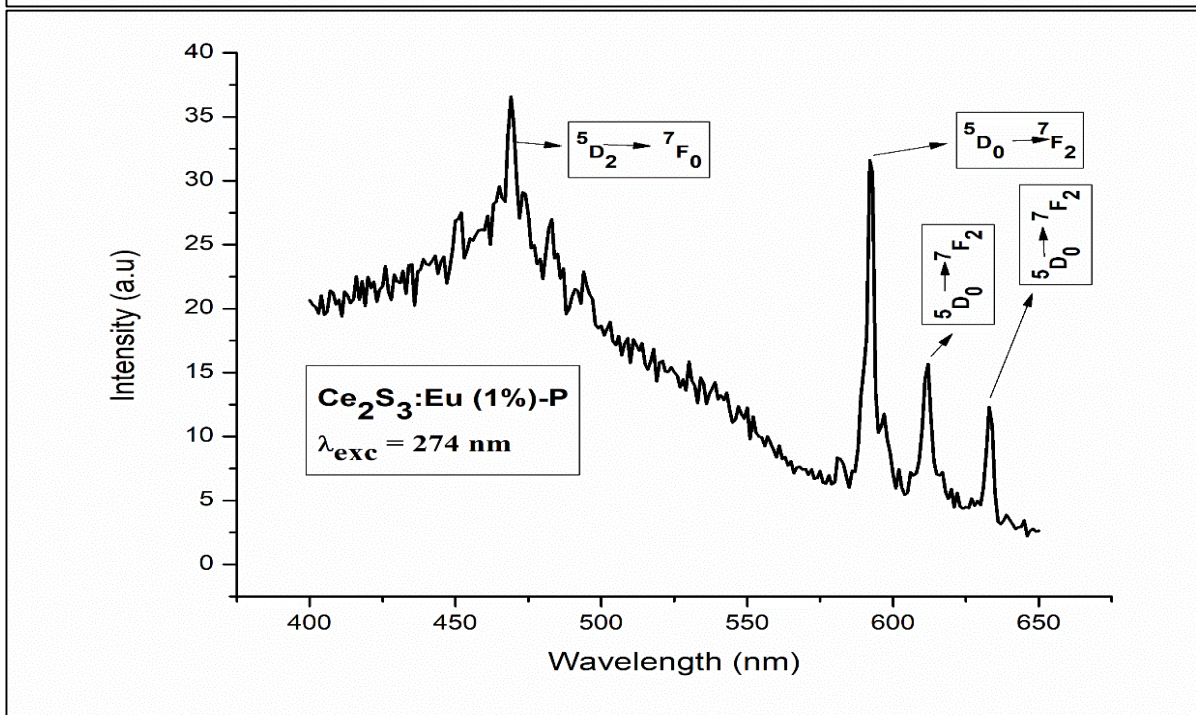
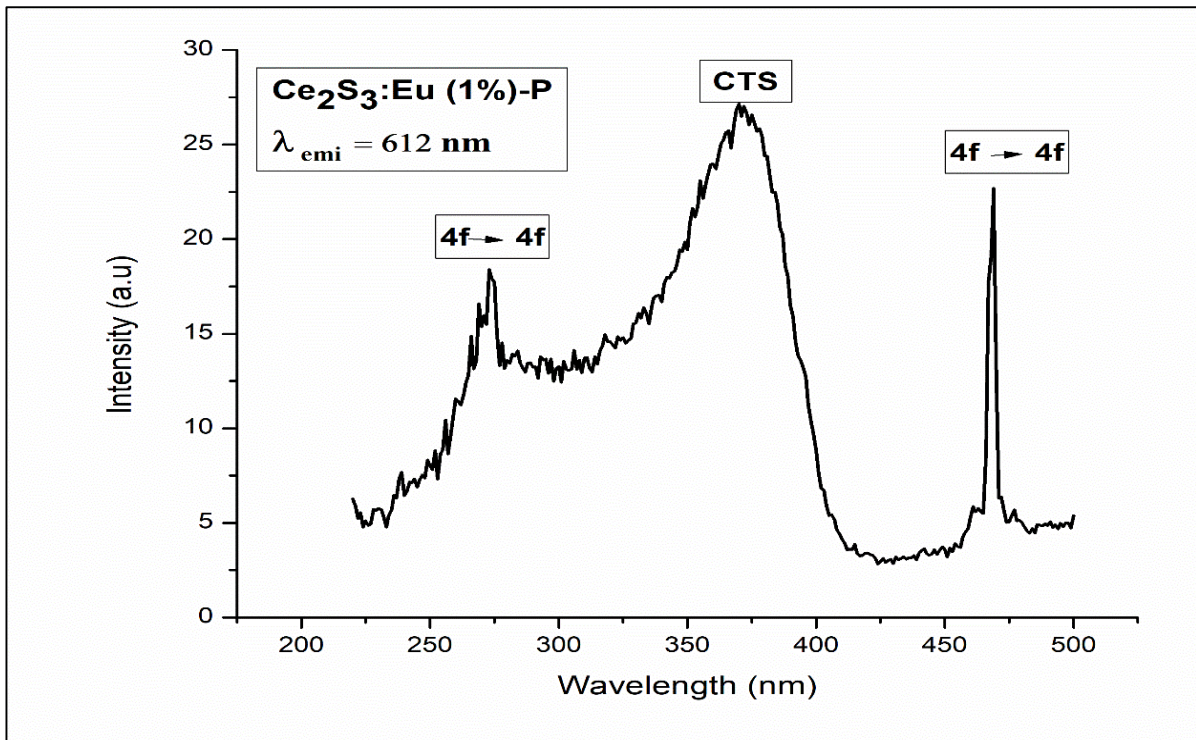
Figure 4-69: Photoluminescence spectra for  $Y_2S_3:Tb (3\%)$   
 [(a) YT3-SS Excitation at  $\lambda_{emi}$  of 550 nm (b) YT3-SS Emission at  $\lambda_{exc}$  of 287 nm]

The Photoluminescence characteristics of Yttrium sulphide ( $Y_2S_3$ ) with 1%, 2% and 3% of Tb doping are shown in Fig. 4-66 to 4-68. The excitation spectrum shows an intense peak at 287 nm for all the doping percentages of Tb which is due to the  $4f^8 \rightarrow 4f^7 5d^1$  transition of  $Tb^{3+}$  ion.

The emission spectrum consists of a series of peaks in the green region at 492 nm, 548 nm, 585 nm, 596 nm and 624 nm corresponding to the  $^5D_4 \rightarrow ^7F_6$ ,  $^5D_4 \rightarrow ^7F_5$ , and  $^5D_4 \rightarrow ^7F_4$  (585 nm and 596 nm) and  $^5D_4 \rightarrow ^7F_3$  transitions of  $Tb^{3+}$  ion respectively, out of which the peaks at 492 nm and 548 nm have high intensity. No appreciable change in intensity is found with different doping concentrations of Tb. It can also be observed that Yttrium sulphide does not give emission lines in the blue region of the spectrum. This is a major change in the results obtained for the same sample synthesized by Precipitation method, that is discussed elsewhere.

## Samples synthesized by Precipitation Method

### 4.5.8 PL of Europium (Eu) Doped Cerium Sulphide ( $\text{Ce}_2\text{S}_3$ ) synthesized by Precipitation Method



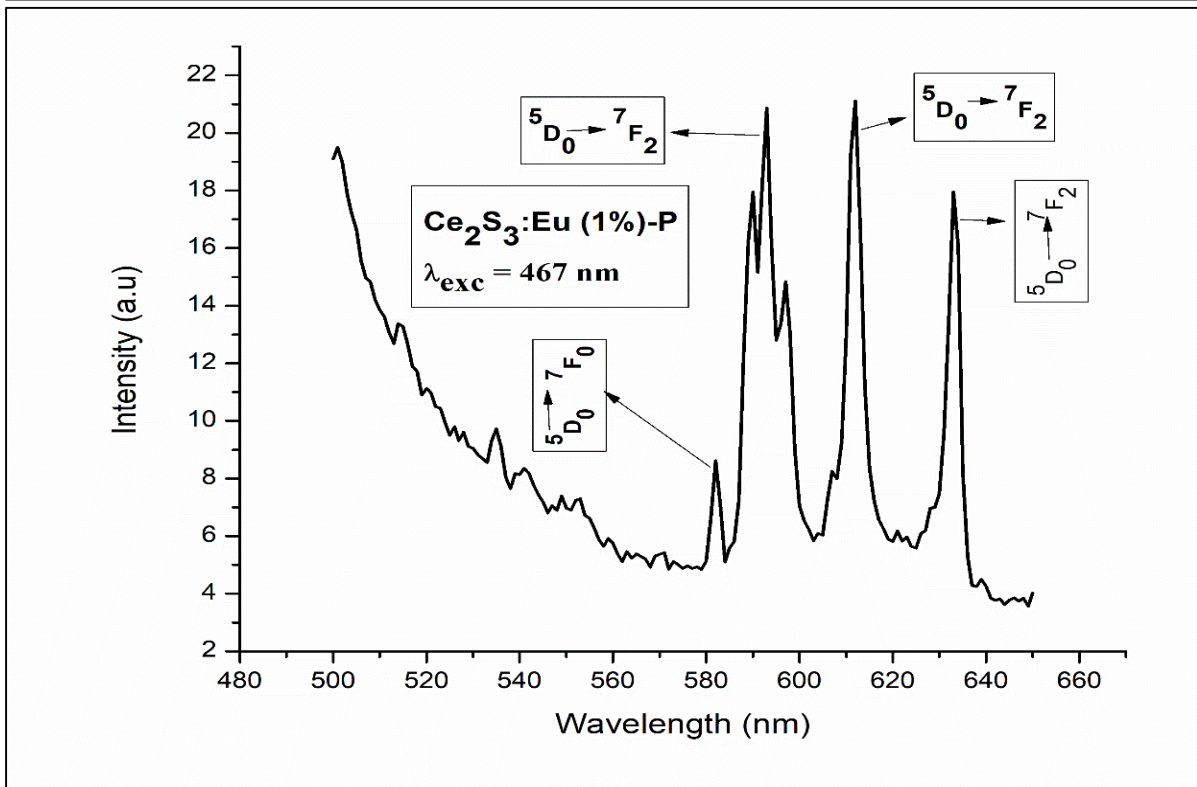
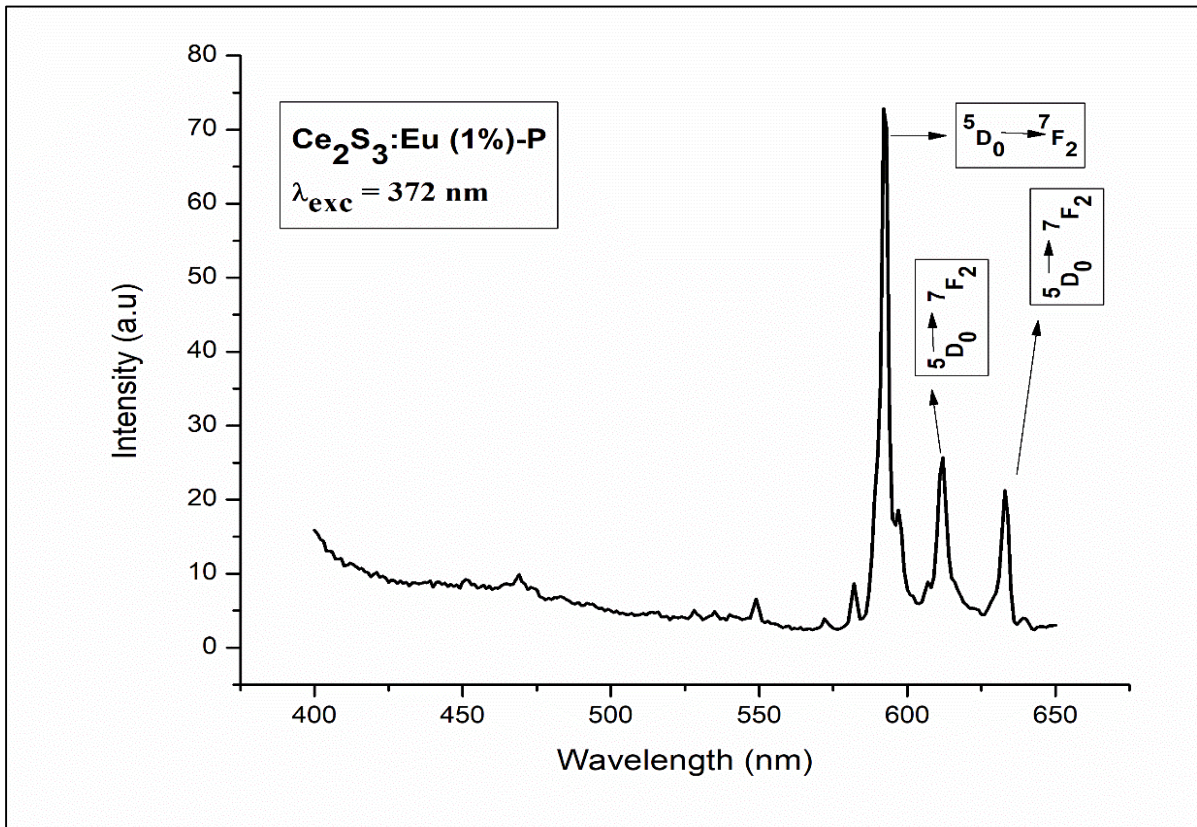
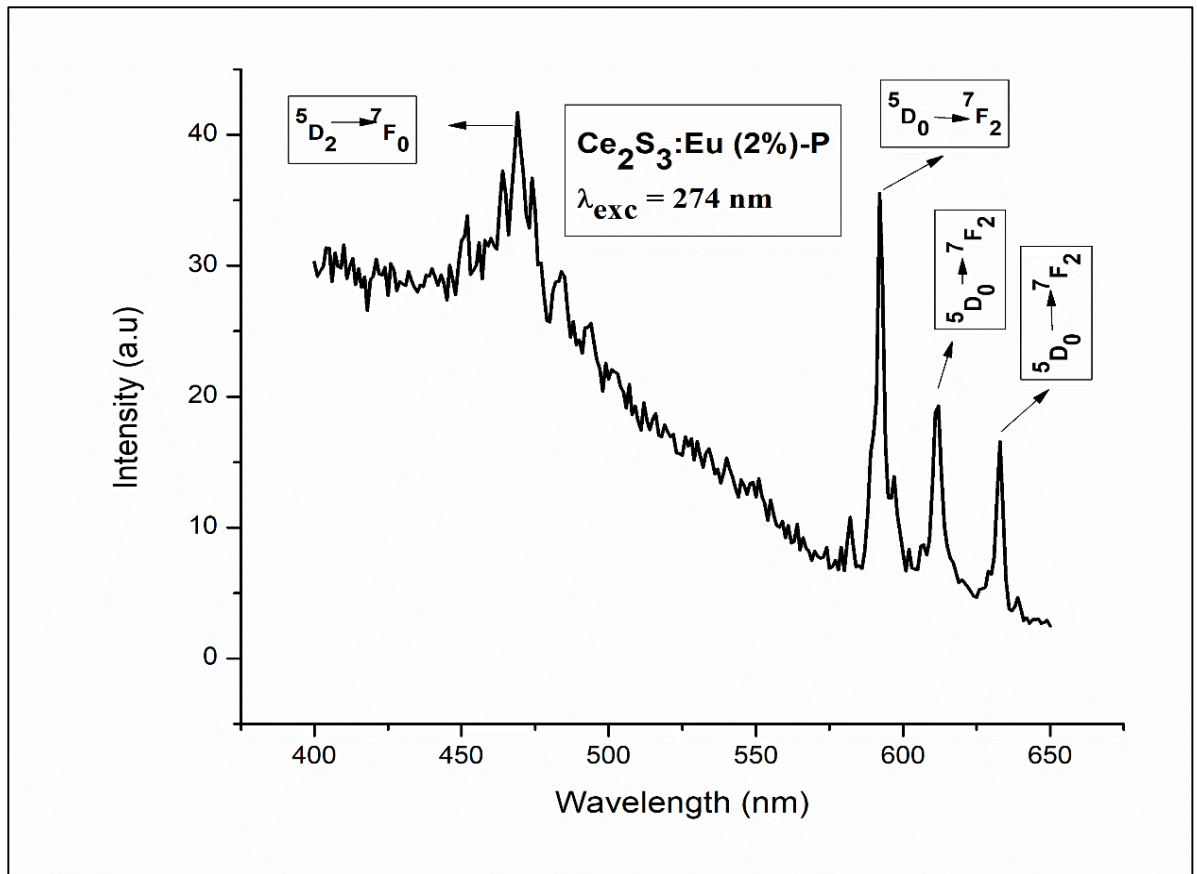
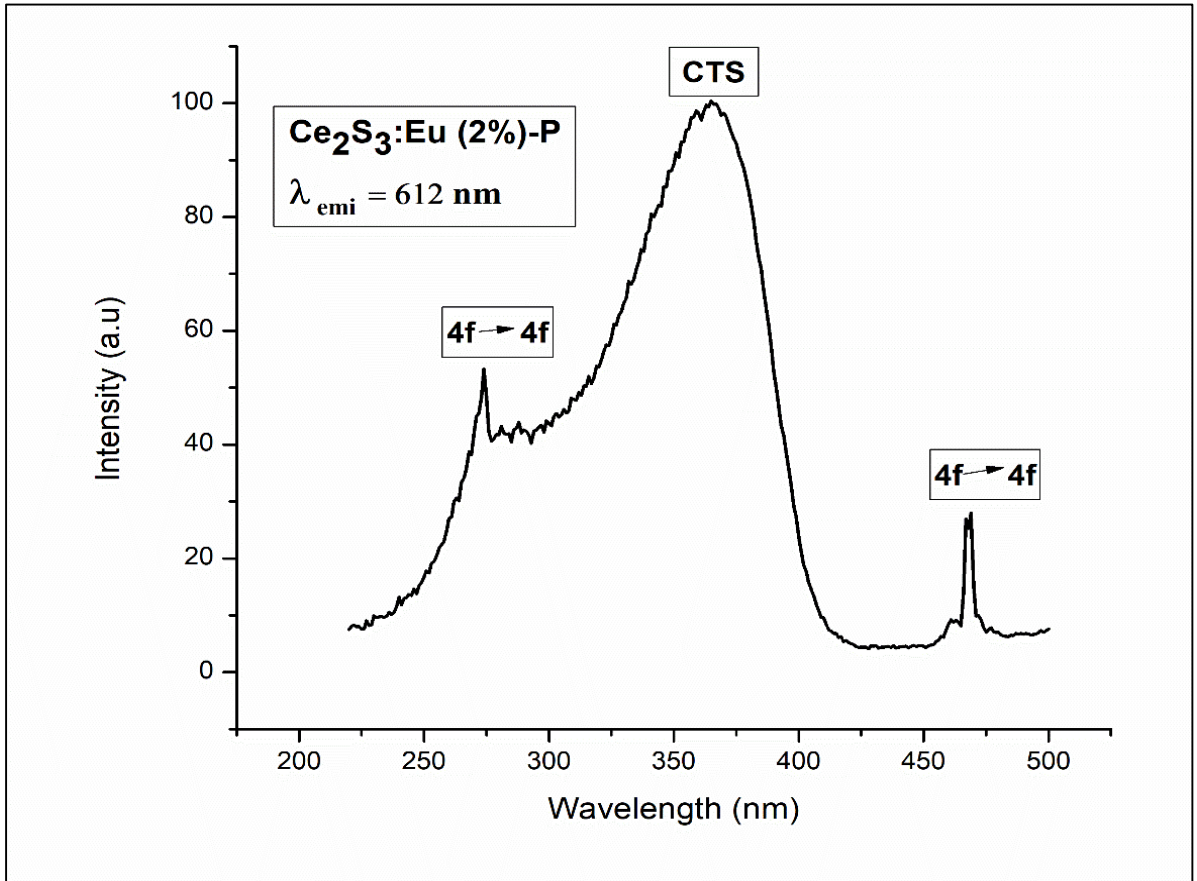


Figure 4-70: Photoluminescence spectra for Ce<sub>2</sub>S<sub>3</sub>:Eu (1%)  
 [(a) CeE1-P Excitation at  $\lambda_{emi}$  of 612 nm (b) CeE1-P Emission at  $\lambda_{exc}$  of 274 nm  
 (c) CeE1-P Emission at  $\lambda_{exc}$  of 372 nm (d) CeE1-P Emission at  $\lambda_{exc}$  of 467 nm]



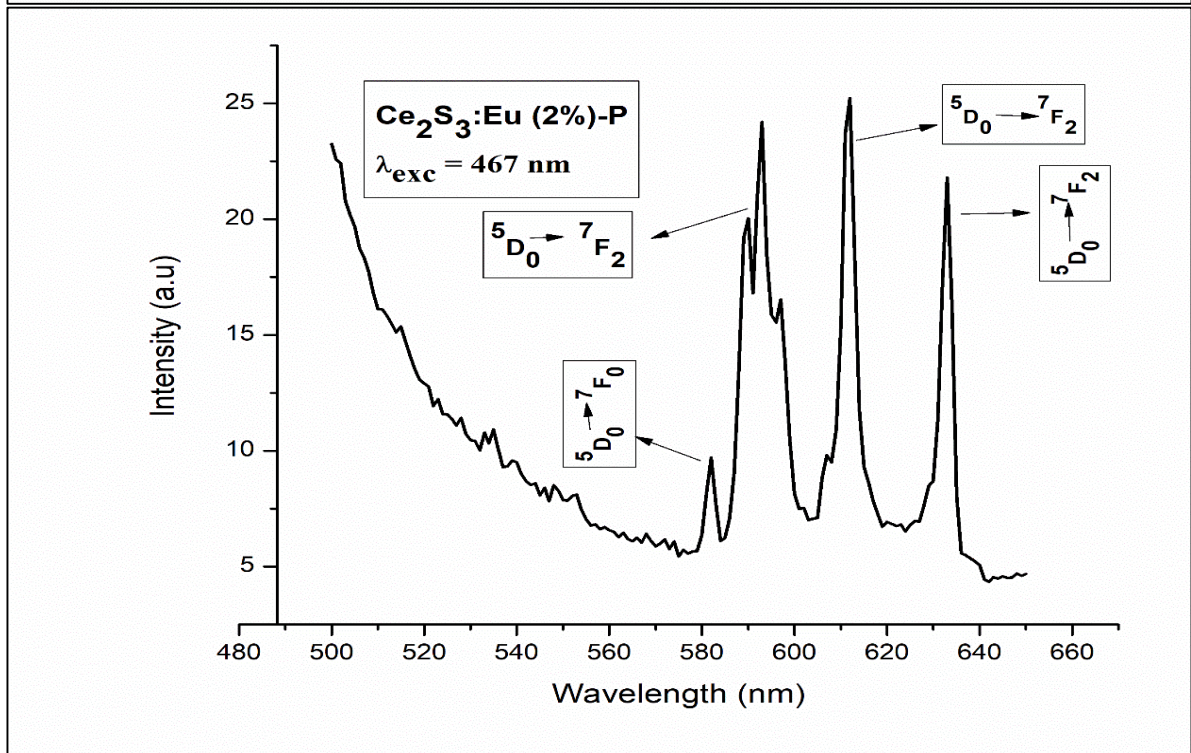
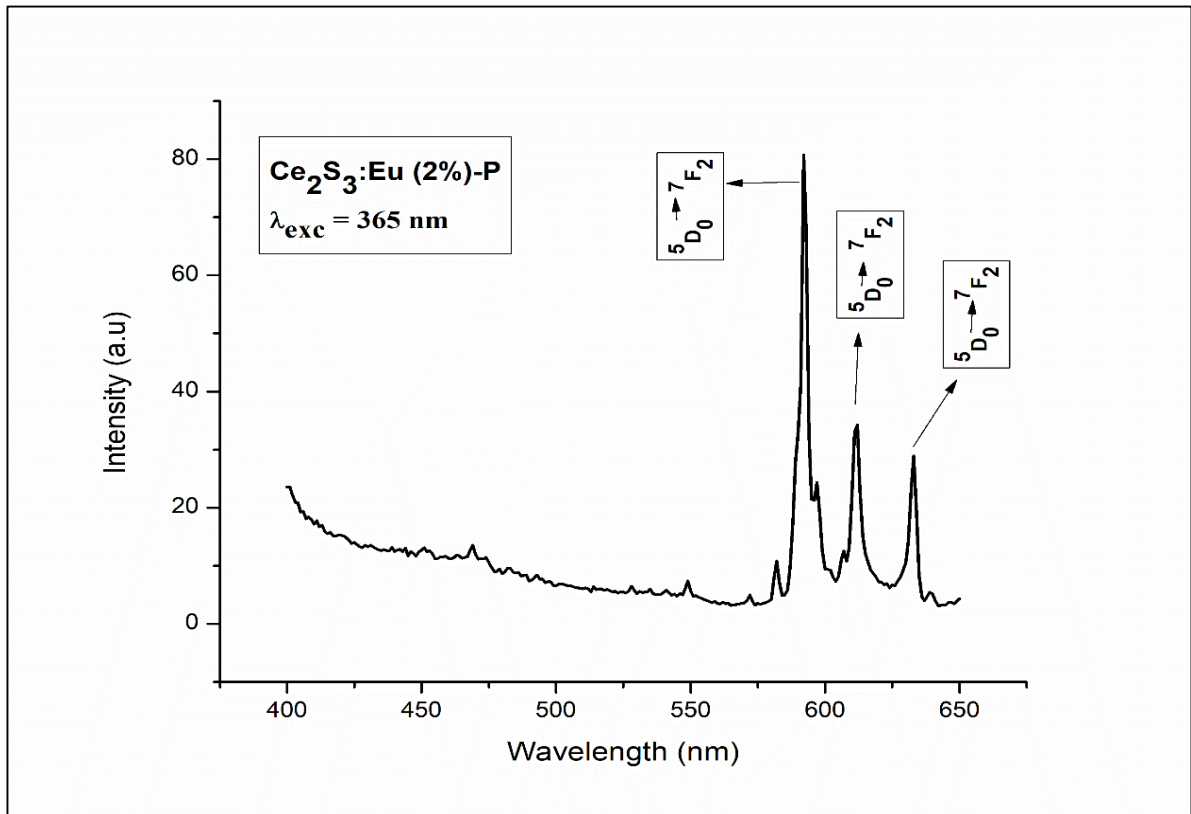
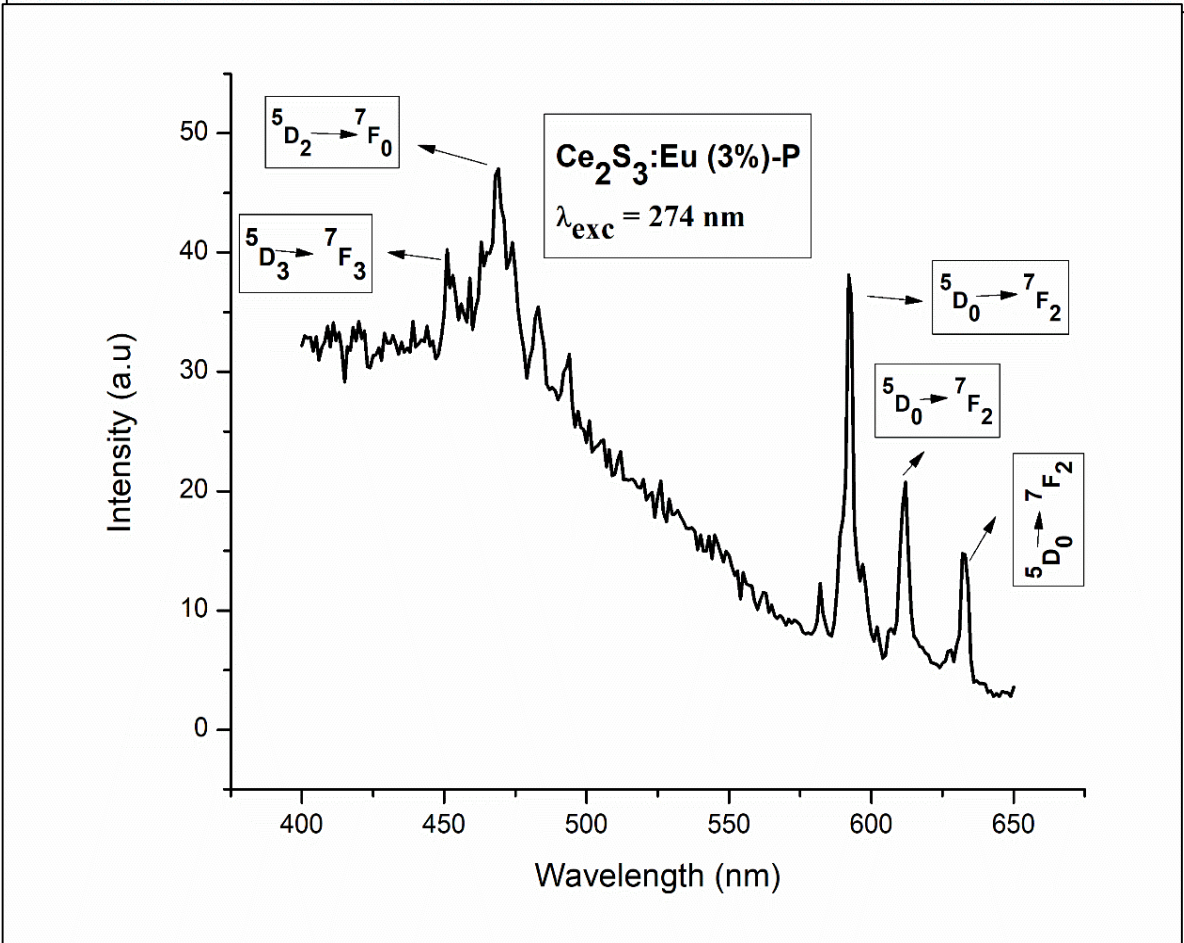
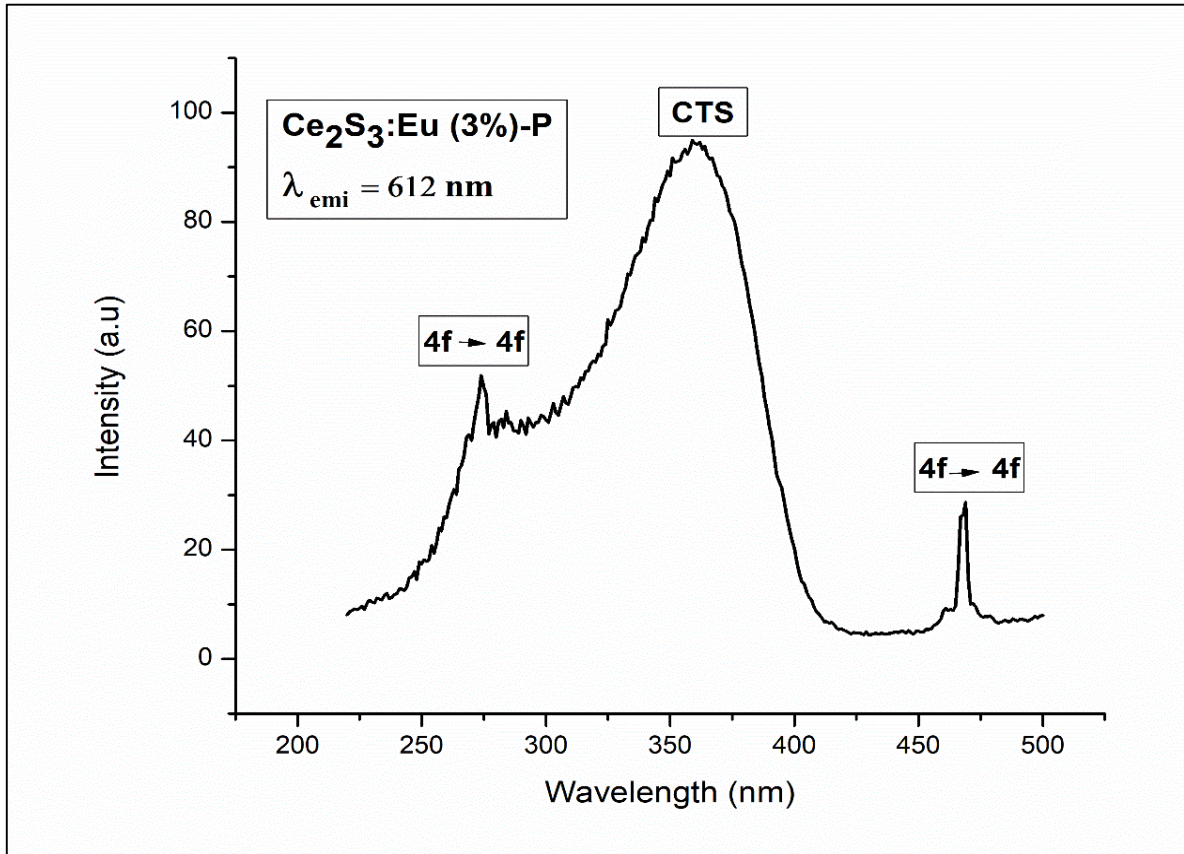


Figure 4-71: Photoluminescence spectra for Ce<sub>2</sub>S<sub>3</sub>:Eu (2%)

[(a) CeE2-P Excitation at  $\lambda_{\text{emi}}$  of 612 nm (b) CeE2-P Emission at  $\lambda_{\text{exc}}$  of 274 nm  
(c) CeE2-P Emission at  $\lambda_{\text{exc}}$  of 365 nm (d) CeE2-P Emission at  $\lambda_{\text{exc}}$  of 467 nm]



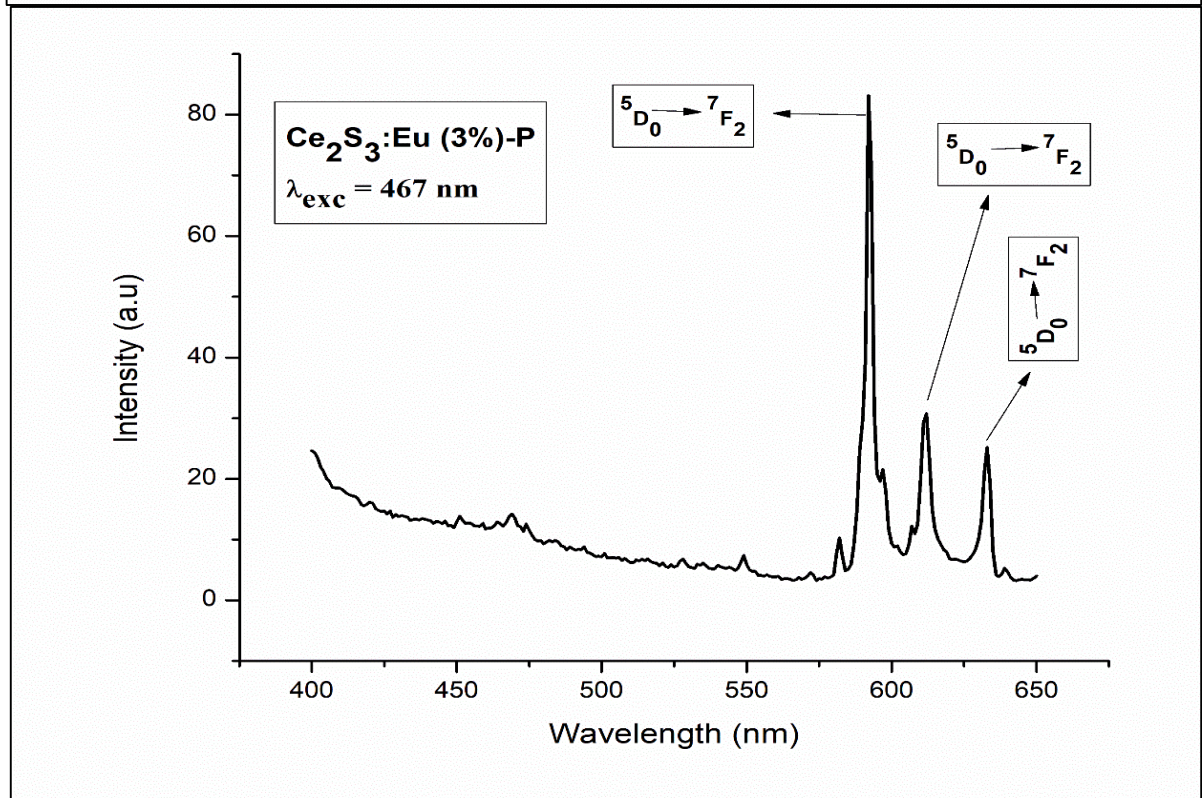
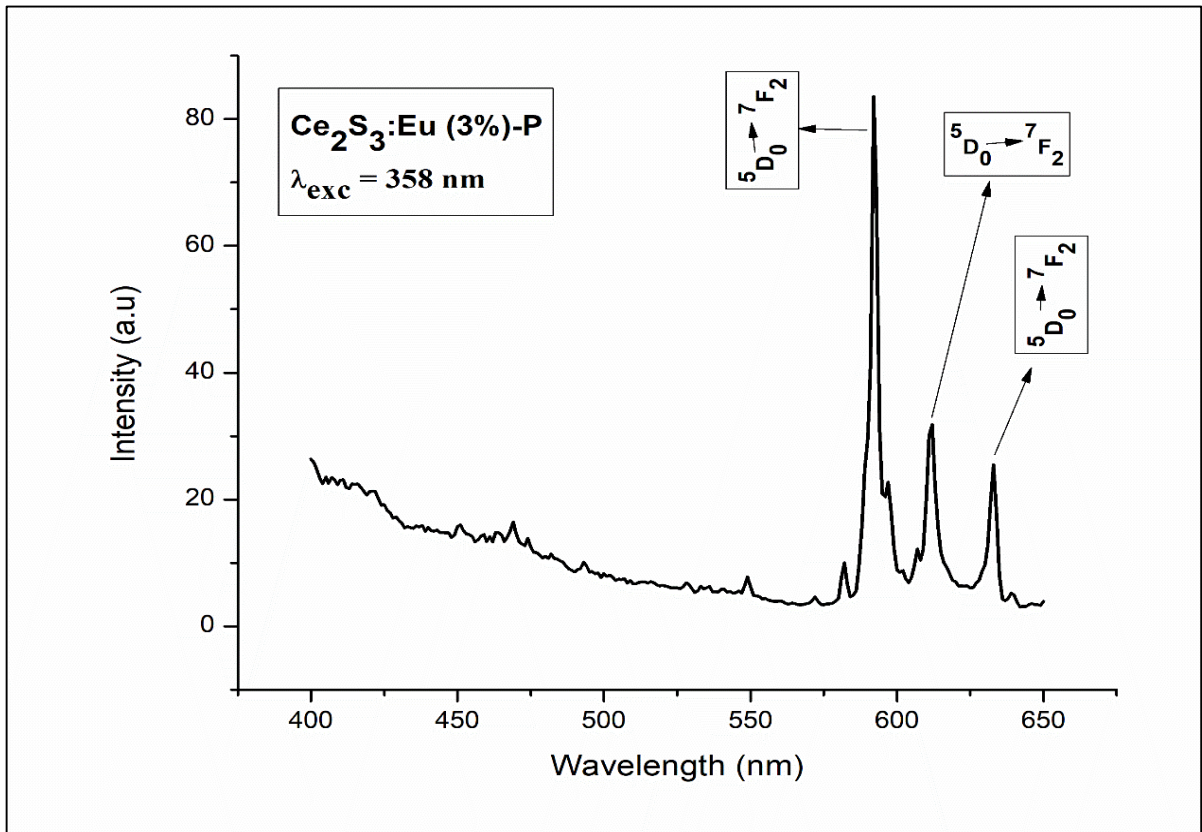


Figure 4-72: Photoluminescence spectra for Ce<sub>2</sub>S<sub>3</sub>:Eu (3%)

[(a) CeE3-P Excitation at  $\lambda_{\text{emi}}$  of 612 nm (b) CeE3-P Emission at  $\lambda_{\text{exc}}$  of 274 nm  
(c) CeE3-P Emission at  $\lambda_{\text{exc}}$  of 358 nm (d) CeE3-P Emission at  $\lambda_{\text{exc}}$  of 467 nm]

The graphs in Fig. 4-70, 4-71 and 4-72 show excitation and emission spectra of Ce<sub>2</sub>S<sub>3</sub> with 1%, 2% and 3% of Eu doping. The excitation spectra of all three samples show peaks at 274 nm and 467 nm which can be attributed to the 4f–4f transitions of Eu<sup>3+</sup> ions. The maximum intensity peak in 1% doping is at 372 nm, for 2% doping it is at 365 nm and that for 3% Eu doping it is at 358 nm. All these broadband peaks are attributed to the charge transfer (CTS) transition of Eu<sup>3+</sup> ions.

The emission spectrum shows an intense peak at 592 nm and second intense peak at 612 nm corresponding to the <sup>5</sup>D<sub>0</sub> → <sup>7</sup>F<sub>2</sub> transition for all excitations in all samples with different doping amount. All three samples give peaks at 468 nm corresponding to the transition <sup>5</sup>D<sub>2</sub> → <sup>7</sup>F<sub>0</sub> apart from peaks at 592 nm, 612 nm and 633 nm corresponding to the transition <sup>5</sup>D<sub>0</sub> → <sup>7</sup>F<sub>2</sub> for their common excitation wavelength of 274 nm. However, an additional peak is observed at 451 nm corresponding to <sup>5</sup>D<sub>3</sub> → <sup>7</sup>F<sub>3</sub> transition for 3% Eu doping.

Peaks are observed at 592 nm, 612 nm, and 633 nm corresponding to the <sup>5</sup>D<sub>0</sub> → <sup>7</sup>F<sub>2</sub> transition in 1%, 2% and 3% Eu doping for their respective excitation wavelengths of 372 nm, 365 nm and 358 nm respectively. For excitation of 467 nm, the common peaks at 592 nm, 612 nm and 633 nm corresponding to the <sup>5</sup>D<sub>0</sub> → <sup>7</sup>F<sub>2</sub> transitions of Eu<sup>3+</sup> ions are present in all three samples. However, in 1% and 2% Eu doping, an additional peak is seen at 582 nm which can be associated to the <sup>5</sup>D<sub>0</sub> → <sup>7</sup>F<sub>0</sub> transitions of Eu<sup>3+</sup> ions. The intensity of emission is found to increase with increase in doping percentage.

The Terbium (Tb) doped Ce<sub>2</sub>S<sub>3</sub> samples being dark in colour did not give luminescence and hence their excitation and emission spectra could not be obtained.

#### 4.5.9 PL of Europium (Eu) Doped Gadolinium Sulphide ( $Gd_2S_3$ ) synthesized by Precipitation Method

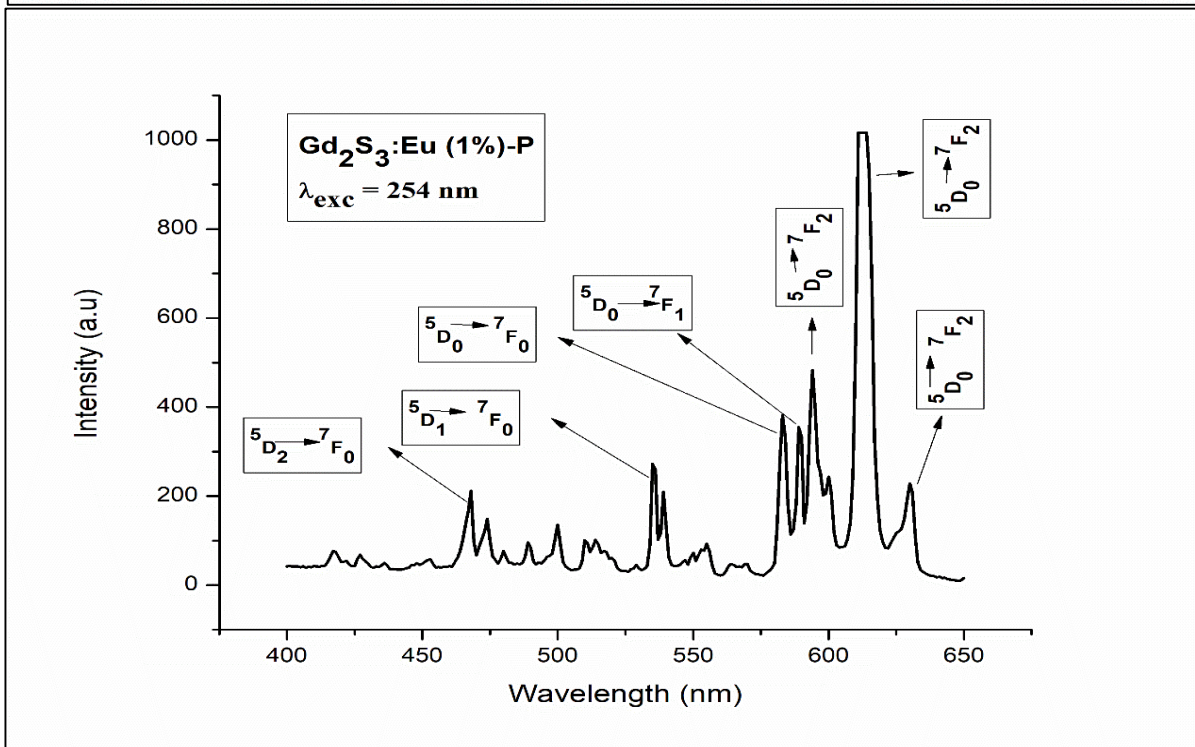
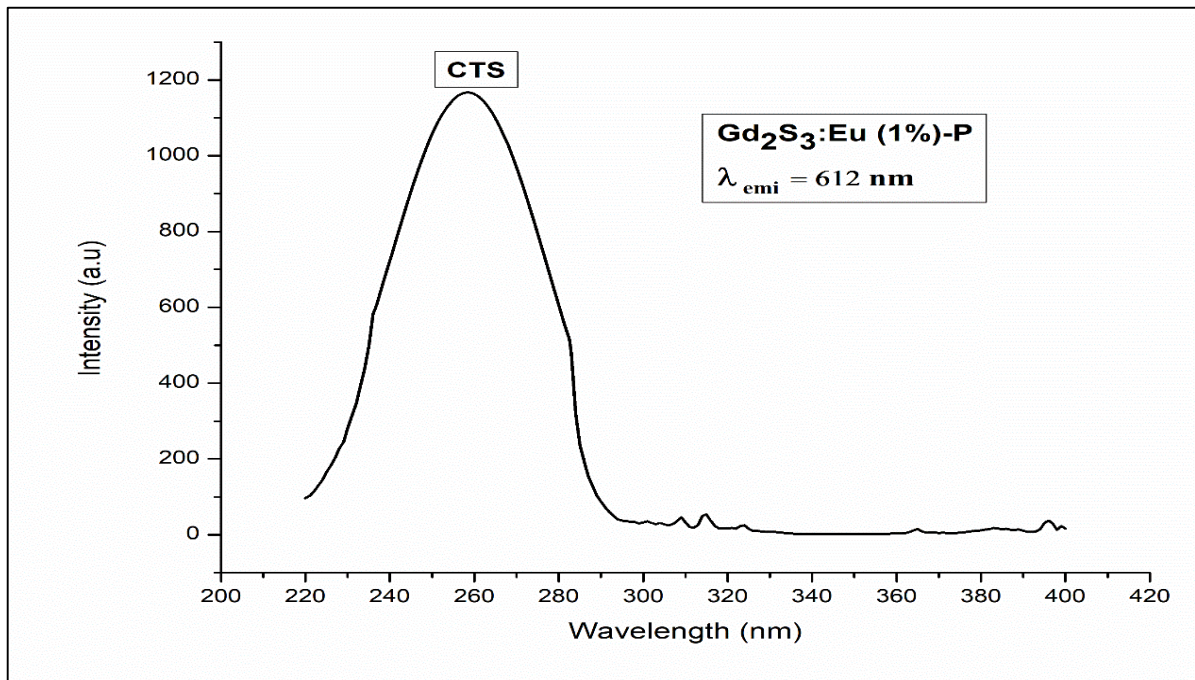
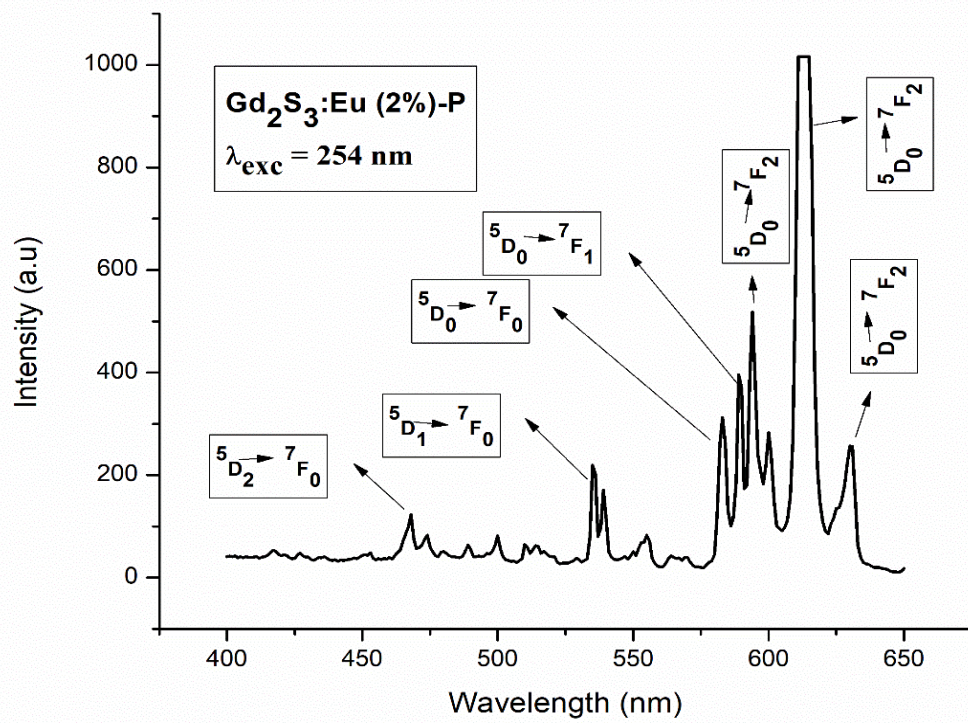
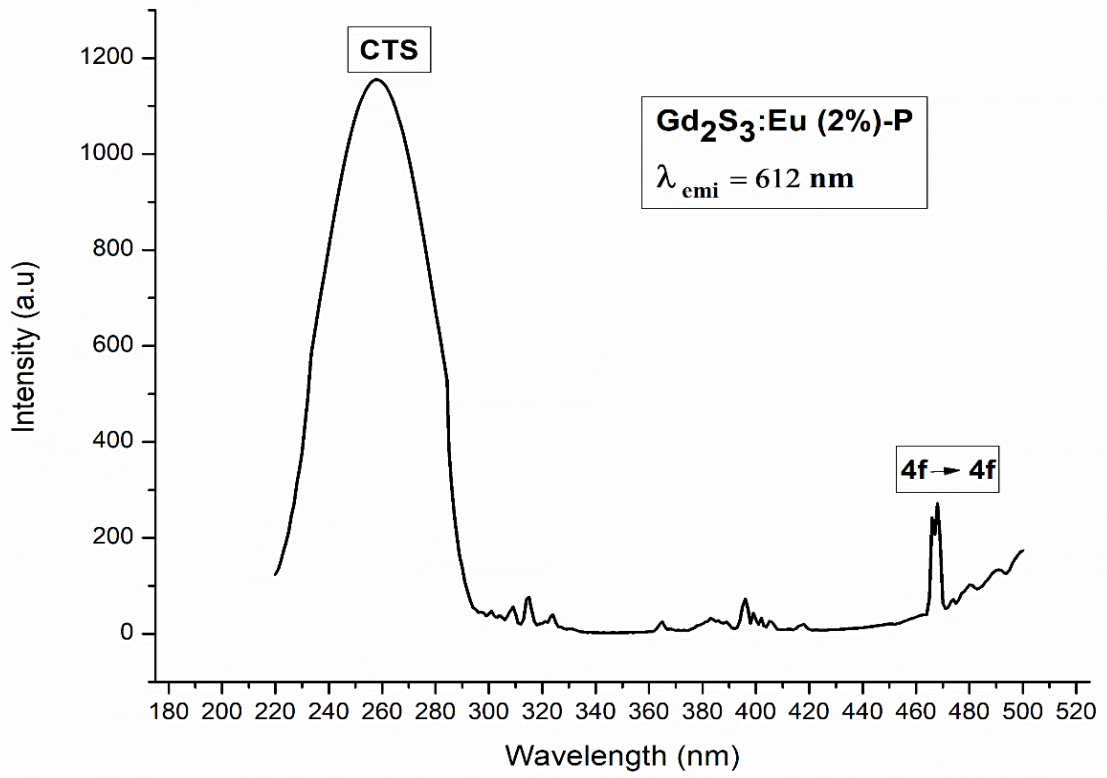


Figure 4-73: Photoluminescence spectra for  $Gd_2S_3:Eu (1\%)$   
[(a)  $GdE1-P$  Excitation at  $\lambda_{emi}$  of 612 nm (b)  $GdE1-P$  Emission at  $\lambda_{exc}$  of 254 nm]



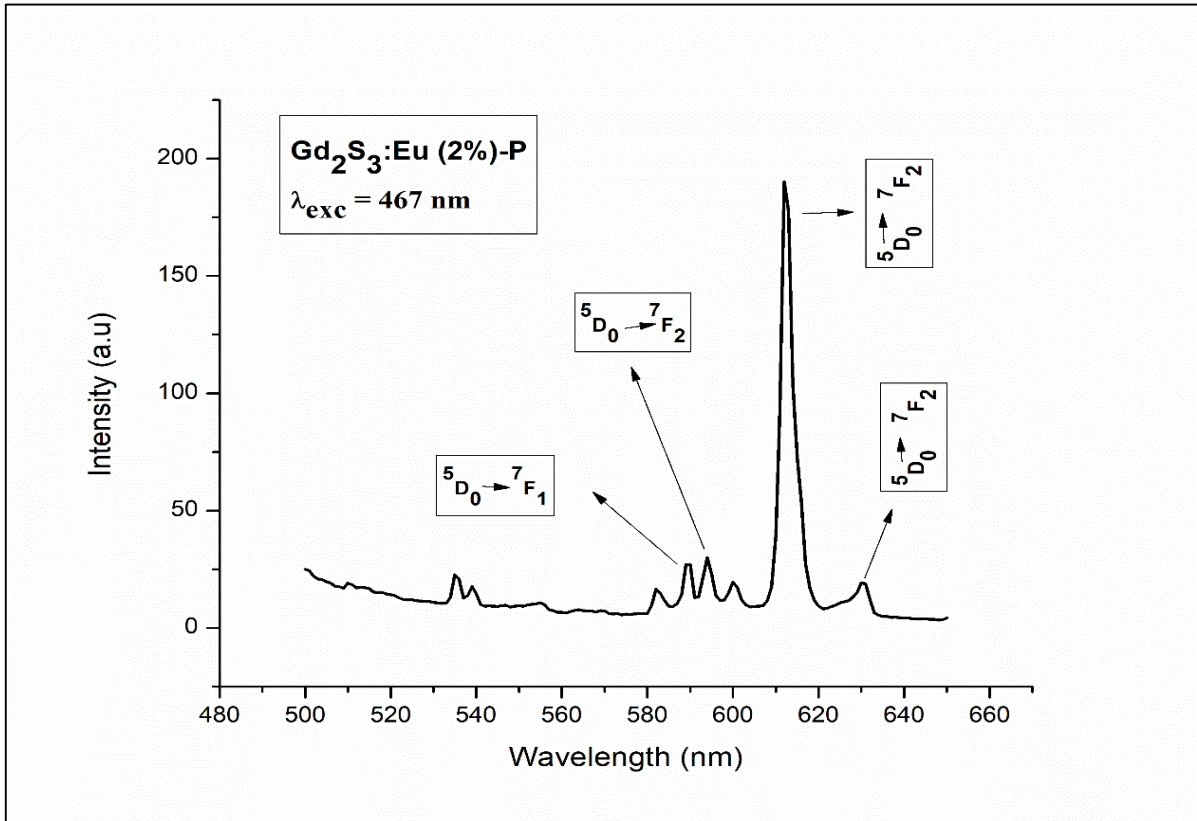
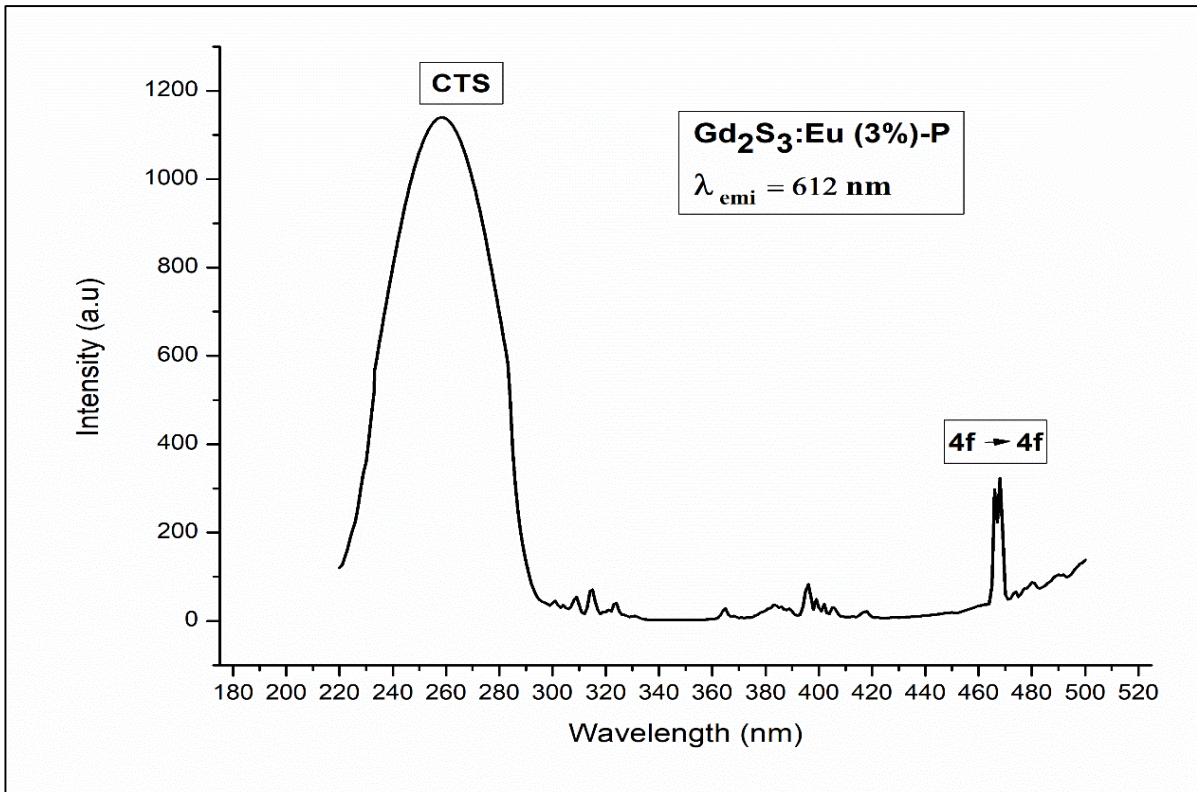


Figure 4-74: Photoluminescence spectra for  $\text{Gd}_2\text{S}_3:\text{Eu (2\%)}$   
 [(a)  $\text{GdE2-P}$  Excitation at  $\lambda_{\text{emi}}$  of 612 nm (b)  $\text{GdE2-P}$  Emission at  $\lambda_{\text{exc}}$  of 254 nm  
 (c)  $\text{GdE2-P}$  Emission at  $\lambda_{\text{exc}}$  of 467 nm]



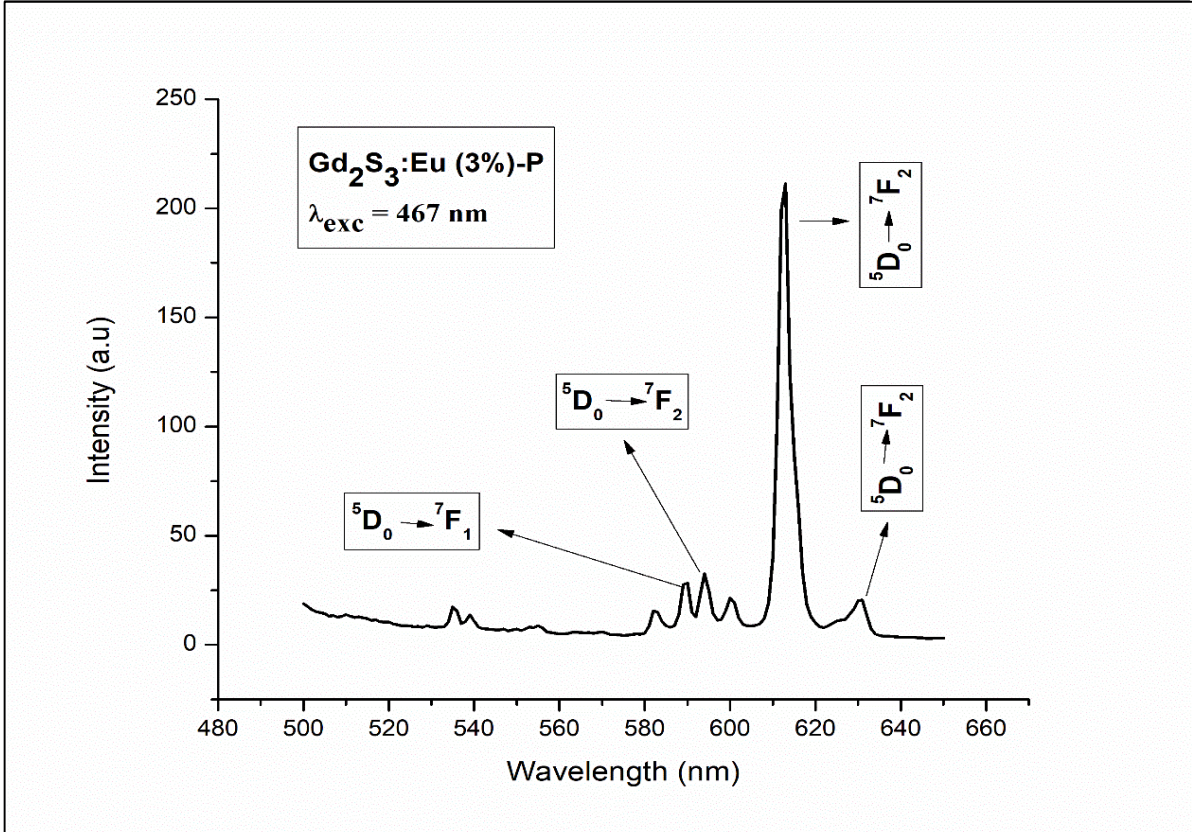
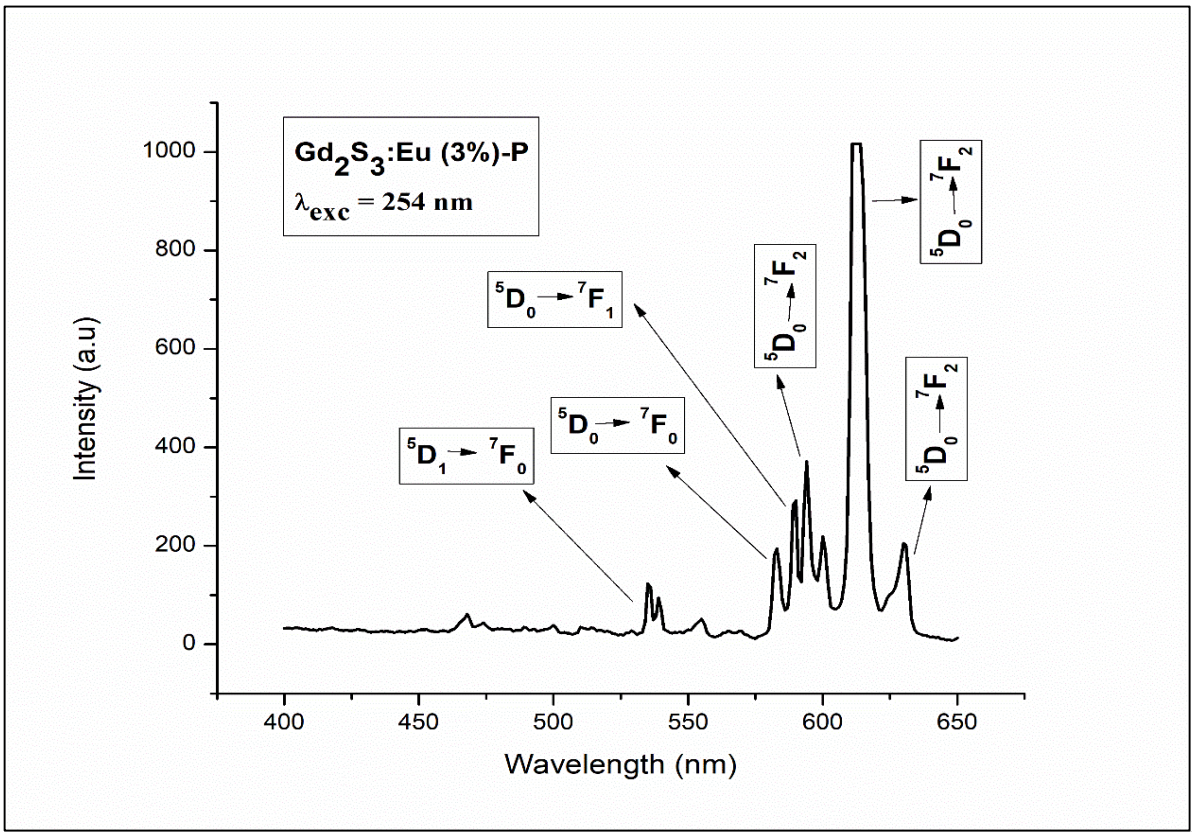


Figure 4-75: Photoluminescence spectra for  $Gd_2S_3:Eu$  (3%)  
 [(a) GdE3-P Excitation at  $\lambda_{emi}$  of 612 nm (b) GdE3-P Emission at  $\lambda_{exc}$  of 254 nm  
 (c) GdE3-P Emission at  $\lambda_{exc}$  of 467 nm]

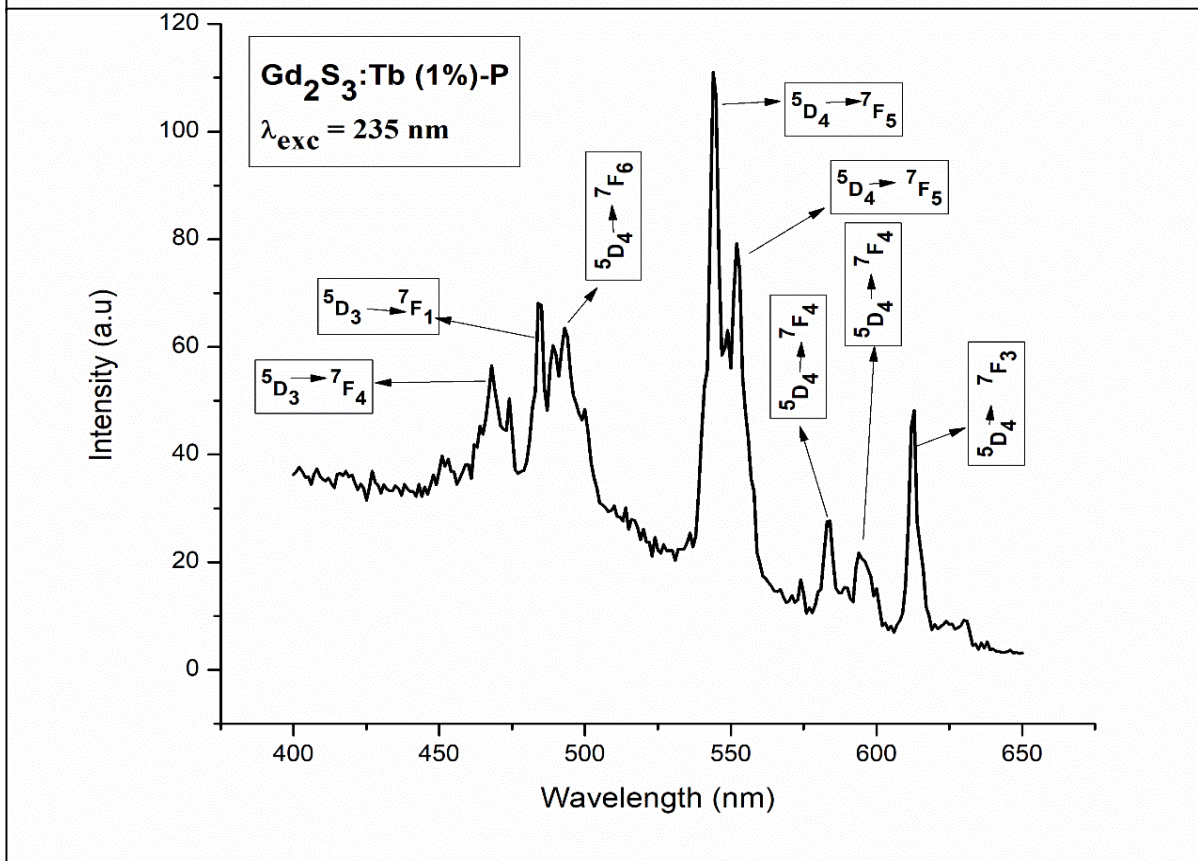
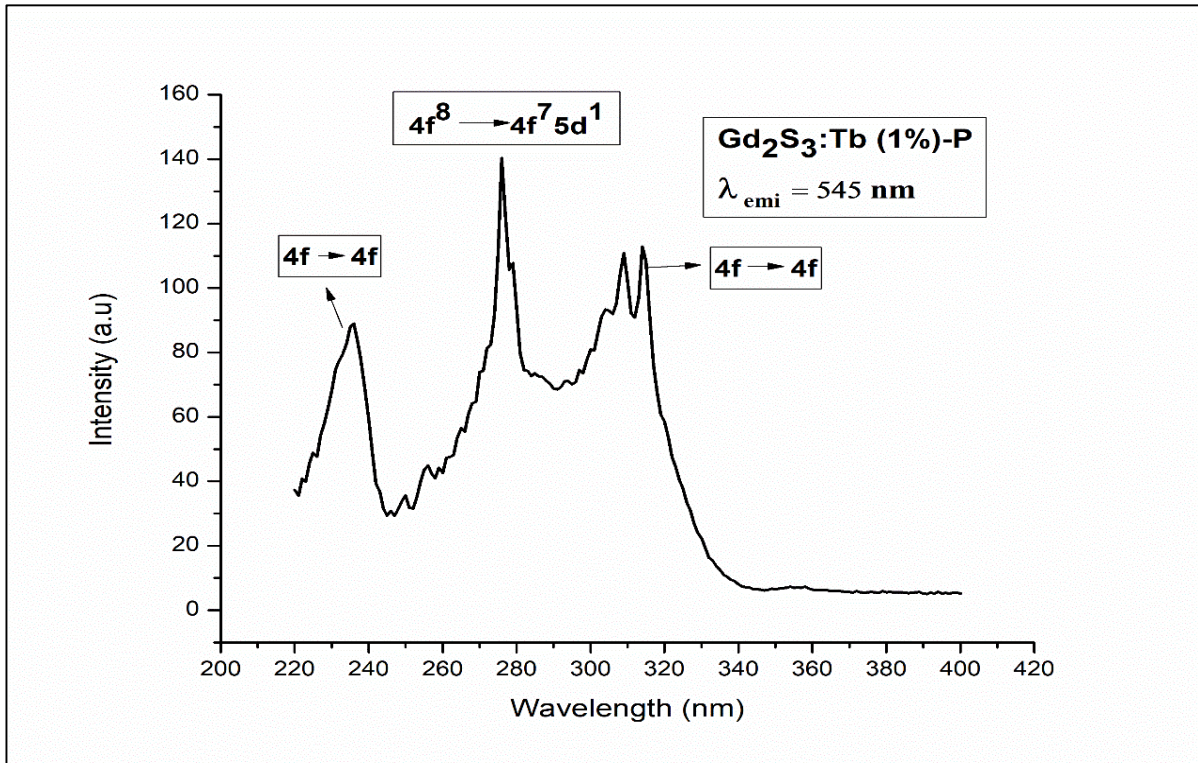
The graphs in Fig. 4-73 to 4-75 show excitation and emission spectra of 1%, 2% and 3% Eu doped Gd<sub>2</sub>S<sub>3</sub>. The excitation spectra of all three samples show an intense peak at 254 nm which is due to the charge transfer (CTS) transition of Eu<sup>3+</sup> ions while in 2% and 3% Eu doping, there is an additional small peak at 467 nm due to the 4f–4f transitions of Eu<sup>3+</sup> ions.

The emission spectrum of 1%, 2% and 3% Eu doping at an excitation of 254 nm shows an intense peak at 613 nm corresponding to the transition  $^5D_0 \rightarrow ^7F_2$  and two weak peaks at 594 nm and 630 nm associated with the same transition. The separation is on account of Stark splitting. The other peaks at 467 nm, 534 nm, 582 nm and 588 nm can be associated to the transitions  $^5D_2 \rightarrow ^7F_0$  (467 nm),  $^5D_1 \rightarrow ^7F_0$  (534 nm),  $^5D_0 \rightarrow ^7F_0$  (582 nm) and  $^5D_0 \rightarrow ^7F_1$  (588 nm) of Eu<sup>3+</sup> ions. The 467 nm peak is missing in 3% of Eu doping.

When excited at 467 nm, the PL spectra of 2% and 3% Eu doped samples shows the same intense peak at 613 nm corresponding to the  $^5D_0 \rightarrow ^7F_2$  transition along with two more peaks at 594 nm and 630 nm due to the same transition. It also shows a peak at 588 nm due to  $^5D_0 \rightarrow ^7F_1$  transition.

The photoluminescence intensity is found to increase with increase in doping percentage.

### 4.5.10 PL of Terbium (Tb) Doped Gadolinium Sulphide ( $Gd_2S_3$ ) synthesized by Precipitation Method



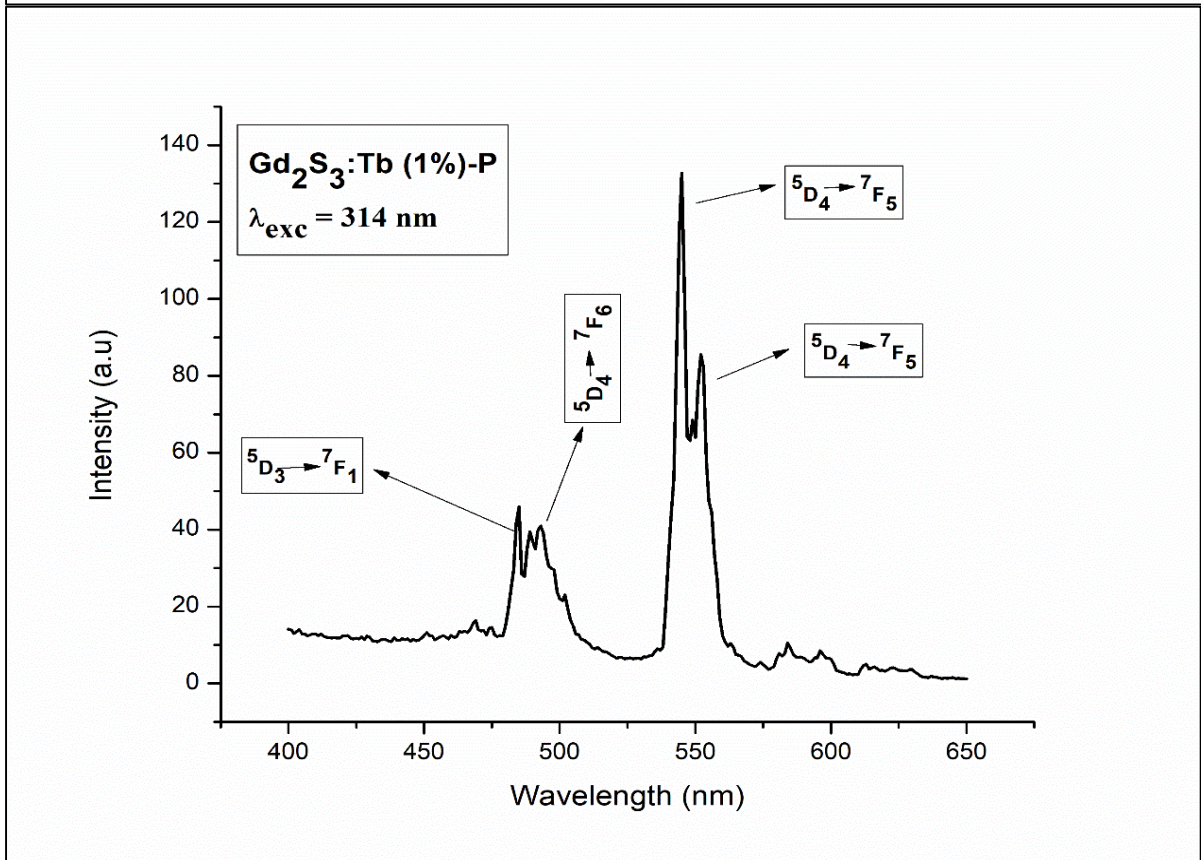
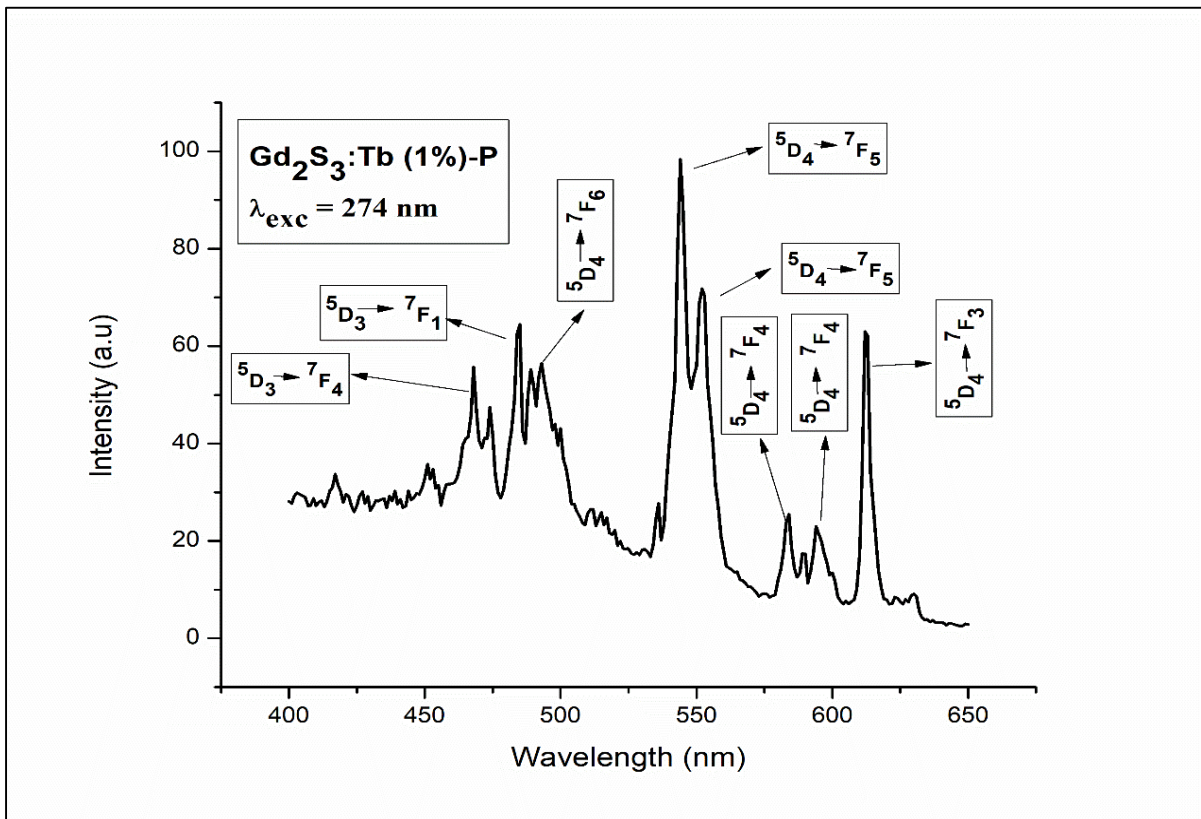
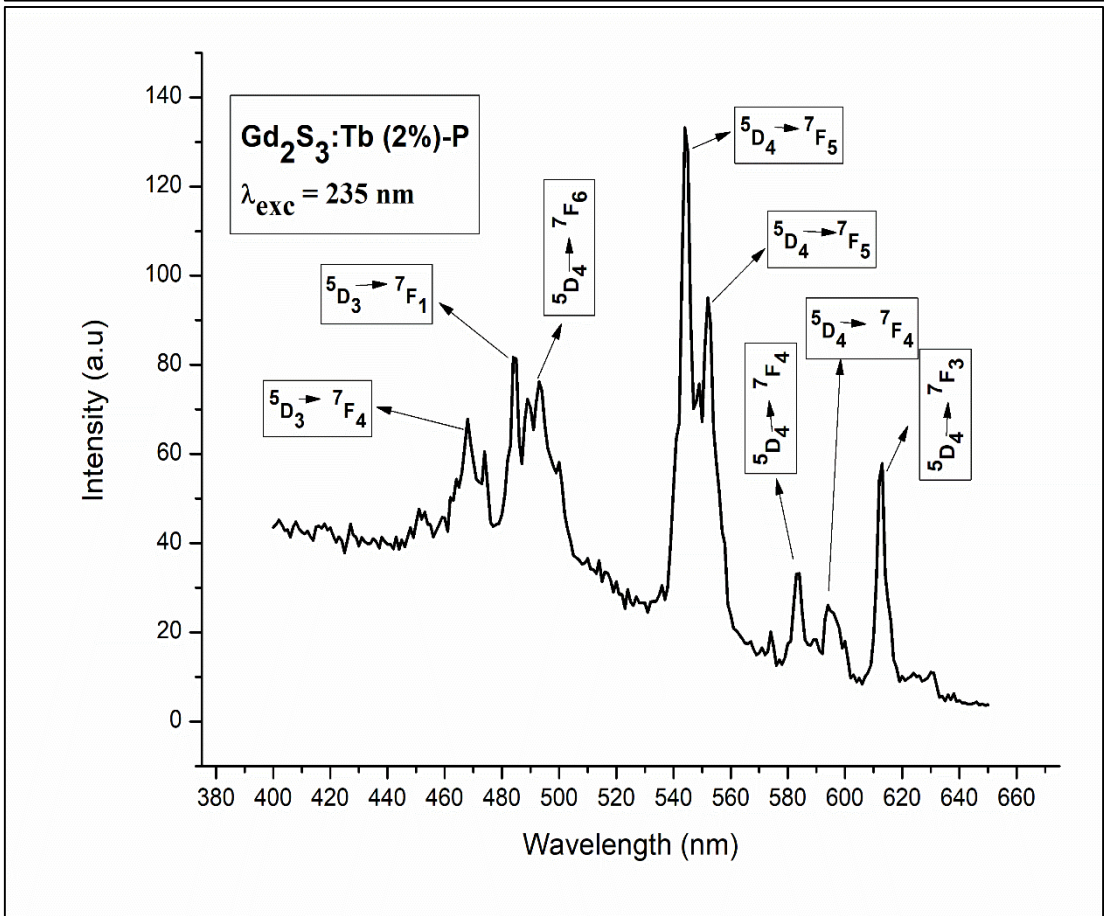
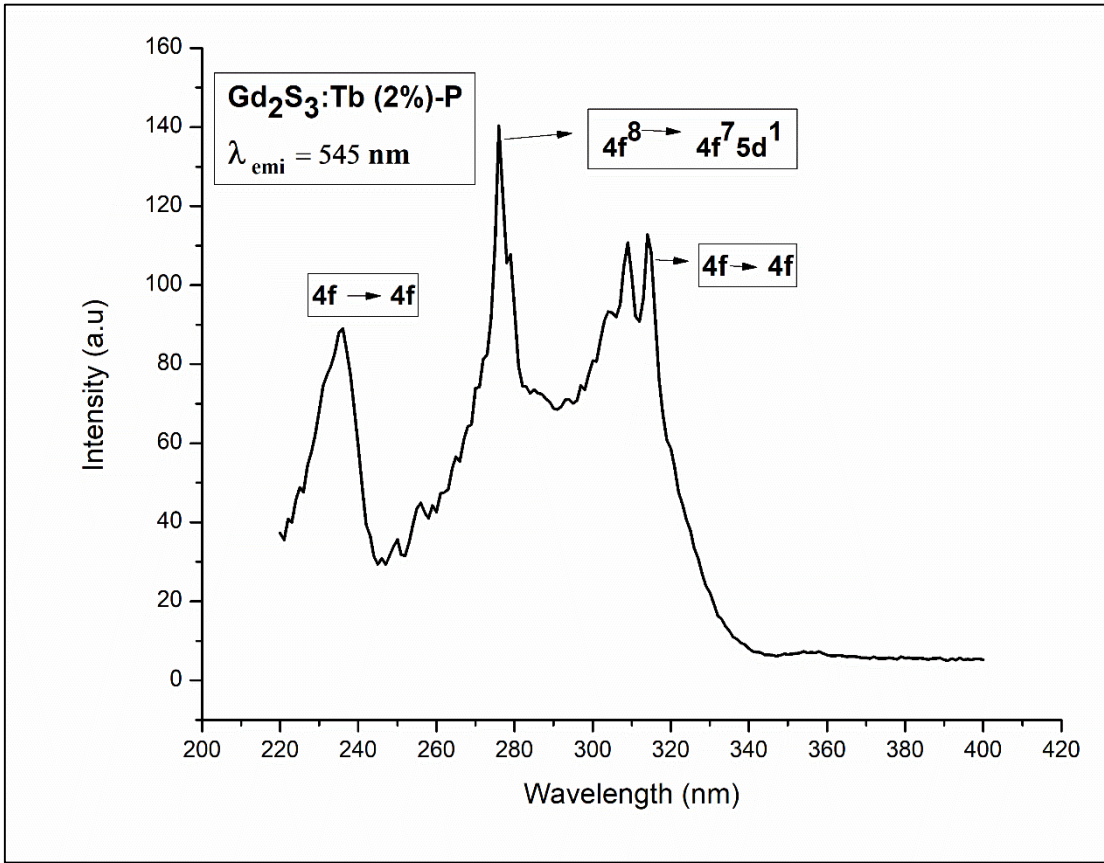


Figure 4-76: Photoluminescence spectra for Gd<sub>2</sub>S<sub>3</sub>:Tb (1%)  
 [(a) GdT1-P Excitation at  $\lambda_{\text{emi}}$  of 545 nm (b) GdT1-P Emission at  $\lambda_{\text{exc}}$  of 235 nm  
 (c) GdT1-P Emission at  $\lambda_{\text{exc}}$  of 274 nm (d) GdT1-P Emission at  $\lambda_{\text{exc}}$  of 314 nm]



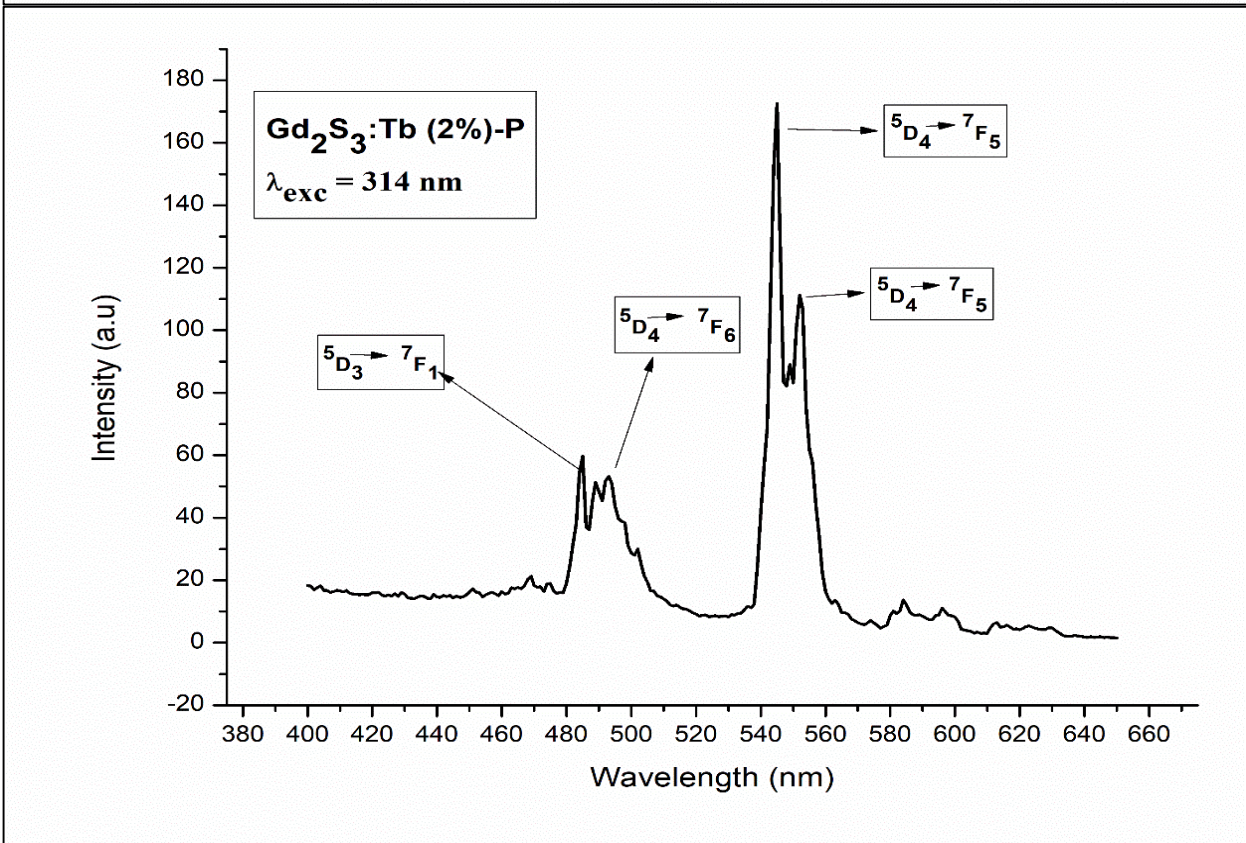
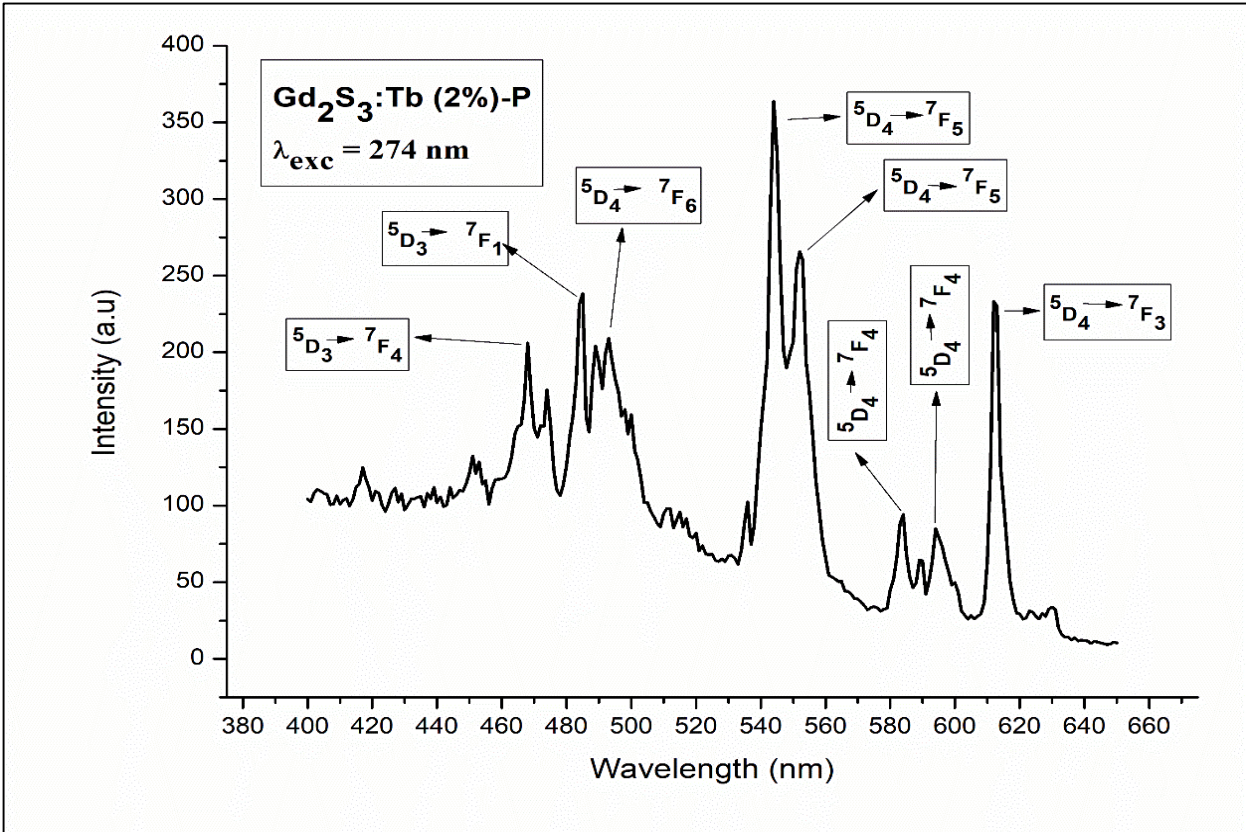
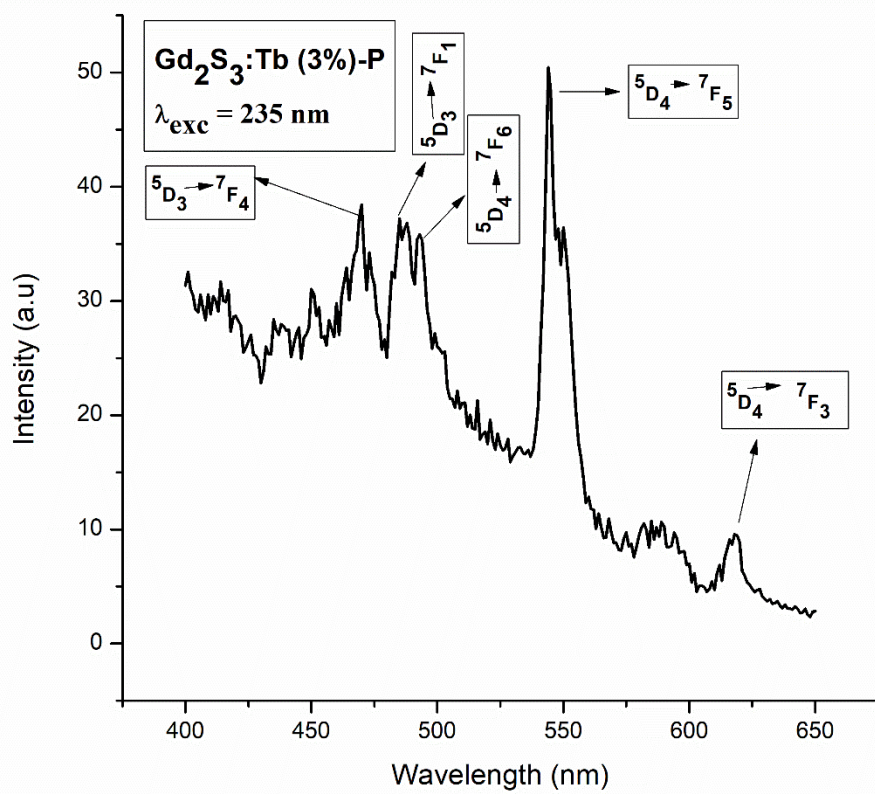
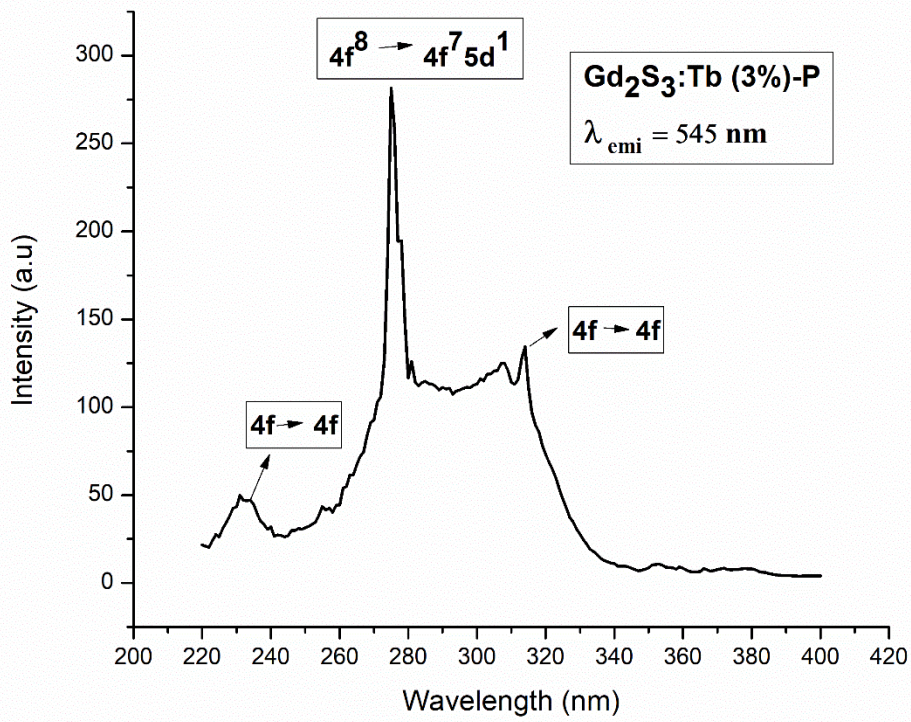


Figure 4-77: Photoluminescence spectra for Gd<sub>2</sub>S<sub>3</sub>:Tb (2%)  
 [(a) GdT2-P Excitation at  $\lambda_{\text{emi}}$  of 545 nm (b) GdT2-P Emission at  $\lambda_{\text{exc}}$  of 235 nm  
 (c) GdT2-P Emission at  $\lambda_{\text{exc}}$  of 274 nm (d) GdT2-P Emission at  $\lambda_{\text{exc}}$  of 314 nm]



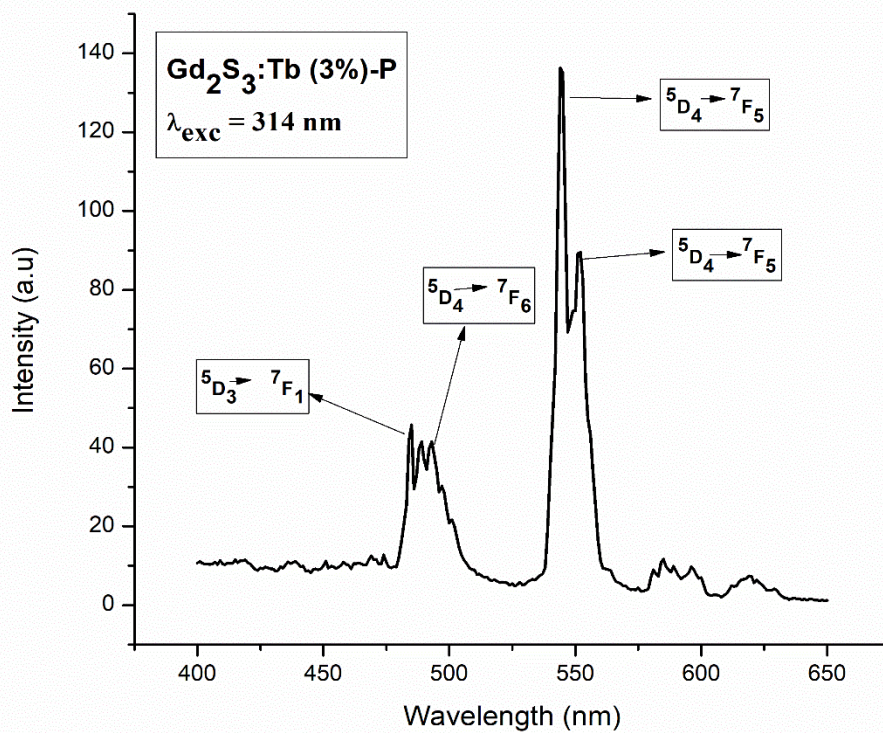
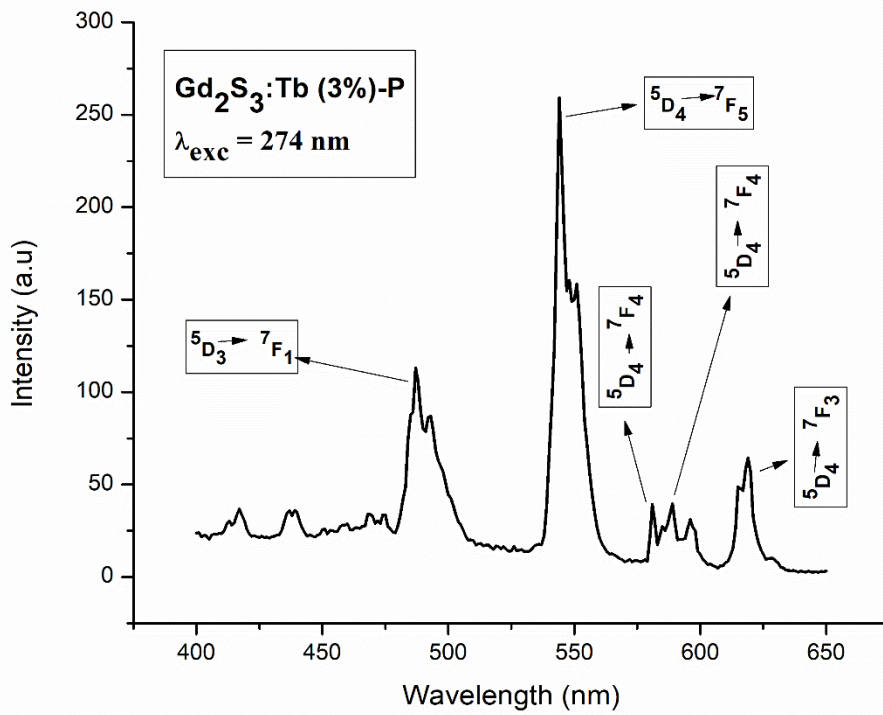


Figure 4-78: Photoluminescence spectra for  $\text{Gd}_2\text{S}_3:\text{Tb}$  (3%)

[(a)  $\text{Gd}_2\text{S}_3:\text{Tb}$ -P Excitation at  $\lambda_{\text{emi}}$  of 545 nm (b)  $\text{Gd}_2\text{S}_3:\text{Tb}$ -P Emission at  $\lambda_{\text{exc}}$  of 235 nm (c)  $\text{Gd}_2\text{S}_3:\text{Tb}$ -P Emission at  $\lambda_{\text{exc}}$  of 274 nm (d)  $\text{Gd}_2\text{S}_3:\text{Tb}$ -P Emission at  $\lambda_{\text{exc}}$  of 314 nm]

The excitation and emission spectra of 1%, 2% and 3% Tb doped Gd<sub>2</sub>S<sub>3</sub> are shown in fig. 4-76 to 4-78. The excitation spectrum for all doping concentrations shows an intense peak at 274 nm which is due to the  $4f^8 \rightarrow 4f^7 5d^1$  transition of Tb<sup>3+</sup> ion while the two additional peaks at 235 nm and 314 nm are attributed to the 4f–4f transitions of Tb<sup>3+</sup> ions.

The emission spectrum of 1% and 2% Tb doped Gd<sub>2</sub>S<sub>3</sub> consists of both, the blue and green emission lines when excited at 235 nm and 274 nm. The blue emission peaks are at 467 nm and 485 nm corresponding to the  $^5D_3 \rightarrow ^7F_4$  and  $^5D_3 \rightarrow ^7F_1$  transitions while the green emission peaks are at 493 nm, 552 nm, 582 nm along with the sharp and intense peak at 545 nm ( $^5D_4 \rightarrow ^7F_5$ ). The peaks at 493 nm, 552 nm and 582 nm are associated with  $^5D_4 \rightarrow ^7F_6$ ,  $^5D_4 \rightarrow ^7F_5$ ,  $^5D_4 \rightarrow ^7F_4$  transitions of Tb<sup>3+</sup> ions. Additional peaks at 592 nm ( $^5D_4 \rightarrow ^7F_4$ ) and 613 nm ( $^5D_4 \rightarrow ^7F_3$ ) are also seen in the graph.

On excitation at 314 nm, only four peaks corresponding to the transitions  $^5D_3 \rightarrow ^7F_1$  (485 nm),  $^5D_4 \rightarrow ^7F_6$  (493 nm) and  $^5D_4 \rightarrow ^7F_5$  (545 nm and 552 nm) are observed for all doping percentages.

For 3% Tb doping samples, for an excitation of 235 nm and 274 nm, peaks corresponding to the same transitions are observed but the number of peaks is reduced. The range of emission is extending further to 616 nm and 619 nm corresponding to the  $^5D_4 \rightarrow ^7F_3$  transition of Tb<sup>3+</sup> ion. The luminescent intensity increases from 1% to 2% of Tb doping and decreases when doping percentage becomes 3%.

### 4.5.11 PL of Europium (Eu) Doped Lanthanum Sulphide ( $\text{La}_2\text{S}_3$ ) synthesized by Precipitation Method

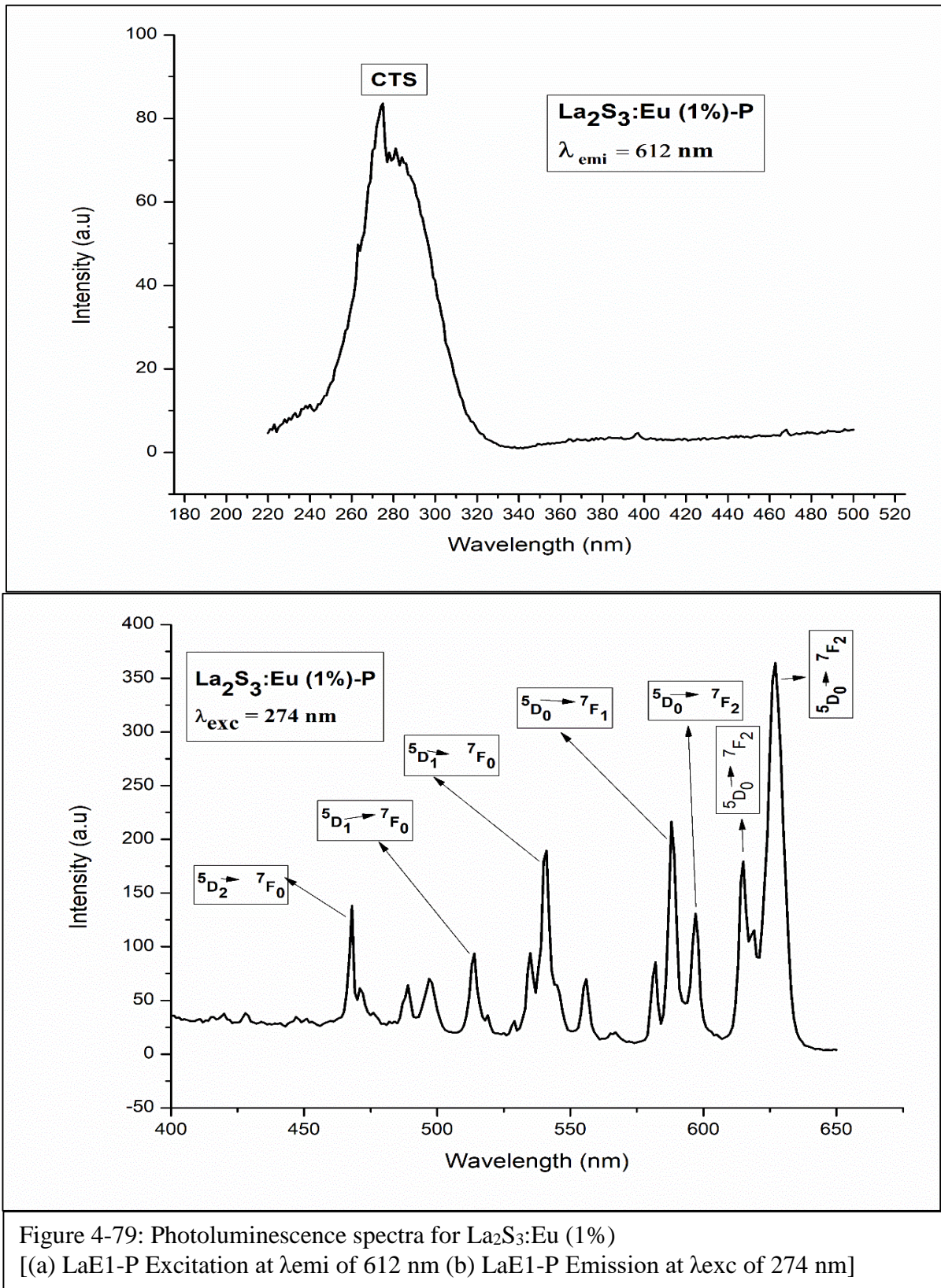


Figure 4-79: Photoluminescence spectra for  $\text{La}_2\text{S}_3:\text{Eu (1\%)}$   
 [(a)  $\text{LaE1-P}$  Excitation at  $\lambda_{\text{emi}}$  of 612 nm (b)  $\text{LaE1-P}$  Emission at  $\lambda_{\text{exc}}$  of 274 nm]

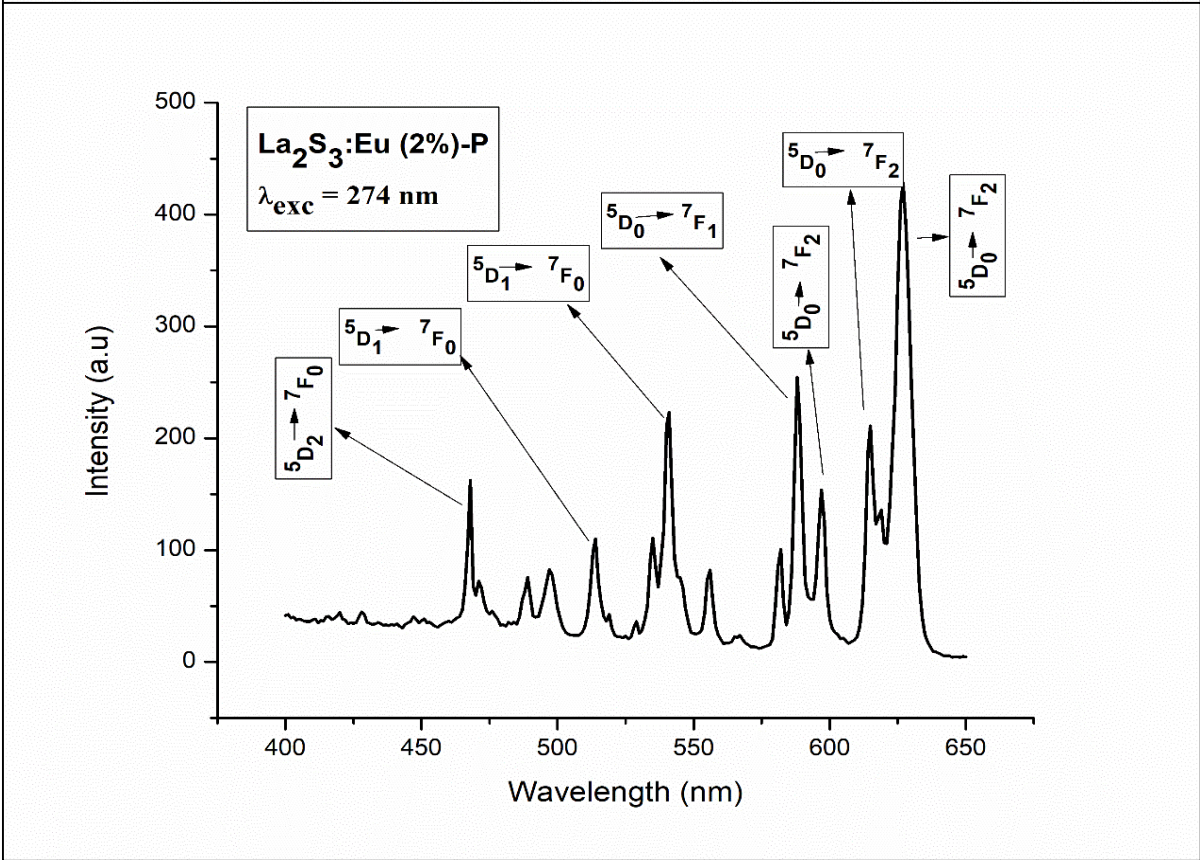
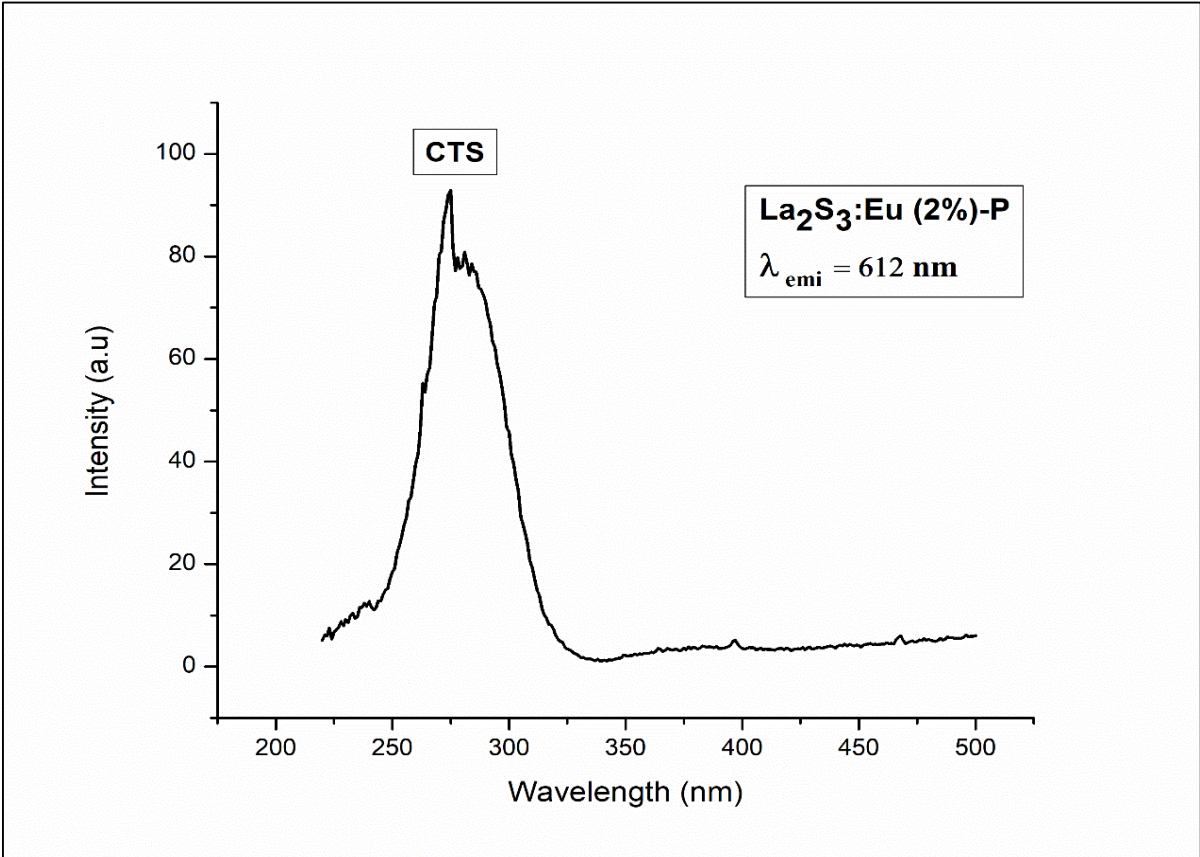


Figure 4-80: Photoluminescence spectra for  $\text{La}_2\text{S}_3:\text{Eu (2\%)}$   
 [(a) LaE2-P Excitation at  $\lambda_{\text{emi}}$  of 612 nm (b) LaE2-P Emission at  $\lambda_{\text{exc}}$  of 274 nm]

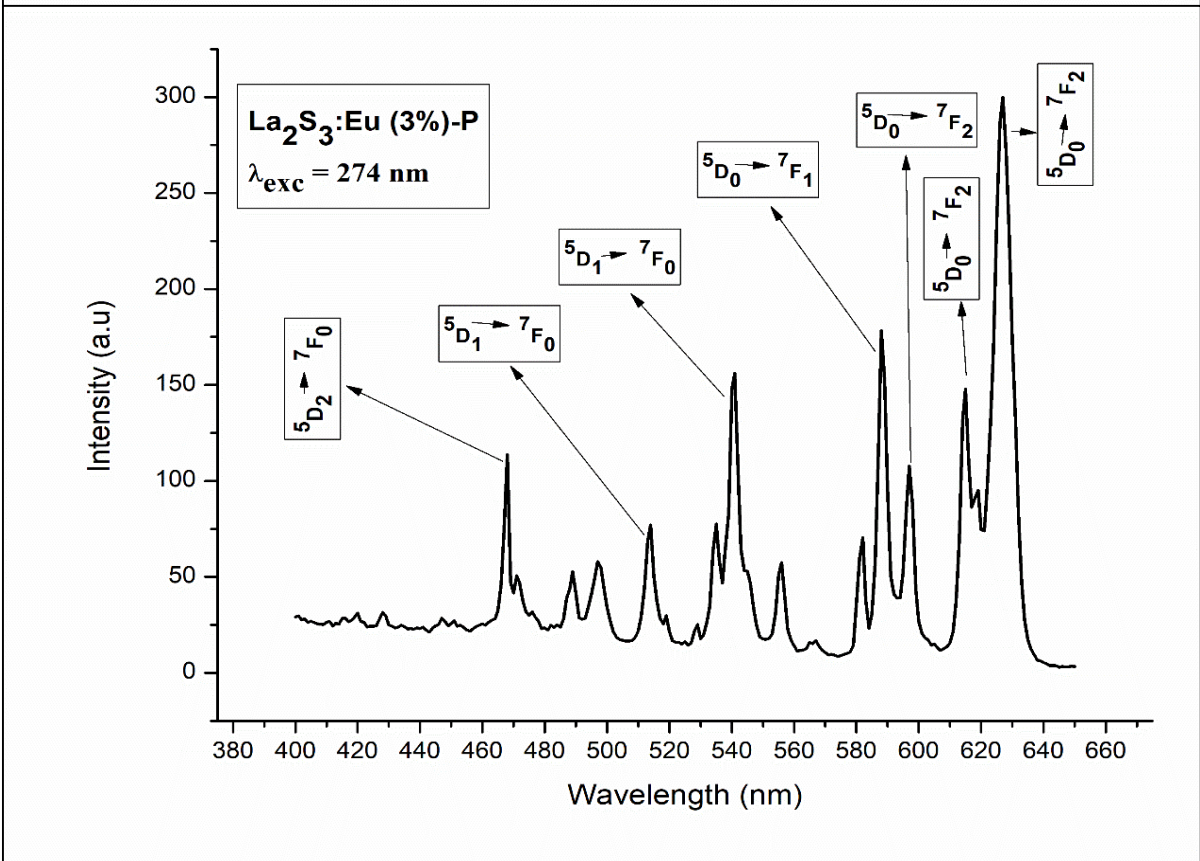
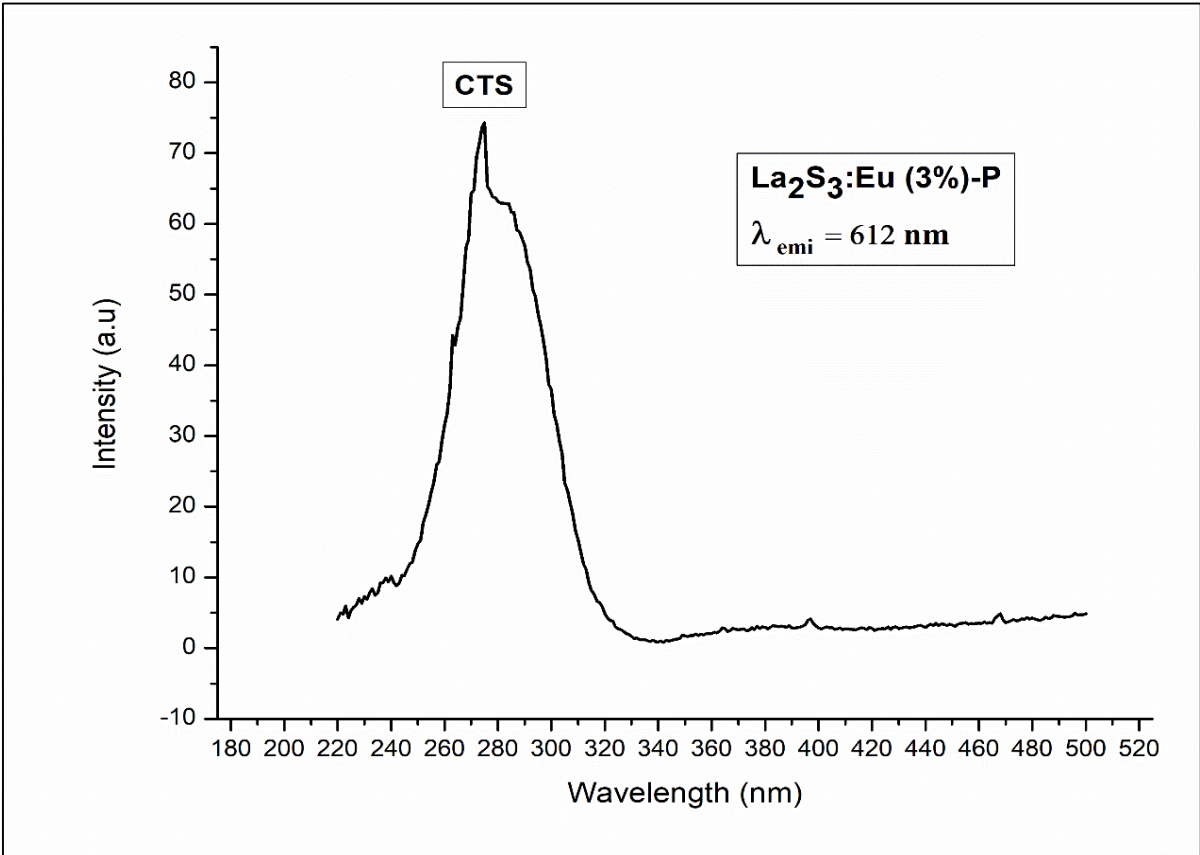


Figure 4-81: Photoluminescence spectra for  $\text{La}_2\text{S}_3:\text{Eu (3\%)}$   
 [(a) LaE3-P Excitation at  $\lambda_{\text{emi}}$  of 612 nm (b) LaE3-P Emission at  $\lambda_{\text{exc}}$  of 274 nm]

The graph in Fig. 4-79 to 4-81 show excitation and emission spectra of  $\text{La}_2\text{S}_3$  with 1%, 2% and 3% Eu doping. The excitation spectra of  $\text{La}_2\text{S}_3$  for all doping percentages of Eu doping shows an intense peak at 274 nm which is due to the charge transfer (CTS) transition of  $\text{Eu}^{3+}$  ions.

For an excitation of 274 nm, the emission spectrum shows an intense peak at 627 nm corresponding to the  $^5\text{D}_0 \rightarrow ^7\text{F}_2$  transition. Other peaks observed are observed at 467 nm, 513 nm, 540 nm, 588 nm, 595 nm and 615 nm which are assigned to the transitions  $^5\text{D}_2 \rightarrow ^7\text{F}_0$ ,  $^5\text{D}_1 \rightarrow ^7\text{F}_0$ ,  $^5\text{D}_1 \rightarrow ^7\text{F}_0$ ,  $^5\text{D}_0 \rightarrow ^7\text{F}_1$ ,  $^5\text{D}_0 \rightarrow ^7\text{F}_2$  and  $^5\text{D}_0 \rightarrow ^7\text{F}_2$  respectively of  $\text{Eu}^{3+}$  ions. The intensities of a number of peaks is quite high which shows a broad range of emission of Lanthanum Sulphide. It is seen that the photoluminescence intensity increases with increase in doping concentration from 1% to 2% and then decreases when doping concentration becomes 3%.

The excitation and emission spectra of Terbium (Tb) doped  $\text{La}_2\text{S}_3$  samples could not be obtained.

#### 4.5.12 PL of Europium (Eu) Doped Yttrium Sulphide ( $Y_2S_3$ ) synthesized by Precipitation Method

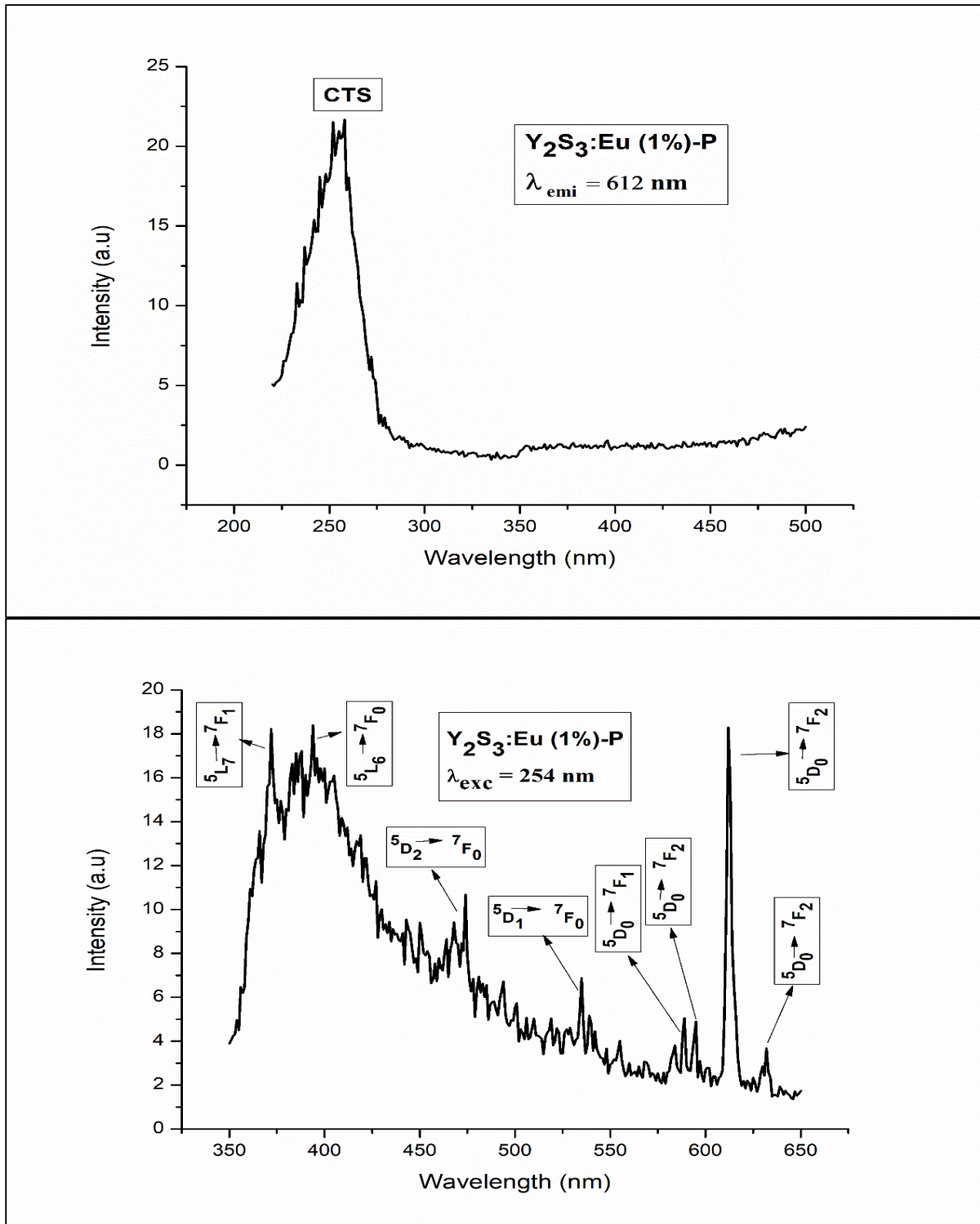
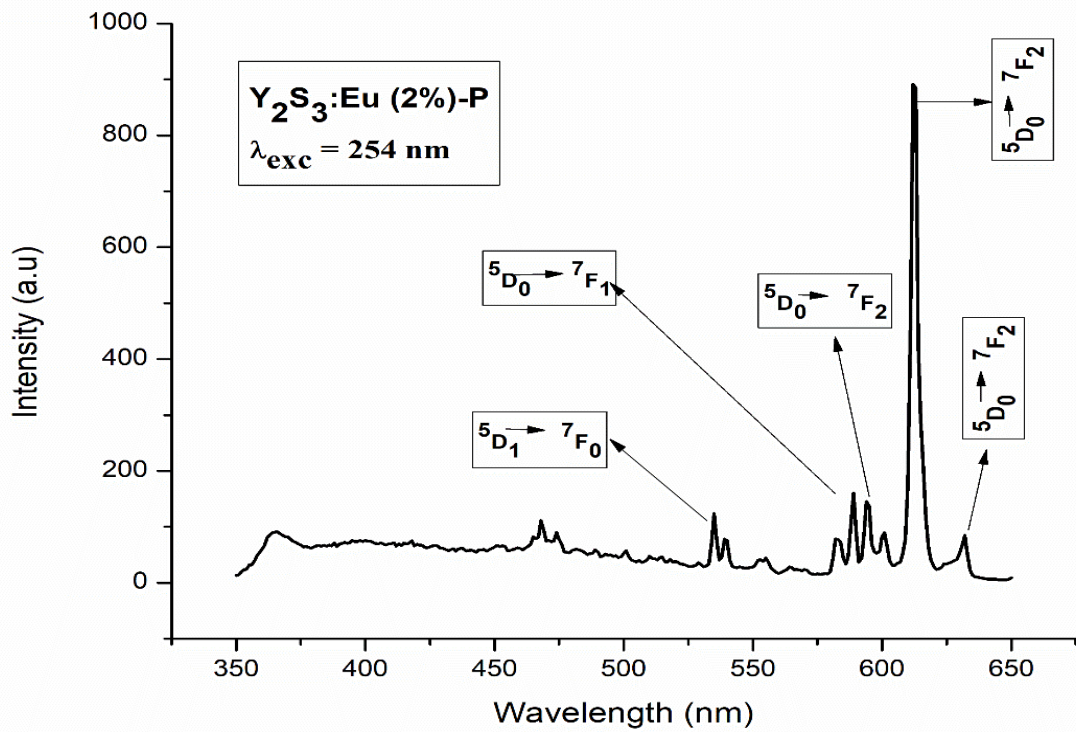
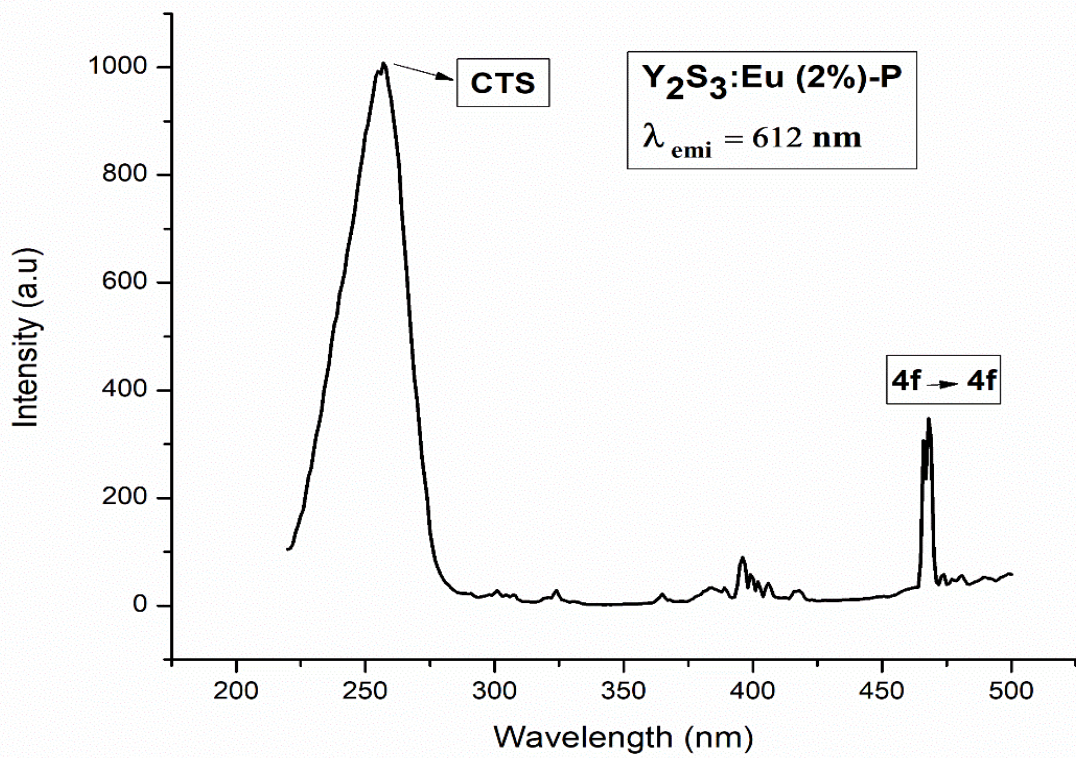


Figure 4-82: Photoluminescence spectra for  $Y_2S_3:Eu$  (1%)  
 [(a) YE1-P Excitation at  $\lambda_{emi}$  of 612 nm (b) YE1-P Emission at  $\lambda_{exc}$  of 254 nm]



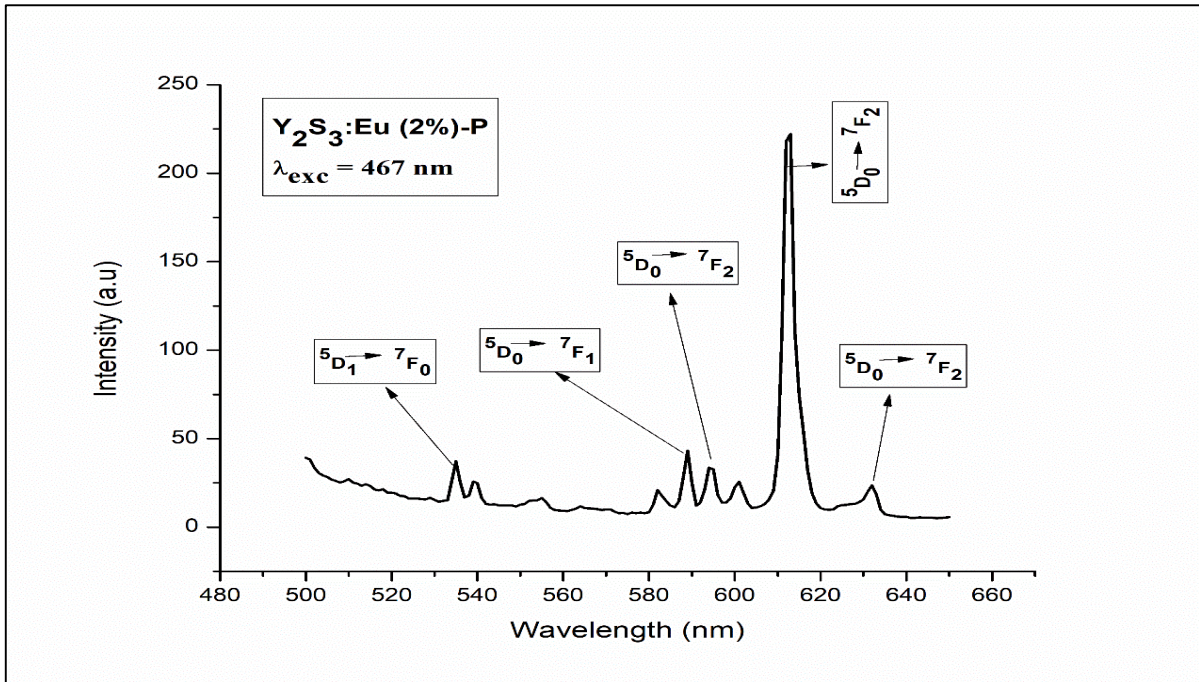
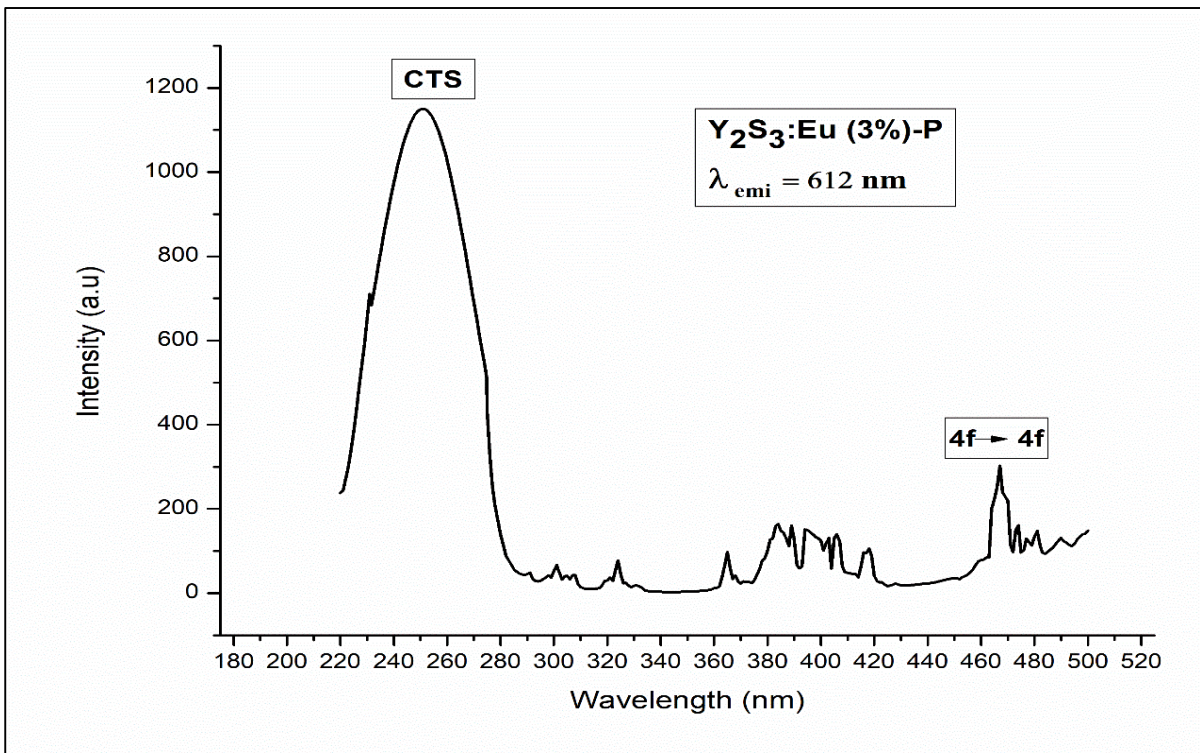


Figure 4-83: Photoluminescence spectra for Y<sub>2</sub>S<sub>3</sub>:Eu (2%)  
 [(a) YE2-P Excitation at λ<sub>emi</sub> of 612 nm (b) YE2-P Emission at λ<sub>exc</sub> of 254 nm  
 (c) YE2-P Emission at λ<sub>exc</sub> of 467 nm]



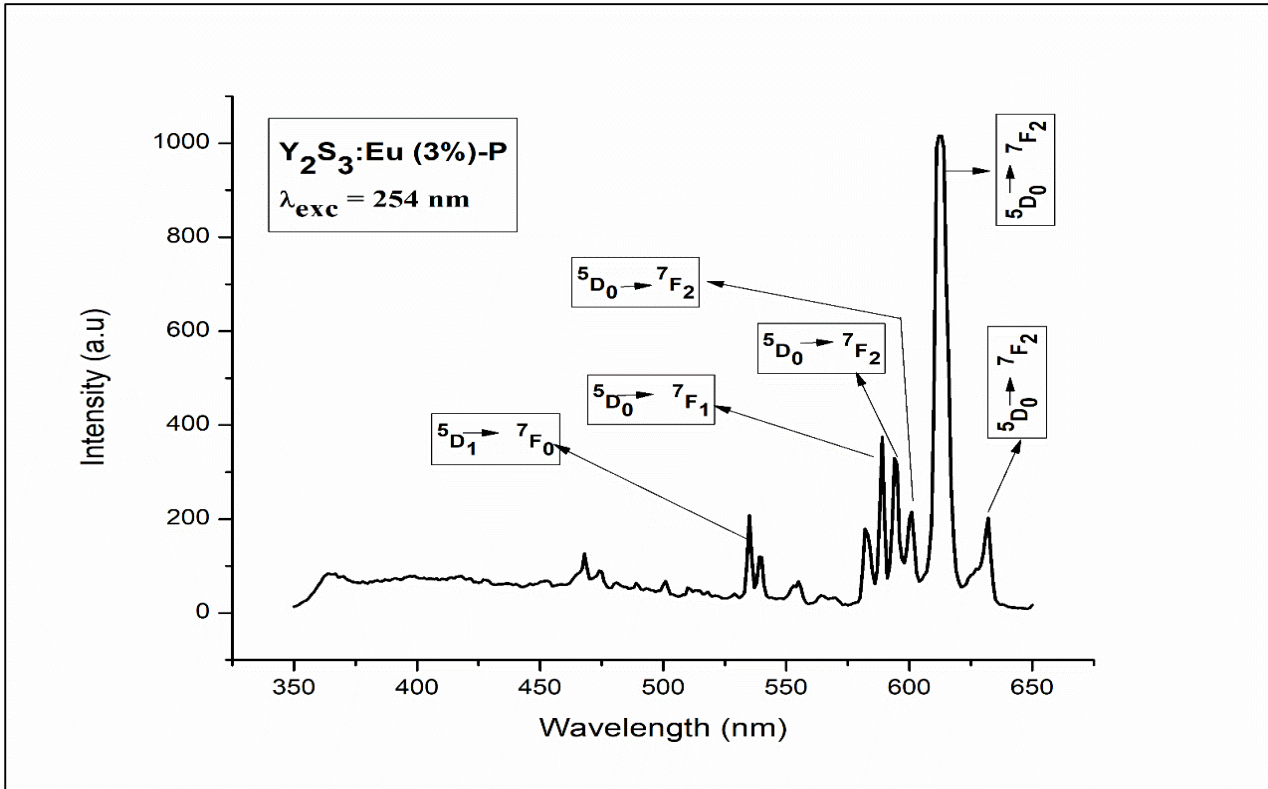


Figure 4-84: Photoluminescence spectra for  $Y_2S_3:Eu$  (3%)  
 [(a) YE3-P Excitation at  $\lambda_{emi}$  of 612 nm (b) YE3-P Emission at  $\lambda_{exc}$  of 254 nm]

Figures. 4-82 to 4-84 show the excitation and emission spectra of  $Y_2S_3$  doped with 1%, 2% and 3% of Eu. The excitation spectra of  $Y_2S_3$  for all the doping percentages of Eu shows an intense peak at 254 nm which is due to the charge transfer (CTS) transition of  $Eu^{3+}$  ions. An additional peak at 467 nm due to the 4f–4f transitions of  $Eu^{3+}$  ions is observed in 2% Eu doping.

The emission spectrum for the excitation with 254 nm, of all three samples shows an intense peak at 612 nm corresponding to the  $^5D_0 \rightarrow ^7F_2$  transition. In 1% Eu doping, the other peaks observed are located at 371 nm, 393 nm, 474 nm, 587 nm, 595 nm and 632 nm which can be attributed to the transitions  $^5L_7 \rightarrow ^7F_1$ ,  $^5L_6 \rightarrow ^7F_0$ ,  $^5D_2 \rightarrow ^7F_0$ ,  $^5D_0 \rightarrow ^7F_1$ ,  $^5D_0 \rightarrow ^7F_2$  and  $^5D_0 \rightarrow ^7F_2$  of  $Eu^{3+}$  ions. In 2% and 3% Eu doping, the transitions and peaks are  $^5D_1 \rightarrow ^7F_0$  (534 nm),  $^5D_0 \rightarrow ^7F_1$  (589 nm) and  $^5D_0 \rightarrow ^7F_2$  (595 nm and 632 nm). An additional small peak is observed at 600 nm for 3% Eu doping which can be attributed to the  $^5D_0 \rightarrow ^7F_2$  transition of  $Eu^{3+}$  ions.

When excited at 467 nm, the 2% Eu doped sample, which has this additional excitation peak, gives the same peaks as 254 nm excitation but with reduced intensity. The emission intensity is found to increase with increase in doping percentage.

### 4.5.13 PL of Terbium (Tb) Doped Yttrium Sulphide ( $Y_2S_3$ ) synthesized by Precipitation Method

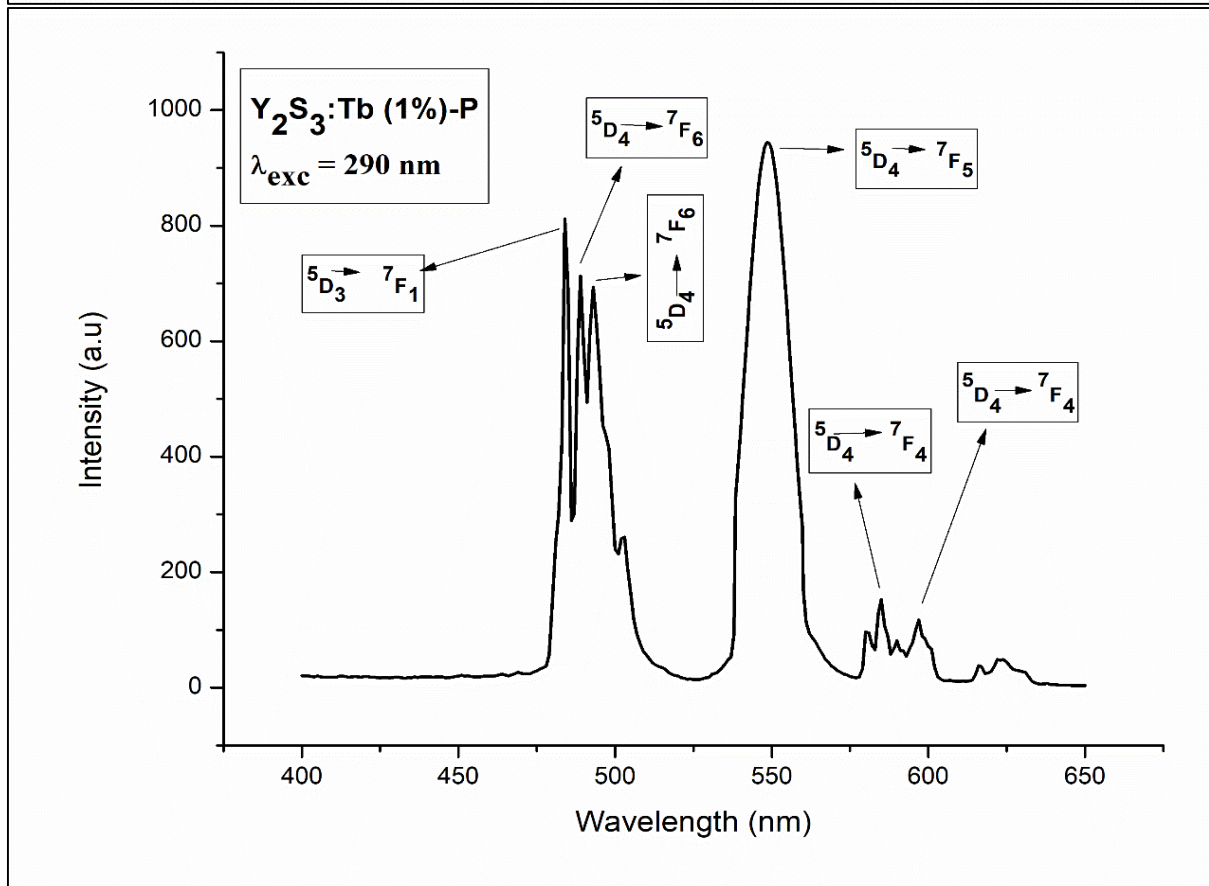
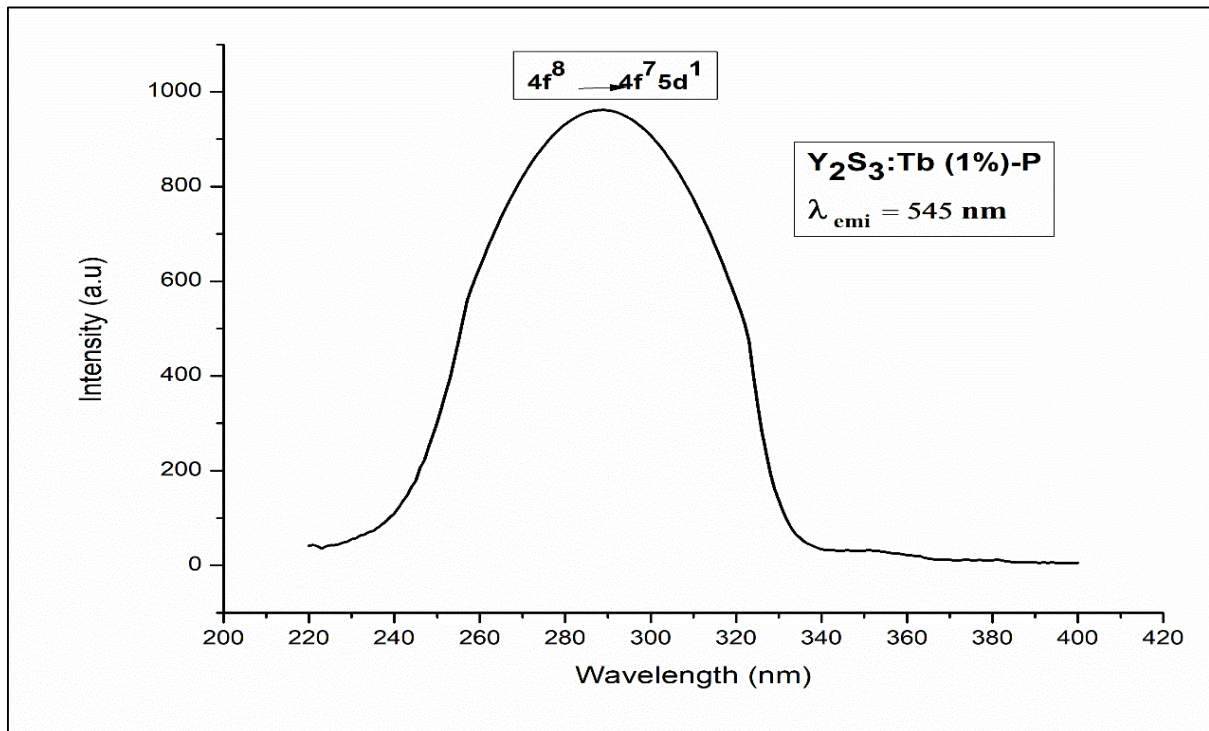


Figure 4-85: Photoluminescence spectra for  $Y_2S_3:Tb (1\%)$   
 [(a) YT1-P Excitation at  $\lambda_{emi}$  of 545 nm (b) YT1-P Emission at  $\lambda_{exc}$  of 290 nm]

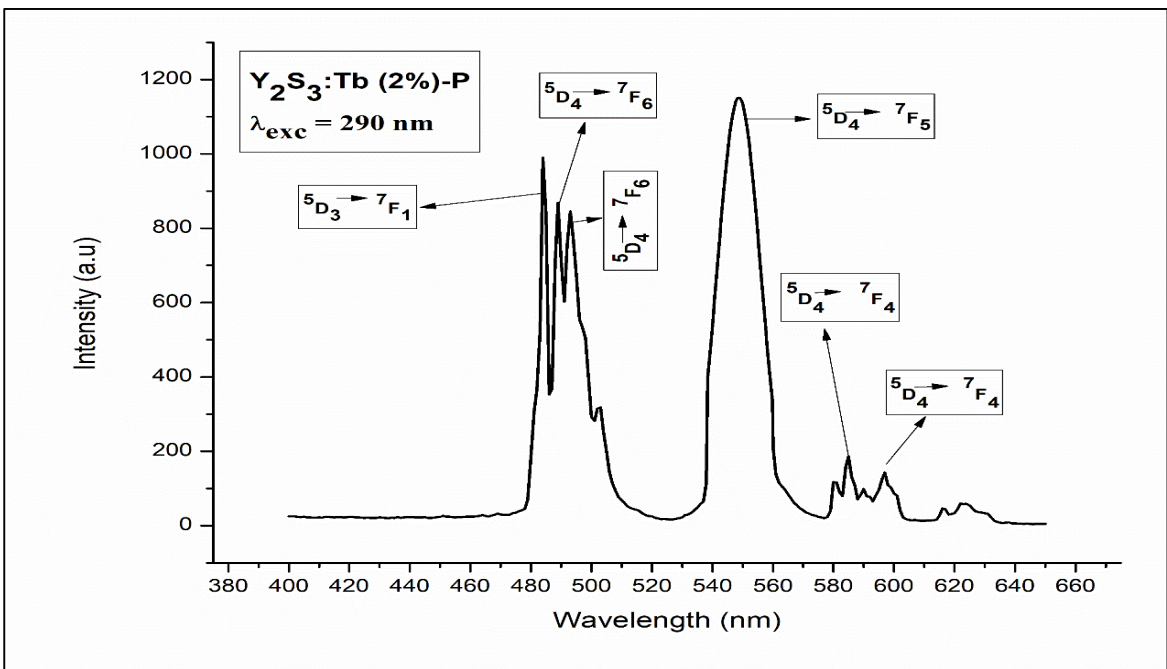
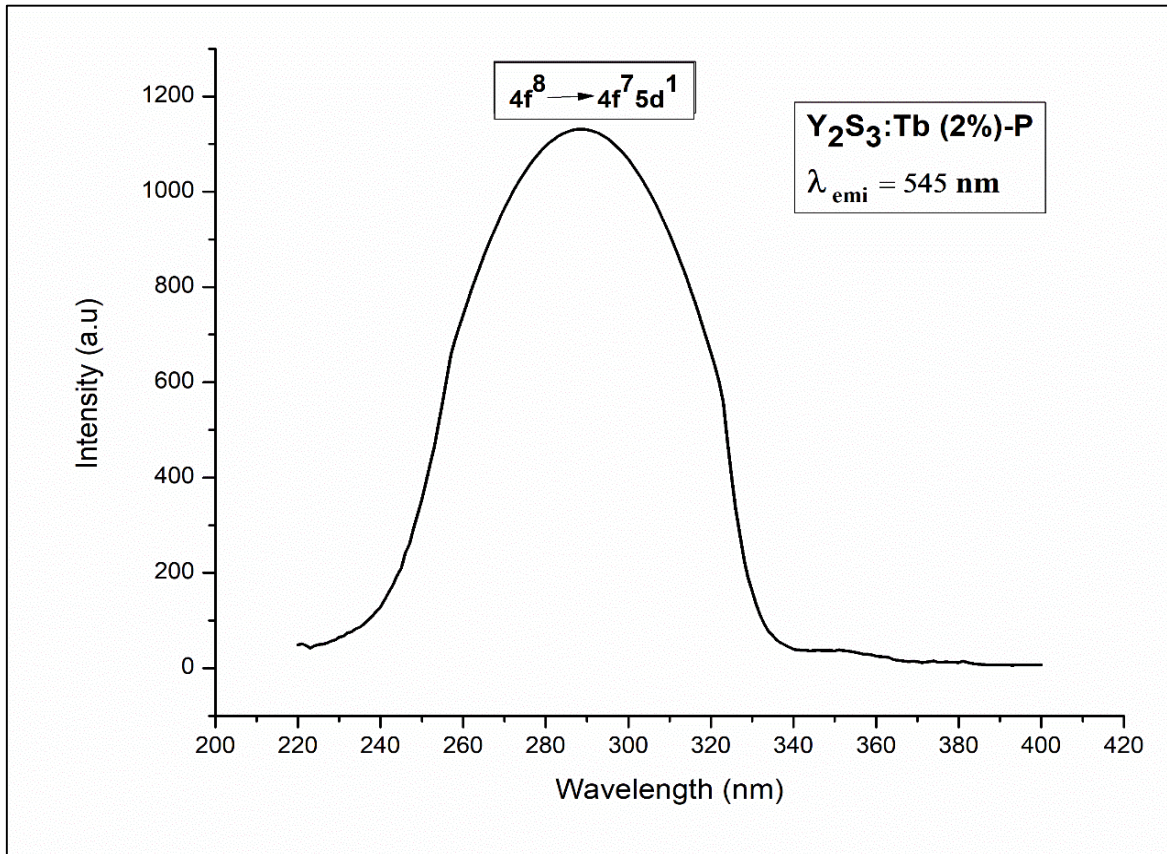


Figure 4-86: Photoluminescence spectra for  $\text{Y}_2\text{S}_3:\text{Tb} (2\%)$   
 [(a) YT2-P Excitation at  $\lambda_{\text{emi}}$  of 545 nm (b) YT2-P Emission at  $\lambda_{\text{exc}}$  of 290 nm]

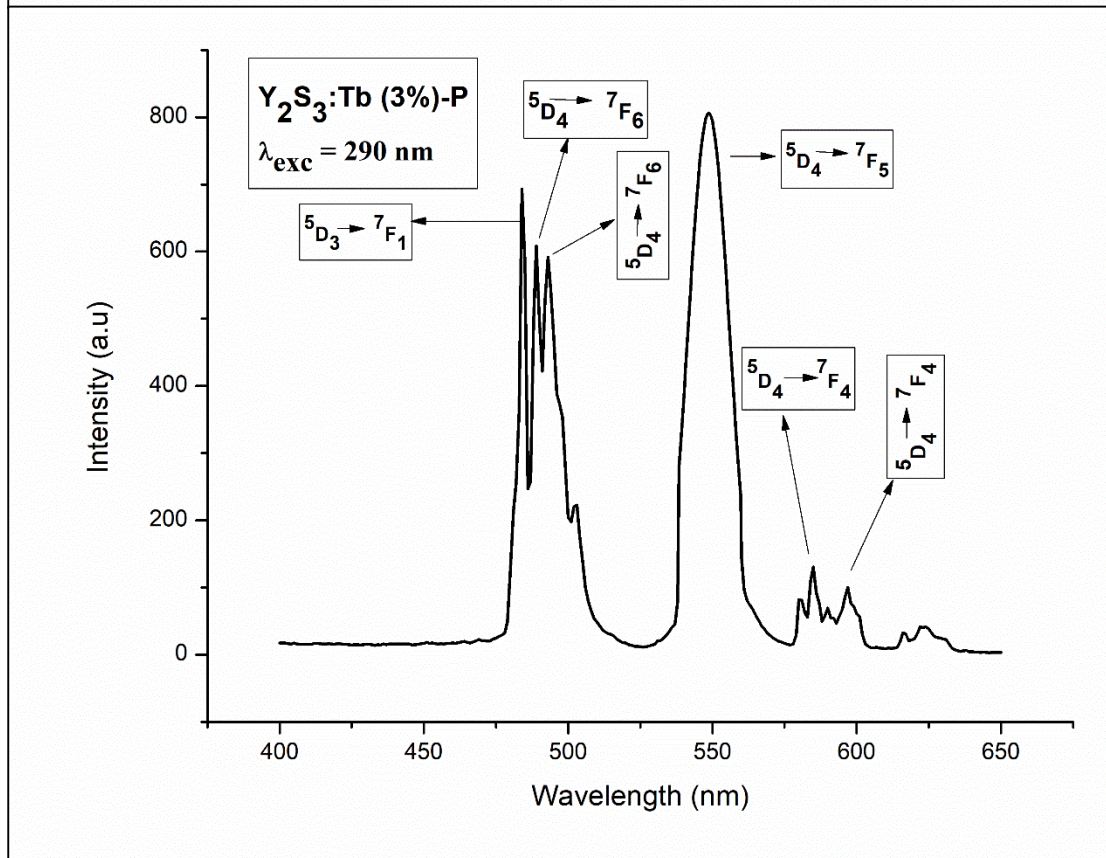
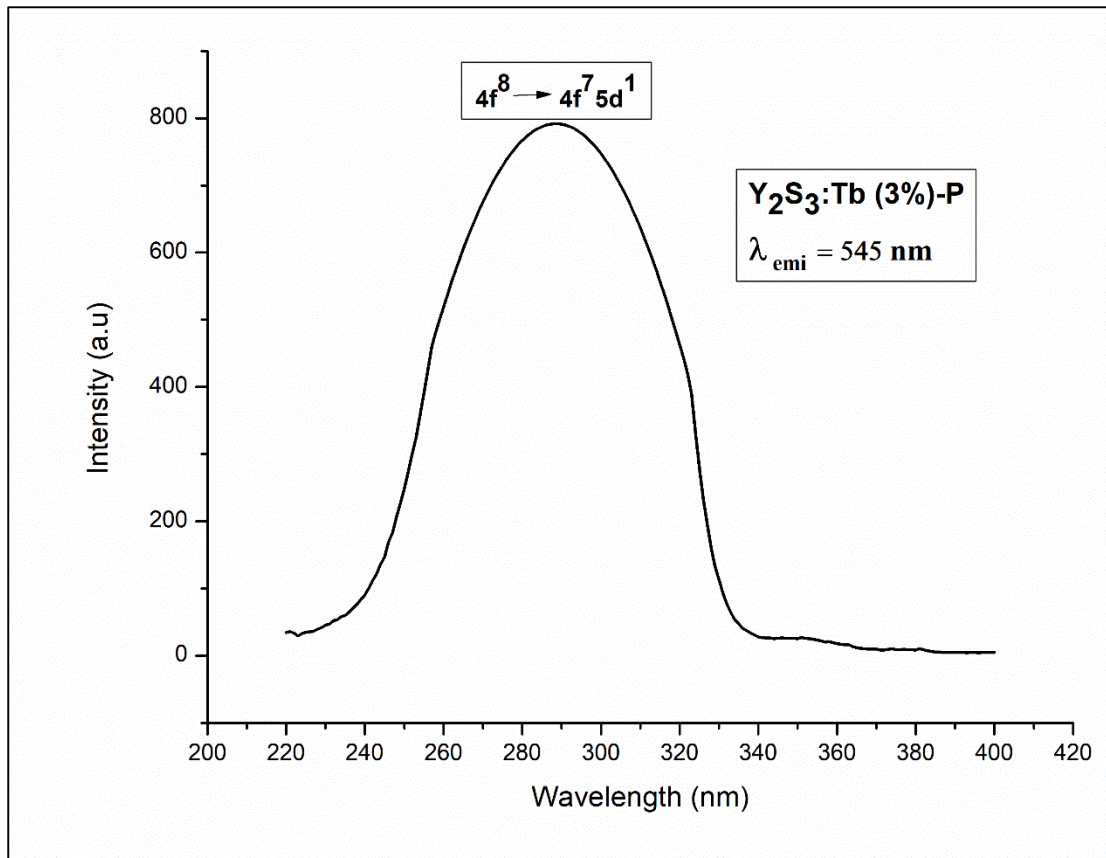


Figure 4-87: Photoluminescence spectra for  $Y_2S_3:Tb (3\%)$   
 [(a) YT3-P Excitation at  $\lambda_{emi}$  of 545 nm (b) YT3-P Emission at  $\lambda_{exc}$  of 290 nm]

The Photoluminescence excitation and emission spectra of  $Y_2S_3$  with 1%, 2% and 3% Tb doping is shown in the Fig. 4-85 to 4-87. The excitation spectra of all three samples show an intense peak at 290 nm which can be attributed to the  $4f^8 \rightarrow 4f^75d^1$  transition of  $Tb^{3+}$  ions.

All the Tb doped samples on excitation of 290 nm, show intense emission features both in the blue and green regions. The intense peak in the blue region at 485 nm and small peak at 488 nm are associated with the transitions  $^5D_3 \rightarrow ^7F_1$  and  $^5D_4 \rightarrow ^7F_6$  while the intense peak in the green region at 548 nm along with small peaks at 493 nm, 586 nm and 597 nm correspond to the transitions  $^5D_4 \rightarrow ^7F_5$ ,  $^5D_4 \rightarrow ^7F_6$ ,  $^5D_4 \rightarrow ^7F_4$  and  $^5D_4 \rightarrow ^7F_4$  of  $Tb^{3+}$  ions.

From the graphs, it is observed that the photoluminescence intensity increases from 1% to 2% of Tb doping and then decreases when doping percentage becomes 3%.

When compared with the PL spectra of Solid State samples, Tb doped  $Y_2S_3$  synthesized by Precipitation method gives emission in both the blue and green range while the PL spectra of Tb doped  $Y_2S_3$  synthesized by Solid State method gives only green emission.

## 4.6 Comparative Study of Photoluminescence Spectra

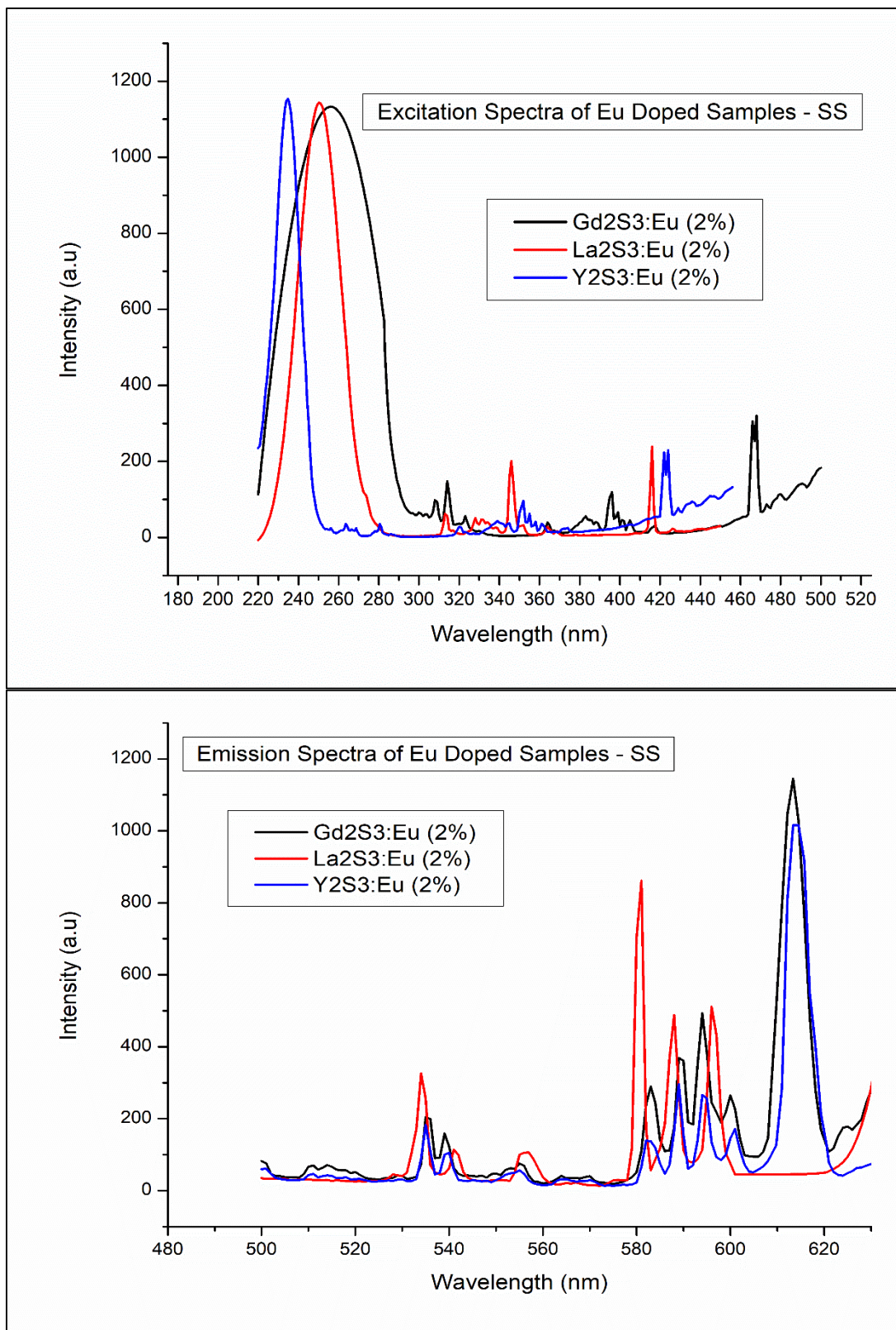


Figure 4-88: Excitation and Emission spectra of Eu doped samples synthesized by Solid State method (a) Excitation spectra of GdE2-SS, LaE2-SS and YE2-SS (b) Emission spectra of GdE2-SS, LaE2-SS and YE2-SS

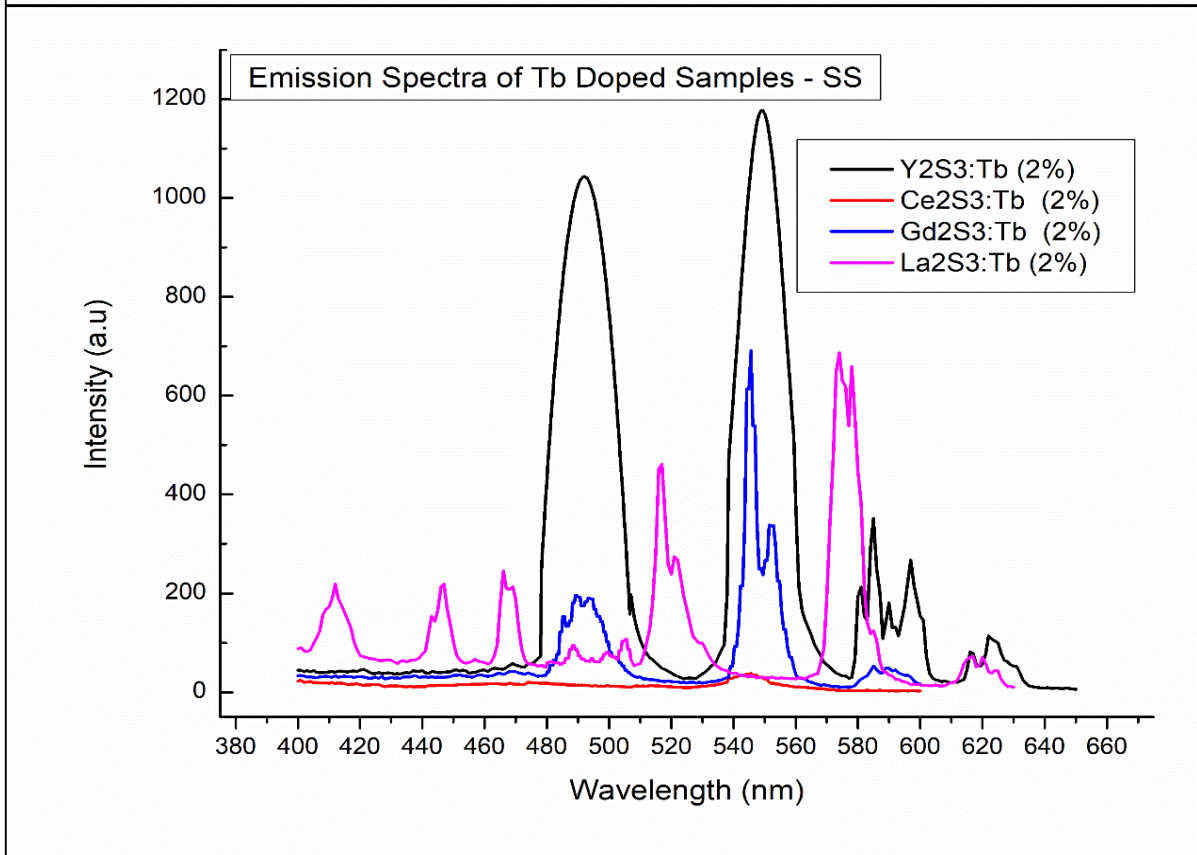
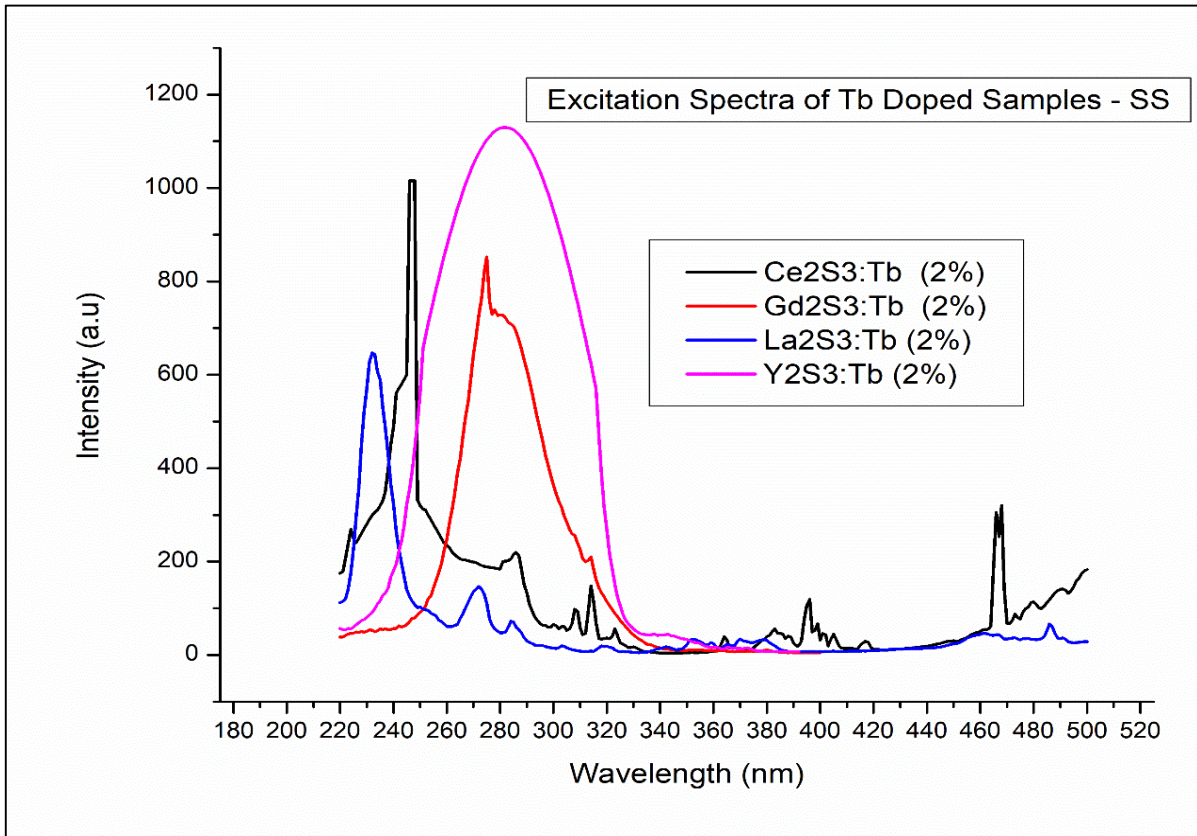


Figure 4-89: Excitation and Emission spectra of Tb doped samples synthesized by Solid State method (a) Excitation spectra of CeT<sub>2</sub>-SS, GdT<sub>2</sub>-SS, LaT<sub>2</sub>-SS and YT<sub>2</sub>-SS (b) Emission spectra of CeT<sub>2</sub>-SS, GdT<sub>2</sub>-SS, LaT<sub>2</sub>-SS and YT<sub>2</sub>-SS

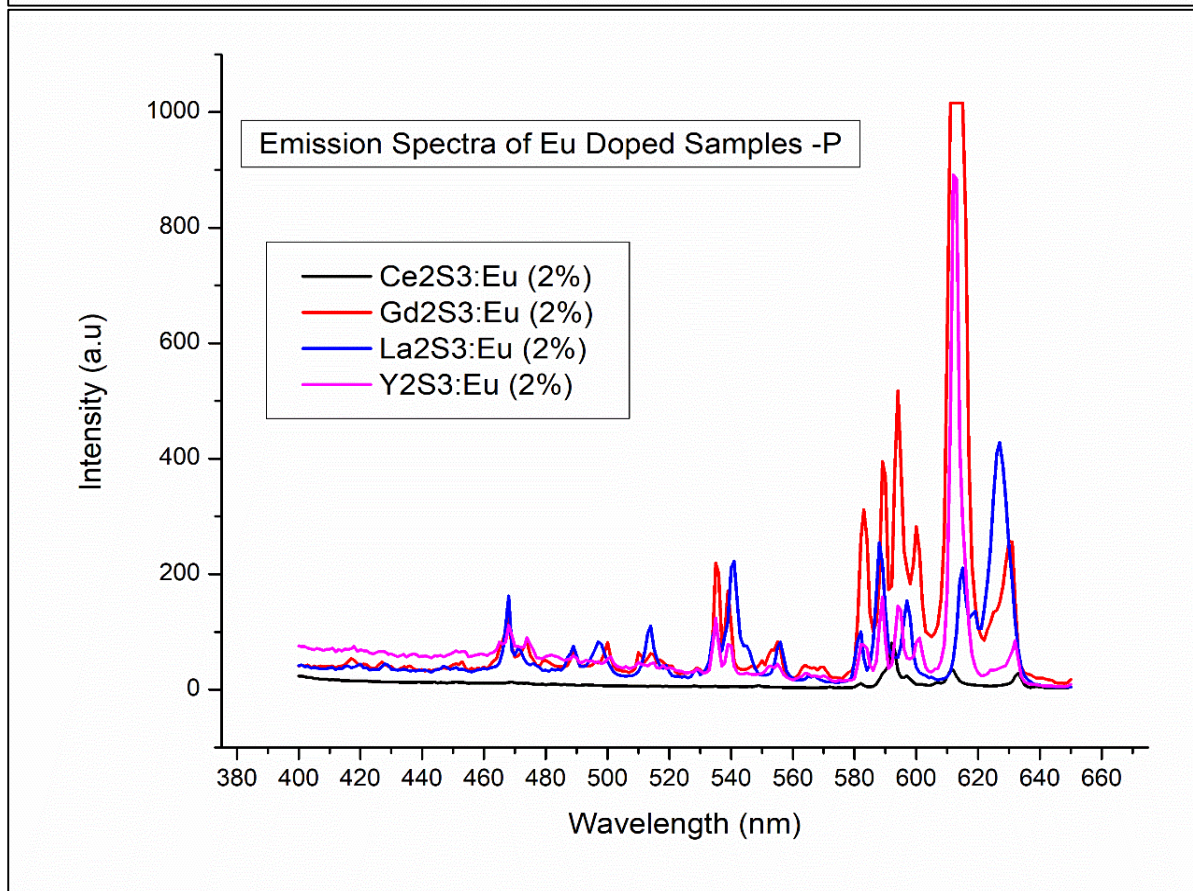
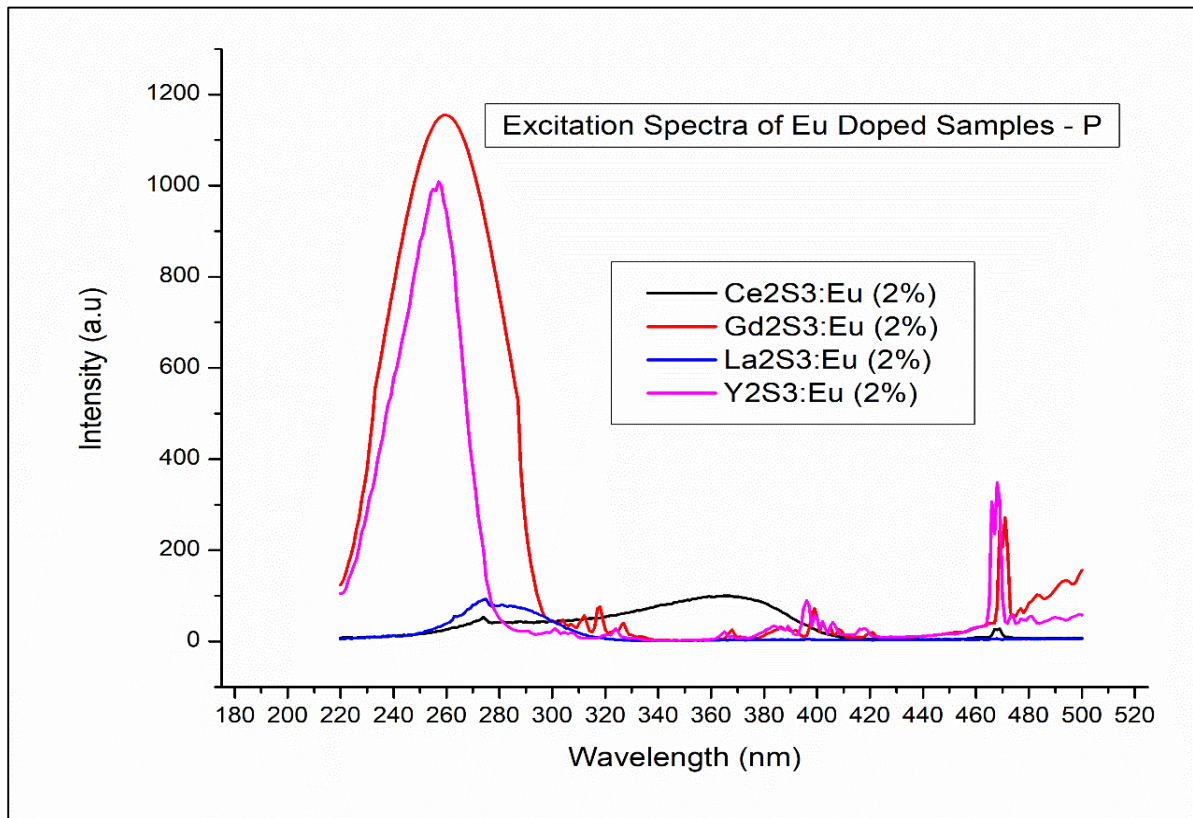


Figure 4-90: Excitation and Emission spectra of Eu doped samples synthesized by Precipitation method (a) Excitation spectra of CeE2-P, GdE2-P, LaE2-P and YE2-P (b) Emission spectra of CeE2-P, GdE2-P, LaE2-P and YE2-P

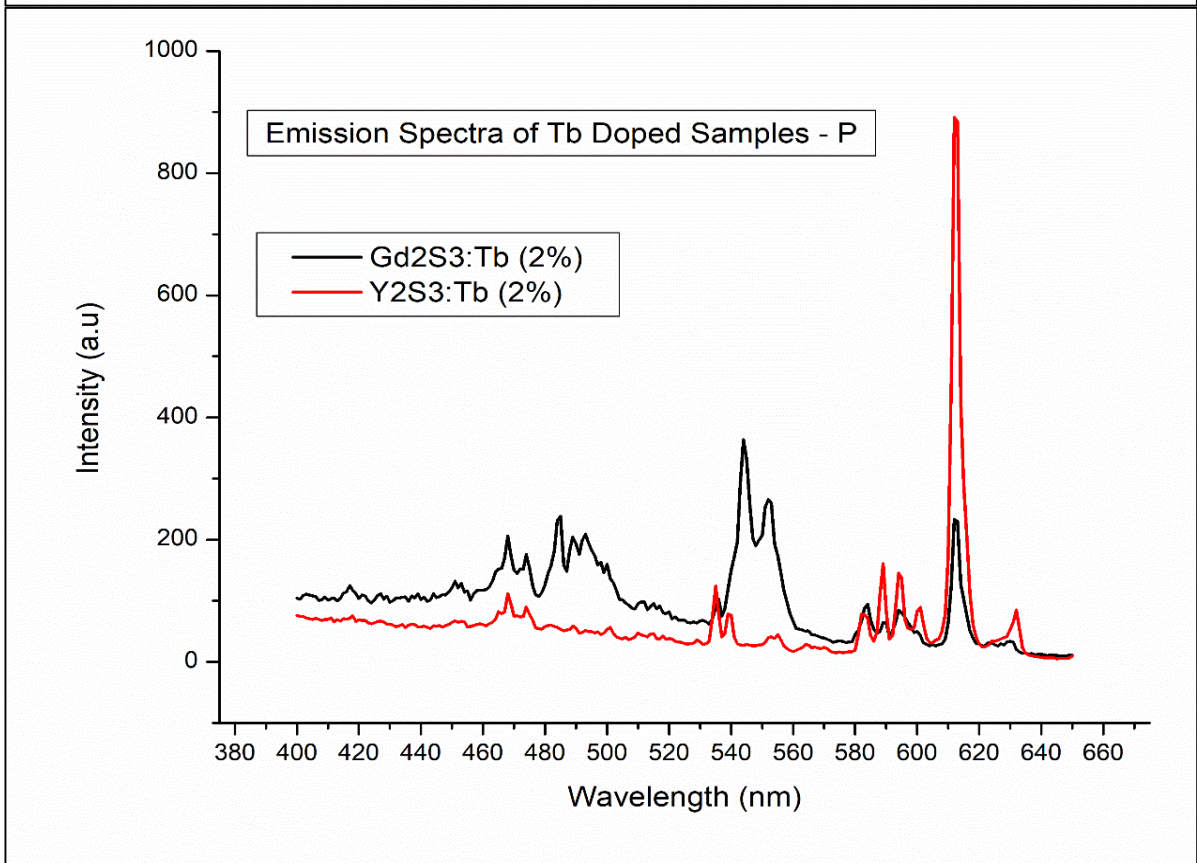
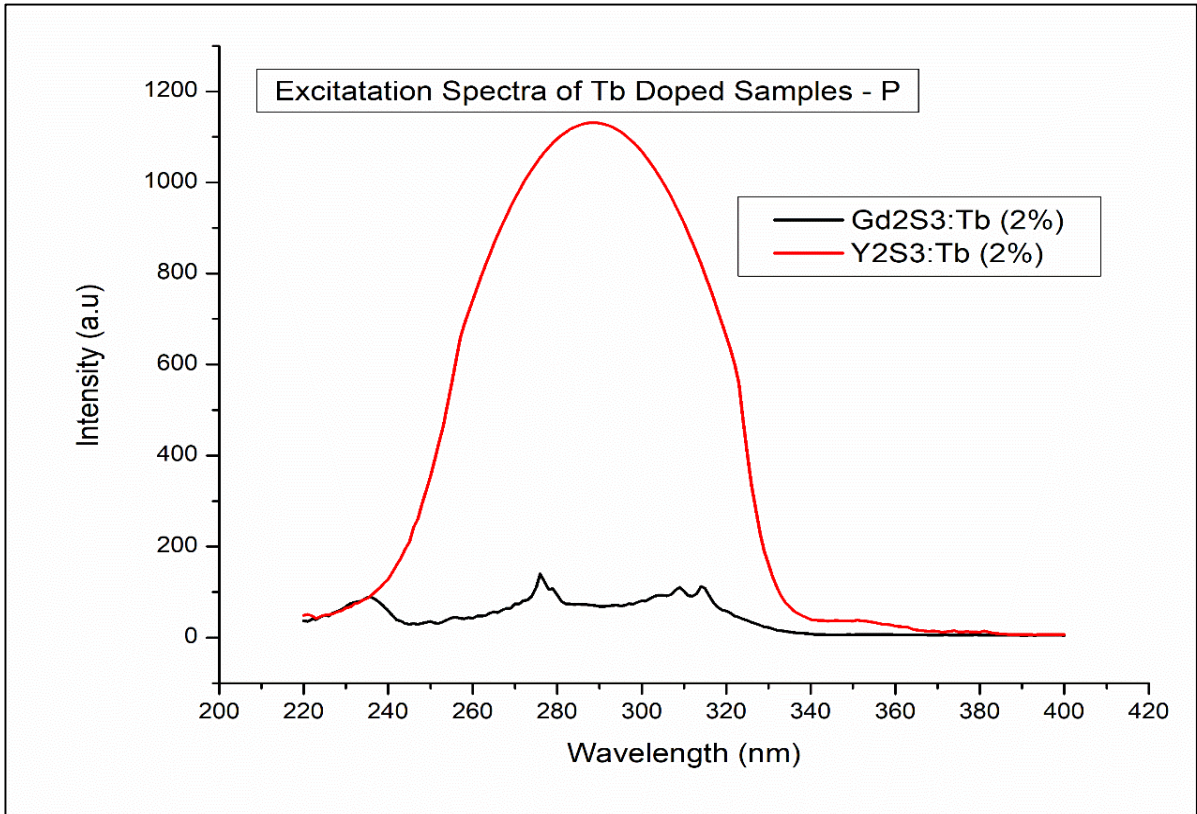


Figure 4-91: Excitation and Emission spectra of Tb doped samples synthesized by Precipitation method (a) Excitation spectra of GdT2-P and YT2-P (b) Emission spectra of GdT2-P and YT2-P

Figure 4-88 and 4-89 show the excitation and emission spectra of 2% Eu and Tb doped samples synthesized by Solid State method while Figs. 4-90 and 4-91 show the excitation and emission spectra of samples synthesized by Precipitation method. The excitation spectra of the most intense excitation line have been shown here.

It is seen that the intensity of the excitation peaks is almost similar in Eu doped samples while there is a difference in intensity for Tb doped samples. In both the excitation graphs, there is a shift in the peak wavelengths which can be attributed to the crystal field of different host materials.

The emission spectrum shows peaks at almost the same wavelengths for samples prepared by either method. These narrow band features are attributed to the properties of dopants  $\text{Eu}^{3+}$  and  $\text{Tb}^{3+}$ .

It is also observed that the emission intensity of  $\text{La}_2\text{S}_3$  is less as compared to the intensities of  $\text{Y}_2\text{S}_3$  and  $\text{Gd}_2\text{S}_3$  for samples synthesized by both the methods. However, it is seen to cover an extended region of the spectrum of visible light, more distinctly in case of Tb doping.

The excitation and emission intensities of  $\text{Y}_2\text{S}_3$  and  $\text{Gd}_2\text{S}_3$  are almost equal in case of Eu doping for both Solid State and Precipitation synthesis while, in case of Tb doping, the intensity of  $\text{Y}_2\text{S}_3$  is higher as compared to  $\text{Gd}_2\text{S}_3$  for both the synthesis methods.

The PL spectra of  $\text{Y}_2\text{S}_3$  gives only green emission when synthesized by Solid State method while it gives emission in both blue and green regions when synthesized by Precipitation method.

In Solid State synthesis, the excitation and emission spectra for Eu doped  $\text{Ce}_2\text{S}_3$  could not be obtained because of its dark colour while in Precipitation synthesis, spectra of Tb doped  $\text{Ce}_2\text{S}_3$  could not be obtained for the same reason.

The emission intensity of  $\text{Ce}_2\text{S}_3:\text{Tb}$  in case of Solid State synthesis and  $\text{Ce}_2\text{S}_3:\text{Eu}$  in case of Precipitation synthesis is found be least as compared to the other samples.

The width of the CTS band is maximum for  $\text{Gd}_2\text{S}_3$  for both the synthesis methods followed by  $\text{Y}_2\text{S}_3$ . In case of Solid State method, the intensities of peaks of  $\text{Gd}_2\text{S}_3$  and  $\text{Y}_2\text{S}_3$  are almost equal which implies that the absorption in Gadolinium Sulphide is higher. The CTS

band of  $\text{La}_2\text{S}_3$  is quite wide and intense in case of Solid State synthesis but it diminishes greatly for Precipitation synthesis.

Gadolinium Sulphide gives highest intensity emission in case of Eu doping while Yttrium Sulphide gives highest intensity emission in case of Tb doping in Solid State method.

**Table 4-12: Comparative study of Excitation and Emission Characteristics of Eu<sup>+3</sup> ions in samples X<sub>2</sub>S<sub>3</sub> [X = Ce, Gd, La, Y] prepared by both the methods**

Sample Name	Excitation Line	Emission Lines									
Gd <sub>2</sub> S <sub>3</sub> :Eu(1%) -SS	254							593	<b>612</b>	625	
La <sub>2</sub> S <sub>3</sub> :Eu(1%) - SS	274				534	580	589	596	<b>618</b>		
Y <sub>2</sub> S <sub>3</sub> :Eu(1%) - SS	<b>254</b>				535		588	595	<b>613</b>	631	
	466				535		588	595	<b>613</b>	632	
Ce <sub>2</sub> S <sub>3</sub> :Eu(1%) - P	274		468						<b>592</b>	612	633
	<b>372</b>								<b>592</b>	612	633
	467					582			<b>592</b>	<b>612</b>	633
Gd <sub>2</sub> S <sub>3</sub> :Eu(1%) - P	254		467		534	582	588	594	<b>613</b>	630	
La <sub>2</sub> S <sub>3</sub> :Eu(1%) - P	274		467	513	540		588	595	<b>615</b>	627	
Y <sub>2</sub> S <sub>3</sub> :Eu(1%) - P	254	371 393	474		535		587	595	<b>612</b>	632	
Gd <sub>2</sub> S <sub>3</sub> :Eu(2%) -SS	<b>254</b>				535	583	588	593	<b>613</b>	630	
	395						588	593	<b>613</b>	625 630	
	466						588	593	<b>612</b>	630	
La <sub>2</sub> S <sub>3</sub> :Eu(2%) - SS	<b>274</b>				534	580	589	596	<b>618</b>	627	
	396				534	580	587	595	<b>618</b>	627	
	466				534	580	587	596	<b>618</b>	627	
Y <sub>2</sub> S <sub>3</sub> :Eu(2%) - SS	<b>254</b>				535		588	595	600 <b>613</b>	631	
	466				535		588	595	600 <b>613</b>	631	

Sample Name	Excitation Line	Emission Lines								
Ce <sub>2</sub> S <sub>3</sub> :Eu(2%) - P	274		468					<b>592</b>	<b>612</b>	633
	<b>365</b>							<b>592</b>	612	633
	467					582		<b>592</b>	<b>612</b>	633
Gd <sub>2</sub> S <sub>3</sub> :Eu(2%) - P	<b>254</b>		467		535	582	588	594	<b>613</b>	630
	467						588	594	<b>613</b>	630
La <sub>2</sub> S <sub>3</sub> :Eu(2%) - P	274		467	513	540		588	595	<b>615</b>	<b>627</b>
Y <sub>2</sub> S <sub>3</sub> :Eu(2%) - P	<b>254</b>				534		589	595	<b>612</b>	632
	467				535		589	595	<b>612</b>	632
Gd <sub>2</sub> S <sub>3</sub> :Eu(3%) -SS	254					582	590	593	<b>613</b>	630
La <sub>2</sub> S <sub>3</sub> :Eu(3%) - SS	274				534	580	589	596	<b>618</b>	627
Y <sub>2</sub> S <sub>3</sub> :Eu(3%) - SS	<b>254</b>				535		588	595	600 <b>613</b>	631
	466				535		588	595	600 <b>613</b>	
Ce <sub>2</sub> S <sub>3</sub> :Eu(3%) - P	274	451	468					592	<b>612</b>	633
	<b>358</b>							592	<b>612</b>	633
	467							592	<b>612</b>	633
Gd <sub>2</sub> S <sub>3</sub> :Eu(3%) - P	<b>254</b>				535	582	588	594	<b>613</b>	630
	467						588	594	<b>613</b>	630
La <sub>2</sub> S <sub>3</sub> :Eu(3%) - P	274		467	513	540		588	595	<b>615</b>	<b>627</b>
Y <sub>2</sub> S <sub>3</sub> :Eu(3%) - P	254				535		589	593	600 <b>612</b>	632

From table 4-12, it is seen that

- For Eu<sup>3+</sup> doped samples, the maximum excitation intensity due to CTS transition is found to be 254 nm in Gd<sub>2</sub>S<sub>3</sub> and Y<sub>2</sub>S<sub>3</sub>, while it is 274 nm in La<sub>2</sub>S<sub>3</sub>. This is true for all samples prepared by both Solid State and Precipitation method.

- In case of  $\text{Ce}_2\text{S}_3$  synthesized by Precipitation method, the intensity of the most intense excitation line changes from 372 nm to 365 nm to 358 nm for 1%, 2% and 3% of Eu doping respectively. The Photoluminescence spectra of  $\text{Ce}_2\text{S}_3$  synthesized by Solid State method could not be obtained as mentioned earlier.
- The intensity of the most intense excitation line is almost the same for all 2% Eu doped samples synthesized by Solid State method, while it varies for samples synthesized by Precipitation method. In Precipitation synthesis,  $\text{Gd}_2\text{S}_3$  has the highest excitation intensity followed by  $\text{Y}_2\text{S}_3$  while  $\text{Ce}_2\text{S}_3$  and  $\text{La}_2\text{S}_3$  have almost same intensity which is very much less as compared to the other two samples.
- In Eu doped samples prepared by Solid State method, the intensities of the most intense excitation line remain almost constant in case of  $\text{Gd}_2\text{S}_3$  and  $\text{Y}_2\text{S}_3$  for all doping percentages, while in case of  $\text{La}_2\text{S}_3$ , it increases from 1% to 2% and then decreases for 3% of Eu doping. In samples prepared by Precipitation method, the intensities of the most intense excitation lines are found to increase from 1% to 2% of Eu doping and then decrease with 3% of Eu doping in case of  $\text{Ce}_2\text{S}_3$  and  $\text{La}_2\text{S}_3$ , while it remains almost same for  $\text{Gd}_2\text{S}_3$  and increases with increase in doping percentage for  $\text{Y}_2\text{S}_3$ .
- The emission spectra gives maximum intensity peak around 612 nm which is the characteristic wavelength for  $\text{Eu}^{3+}$  dopant in red region for all the samples synthesized by both the methods except  $\text{La}_2\text{S}_3$ . For  $\text{La}_2\text{S}_3$ , the most intense emission line is obtained at 618 nm. However, the transition levels remain the same.
- For Eu doped samples prepared by Solid State method, the intensities of the emission lines are found to increase with increase in doping percentage from 1% to 2% while it decreases when Eu doping percentage becomes 3% for all the samples. This is not the case for samples prepared by Precipitation method. The intensities of the emission lines are found to increase with increase of Eu doping from 1% to 3% for all the samples except  $\text{La}_2\text{S}_3$  for which the intensity increases with 1% to 2% Eu doping and then decreases for 3% of Eu doping.
- The emission lines are obtained at almost the same wavelengths for all the samples synthesized by Solid State method for all doping percentages of Eu. Additional lines on the lower wavelength side are found along with common emission lines in samples synthesized by Precipitation method. The number of emission peaks are maximum for 1% and 2% of Eu doping while it decreases when doping percentage becomes 3%.

- The overall emission intensity for samples synthesized by Precipitation method is less as compared to the emission intensities of samples prepared by Solid State method for all the doping percentages of Eu.
- Out of all the synthesized samples, the luminescence intensity is found to be highest in case of  $\text{Gd}_2\text{S}_3:\text{Eu}$  which suggests that it is a better material for Eu doped samples. This is true for samples synthesized by both the methods.

**Table 4-13: Comparative study of Excitation and Emission Characteristics of Tb<sup>+3</sup> ions in samples X<sub>2</sub>S<sub>3</sub> [X = Ce, Gd, La, Y] prepared by both the methods**

Sample Name	Excitation Line	Emission Lines								
Ce <sub>2</sub> S <sub>3</sub> :Tb(1%) -SS	247		468	474			<b>545</b>			
Gd <sub>2</sub> S <sub>3</sub> :Tb(1%) -SS	273			484	489	492	<b>544</b>	552		
La <sub>2</sub> S <sub>3</sub> :Tb(1%) - SS	<b>232</b>	415 <b>436</b>	457	475	486		<b>544</b>	547		
	273	415 436	468		487	492	<b>544</b>			
Y <sub>2</sub> S <sub>3</sub> :Tb(1%) - SS	287					<b>492</b>	<b>548</b>		585	596 624
Gd <sub>2</sub> S <sub>3</sub> :Tb(1%) - P	235		467	485		493	<b>545</b>	552	582	595 613
	<b>274</b>		467	485		493	<b>545</b>	552	582	592 613
	314			485		493	<b>545</b>	552		
Y <sub>2</sub> S <sub>3</sub> :Tb(1%) - P	290			485	488	493	<b>548</b>		586	597
Ce <sub>2</sub> S <sub>3</sub> :Tb(2%) -SS	247			474			<b>545</b>			
Gd <sub>2</sub> S <sub>3</sub> :Tb(2%) -SS	273			484	489	493	<b>544</b>	552		
La <sub>2</sub> S <sub>3</sub> :Tb(2%) -SS	<b>232</b>	383 416	435		487		<b>544</b>	547		
	273	383 416	435 468		487		<b>544</b>	547		
Y <sub>2</sub> S <sub>3</sub> :Tb(2%) - SS	287					492	<b>548</b>		585	596 624
Gd <sub>2</sub> S <sub>3</sub> :Tb(2%) - P	235		467	485		493	<b>545</b>	552	582	595 613
	<b>274</b>		467	485		493	<b>545</b>	552	582	592 613
	314			485		493	<b>545</b>	552		
Y <sub>2</sub> S <sub>3</sub> :Tb(2%) - P	290			485	488	493	<b>548</b>		586	597
Ce <sub>2</sub> S <sub>3</sub> :Tb(3%) -SS	247		468	474			<b>545</b>			
Gd <sub>2</sub> S <sub>3</sub> :Tb(3%) -SS	273			484	489	493	<b>544</b>	552		

Sample Name	Excitation Line	Emission Lines								
La <sub>2</sub> S <sub>3</sub> :Tb(3%) -SS	<b>232</b>	383 416	435		487		<b>544</b>	547		
	273	383 416	435 468		487		<b>544</b>	547		
Y <sub>2</sub> S <sub>3</sub> :Tb(3%) - SS	287					492	<b>548</b>		585	596 622
Gd <sub>2</sub> S <sub>3</sub> :Tb(3%) - P	235		467	485		493	<b>544</b>			616
	<b>274</b>			485			<b>544</b>		580 589	619
	314			485		493	<b>545</b>	552		
Y <sub>2</sub> S <sub>3</sub> :Tb(3%) - P	290			485	488	493	<b>548</b>		586	597

From table 4-13, it can be seen that

- For Tb<sup>3+</sup> doped samples, the maximum intensity excitation wavelength is different for different samples. It is found to be 247 nm and 232 nm for Ce<sub>2</sub>S<sub>3</sub> and La<sub>2</sub>S<sub>3</sub> synthesized by Solid State method. Photoluminescence spectra for these two samples synthesized by Precipitation method could not be obtained. The most intense excitation peak is found at 273 nm and 274 nm for Gd<sub>2</sub>S<sub>3</sub> synthesized by Solid State and Precipitation method respectively, while it is obtained at 287 nm and 290 nm in Y<sub>2</sub>S<sub>3</sub> for the respective methods. These values are found to remain the same for all doping percentages of Tb.
- In contrast to 2% Eu doped samples, the 2% Tb doped samples have varying intensities of excitation lines for samples synthesized by both Solid State and Precipitation methods. The excitation intensity decreases in the order Y<sub>2</sub>S<sub>3</sub> → Ce<sub>2</sub>S<sub>3</sub> → Gd<sub>2</sub>S<sub>3</sub> → La<sub>2</sub>S<sub>3</sub> in case of samples synthesized by Solid State method while in case of 2% Tb doped Precipitation method samples, the intensity of Y<sub>2</sub>S<sub>3</sub> is much higher as compared to Gd<sub>2</sub>S<sub>3</sub>.
- In Tb doped samples synthesized by Solid State method, the intensity of the most intense excitation peak remains almost the same in case of Ce<sub>2</sub>S<sub>3</sub> and Y<sub>2</sub>S<sub>3</sub> for all doping percentages of Tb. The intensity of excitation line of Gd<sub>2</sub>S<sub>3</sub> shows a steady decrease with increase in doping percentage while the intensity of La<sub>2</sub>S<sub>3</sub> excitation line increases from 1% to 2% of doping and then decreases for 3% of Tb doping. In samples prepared

by Precipitation method, the intensities of the excitation peaks increase for doping percentage of Tb from 1% to 2% and then decreases for 3% of Tb doping for both  $Gd_2S_3$  and  $Y_2S_3$ .

- The emission spectra give maximum intensity around 545 nm which is the characteristic emission wavelength of  $Tb^{3+}$  in green region. This applies for all the samples synthesized by both Solid State and Precipitation method. All the samples except  $Y_2S_3$  give emission lines in both blue and green regions for all samples synthesized by both the methods.
- In case of  $Y_2S_3$ , blue emission lines are absent in Solid State samples while in case of Precipitation samples, both blue and green emission lines are obtained.
- The intensities of emission lines of Tb doped samples prepared by Solid State method is found to increase with doping percentage from 1% to 2% and then decrease for 3% Tb doping for  $La_2S_3$ . It decreases with increase in doping percentage from 1% to 3% for  $Gd_2S_3$  and remains almost constant for  $Ce_2S_3$  and  $Y_2S_3$ . In case of all the samples prepared by Precipitation method, the intensities are found to increase with increase in Tb doping from 1% to 2% and then decreases when doping percentage becomes 3%.
- The emission lines are obtained at almost the same wavelengths for all the samples synthesized by Precipitation method for all the doping percentages of Tb. Additional emission lines in the blue region are found in samples synthesized by Solid State method for all doping percentages of Tb.
- $La_2S_3$  is seen to exhibit the widest wavelength range of emission lines with almost equal intensities.
- The overall emission intensity for samples synthesized by Precipitation method is less as compared to the emission intensities of samples synthesized by Solid State method for all doping percentages of Tb.
- Of all the synthesized samples, the luminescence intensity is found to be highest in case of  $Y_2S_3:Tb$  which suggests that it is a better material for Tb doped samples.

## 4.7 Thermoelectric Properties

This section provides thermoelectric power conversion application trials of the synthesized materials with dopants for further possible power applications. The thermoelectric properties of the synthesized rare-earth sulphides like Lanthanum Sulphide, Cerium Sulphide, Gadolinium Sulphide and Yttrium Sulphide with Manganese, Europium and Terbium as dopants were studied using their Resistance  $\rightarrow$  Temperature graphs. The change in resistance of rare earth sulphides was studied with an increase in temperature in the range of 308°K to 378°K (35°C to 105 °C) under laboratory conditions. All the samples were prepared using the same pellet press and die and hence in this case, resistance can be considered to be equivalent to resistivity as the dimensions and area of all samples was the same. Thus, the Resistance  $\rightarrow$  Temperature graphs can be considered to be replicas of Resistivity  $\rightarrow$  Temperature graphs.

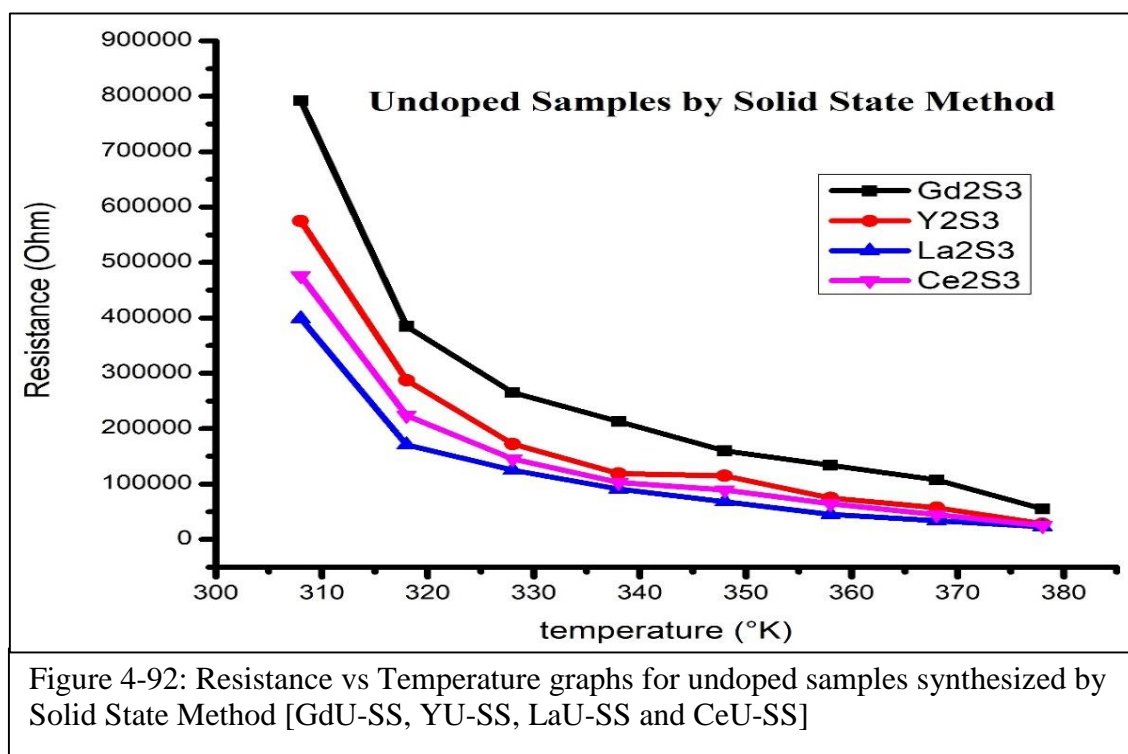


Figure 4-92 shows the Resistance  $\rightarrow$  Temperature curve for the undoped samples synthesized by Solid State Method. As seen in the above Figure, the resistance is in the order

of  $10^5 \Omega$  which decreases significantly with increase in temperature. Thus, the rare earth sulphides of Cerium, Gadolinium, Lanthanum and Yttrium exhibit semiconductor and Negative Temperature Coefficient Thermistor like properties. It is seen that the resistance of the samples decreases in the order of  $Gd_2S_3$  to  $Y_2S_3$  to  $Ce_2S_3$  to  $La_2S_3$  which can be understood on the basis of their Electronic Configuration and Ionization energies.

Samsonov has discussed the effect of incomplete f-shell electrons on the bonding capacity of s-shell electrons when these metals enter into chemical combination with Sulfur atoms. The influence of the f-electrons on the state of the s-electrons is felt more strongly, the greater the degree of incompleteness of the f-electron level. This would imply that the lesser filled the f-shell, higher is the bonding capacity when bonded with sulfur. As lanthanum has no 4f-shell electron, lanthanum sulfide possesses lowest resistivity and as Gadolinium has half-filled 4f-shell, it has highest resistivity which is seen in our results [13].

The electronic configuration of Gadolinium is  $[Xe] 4f^7 5d^1 6s^2$  which is a half-filled orbital configuration. Its first ionization energy is also 593 KJ/Mol which is the highest among all lanthanides. The half-filled  $4f^7$  orbit is considered more stable owing to symmetrical distribution of electrons resulting into strongly bounded electrons in the 4f sub shell. As a result, Gadolinium offers the highest resistance. Thus half-filled symmetrically organized sub shell is the reason for higher resistance of  $Gd_2S_3$ . As the temperature increases in semiconducting materials, we know that the forbidden energy gap decreases and electrons move from valence band to conduction band thus making free electrons available resulting into decrease in resistance.

Yttrium has  $[Kr] 4d^1 5s^2$  electronic configuration and ionization energy of 616 KJ/Mol. As the f-shell is absent in Yttrium, its s-shell bonding capacity with Sulfur is relatively higher compared to Gadolinium thus lowering the resistivity, even though it has relatively higher ionization energies than the lanthanides with one less filled shell [14].

In the case of Cerium with electronic configuration  $[Xe] 4f^1 5d^1 6s^2$ , the partially filled f-shell leads to relatively less s-shell bonding capacity with sulfur atoms as compared to Lanthanum, resulting into relatively higher resistance when compared to Lanthanum which does not have f-shell electrons at all. Its ionization energy is 534 KJ/Mol which is almost comparable to that of Lanthanum having ionization energy of 538 KJ/Mol.

Lanthanum has an electric configuration of  $[Xe] 5d^1 6s^2$  which is almost similar to the electronic configuration of Yttrium. They both do not have f-shell electrons.

However, Lanthanum has electrons in the 5d orbitals which are relatively distant than Yttrium's 4d orbital electrons. Thus, Lanthanum ought to have decreased resistivity compared to Yttrium. This is observed in our results as shown in figure 4-92.

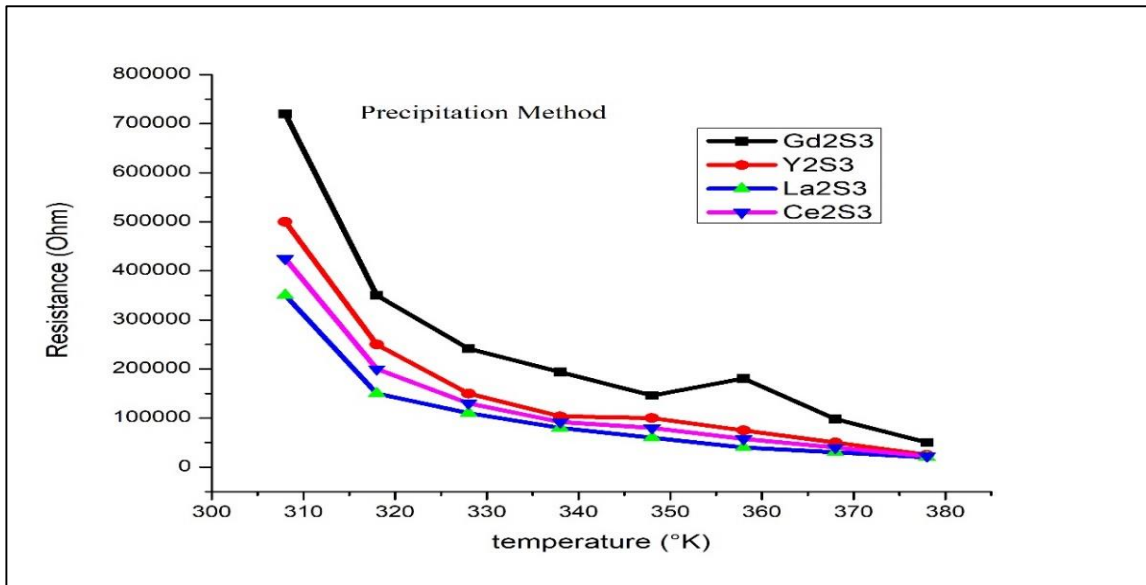


Figure 4-93: Resistance vs Temperature graphs for samples synthesized by Precipitation Method [GdU-P, YU-P, LaU-P and CeU-P]

Figure 4-93 shows the change in the resistance of rare earth sulphides with increase in temperature in the range of 308°K to 378°K (35°C to 105 °C) for samples synthesized by Precipitation method. The resistance of the same samples prepared by Precipitation method is less than the ones prepared by Solid State method. Thus the preparation method affects the resistance of the samples substantially. In case of Precipitation method also, it is seen that the resistance of the samples decreases in the order of Gd<sub>2</sub>S<sub>3</sub> to Y<sub>2</sub>S<sub>3</sub> to Ce<sub>2</sub>S<sub>3</sub> to La<sub>2</sub>S<sub>3</sub>. This sequence of resistance properties of synthesized materials with increase in temperature is shown in figure 4-93, which can be explained for the same reasons as discussed above.

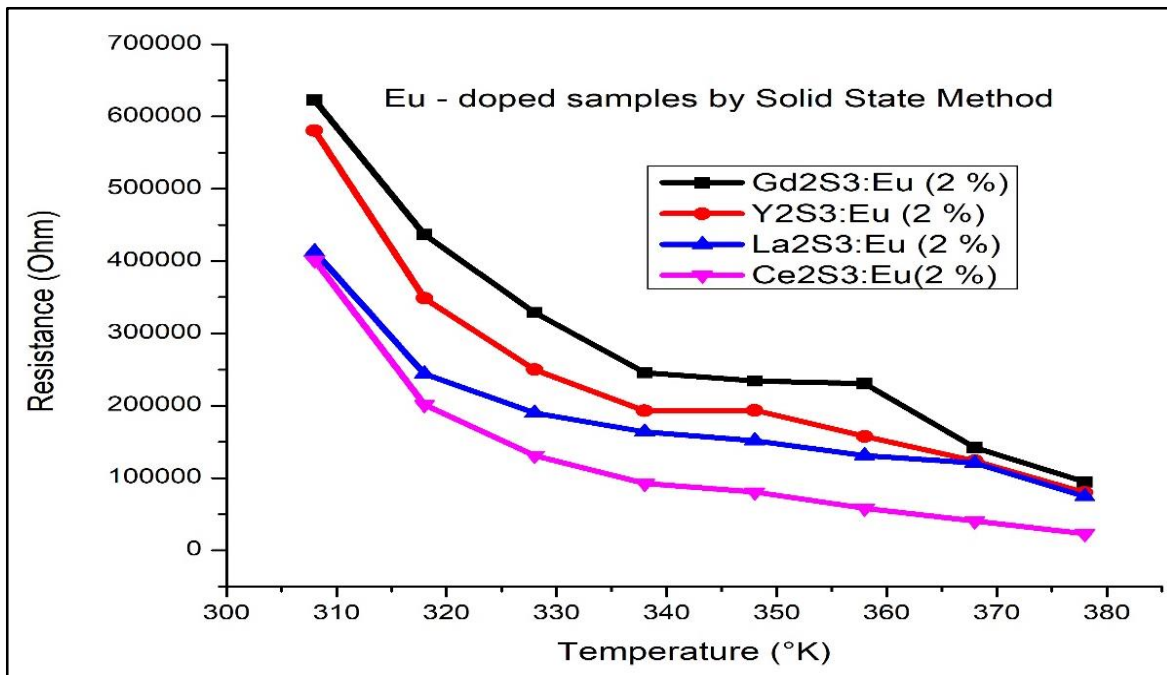


Figure 4-94: Resistance vs Temperature graphs for Eu doped samples synthesized by Solid State Method [GdE2-SS, YE2-SS, LaE2-SS and CeE2-SS]

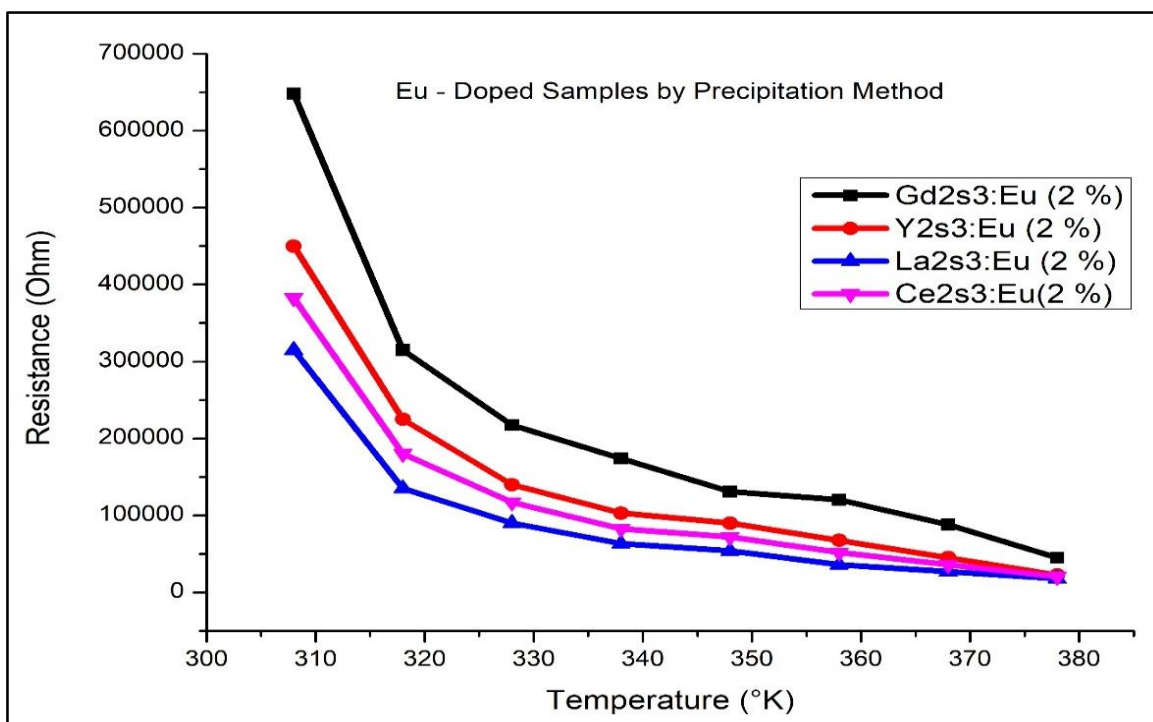


Figure 4-95: Resistance vs Temperature graphs for Eu doped samples synthesized by Precipitation Method [GdE2-P, YE2-P, LaE2-P and CeE2-P]

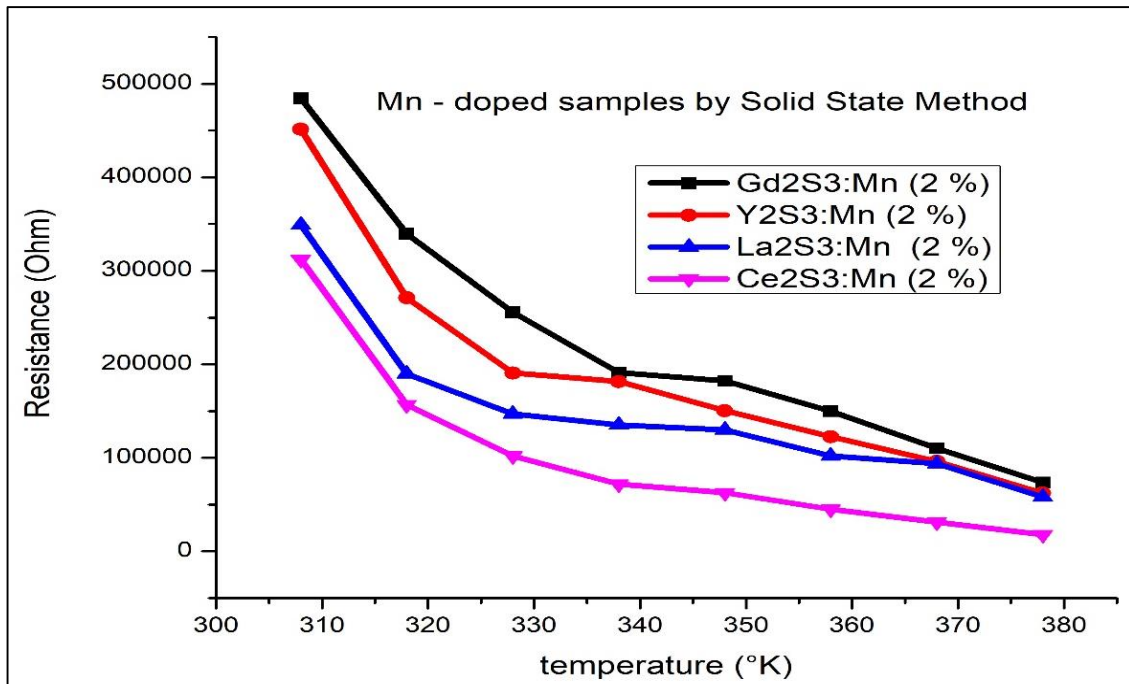


Figure 4-96: Resistance vs Temperature graphs for Mn doped samples synthesized by Solid State Method [GdM2-SS, YM2-SS, LaM2-SS and CeM2-SS]

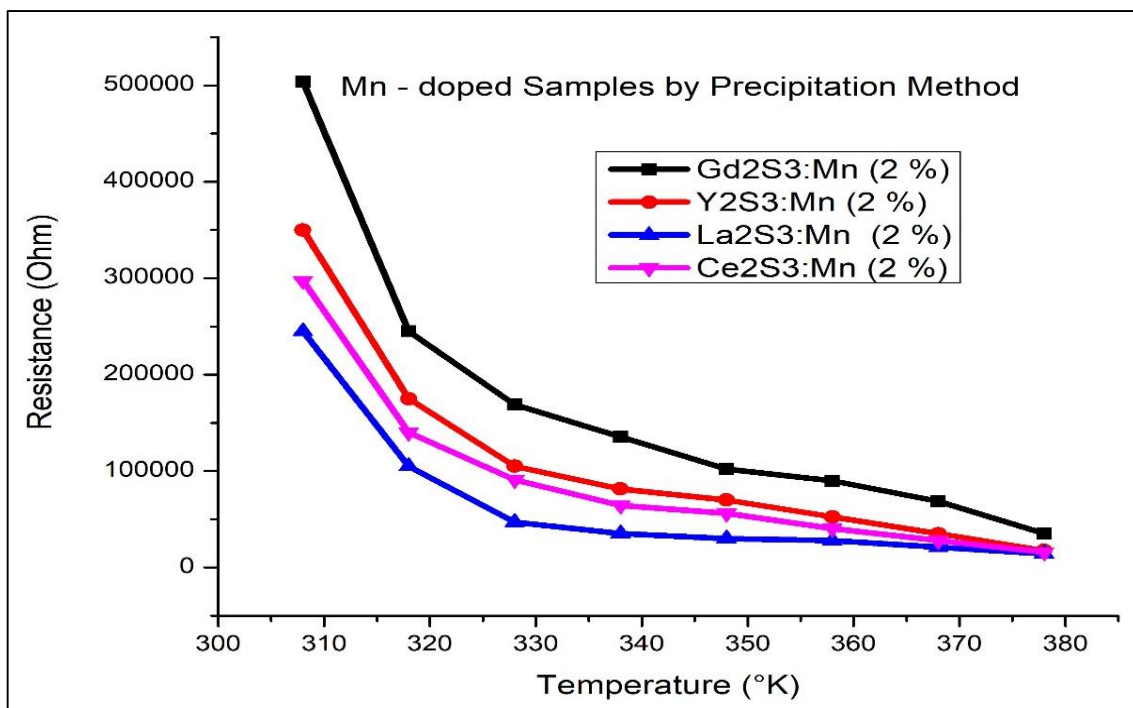


Figure 4-97: Resistance vs Temperature graphs for Mn doped samples synthesized by Precipitation Method [GdM2-P, YM2-P, LaM2-P and CeM2-P]

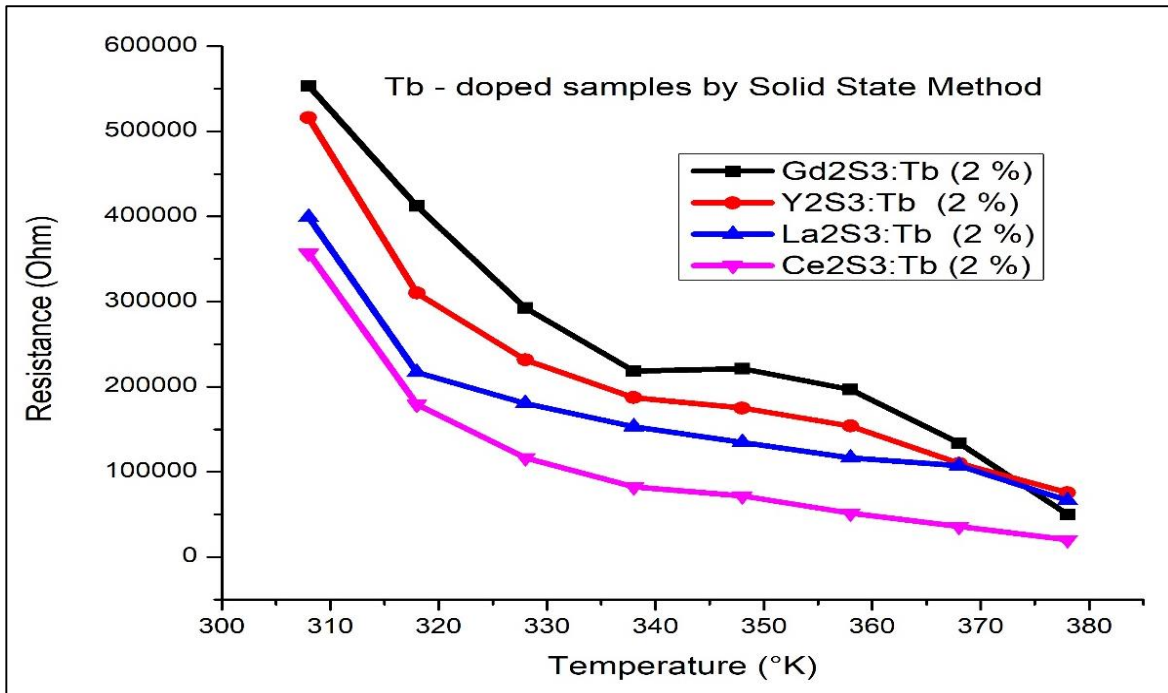


Figure 4-98: Resistance vs Temperature graphs for Tb doped samples synthesized by Solid State Method [GdT<sub>2</sub>-SS, YT<sub>2</sub>-SS, LaT<sub>2</sub>-SS and CeT<sub>2</sub>-SS.]

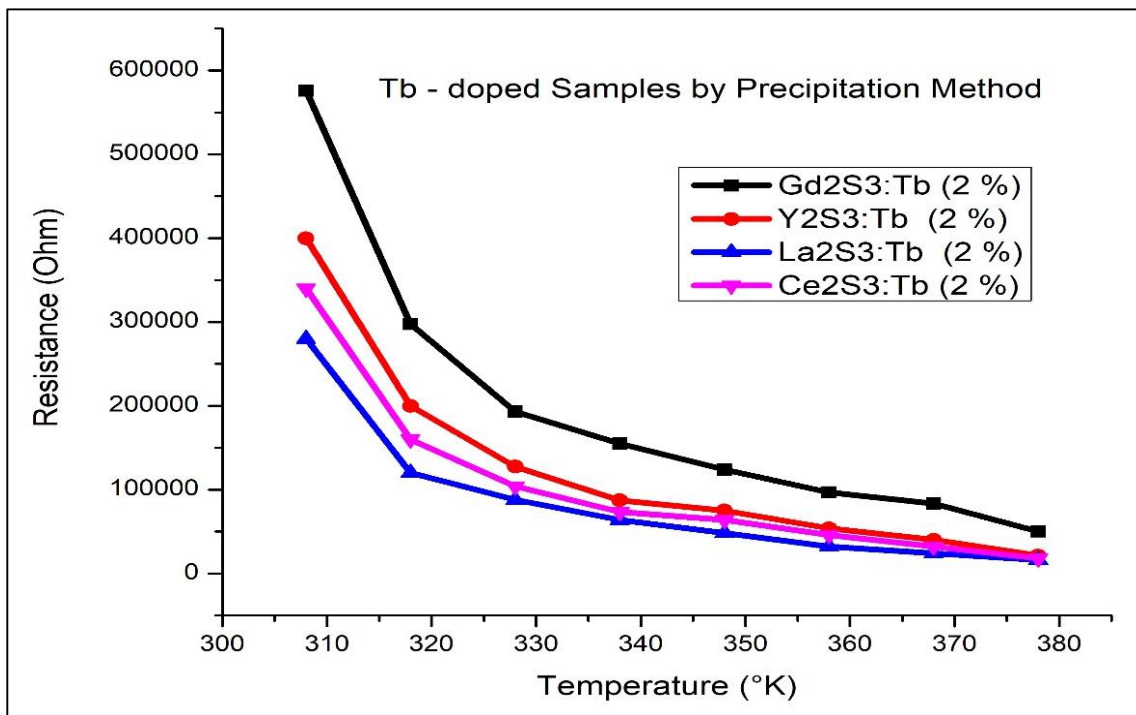


Figure 4-99: Resistance vs Temperature graphs for Tb doped samples synthesized by Precipitation Method [GdT<sub>2</sub>-P, YT<sub>2</sub>-P, LaT<sub>2</sub>-P and CeT<sub>2</sub>-P]

Fig. 4-94 and 4-95 show the Resistance vs Temperature behaviour of 2% Eu-doped samples of Gadolinium, Yttrium, Cerium and Lanthanum Sulfides synthesized by Solid State method and Precipitation method. Similarly, Fig. 4-96 and 4-97 show the behaviour of 2% Mn-doped samples synthesized by Solid State and Precipitation methods while fig. 4-98 and 4-99 show the Resistivity vs Temperature behaviour of 2% Tb-doped samples of Gadolinium, Yttrium, Cerium and Lanthanum Sulfides synthesized by Solid State method and Precipitation methods.

It is evident from the above figures 4-94 to 4-99 that doping decreases the resistance of the material. All the doped samples show similar behaviour as undoped samples with increase in temperature, except that doped samples have relatively lesser resistance which can be attributed to the fact that doping increases availability of conduction electrons and hence causes decrease in resistivity. A unique feature of these results was that in doped samples prepared by Solid State method, the resistance of Lanthanum Sulphide samples was found to be higher than Cerium Sulfide samples, which became the lowest in resistance, while in the doped samples prepared by Precipitation method, the sequence remained same as undoped samples. The resistivity anomaly of Cerium Sulfide in specific case of solid state doping method can be attributed to the following.

Cutler et al studied electronic transport in Cerium Sulfide and argued that the cause of the resistivity anomalies is possibly due to local lattice vibrations or by spin scattering by electrons in the 4f shell of the Cerium ions. The local lattice vibrations and spin scattering give rise to increased collisions and disorder resulting into additional electrons besides the electron availability due to doping. This explains the decrease in resistivity of doped Cerium Sulfide. However, this occurs in only Solid State doping method but not in Precipitation method. It is possible that in Solid State method the heating at 1200 °C may be causing such orientation of atoms so as to facilitate increased spin scattering. [15].

From above figures, it is seen that the samples doped with Eu have the highest resistivity among all followed by Tb doped samples and Mn doped samples for all materials prepared by both the methods.

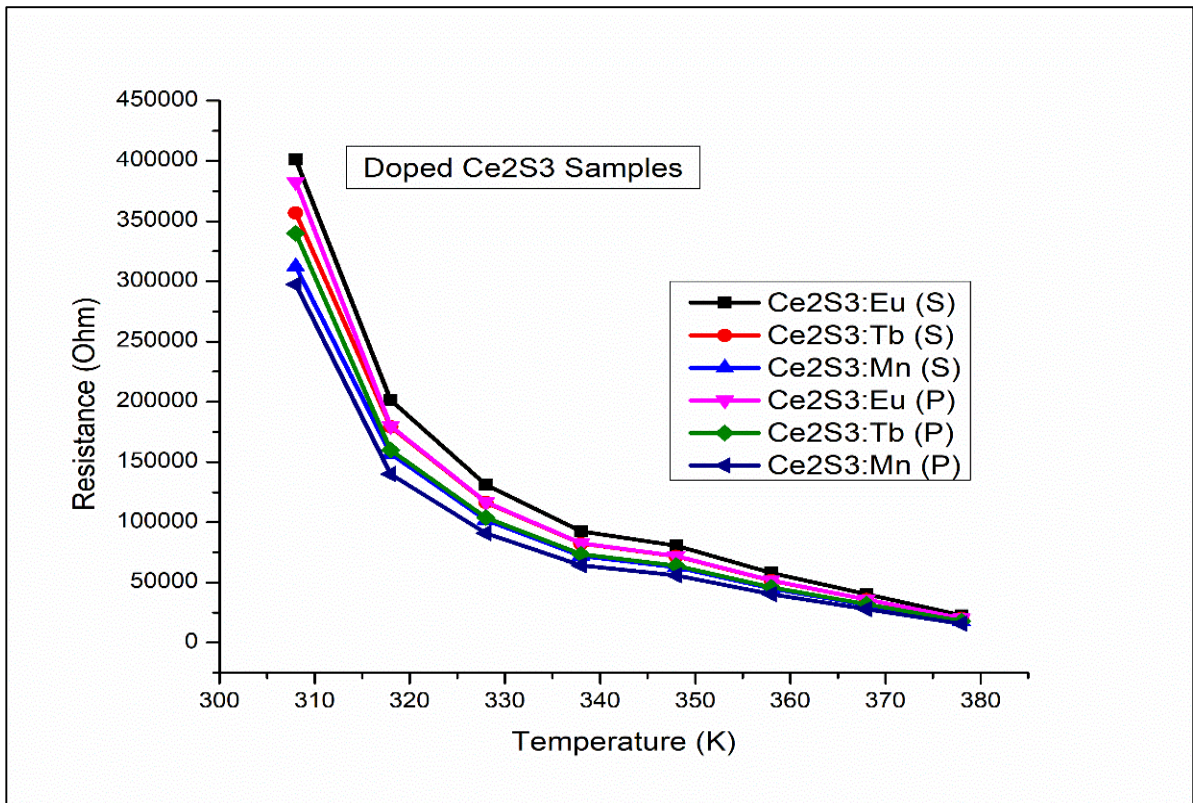


Figure 4-100: Resistance vs Temperature Graphs for Eu, Tb and Mn Doped Cerium Sulphide synthesized by Solid State and Precipitation methods

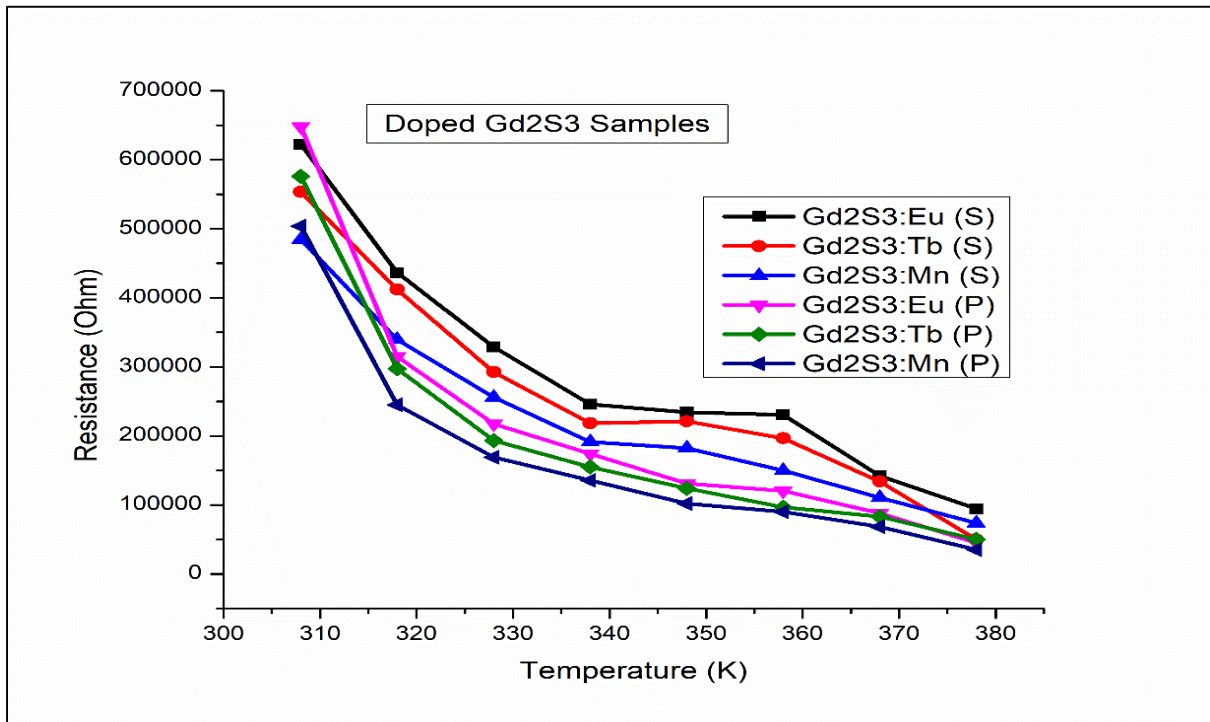


Figure 4-101: Resistance vs Temperature Graphs for Eu, Tb and Mn Doped Gadolinium Sulphide synthesized by Solid State and Precipitation methods

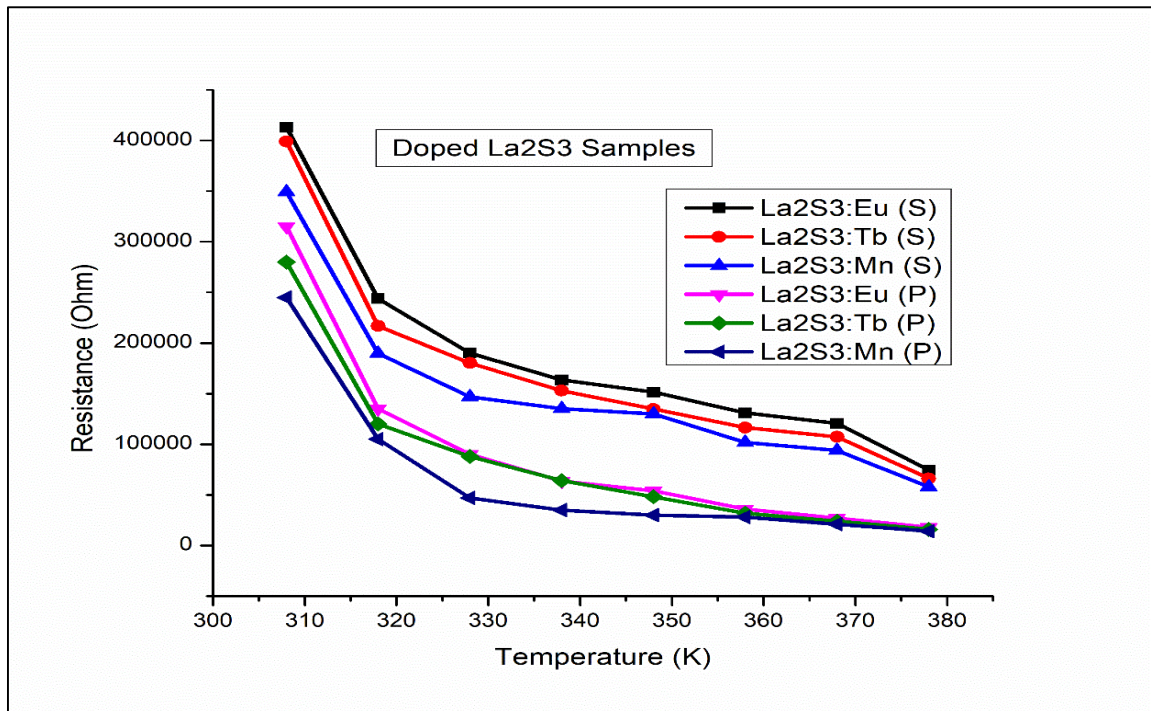


Figure 4-102: Resistance vs Temperature Graphs for Eu, Tb and Mn Doped Lanthanum Sulphide synthesized by Solid State and Precipitation methods

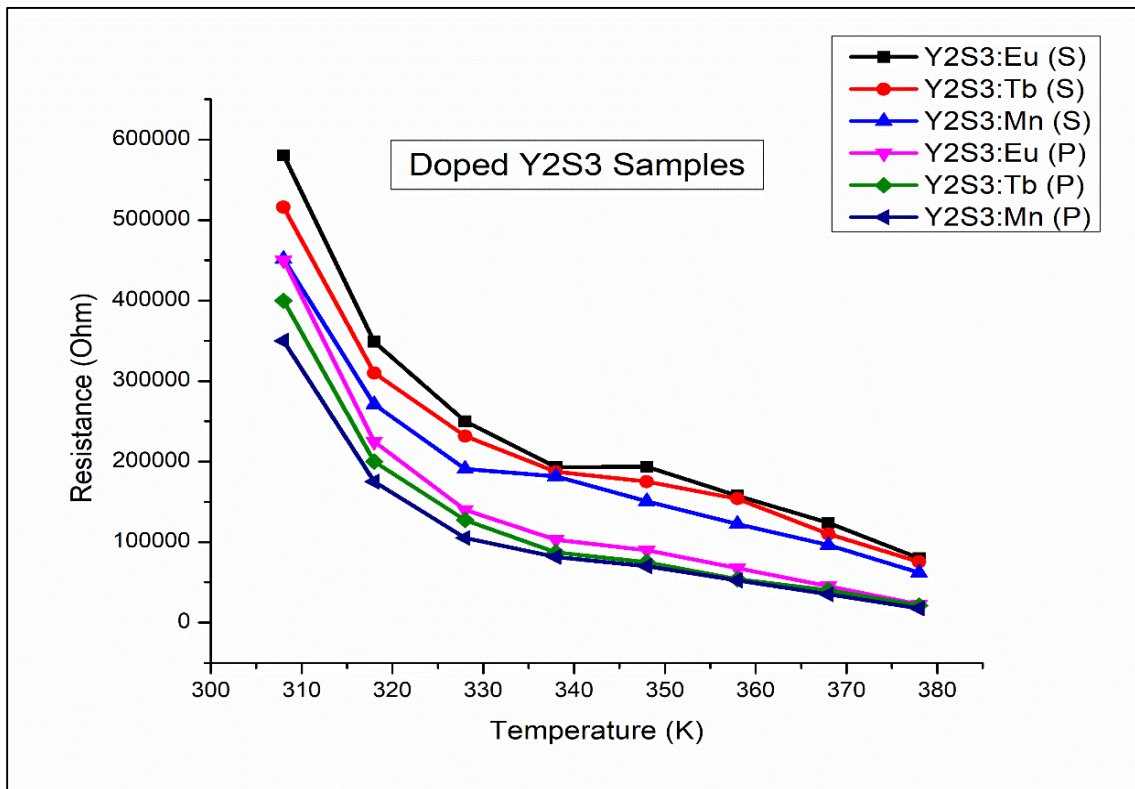


Figure 4-103: Resistance vs Temperature Graphs for Eu, Tb and Mn Doped Yttrium Sulphide synthesized by Solid State and Precipitation methods

Figures 4-100 to 4-103 show the Resistance  $\rightarrow$  Temperature change patterns in the same host with different dopants prepared by the two synthesis methods. The Temperature  $\rightarrow$  Resistance graphs obtained for all the samples can be broadly divided into three sections i.e. the lowest temperature is the steepest region (A) in the temperature range of 308°K to 318 °K, the next region in the temperature range 318°K to 328 °K where it is less steep (B) and the almost linear region (C) beyond this temperature. The Temperature Coefficient of Resistance was calculated for all the samples in these three regions which is shown in the table 4-14 below.

**Table 4-14: Temperature Coefficient of Resistance Calculated for synthesized samples**

Sample Code	Region of the Curve	Gd <sub>2</sub> S <sub>3</sub>	Y <sub>2</sub> S <sub>3</sub>	Ce <sub>2</sub> S <sub>3</sub>	La <sub>2</sub> S <sub>3</sub>
Undoped - SS	A	-0.0519	-0.0464	-0.0529	-0.0572
	B	-0.0290	-0.0410	-0.0338	-0.0265
	C	-0.0180	-0.0180	-0.0159	-0.0274
Eu doped - SS	A	-0.0297	-0.0392	-0.0465	-0.0426
	B	-0.0247	-0.0284	-0.0369	-0.0229
	C	-0.0139	-0.0093	-0.0201	-0.0110
Tb doped - SS	A	-0.0250	-0.0403	-0.0486	-0.0464
	B	-0.0292	-0.0243	-0.0345	-0.0161
	C	-0.0131	-0.0096	-0.0198	-0.0124
Mn doped - SS	A	-0.0302	-0.0414	-0.0499	-0.0463
	B	-0.0247	-0.0278	-0.0345	-0.0216
	C	-0.0138	-0.0163	-0.0194	-0.0123

Sample Code	Region of the Curve	Gd <sub>2</sub> S <sub>3</sub>	Y <sub>2</sub> S <sub>3</sub>	Ce <sub>2</sub> S <sub>3</sub>	La <sub>2</sub> S <sub>3</sub>
Undoped - P	A	-0.0524	-0.0512	-0.0528	-0.0560
	B	-0.0303	-0.0377	-0.0336	-0.0294
	C	-0.0163	-0.0144	-0.0183	-0.0226
Eu doped - P	A	-0.0524	-0.0512	-0.0504	-0.0559
	B	-0.0304	-0.0368	-0.0349	-0.0276
	C	-0.0164	-0.0170	-0.0220	-0.0245
Tb doped - P	A	-0.0478	-0.0502	-0.0539	-0.0577
	B	-0.0344	-0.0358	-0.0337	-0.0276
	C	-0.0151	-0.0158	-0.0209	-0.0245
Mn doped - P	A	-0.0514	-0.0483	-0.0523	-0.0578
	B	-0.0312	-0.0393	-0.0357	-0.0360
	C	-0.0166	-0.0171	-0.0192	-0.0106

Referring to the Temperature Coefficient of Resistance values in these three regions, it is seen that the values do not vary in large measure. The TCR values of all the doped samples is less as compared to the undoped samples for both the methods. The values of TCR are found to be more uniform in samples prepared by Precipitation method when compared to Solid State samples. The values of TCR in the almost linear region (C) are the least for all the samples. This linear region of the curves can be utilized to develop temperature sensing devices. Of all the synthesized samples, Ce<sub>2</sub>S<sub>3</sub> shows the best uniform characteristics and hence is a better candidate for temperature sensing.

The Temperature → Resistance graphs show a certain pattern which was identified to be identical to the power function  $f(x) = k x^n$  where k and n are real numbers. The power function fit curves along with the equation are shown in the fig. 4-104 below.

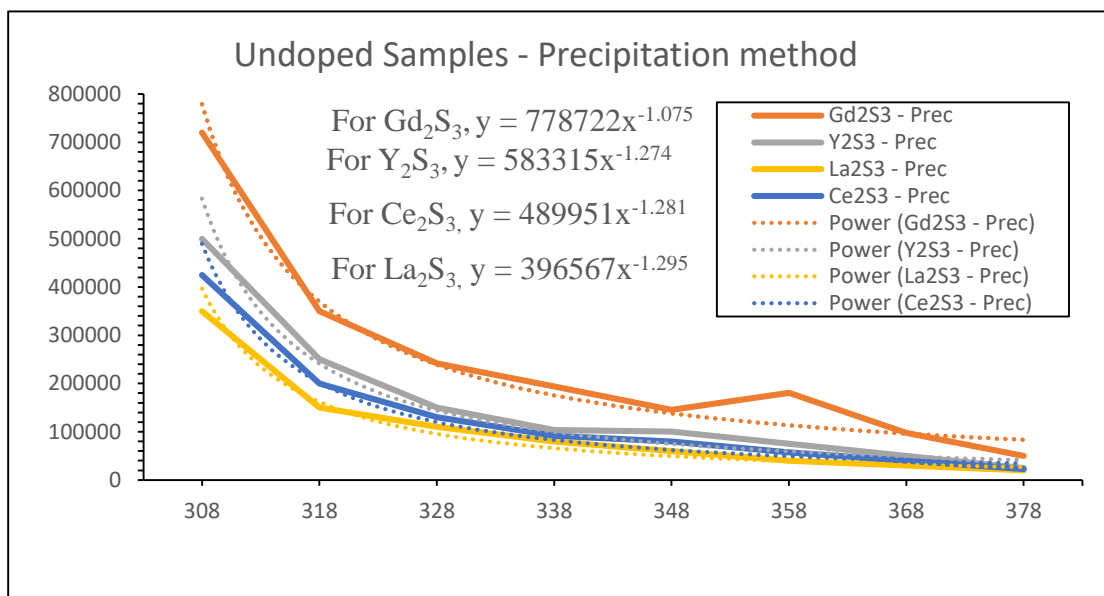
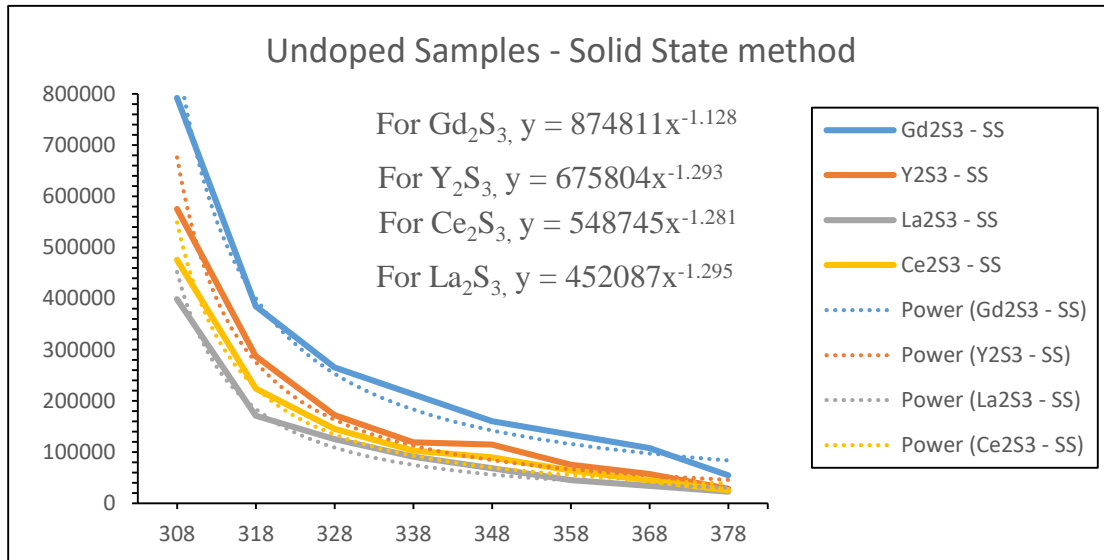


Figure 4-104: The Resistance vs Temperature Graphs Fitted on the Power Function for undoped samples (a) GdU-SS, YU-SS, CeU-SS and LaU-SS (b) GdU-P, YU-P, CeU-P and LaU-P

Using these equations, we can find the resistance of the material at any value of temperature.

The temperature of a running car engine is somewhere between 90° C to 120° C. In this study we have taken TEP data in the range of temperature from 35° C to 105° C. If we use the above equations to find the resistance at a temperature of 120° C, we find that the value of resistance becomes very small and is in a few hundreds. This might not be the actual case

because in semiconductors, there is a saturation after some time which may lead to an almost constant resistance. Yet, there is a large decrease in resistance during the entire temperature range studied here which implies that the current obtained at a temperature of 105° C will be much greater than that which we get at a temperature of 35° C.

The entire set up was operated at a constant voltage of 0.1V and hence, the current obtained at 35° C is in the range of  $\mu\text{A}$  for all the samples. The resistance decreases by a factor of 10 or more, as we increase the temperature from 35° C to 105° C and hence there will be a consequent change in the current for the given voltage. The resistance of doped samples is less than that of undoped samples, in the order from Eu doping to Tb doping to Mn doping. The current obtained in case of doped samples is higher. Maximum current is obtained in the case of  $\text{Ce}_2\text{S}_3$ .

The current being in the range of  $\mu\text{A}$  at 0.1 V, the power obtained would be in the range of microwatt. Though the current and power are relatively less, the generated power may be used to operate various IOT (Internet of Things) devices like sensors, microprocessors and microchips which have found their way in our houses also. The basic IOT functions like switching a device on and off have now been modified to do complicated tasks of collecting data from devices such as television, washing machine etc. and analyzing the same in real time for the purpose of giving them appropriate instructions. Many of such devices can function in the current range of nano and even up to pico amperes.

**Table 4-15: Percentage Decrease in Resistance with Temperature in the range 308°K to 378°K (35° C to 105 °C) for synthesized samples**

Synthesis Method	Gd <sub>2</sub> S <sub>3</sub>	Y <sub>2</sub> S <sub>3</sub>	La <sub>2</sub> S <sub>3</sub>	Ce <sub>2</sub> S <sub>3</sub>
Undoped Solid State – SS	93.05%	95.0%	94.28%	94.7%
Undoped Precipitation – P	93.05%	95.0%	94.28%	94.7%
Eu Doped – P	93.05%	95.0%	94.28%	94.7%
Tb Doped – P	91.31%	94.68%	94.28%	94.7%
Mn Doped – P	93.05%	95.0%	94.28%	94.7%
Eu Doped – SS	84.82%	86.24%	81.96%	94.35%
Tb Doped – SS	90.97%	85.38%	83.40%	94.34%
Mn Doped – SS	84.82%	86.24%	83.40%	94.35%

Table 4-15 shows the percentage decrease in resistance with temperature for the samples synthesized by Solid State and Precipitation method. It is seen that the percentage decrease in resistance is same in undoped samples synthesized by both the methods. In case of doped samples, the percentage decrease in resistance is more in samples synthesized by precipitation method than in those synthesized by Solid State method.

These results show promise to be utilized in futuristic applications of power conversion in industries for the generation of electricity from waste heat from different equipments. There will always remain many important and useful high temperature based applications in manufacturing of materials like ceramics and Silicon heating elements for the industries where these materials can be used as thermoelectric conversion materials. An attempt is made here to realize the thermoelectric properties of Rare Earth Sulphides which can be used for developing better applications.

## 4.8 References:

- [1] E. Eastman, L. Brewer, L. Bromley, P. Gilles, and N. Lofgren, "Preparation and Properties of Refractory Cerium Sulfides," *J. Am. Chem. Soc.*, 72, 2248–50 (1950).
- [2] T. Toide, T. Lkmomiya, M. Sate, Y. Hoshino, T. Hatano of, Y. Akimoto. *Bull. Tokyo Institute Technol.* 117 (1973) 31.
- [3] S. Benazeth, M. Guittard, J. Flahaut. *J. Solid State Chem.* 37 (1981) Patent. R 91-095.9 I I-1 989. 1991. 44.
- [4] B. Le Roland, P. McMillan, P. Colombet. *C.R. Acad. Sci. Paris.*
- [5] C. Wood, High-Temperature Thermoelectric Energy Conversion--II. *Materials Survey, Energy Convers. Mgmt Vol. 24, No. 4 pp. 331 - 343, 1984*
- [6] Christopher Marin, 2016, 'Synthesis and Applications of Lanthanide Sulfides and Oxides', University of Nebraska, Lincoln.
- [7] Manvendra Kumar, Parasmani Rajput, P. K. Singh, A. C. Yadav, S. A. Khan, S. N. Jha, Fouran Singh, A. C. Pandey, On The Europium Activated Gadolinium Sulfide Nanoparticles, *RSC Advances*, 2016, 00, 1-3.
- [8] Chen S, Meng X, Xie G, Gao S, Shi Q. Thermochemistry of the ternary solid complex Gd (C<sub>5</sub>H<sub>8</sub>NS<sub>2</sub>)<sub>3</sub>(C<sub>12</sub>H<sub>8</sub>N<sub>2</sub>). *Russ. J. Inorg. Chem.*, 2006, 51: 445.
- [9] LUO Xixian, MA Lubin, XING Mingming, FU Yao, SUN Min, TAO Pang, Preparation of  $\gamma$ -Gd<sub>2</sub>S<sub>3</sub> via thermolysis of Gd[S<sub>2</sub>CN(C<sub>4</sub>H<sub>8</sub>)]<sub>3</sub>-phen coordination, *Journal Of Rare Earths*, Vol. 30, No. 8, Aug. 2012, P. 802
- [10] M. Ohta, S. Hirai, S. Morita, T. Nishimura, Y. Uemura and K. Simakage: *Proc. 15th Symp. On Functionally Graded Materials (FGM Forum of Japan, 2003) pp. 242–247.*

- [11] Toide T, Utsunomiya T, Sato M, Hoshino Y, Hatano T, Akimoto Y. Preparation of lanthanum sulfides using carbon disulfide as a sulfurizing agent and the change of these sulfides on heating in air. *Bull. Tokyo. Inst. Tech.*, 117 (1973), 41-48.
- [12] ZHENXING DU, QUANSHENG LIU, TIANJIANG HOU, YUE SONG, XIYAN ZHANG and YANYU CUI, The effects of Tb<sup>3+</sup> doping concentration on luminescence properties and crystal structure of BaF<sub>2</sub> phosphor, *Bull. Mater. Sci., Indian Academy of Sciences*, Vol. 38, No. 3, June 2015, pp. 805–809.
- [13] G. V. Samsonov, Crystal-chemical properties of sulfides of the rare-earth metals and actinides, *Poroshkovaya Metallurgiya*, No. 4 (10), July-August 1962, pp 11-19.
- [14] M. Cutler, J. F. Leavy and R. L. Fitzpatrick, Electronic Transport in Semimetallic Cerium Sulfide, *Physical Review*, 113 (1964), A1134-A1152.